COMMUNICATIONS QUARTERLY

THE JOURNAL OF COMMUNICATIONS TECHNOLOGY

Summer 1997

$9.95

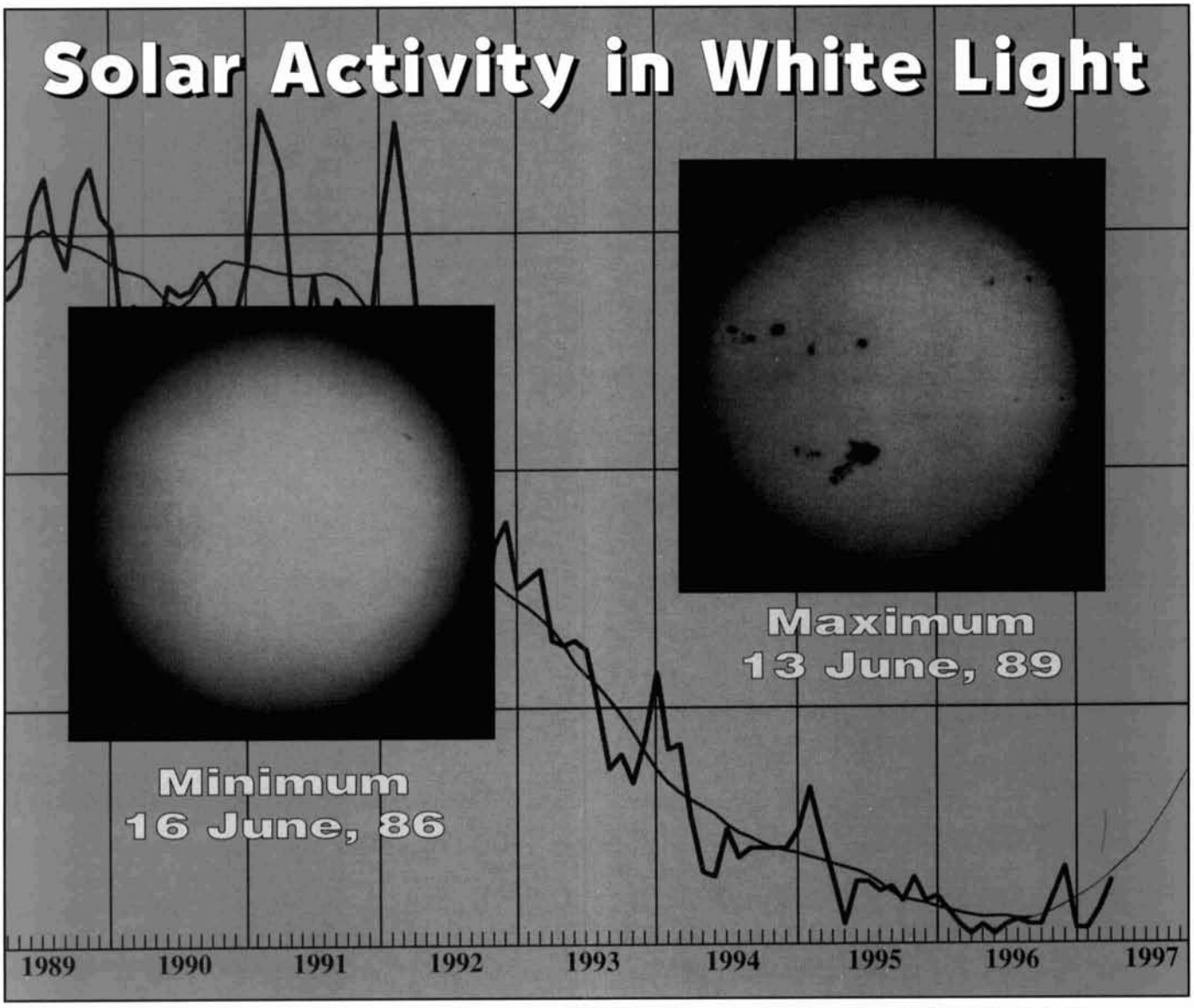

- An Analytical Look at HF Path Losses
- Build a Receiver for Phone Applications with this Low-Cost Monolithic Chip Set
- Loading Profiles for Improved Wideband Antennas
- Measure Coax Cable Loss with Excel
- Broadband Transmission Line Transformers
- The Influence of Ground on Horizontal Antennas
- Recognizing—and Avoiding—"Junk Science"
- The Shrunken Quad Antenna

U.S. $9.95

72>

0 73361 64880 8

The Wireless Solution Site

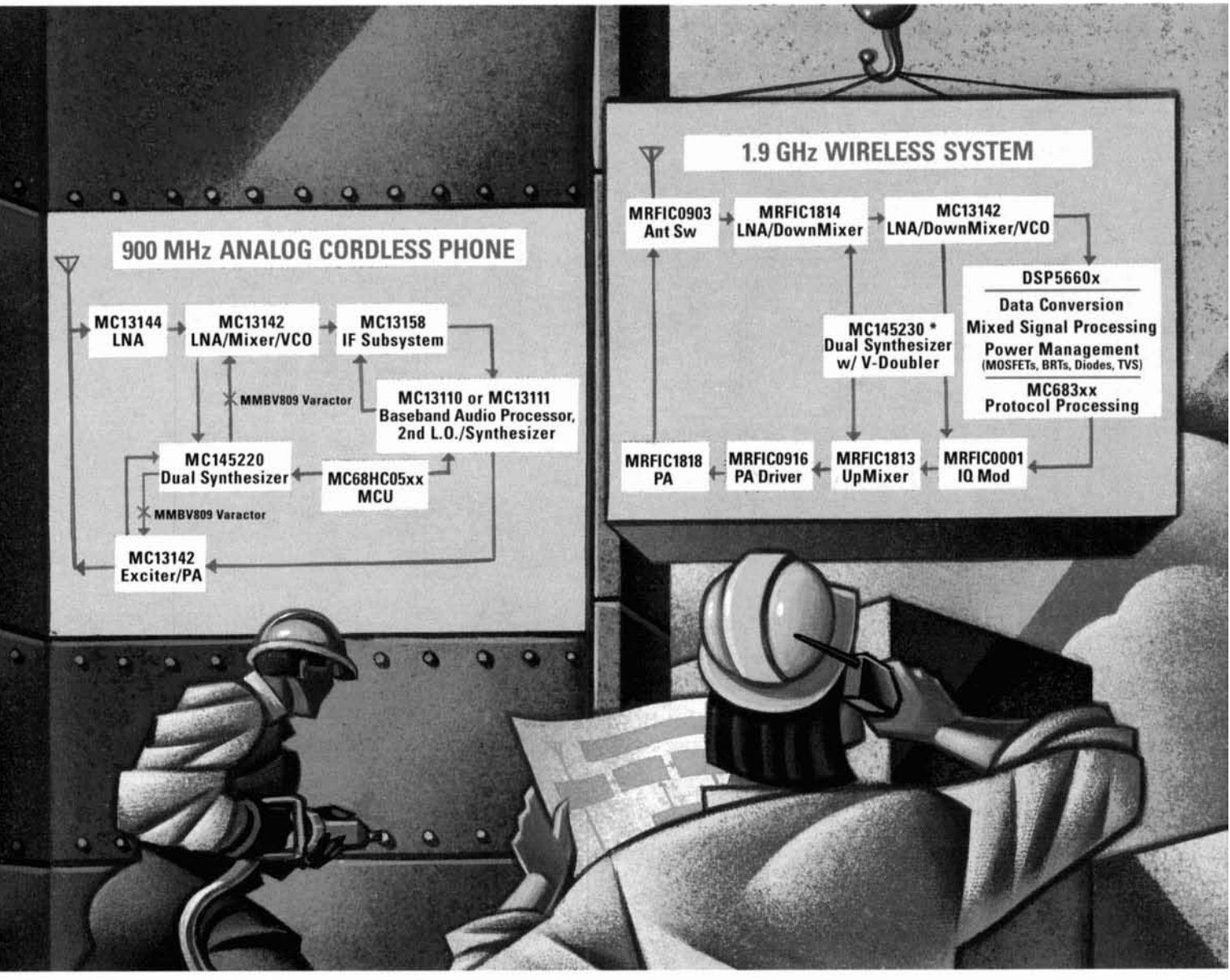

Building the best in RF and baseband components.

We have more than just the blueprints for your success. Built from decades of leadership in ICs for the communications industry, our diverse portfolio of RF, baseband and discrete devices offers superior solutions for a wide range of wireless systems.

Not only do these components award unequaled compatibility and flexibility, each has Motorola's years of experience built right in — from the antenna switches to the PLLs to the baseband processors.

So, no matter what wireless application you're designing, let Motorola's Wireless Solution Site go to work for you.

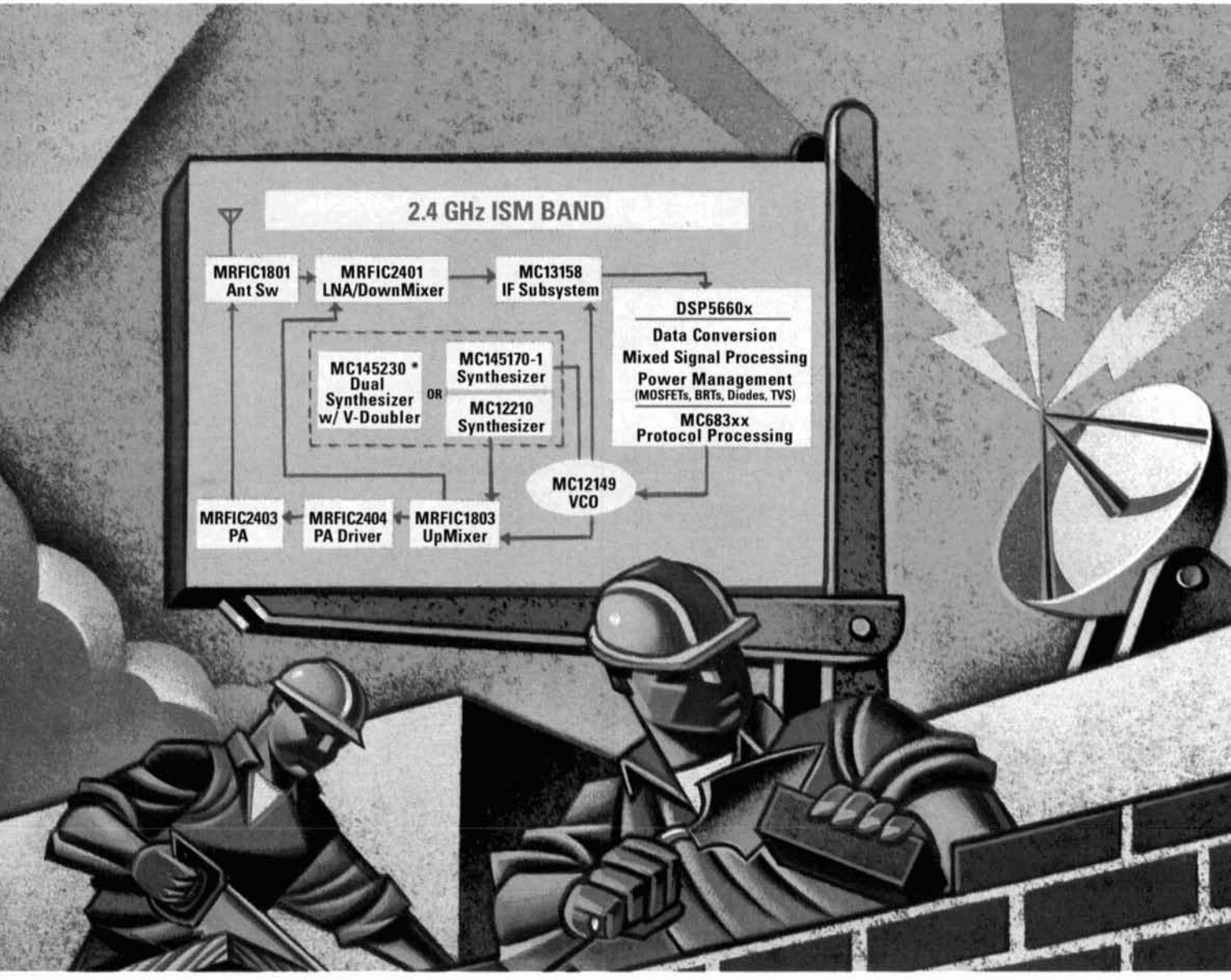

Call **1-800-201-0293** and refer to advertisement number **PLL01** for a comprehensive package of technical data and evaluation kit information. Or visit our web site at **www.mot.com/wireless-solutions**

MOTOROLA

Semiconductor Products Sector

What you never thought possible.™

COMMUNICATIONS QUARTERLY

THE JOURNAL OF COMMUNICATIONS TECHNOLOGY

CONTENTS

Volume 7, Number 3 Summer 1997

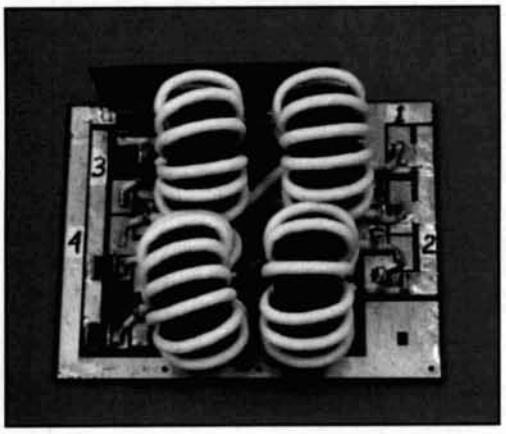

page 45

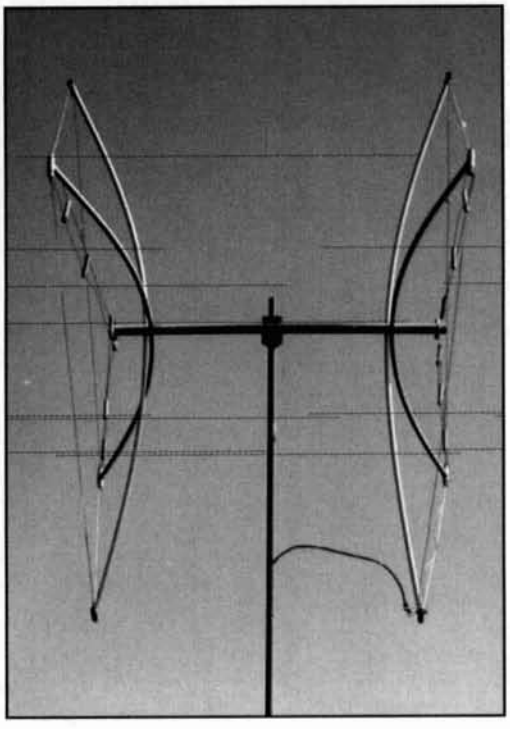

page 71

On the Cover: White-light photographs comparing the inactive sunspot minimum disk of the Sun with sunspot cycle maximum. Photo courtesy of the National Optical Astronomy Observatories/NSO, Sacramento Peak, via Peter O. Taylor. Behind the disks appears a portion of the graph on the Monthly IPS T-index for the Solar Cycle, prepared by the IPS Radio and Space Services in Australia, Dr. Richard Thompson, Director.

.... POWER ON WITH ASTRON
SWITCHING POWER SUPPLIES ....

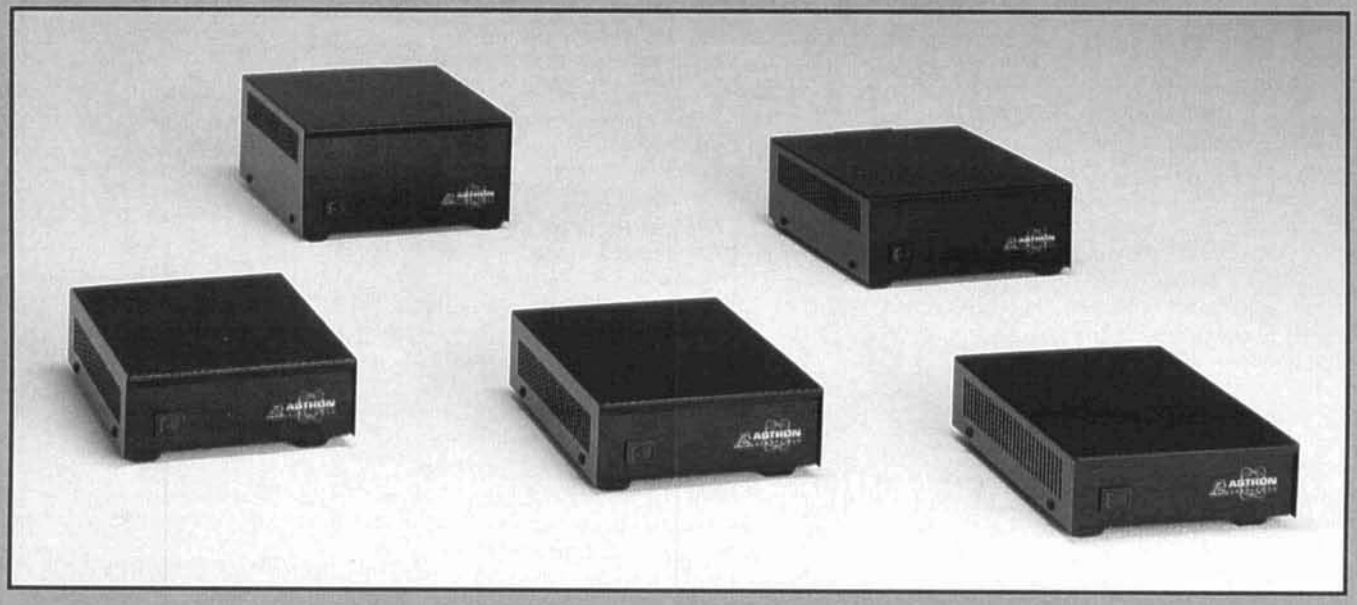

SPECIAL FEATURES:

- HIGH EFFICIENCY SWITCHING TECHNOLOGY SPECIFICALLY FILTERED FOR USE WITH COMMUNICATIONS EQUIPMENT, FOR ALL FREQUENCIES INCLUDING **HF**.
- HEAVY DUTY DESIGN
- LOW PROFILE, LIGHT WEIGHT PACKAGE.
- EMI FILTER
- MEETS FCC CLASS B

PROTECTION FEATURES:

- CURRENT LIMITING
- OVERVOLTAGE PROTECTION
- FUSE PROTECTION
- OVER TEMPERATURE SHUTDOWN

SPECIFICATIONS:

INPUT VOLTAGE: 90-132 VAC 50/60Hz
OR 180-264 VAC 50/60Hz
SWITCH SELECTABLE

OUTPUT VOLTAGE: 13.8 VDC

MODEL	CONT. AMP	ICS	SIZE	WT.(LBS)
SS-10	7	10	1 1/8 x 6 x 9	3.2
SS-12	10	12	1 3/8 x 6 x 9	3.4
SS-18	15	18	1 3/8 x 6 x 9	3.6
SS-25	20	25	2 7/8 x 7 x 9 3/8	4.2
SS-30	25	30	3 3/4 x 7 x 9 5/8	5

ASTRON CORPORATION

9 AUTRY, IRVINE, CALIFORNIA 92618
714-458-7277 FAX 714-458-0826
www.astroncorp.com

EDITORIAL

For a few dollars more...

Our RF spectrum is a precious national, and natural, resource. Unlike many such resources, it has, until now, been a renewable one. We have entrusted our government to manage all these national treasures in the public interest and, historically, there was no question that the airwaves have always belonged to the public. But now our rights appear to be overshadowed by the wants of government and big business...and there are more dark clouds on the horizon.

Rule play

In the early years of RF communications, people who listened to radio transmissions broke no law. Under the Communications Act of 1934 (47 USC 605), you were allowed to listen. What you couldn't do was make use of what you heard, and pass it along to anyone else, unless the information was broadcast or transmitted by amateurs or others for use by the general public.

Enter the laws governing the monitoring of cellular, and then cordless, telephone transmissions. The Electronic Communications Privacy Act (EPCA, 18 USC 2510-2511) passed by Congress in 1986, forbade scanner owners and other listeners from tuning in on communications intended to be private. The cellular rule was followed by another regulation (47 CFR 15.9) that ensured that cellular and cordless phones would be treated alike. Anyone who regularly listens to a scanner knows how easy it is to tap into someone's personal calls, although many who make such calls may be naively unaware that someone might be listening in.

For their part, telecommunications companies have either claimed that the technology to encode such phone conversations is either unavailable or too expensive. As a result, these laws have taken the responsibility from the companies who offer these products and put the onus on the public. Countless scanner listeners are now considered criminals because the telecommunications industry promised false security to its clients and then failed to deliver. Instead of requiring the adoption of encoding technologies, the laws rewarded cellular and cordless phone manufacturers for limiting the rights of others to listen to traffic on the airwaves.

Coming soon, the big auction

In two years, the FCC will start auctioning off the VHF television spectrum. These VHF TV stations will be relocated to the UHF TV spectrum over a 10-year period, as the new HDTV standards are adopted. The auction is expected to raise some 90 billion dollars for the United States government, while paving the way for the emerging technologies. That's another 66 MHz of real estate headed for "ownership" by private industry, and out of the public domain. Television station owners will pay dearly for their new channels in the form of license fees.

As the FCC is continually downsized and stripped of authority by Congress, the agency's role is more and more that of auctioneer than a defender of the airwaves. Our VHF amateur bands are under attack, and the threat from Low Earth Orbiting Satellites (LEOS) is very real. Although their encroachment has been restricted for now, these little satellites may literally kick us right off the spectrum!

Congress, and to some degree the FCC, has always supported amateur radio. Members of the ham community have been entrusted with generous areas of the RF spectrum, as have other citizens across the free world. The amateur bands are a public resource. Any motivated citizen can easily obtain a license and use this service. But how will our "public service" role play against the one billion dollars per megahertz price tag our bands represent?

Unfortunately, our RF resources are "intangible." You can't see, feel, or touch them. This very invisibility leaves the spectrum ripe for plundering when commercial interests outweigh those of the public. How can something so vital to the fabric of our free speech and communication be sold! Remember, we're not talking short-term leases here, we're talking sale. Once this process begins, there's no retreat. Once the spectrum is sold, it's gone.

What can you do?

Contact your Congressmen and Senators. Tell them the facts. Fight to stop this unprecedented plundering of our national resources before there's no public spectrum left, before we have to become expatriates to enjoy what we once enjoyed here at home!

Peter Bertini, K1ZJH
Senior Technical Editor

Terry Littlefield, KA1STC
Editor

A publication of
CQ Communications, Inc.
76 North Broadway
Hicksville, NY 11801-USA

Editorial Offices: P.O. Box 465, Barrington, NH 03825. Telephone/FAX: (603) 664-2515. **Business Offices:** 76 North Broadway, Hicksville, NY 11801. Telephone: (516) 681-2922. FAX: (516) 681-2926.

Communications Quarterly is published four times a year (quarterly) by *CQ Communications, Inc. Communications Quarterly* is the philosophical successor of *Ham Radio Magazine* founded by T.H. "Skip" Tenney, Jr., W1NLB and James R. Fisk, W1HR. Subscription prices (all in U.S. Dollars): Domestic—one year $33.00; two years $62.00. Canada/Mexico—one year $39.00; two years $74.00. Foreign Air Post—one year $46.00; two years $88.00.

Periodical postage paid at Hicksville, NY and additional mailing offices.

Postmaster: Please send change of address to Communications Quarterly, CQ Communications, Inc., 76 North Broadway, Hicksville, NY 11801. ISSN 1053-9344.

Printed in U.S.A.

A Wake-up Call

Dear Editor:

Dick Weber's article on uneven currents in elevated radials (Spring '97 *Communications Quarterly*) was a real wake-up call.

Uneven radial lengths can be a problem as he has shown, but, with some care, they can also be useful in special situations. For example, it is possible to create a low SWR resonance at two points in an elevated radial 80-meter vertical.

A vertical with elevated radials can be modeled as several parallel, open circuited, transmission lines. In the vicinity of quarterwave resonance the equivalent circuit can be approximated by several series resonant networks, one for the vertical and one for each radial as shown in **Figure 1**.

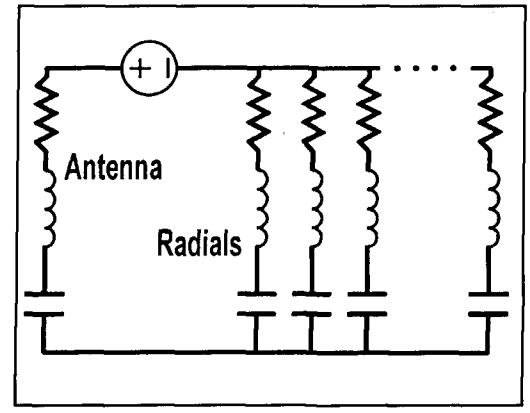

Figure 1.

Basic circuit theory tells us that the driving point of this network can have multiple series resonances (zeros) at different frequencies, *but*

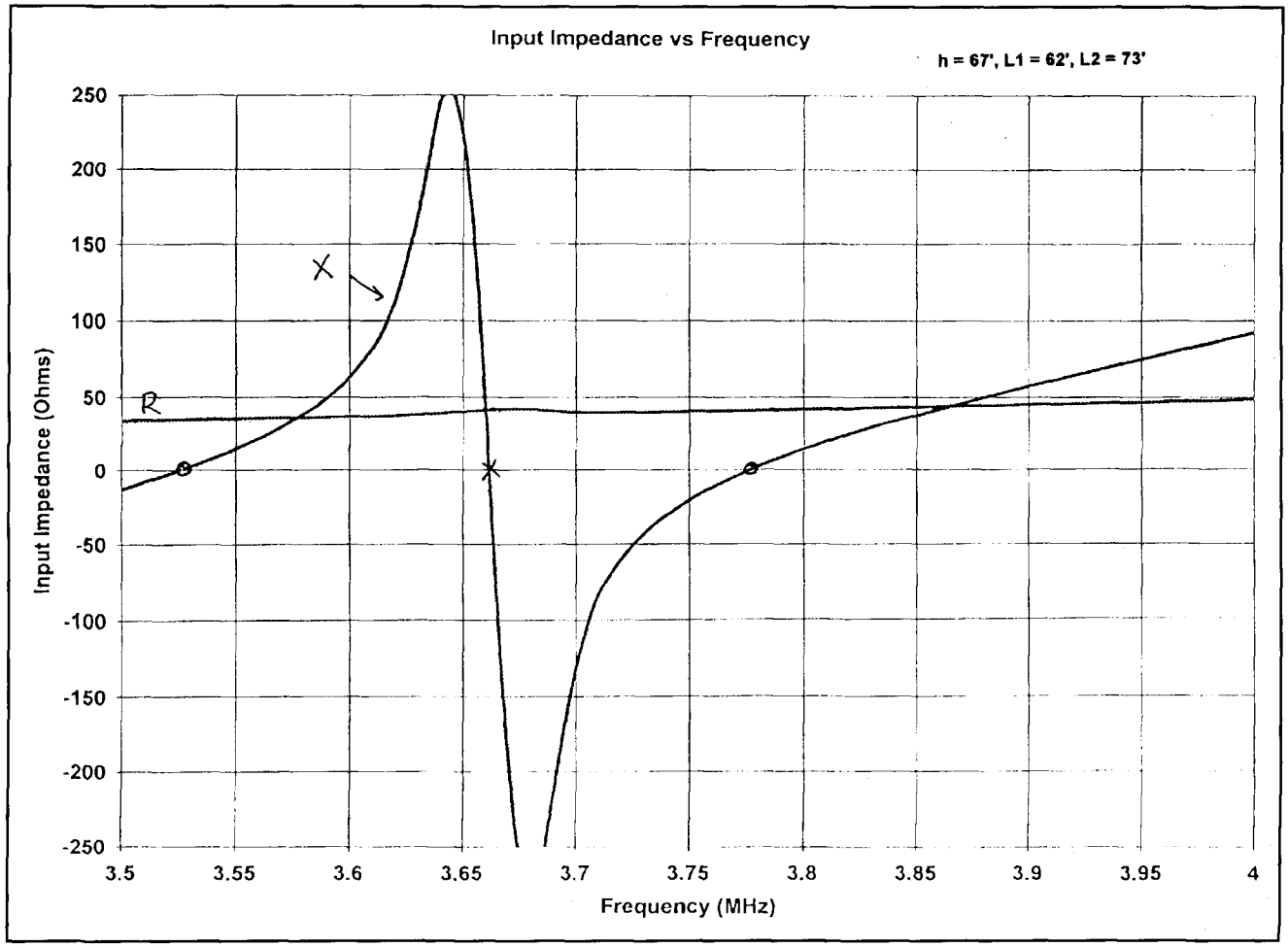

Figure 2.

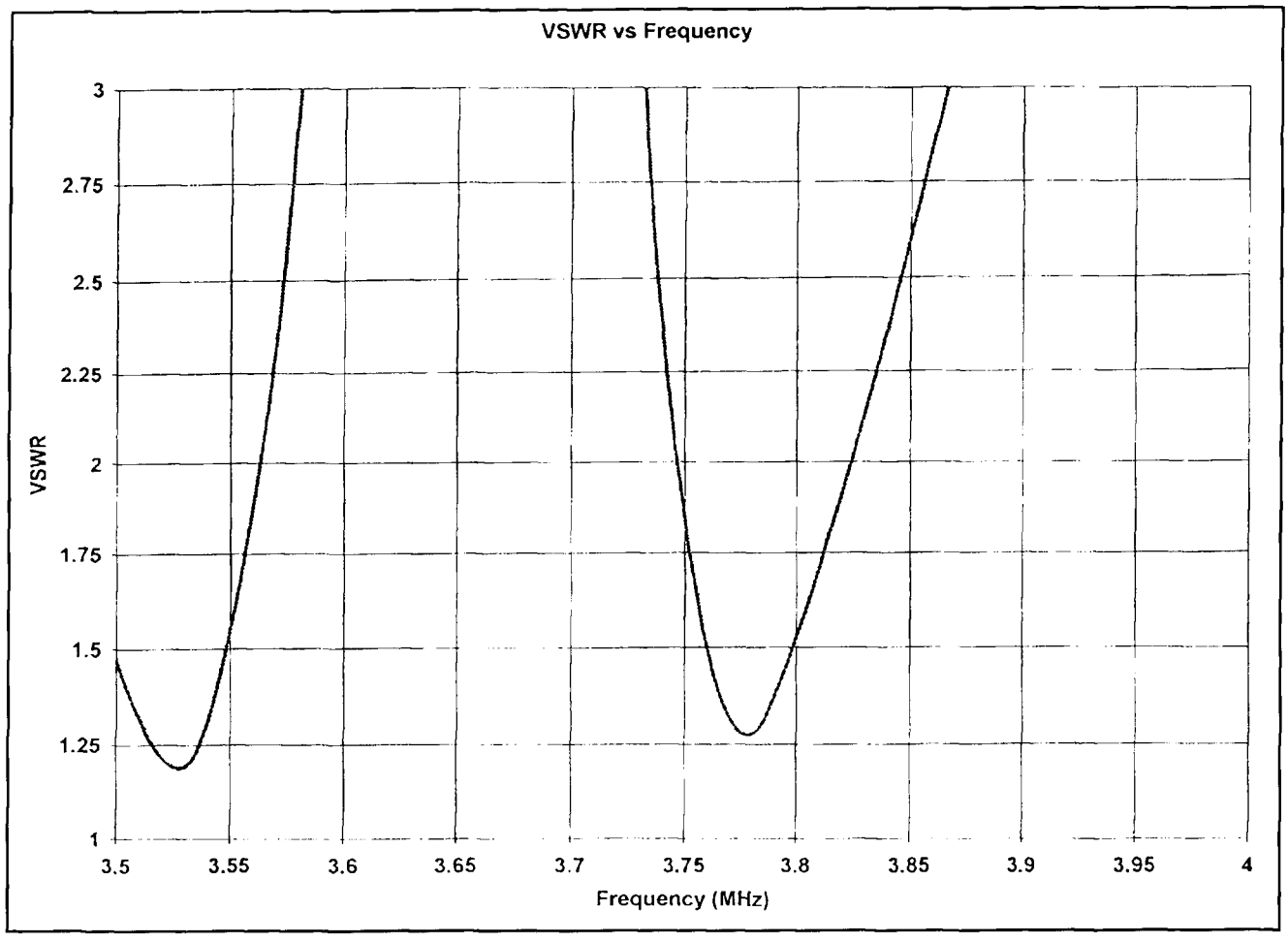

Figure 3.

circuit theory also tells us that between every series resonance there will be a parallel resonance (pole). This results in a very "lumpy" feedpoint impedance in addition to any non-uniformity in radial currents. An example of this effect is given in **Figure 2** for an 80-meter vertical with two pairs of radials with different lengths. **Figure 3** shows the feedpoint SWR with a simple broadband impedance transformer to 50 ohms. There are series resonances at 3.525 and 3.780 MHz which result in low SWR and allow the antenna to be operated in both of the DX widows without adjustment. However, between these two frequencies the SWR is very high and the parallel resonance can be clearly seen in **Figure 2**. The impedance is very lumpy indeed!

Given Dick Weber's insight on quarter-wavelength radials, it would appear that this idea needs to be redone using shorter radials and either:

1. a taller vertical section
2. inductive loading
3. capacitive top loading
4. capacitive loading of the radials
5. some combination of the above

In my article on the Lazy-H antenna, I pointed out how quickly the radials shorten when either a longer vertical section or top loading are used.

The vertical groundplane antenna has been around for a very long time. It's amazing how much we still have to learn about it. Pages 6-5 through 6-9 in the new edition (18th) of the *ARRL Antenna Book* has some interesting information on the input impedance. It's not really 36 ohms, as we frequently assume, but depends on the height above ground and ground characteristics, among other things.

Rudy Severns, N6LF
Cottage Grove, Oregon

Junk Science and Antennas

Dear Editor:

Thank you for your editorial on "Junk Science and Amateur Radio" in the Winter

1997 issue of *Communications Quarterly*. It brought to mind the analysis of why J-match or Zepp-fed antennas do not work (as efficient radiators), done by L.A. Moxon, G6XN, in his book *HF Antennas for All Locations*. His analysis and that of G6CJ in the *RSGB Bulletin* for December 1955 suggest that the radiation from such antennas comes from the unbalanced open wire line quarterwave matching stub. I built one using coax for the matching stub and found the point for a good match; it had a good SWR but did not seem to radiate. The author suggests using a "balancing stub" across the matching stub to correct the unbalance and make the system more efficient.

It is interesting how many articles there are about these antennas in the current ham literature.

Moxon also takes a closer look at other long held ideas concerning antennas.

Len Petraitis, WØNU
Pittsboro, North Carolina

W5OLY's Letter to K5IU

Dear Dick:

Read your article in the Spring 1997 issue of *Communications Quarterly* yesterday. I compliment you on the fine job of highlighting your measured data (which is proof of the pudding) and backing it up with your computed charts. The material to which I objected was omitted. The paper should be much referenced and become a "classic." And thanks for the credit.

Last evening at the Rockwell ham club meeting, one of the retirees asked for a copy of the talk you gave to the club. I recommended he get a copy of this article. I gave a very brief summary of it to the Club for those who didn't hear your talk.

Thanks again for your contribution to the "art and science" of antennas.

Warren Bruene, W5OLY
Dallas, Texas

Reader Requests Assistance

Dear Editor:

Some years ago, Japanese researchers developed an equivalent circuit for free space dipoles and monopoles over perfect ground. By adding elements to their circuit, it became part of a Chebychev bandpass filter and I was thereby able to write a computer program (in GWBASIC) to interactively design antenna matching

networks. Examples of the predicted performance for three different monopoles are:

Frequency Band	Maximum VSWR
3.5 to 4 MHz	1.2:1
68 to 88 MHz	1.25:1
142 to 176 MHz	1.2:1

The only problem is that I no longer have the equipment to verify the accuracy of this predicted performance, thanks to hurricane Hugo. The equivalent circuit is supposed to be accurate to within 10%; circuit analysis programs confirm the program's predictions, but it would be very satisfying to see experimental data showing such bandwidths. I wonder if any of your readers would have the time to check the program's predictions. The program can be found on Version 26 of Hamcalc, or I would be glad to append it together with a .DOC file to an e-mail or, given a disk, I will send it regular mail. My e-mail address is <rdehoney@worldnet.att.com>.

R. Dehoney
Isles of Palms, South Carolina

A Bridge Not Too Far

Dear Editor:

M. Jamet, F9ILX, mentions that it is easier if a bridge uses a modulated signal for the balancing operation. It is also extremely convenient to use an unmodulated signal if the source and the detector are very stable. Modern transceivers have a high degree of stability and can be used as a signal source. Assuming the typical 100 watts output, the voltage into a 50-ohm load would be 70 volts RMS. Under CW space conditions, the output would be around 50 to 60 dB less than this—say 230 millivolts or less. I terminate my rig in a carbon rod (Morganite) resistor, enclosed in a shielding metal tube, and tap the output about a quarter of the way down this. I follow this with a switched attenuator and I have a very stable signal generator. Of course one cannot use the RX side of the unit as the detector, so one requires a second transceiver or receiver to pick up the bridge output.

I have found this arrangement extremely helpful, and it allows one to concentrate using the bridge instead of being distracted by having to retune source and/or detector. It is also useful if one wishes to accurately check the frequency response of aerials or other equipments.

The resistor and its output connection use coaxial connectors so as to minimize direct breakthrough from the transceiver, but I have never found this to be a problem with my IC720A as the source and my IC71 receiver as the detector.

S.F. Brown, G4LU
Shropshire, U.K.

Give Credit to K2BLA

Dear Editor:

In the Winter 1997 *Communications Quarterly* I was pleased to see Mr. Brown write in "Build a 5- to 850-MHz Spectrum Analyzer" about the low-cost use of CATV tuners in spectrum analyzer designs. It is good to see ongoing work in making sophisticated instrumentation more affordable.

I am concerned, though, with Mr. Brown's lack of credit to pioneers in homebrew instrumentation, and, in fact, to the original designer of the CATV-tuner-type spectrum analyzer.

The original article in which a CATV tuner was used for the front-end of a spectrum analyzer was "An Inexpensive Spectrum Analyzer for the Radio Amateur" written by Al Helfrick, K2BLA, in the November 1985 *QST*. In fact, A&A Engineering, of Anaheim, California, has been producing Mr. Helfrick's CATV tuner-based analyzer for a number of years, and it is a well-engineered design and somewhat more refined than Mr. Brown's. I have been using one of the A&A analyzers for a number of years with satisfaction.

Thank you for your notice.

Eric Guinn, AC4LS
Sevierville, Tennessee

Crawford MacKeand, *WA3ZKZ/VP8CMY*
115 South Spring Valley Road
Greenville, Delaware 19807
e-mail: <jcbmck@udel.edu>

PATH LOSSES AT HF

An analytical approach

Shortwave propagation never seems to be the same for two hours together, let alone two days together. But HF signals follow physical laws, and there are good and sufficient reasons for the losses that radio signals incur between two stations on the Earth's surface. Many methods, from experience to manual calculation to sophisticated computer programs, are used to find out how good or bad a path is going to be; but it's worthwhile to go a step further and find out which of the many afflictions that HF signals suffer will prevent a given contact from happening, or conversely help it to S9 status.

If we know which ones control at a given time, then we can intelligently plan our next steps. How do we complete that QSO? Do we need to try another time, or another day, or another frequency, or use a different route. Should we increase power, change antennas, or, as a last resort, move to another location!

Introduction

Even at the height of the sunspot cycle, high band operation is improved by knowledge of the ionosphere and its effects, while at the bottom of the cycle, our relationship with the reflecting layers is an ongoing challenge. The ionosphere can be quite uncooperative, and yet signals are often there if only we know when and where to look. There's no magic in the process of moving a signal from A to B (although it often seems there is); therefore there must be a few good reasons for the changes we notice over time.

Most of the Earth's physical parameters are rather constant. Its temperature (in absolute degrees, that is) isn't wildly different, even from the Arctic to the Equator. The barometric pressure is never all that far from 30 inches of mercury. The global sea level only changes a little, and slowly at that. Gravity is almost a constant everywhere. The ionosphere, however, is another matter. The solar flux changes considerably, but the maximum usable frequency is—to say the least—volatile. It can move from 2 to 50 MHz, and, what's more, it can move a large part of that in a few minutes. No wonder it has the reputation of being the most fickle of all Earth's physical values. And this remarkable variable describes our transmission medium.

If the layers between us and the remote QTH aren't supporting reflection on our chosen band, increased power isn't going to help a bit. If absorption is the problem, power can help, but maybe all we need to do is select another time of day. Possibly, there will be greater chances of good conditions to the south than to the north. To make sense of all the often-conflicting evidence, we need to know the factors at work in a potential contact—and which of them can be modified by changing frequencies, operating habits, or even equipment. We start with antennas, equipment, and locations for both stations. Time of day and year are no problem. Clearly we need ionospheric data, the solar flux, and the A or K indexes that tell us about any ionospheric storms. Data can be found on WWV at 18 minutes past every hour and also on WWVH at 45 minutes past the hour. We need noise levels too, but we'll defer that until later. Let's look at the places where signal strength is lost between the remote and the local station, and hopefully find some pointers to get a better handle on this highly variable environment.

Satisfactory reception of an ionospherically propagated radio signal depends on the signal-to-noise ratio at the receiver, and that depends on three factors. The first and most important is the ability of the ionosphere to reflect signals at the necessary places on the desired path, and at the frequencies, times, and dates to be used. The second and third factors are the resulting signal strength and the ambient noise level at the receiving station, which combine to determine signal-to-noise ratio.

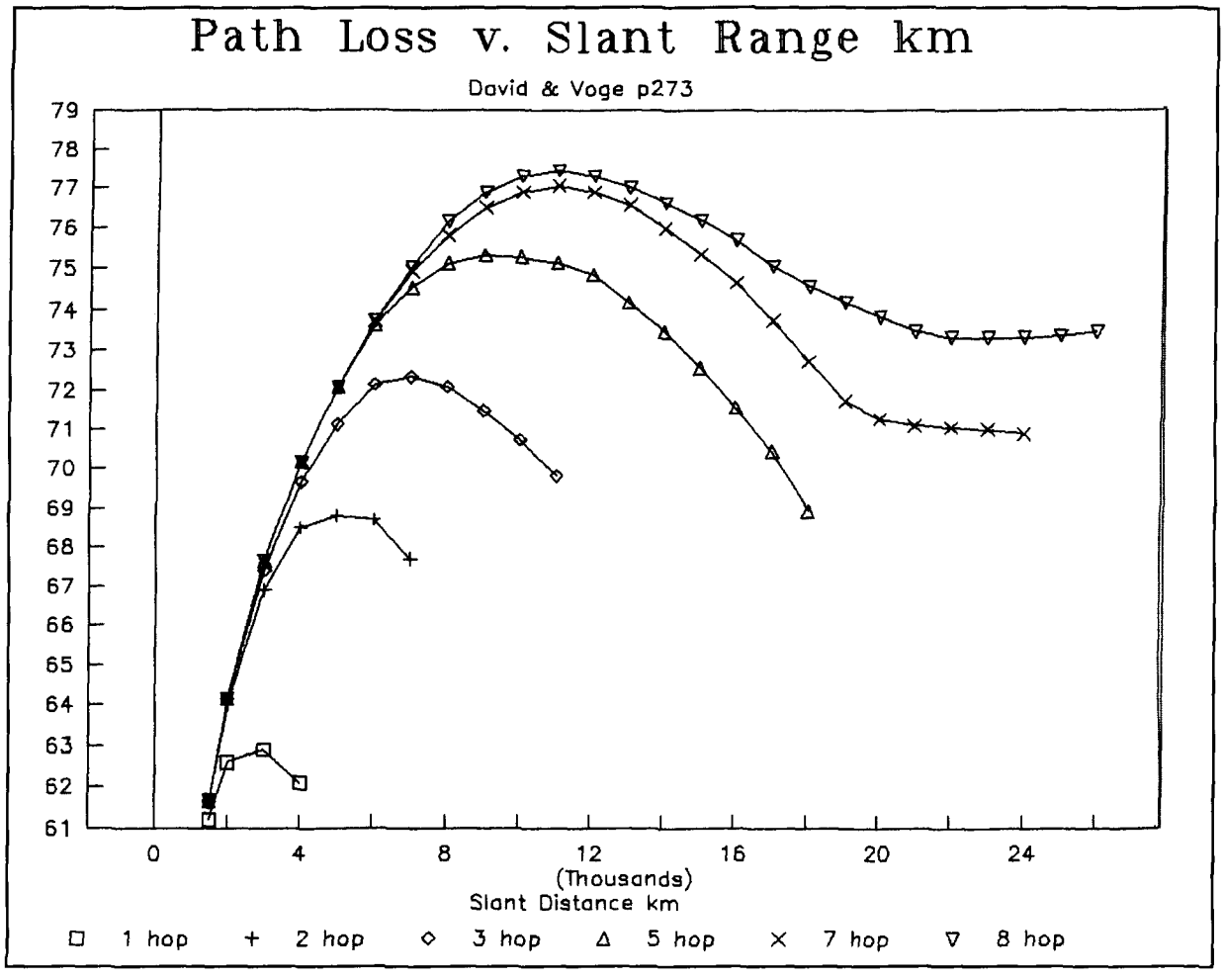

Figure 1. Path loss versus slant range (km) from David and Voge.[6]

Many methods exist to predict the first of these; the central problem is the calculation of maximum usable frequency (MUF) from path geometry, solar flux, and ionospheric storm levels, and their distribution in time and space. But signal strength depends on transmitter power, effective antenna gains, spatial spreading, ionospheric absorption and scattering, focusing and defocusing on reflection, and polarization mismatch. The ambient noise level at the receiver can be determined to a fair approximation from published world noise maps,[1] with some allowance for local manmade noise at the receiver. To predict signal-to-noise ratio, we have to work in all these factors. We will also need the system bandwidth, which determines how much of the noise we'll actually hear.

Estimates

Propagation cannot be calculated exactly; it can only be estimated, and estimates, by their very nature, suffer from a combination of many different uncertainties. One certainty in estimating is that it's far better to use educated experience than no estimate at all, and an estimate honed against actual field results is more credible than any other. Working for us is the probability that errors in the individual components of an estimate are unlikely to err systematically in the same direction, or by the same amount. Finally, there's no merit in improving the accuracy of the individual parts of the estimate much beyond that of the other parts, if they are equally important.

In this approach, we calculate all known components of the system loss, and by approximating, adding, and subtracting, simplifying and curve-fitting, it's possible to obtain a fairly complete picture. Just looking at the picture is interesting, but we also want to know more about the details. If we don't find a good path to the desired remote site, is there anything we can do about it? Is the problem regular D-layer absorption, or should we wait a couple of days until the K Index is lower? Or should we just wait a few hours? Any picture of the ionosphere and its propagation must start with the fundamental questions: Is any propagation like-

ly to be possible on the chosen path? Are we below or above the maximum usable frequency, the MUF?

Will there be any signal at all?

Many excellent computer programs and some manual and semi-manual methods will help determine whether we are above or below the MUF, and some will tell us the probability of there being a useful signal on the route of interest. All of these methods require the knowledge of the solar radiation at all the places on the route where the signals will encounter the ionospheric layers, so locations and times of day are both obviously controlling factors. They account for the great differences between temperate zone routes, such as the U.S. to Europe, and transequatorial routes, such as Europe to South Africa, or the U.S. to southern South America.

The classic MUF is so defined that there is a 50 percent chance of propagation at the MUF itself, a rapidly diminishing probability at higher frequencies, and a chance near 100 percent for signal propagation at frequencies lower than about 80 percent of the MUF. There's also data to support an "over-MUF" signal loss, which may relate to the decreasing ability of the reflecting layers to act as good mirrors when the frequency is close to the limit.[2] But there is a host of other ways to lose that reflected energy before it reaches us. Let's consider what the signal has to endure en route, and we'll see how we can use that information to improve our operations.

Where the signal went

We must begin with some assumptions about the remote station and its antenna, unless we have a scheduled contact with a known station. Whatever the data, we aren't likely to be able to change it; but the type and height of the remote antenna will determine the strength of the signals emitted in our direction, just as will the power of the remote transmitter. Our own antenna configuration has to be taken into account, too, but at least we have some control over that from time to time.

Spreading and focusing

The radio-frequency energy from the remote station isn't coming only to our station, and clearly it spreads wider and thinner the farther it proceeds. If we were both operating from spacecraft, with no Earth and ionosphere to bother about, the energy would spread out pretty evenly in all directions, but Earth-bound amateurs must contend with reflection from both.

Calculations of the spreading loss start with an isotropic antenna (one which radiates uni-

Table 1. Solar flux versus 14-MHz signal strength

Level	**A**	**B**	**C**	**D**	**E**
Nominal dB	**50**	**25**	**0**	**-25**	**-50**
W4-JA Solar Flux		137.5	116	92	94
Std. Dev.		11	20	9	10
Rel. dB	64.5	39.5	14.5	-10.5	-35.5
W4-VK Solar Flux	136	113	107	87	
Std. Dev.	32	14	9	1.5	
Rel. dB	47	22	-3	-28	-53
W4-UA9 Solar Flux		126	114	110	
Mar- Std. Dev.		22	13		
May Rel. dB	41	16	-9	-34	-59
W4-UA9 Solar Flux	120	126	93	99	
Aug- Std. Dev.	34		20	13	15
Oct Rel. dB	42.3	17.3	-7.7	-32.7	-57.7

formly in all directions) at each end, and then modify the results for the real antennas in use and their actual locations. The loss calculation requires knowledge of the slant range, which includes the up and down distances, rather than the range measured on the ground. It also must take into account the shape of the Earth and the layers, which are both assumed to be spherical.[3,4] The reflecting layers aren't so far from flat that they greatly distort the paths, yet they are different enough to cause some interesting losses, and gains too on occasion, for the remotest of terrestrial contacts.

There seem to have been two distinct views on calculation of distance or spreading loss. Davies, the "grand old man" of the National Bureau of Standards, says[5] that "in general it is too complicated to take into account the detailed effects of focusing etc.," and he, therefore, uses slant range as the effective distance. On the other hand, Rawer[3] in the French ionospheric service, using a more detailed geometry shows losses that relate to the number of hops as well as to the distance. Although his curves look rather complex, if we reconfigure them to use slant range instead of surface range, they are greatly simplified (**Figure 1**, taken from **Reference 6**), and the loss can be calculated from a fairly friendly set of algorithms. Comparing the results with my own experience, and that of others,[4] the Rawer curves seem to provide a closer match, with Davies' method being somewhat on the pessimistic side.

If the two stations are at antipodean locations, all the possible great circle routes can join in providing a signal path. And, if the ionosphere is very stable, Rawer's approach shows the possibility of signal enhancements of up to 20 dB. While so much gain is unlikely, real gains do appear to be quite common in the HF broadcast experience,[7] and, for amateur purposes, this source of signal enhancement is something we don't want to ignore.

Reflection

There are also losses at the actual points of reflection. If the signal has to bounce off the ocean, well and good, as the loss there is quite small. If it has to bounce off a desert, the loss may be quite large, maybe 4 or 5 dB, or more.[5] Both of these losses have been pretty well determined, although it would be somewhat laborious to look at every path and determine the characteristics of the Earth at all possible points of reflection. So a calculation must use estimates, both of the likely reflectivity and of the distribution of that reflectivity between better and poorer locations. The angle is important, too, but the value will be inherent in any path calculations. As far as reflections up above are concerned, the *F* layer seems to be a pretty good reflector, while the *E* layer is not so good.[8]

D-layer absorption

In addition to the losses on reflection, some parts of the ionosphere are no help at all! The worst actor for HF is the lowest, or *D* layer. It's so thin that it can only reflect very low frequencies, well below the MF bands; however, it's thick enough during daylight hours that it can absorb RF energy well into the shortwave region. The absorption of RF wave energy is greatest at the gyro-frequency, where the *D*-layer electrons resonate most energetically under the influence of the impinging RF and under the constraint of the Earth's magnetic field. This is around 1.4 MHz, and losses from the resonant motion decrease both above and below that frequency. Fortunately, these losses tend to vanish at the high end of the HF spectrum, allowing us the delight of low-power worldwide QSOs on 10 meters when the MUF is high enough.

The *D* layer is almost entirely a daytime phenomenon and is dependent on the strength of the ionizing radiations from the sun, mainly ultraviolet, which cause the *D* layer to exist in the first place—hence the nighttime AM band interference we're all familiar with. The loss, therefore, depends on place and season and time of day along the route, as these can tell us the strength of solar radiation. It also depends on the selected frequency and, to a smaller extent, on the Earth's magnetic field as it varies along the path of interest, setting gyro-frequencies at those points on the route where the signal must pass through the *D* layer. Calculation methods for *D*-layer absorption seem to be well established and in relatively good agreement.[5,9]

Other absorption

Unfortunately, as those who live in the more northerly parts of the world (and also those few who inhabit the Far South) well know, there are other sources of absorption, too. The star actors are ionospheric storms, in which the Sun dumps cascades of energetic particles onto the Earth's magnetopause. Most of these, very fortunately for us, flow on past into the night, forming the magnetosheath. But a few find their way through the protective regions up above, and spiral down to Earth in the sub-Polar regions, where our magnetic lines of force come down vertically.

Concentrated in the auroral ring—which usually lies at some 60 to 70 degrees north or south, roughly concentric with the magnetic poles—they cause not only the Northern Lights

(Aurora Borealis) and its more rarely seen southern counterpart, but also strong absorption of HF radio signals. The ring or oval moves closer to the equator in times of ionospheric storm, and, because of the location of the magnetic pole, the very popular paths from the U.S. to Northern Europe are among those most noticeably affected.

To calculate this factor, we must find out how much of the path lies within the auroral ring, and how many passes the path must make through the relevant layers (the auroral regions, which are close to the *E* layer) as the signal bounces up and down on its way to its final destination. The ring position must be estimated, as it depends on the storm level, which relates to the A or K index broadcast by WWV. Auroral absorption also depends on local time where the path crosses the ring[2] and on particle density, which also relates to the A or K index.

Other losses

Polarization mismatch is easy to handle for line-of-sight VHF circuits; but polarization shifts on reflection make this an unpredictable will-o'-the-wisp at HF and we have to ignore it. When we considered the calculation of MUF, we noted that the literature talks about an over-MUF loss. It seems to be general experience that signals on any given band are better in the heights of the sunspot cycle than in the doldrums of low solar flux.

To back this up, a correlation was attempted for data given by Jacobs and Cohen[4] on four paths at various solar fluxes. Basic ionospheric propagation theory says that the higher the solar flux, the higher the *D*-layer absorption. Any gains in propagation would then be solely due to higher MUFs permitting operation at higher frequencies, where absorption falls off as the square of the frequency. But, this isn't what the Jacobs and Cohen results show. A quick visual examination (**Table 1**) of their data shows that better signals at constant frequency are achieved at higher fluxes, and this seems to be true of all four 14-MHz paths. (See **Appendix** for calculations.)

A check of several propagation programs showed that none of them predicted this effect for the cited conditions, but incorporating over-MUF loss, quite a reasonable agreement appears. Maybe the *F*2 layer at the higher solar fluxes presents a cleaner more mirror-like reflector with less scattering, or a more efficient reflector from some other point of view.

Basic calculations

Having adopted a suitable MUF calculation, it also seems worthwhile to try allowing for the A index in another effect of ionospheric storms, the depression of the *F*2 critical frequencies, which control the MUF, in temperate and high latitudes. Considering the results given by Davies[5] for Matsushita's work, and a comparison with geomagnetic storm descriptions given by Chapman,[10] a simple algorithm allowing for this effect was derived. It modifies critical frequency at each successive hop, depending on magnetic latitudes and A index, to give the depression of the MUF. The database seems quite thin, but despite this, the match has seemed to be as good as could have been hoped wherever a comparison has been possible. Any further information that might lead to an improved correlation would be of interest.

Noise levels

Noise level calculations are readily made using CCIR Report 322 and setting up an algorithm for the CCIR noise maps. There is a regularity to the sets of correction curves presented in CCIR 322, in time, seasonn and frequency, and a workable algorithm was obtained, with errors of less than about one standard deviation over most of the range. The curves illustrate the analysis used, with frequency-based correction factors centered at 4 and 16 MHz, and a small fall anomaly in addition to the main seasonal changes observed. Seasonal changes are assumed to be gradual, and a straight line segment variation based on the Julian date makes these corrections.

All the factors are applied to data for a frequency of 1 MHz for each receiving site, extracted directly from the CCIR 322 maps, which are published for four seasons, at six times of the day. Commercial operators use a worst case estimate, correcting from a standard deviation curve to the noise value obtained. But for amateur use, the uncorrected value seems more appropriate. It represents the most likely value rather than worst case, and amateurs normally look for the most probable condition rather than calculating a safe margin for service reliability. Of course, a contest station making pre-contest evaluations might wish to use the commercial approach!

Galactic noise can also be predicted from CCIR 322 curves, but an additional calculation is needed for transmission through the ionosphere, which depends on critical frequency and other MUF-related values. Noise coming at us from the galaxy does have to make it through the ionosphere from the other side, so we might as well take advantage of this useful screening when we can! Values for manmade site noise were also obtained from the curves in CCIR 322, although it would be interesting to estimate data for local weather and distance from

high voltage lines and highways.[11] This could not pretend to great accuracy, but, again, anything which can be particularized has a good chance of being better than general data.

Signal strength

Signal strength can be computed from algorithms discussed by Davies in his book on ionospheric propagation[5] or from an ESSA report which has been very widely used.[9] Several sources of information exist on auroral activity and on its relation to HF path loss.[2,5,9,12]

The next necessity is an allowance for antenna gain. The usual values cited are for the optimum ray angle for the antenna in question, which has little relation to gain at the actual ray angle. To calculate the signal strength, we need

Computer program

It's easy to conclude that a computer program is needed to make sense of all this in any reasonable time frame. Such a program was started some years ago based on MINIMUF 3.5.[14] But, at the urging of Bob Brown, NM7M, the basis was changed to a more recent algorithm for MUF calculations developed by R. Fricker of the BBC's External Services,[15] which is widely regarded as having better accuracy.[16]

The main objective was not to have yet another propagation program, but to understand the contribution of the various different loss mechanisms to HF signal strength. Most modern programs offer excellent graphics with maps and even pictorial path displays, but it seems equally important to know the details of signal loss.

A graphic bar-chart display (**Photo A**) of loss types and noise sources shows, together with a detailed tabular analysis, the probable makeup of the selected signal on its path. Thus the user can see, especially for a failing path, the problems and the possibilities. The data are presented for the most likely ray angle and the next most likely angle, too. Distance and *D*-layer absorption losses are shown, in addition to the auroral zone or polar losses and the over-MUF contribution. The local noise level factors are given individually, along with much more other important data, such as the *E*-layer cutoff frequency for *F*-layer propagation, and the probable error limits for the MUF calculation. Paths are well characterized, with beam headings, geographic and magnetic coordinates of the control points used in the calculations, and the takeoff angles likely for the calculated layer heights.

The program, SNAPmax, also includes a more conventional numerical display of probable signal-to-noise ratio for a given path over a 24-hour period. The *CCIF/CCIT/CCIR Red Book*[17] and other sources quote bandwidths and the signal-to-noise ratios required for different modes, and it's clearly of interest to use this "required signal-to-noise" data to analyze a number of routes for a given date, time, frequency, and operating mode. Therefore a "band open" display shows probable openings at one preselected frequency for a group of preselected remote sites for one selectable mode.

SNAPmax accepts station entry by callsign prefix, by latitude and longitude, or by U.S. state. Noise map data are built in for the U.S. and Canadian call areas, and for a few foreign countries (G, CE, VP8), with a default basis for the rest of the world. Data for any other area may be added and saved by the user with the aid of CCIR noise maps. The program can be purchased (for $30) from the author at 115 S. Spring Valley Road, Greenville, Delaware 19807, U.S.A.

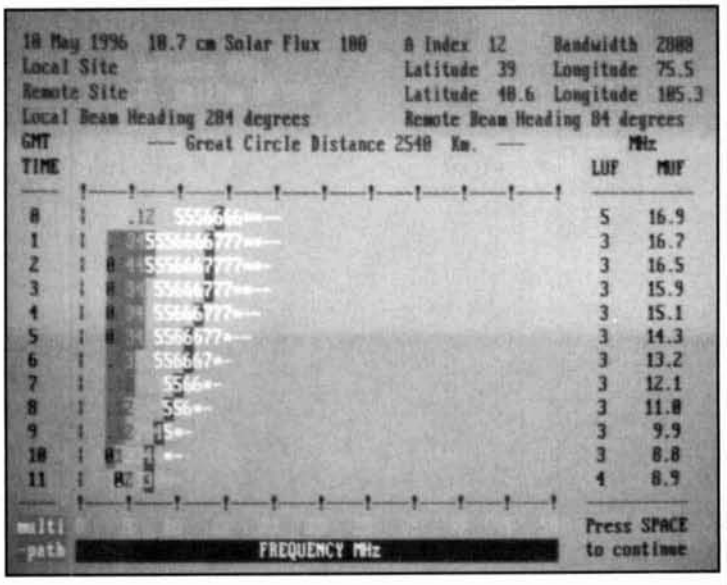

Photo A. Graphic bar-chart display of loss types and noise sources.

to obtain gain versus angle curves, and it is useful to calculated or adopted values for three common antennas over real ground: a three-element beam, a wire dipole, and a ground-based quarterwave vertical. The beam and dipole curves were also analyzed for the effect of antenna height.

These antennas develop nulls at some elevations, which would considerably complicate the picture. However, because real height over electrical ground is unknown, and as the parasitic radiations from other local conductors tend to fill in such nulls, it seemed appropriate to fit an envelope to the curves and ignore the nulls, which are, in fact, often quite narrow. Most of the data is from curves produced using ELNEC,[13] and assumes the antenna points towards the other station!

Bandwidth

In the 1920s, well-known English radio engineer P.P. Eckersley said "the wider you open the window, the more dirt blows in." Signals are constant with increasing bandwidth, as long as we have enough bandwidth to handle them properly, but noise power will increase linearly. We need, therefore, to use the actual receive bandwidth and adjust signal-to-noise computations to suit.

Conclusions

Presenting the results diagrammatically, we can show signal-to-noise relationships for a given time, date, circuit, frequency, and solar flux. It is then easy to change circuit constants. A short time playing with the variables shows that most of us are living close to the ragged edge of practicality for consistent long-distance HF contacts, unless we choose a low bandwidth mode, such as CW or one of the digital systems. The difference made by a higher or better antenna, or even, to a smaller extent, by increased power is quite dramatic.

Data appropriate for shortwave broadcasting show the greater power needed for regular DSB/AM with the 20-dB signal-noise ratio that comfortable BC listing requires. Looking at all the benefits of a low noise location, you might decide to move to the Outer Boondock islands with all possible speed and vigor. Even in the U.S., Hawaii, for example, has a real edge over the rest of us. ■

REFERENCES

1. "World Distribution and Characteristics of Atmospheric Radio Noise," *Report 322*, International Radio Consultative Committee (CCIR), Geneva. (International Telecommunication Union) (NTIS Document PB 255 060)
2. Kenneth Davies, *Ionspheric Radio*, Peter Peregrinus Ltd., London, 1987, page 459.
3. K. Rawer, "Calculation of Sky-Wave Field Strength, Wireless Engineer, November 1952, pages 287–301.
4. G. Jacobs, W3ASK, T.J. Cohen, N4XX, and R.B. Rose, K6GKU, *The NEW Shortwave Propagation Handbook*, CQ Communications, Inc., 1995.
5. Kenneth Davies, *Ionspheric Radio Propagation*, Dover, 1996, originally published as *NBS Monograph 80*, 1965.
6. P. David and J. Voge, *Propagation of Waves*, Pergamon Press, Oxford, England, 1969, (translation of French *Propagation des Ondes*, Eyrolles, Paris, 1966).
7. K.J. Hortenbach and F. Rogler, "On the propagation of short waves over very long distances," *Telecommunications Journal, Volume 46*, 1979, pages 320-327.
8. L.F. Mcnamara, *The Ionosphere: Communications, Surveillance & Direction Finding*, Orbit/Krieger, Malabar, Florida, 1991.
9. A.F. Barghausen, J.W. Finney, L.L. Procter, and L.D. Schultx, "Predicting Long-Term Operational Parameters of High-Frequency Sky-Wave Telecommunication Systems, U.S. Department of Commerce, *ESSA Technical Report ERL 110-ITS 78*.
10. S. Chapman, *The Earth's Magnetism*, Methuen, London, 1936.
11. E.N. Skomal, *Man-Made Radio Noise*, Van Nostrand Reinhold, New York, 1978.
12. *Radio Wave Propagation and the Ionosphere*, Al'pert Ya. L., Consultants Bureau, New York, 1963.
13. R.W. Lewallen, W7EL, ELNEC, Beaverton, Oregon, 1991.
14. R.B. Rose, "MINIMUF, A Simplified MUF Prediction Program for Microcomputers," *QST*, Vol. LXVI, No. 12, December 1982, pages 36–38.
15. R. Fricker, "A Microcomputer Program for the Critical Frequency and Height of the *F* Layer of the Ionosphere," *4th International Conference on Antennas and Propagation* (ICAP 85), 16–18 April 1985, pages 546-550.
17. *Compendium of the Technical Recommendations*, issued by CCIF, CCIT, CCIR of the International Telecommunications Union (*The CCIF Red Book*), Automatic Telephone and Electric Company, Ltd., Liverpool, 1956.
16. Private correspondence, Bob Brown, NM7M, March 1995.

Appendix

Rearranging Jacobs and Cohen's graphs, while ignoring the minor effect of the A index for this purpose, arbitrary dB values were assigned to their A–E levels relative to level C as shown in **Table 2**:

A mean dB level for each circuit was obtained and the dB values of A-E were then recalculated as differences from the mean signal for that route in order to remove circuit-to-circuit bias and consider only the differences on each circuit due to the solar flux changes. Each point in the charts can now be assigned a dB level and a solar flux. The results shown in **Table 1** for each level were then plotted in **Figure 2**, and it's clear that there is a positive

Table 2. Arbitrary dB values for A-E signal levels relative to level C.

Level	Description	dB Value rel. to C
A	S9+30	50
B	S9	25
C	S5	0
D	S1	-25
E	No signals	-50

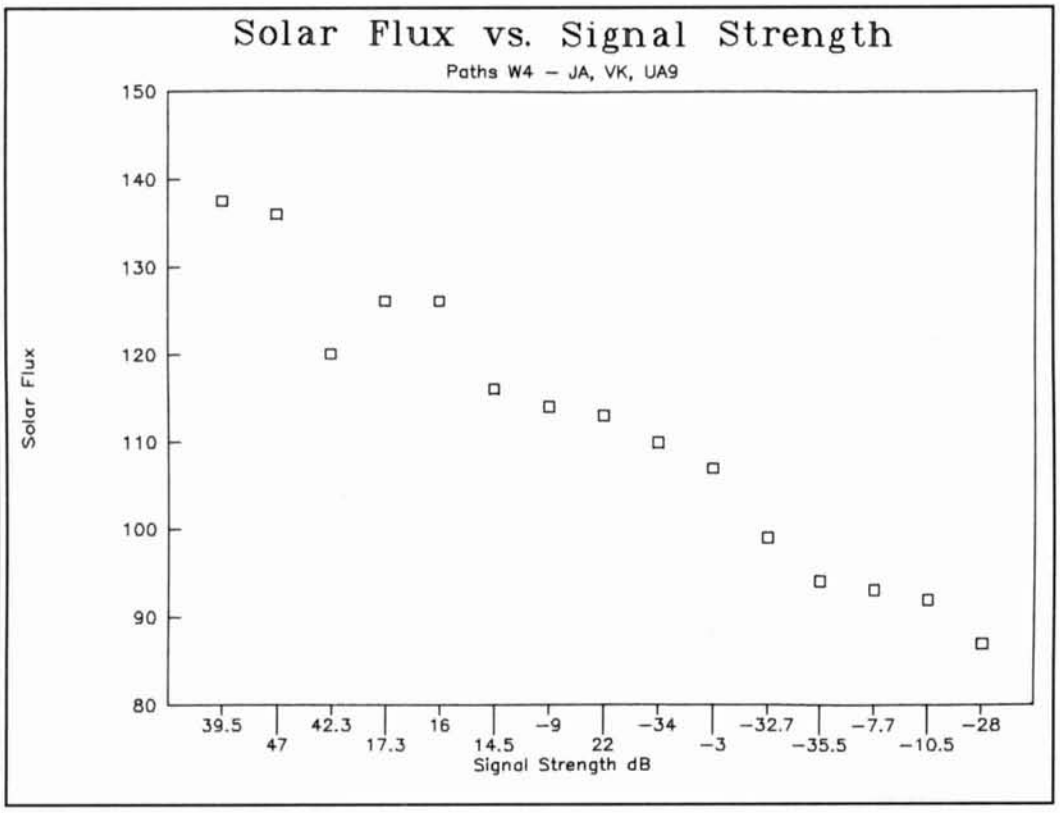

Figure 2. Solar flux versus signal strength.

slope to the data, showing stronger signals at higher fluxes.

The data were also separately run through a correlation program, as a straight line curve fit, showing approximately 2 dB increase in signal strength for each solar flux unit. The correlation coefficient was R = 0.62; a real dependency, though obviously there are large random variations due to local conditions and the general variability of the medium.

PRODUCT INFORMATION

Phillips ECG Introduces New Improved U-105 Antenna Rotator

Phillips ECG introduces the U-105 Antenna Rotator, which includes automatic controller, rotator drive unit, mounting hardware, and installation and operating instructions. The optional TB-105 support bearing is available for extra-rigid installation.

The U-105 Antenna Rotator is a durable, precision-built rotator designed to turn and position even the largest flat wedge-type TV-FM antenna.

Its features include precision cut steel gears hardened for long service life; rugged, one-piece cast aluminum housing designed for greatest strength in high stress areas; large bearing surfaces and strong reinforced mast for lateral load support (vertical load 45 Kg (99 lbs) maximum); ball bearing provided for thrust (160 lbs-inches of motor torque); high torque-

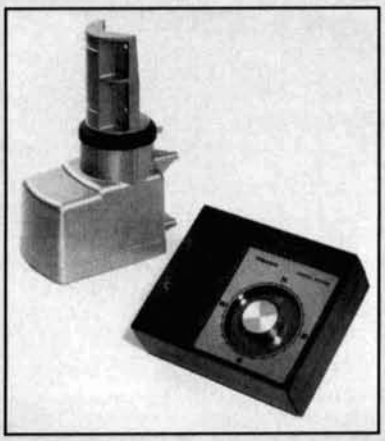

easily handles largest TV/FM antenna arrays; built to take high winds and harshest weather extremes-water tight seal, fully lubricated drive train; completely automatic control indicator accurately shows orientation of antenna; control designed for smoother, quieter operation; and UL and CSA listed.

To locate the nearest distributor of ECG Electronics manufacturing and maintenance products, call toll-free 1-(800) 526-9354.

Harry J. Swanson
Motorola, Inc., Analog IC Division
2100 East Elliot Road, M/S EL340
Tempe, Arizona 85284

DUAL-CONVERSION FM NARROWBAND RECEIVER

Uses low-cost monolithic IC chip set

Here's an analog narrowband FM receiver designed for cellular and 902- to 928-MHz ISM Band Part 15 cordless phone applications.[1] The receiver is a dual-conversion superheterodyne incorporating a low-cost silicon monolithic IC chip set. This is made up of an integrated LNA, mixer and VCO RF front-end IC (MC13142) and a single conversion, split IF and coil-less detector back-end IC (MC13150). Surface mount components, small-size pc board layout, and few external components allow fabrication of a receiver suitable for cellular and portable applications. Performance is verified in a demonstration receiver. I'll discuss how design techniques to optimize the receiver sensitivity and noise performance were analyzed and developed, as well as the trade-offs in signal handling and power management.

Figure 1 shows a simplified block diagram of an analog/digital FM narrowband RF section commonly used on low-cost, high-volume analog cellular services today. The receiver topolo-

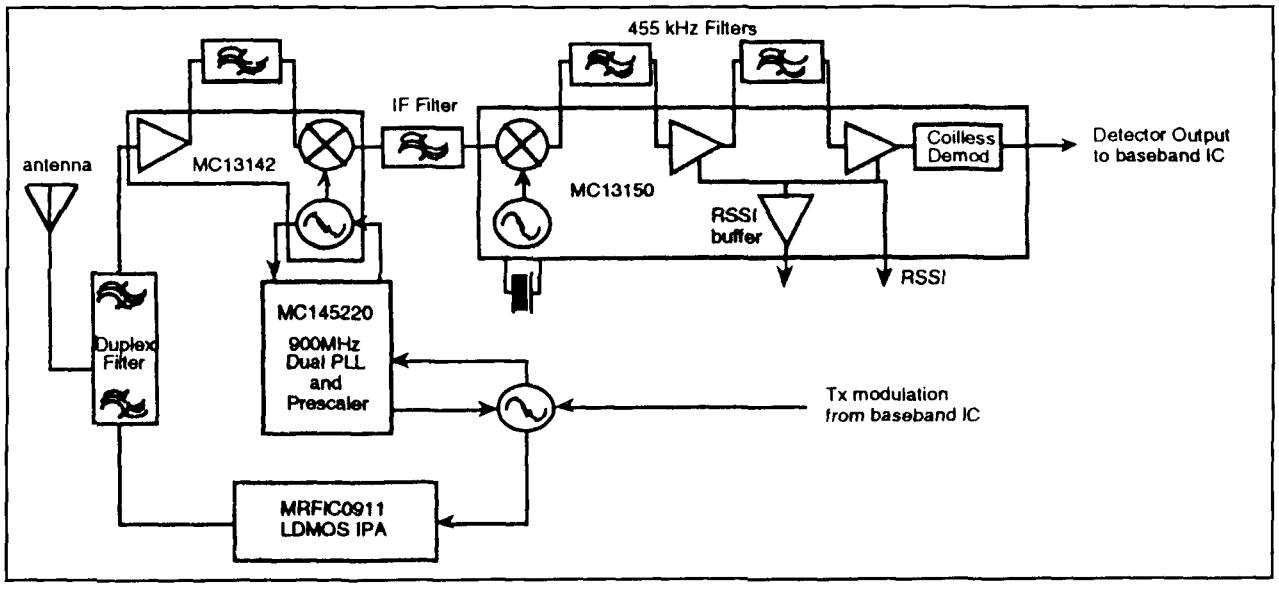

Figure 1. Analog/digital FM narrowband RF section.

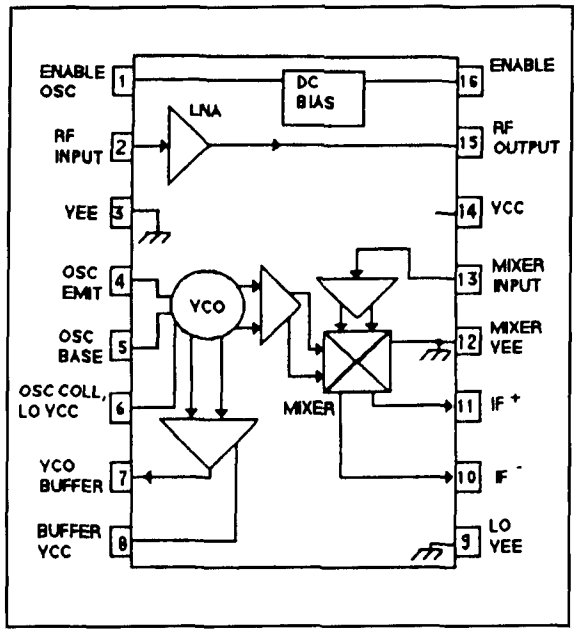

Figure 2. MC13142D pin connections.

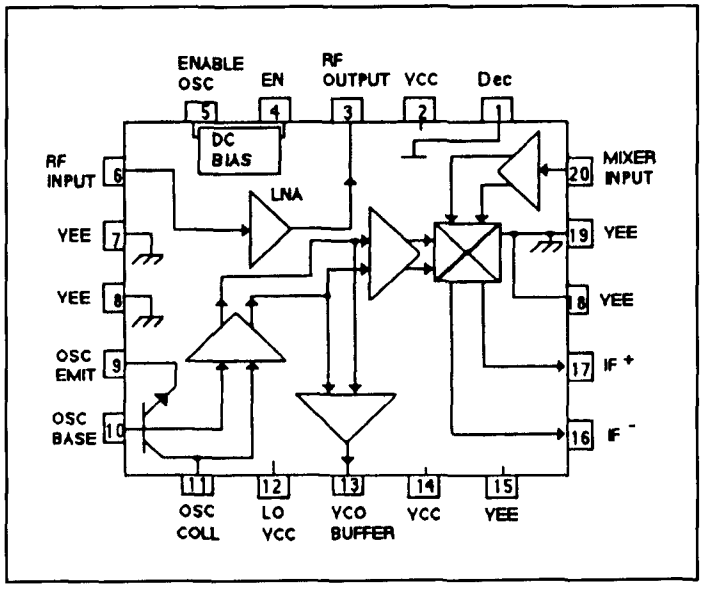

Figure 3. MC13142FTB pin connections.

gy may be used to implement popular wireless communications applications like 100 channel 900- to 928-MHz cordless phones, Cellular Packet Radio, Special Mobile Radio (SMR), Narrowband PCS (covers messaging and paging services), and the newly proposed Family Radio Services at 462 and 467 MHz for very short distance two-way radio service (FCC 95-261 released August 2, 1995).[1]

Description of the chip set

Front-end receiver IC. The MC13142[2] is intended to be used as the first amplifier, voltage-controlled oscillator, and down converter. It features wideband operation, low noise, high gain, and excellent linearity while maintaining low current consumption. The circuit consists of a low-noise amplifier (LNA), a voltage-controlled oscillator (VCO), a buffered oscillator output, a doubly balanced mixer, a wideband IF amplifier, and a DC control section. The wideband IF amp allows this IC to also be used as an up converter and exciter amplifier.

The IC is offered in two packages: 1) a 16-pin SOIC and 2) a 20-pin thin quad flat package (TQFP). **Figures 2** and **3** show the MC13142 pin connections in both packages. In the TQFP package, a pin is provided for linearity adjustment of the mixer; the input intercept point may be increased up to +20 dBm. Other features include:

- Low-power operation: 13 mA at V_{CC} = 2.7–6.5 volts DC
- High mixer linearity: Input IP3 = +3.0 dBm
- Single-ended 50-ohm mixer input
- Double balanced mixer operation
- Open collector mixer output
- Single transistor oscillator with collector, base, and emitter pinned out
- Buffered oscillator output
- Mixer and oscillator capable of being enabled independently

Back-end receiver. The MC13150[3] is designated for use as the back end in analog narrowband FM systems like cellular, 900-MHz cordless phones, and narrowband data links with data rates up to 9.6 kbaud. The MC13150 is a very low power single-conversion narrowband FM receiver incorporating a split IF. It consists of a doubly balanced mixer, common collector transistor oscillator, extended range received signal strength indicator (RSSI), RSSI buffer, IF amplifier, limiting IF, a unique coil-less quadrature detector, and a device-enable function (refer to **Figure 4**). The following are key features of this unique IC:

- Unique coil-less detector
- Low-frequency corner adjustable to <1 Hz for paging and messaging applications
- Low current at 1.7 mAdc at 2.3–6.5 volts DC
- 110 dB RSSI dynamic range
- 12 dB SINAD sensitivity = -100 dBm
- Available in 32 and 24 pin TQFP packages

For those who want more information, the "MC13150 Advance Information Data Sheet" contains details on the IC description and possible applications.

The MC13175D[4] UHF PLL System is used as the 1/8 prescalar and phase detector for the second LO PLL. Other ICs include the MC33111[5] compander, the MC33269-3[6] 3.3-volt, low dropout regulator (LDO), the

Table 1. Noise Analysis Front and Back-End Circuits.

Input Power = 30 dBm

Circuit Reference Number	Circuit Configuration Description	Cascaded Gain (dB)	Cascaded NF (dB)	Input IP3 (dBm)	Minimum Detectable Signal (dBm)	Output IP3 IM3 O/P Level (dBm)
1 (Figure 10)	MC13142 w/o Preamp	11.0	6.17	-10.6	-104.8	0.36 -57.7
2 (Figure 10)	MC13142 w Preamp	21	5.05	-20.7	-105.9	0.34 -27.7
3 (Figure 12)	MC13150 w/o preamp	106.5	21.8	3.0	-107.4	109.5 10.5
4 (Figure 12)	MC13150 w preamp	124.5	6.28	-15	-122.9	109.5 64.6

MC145220[7] dual PLL synthesizer, and the MRF944L[8] RF low-noise transistor.

Receiver system design

LNA/1st mixer. **Figure 5**, the block diagram of the receiver system, shows the implementation of the front and back-end ICs. In this receiver, a discrete LNA, MRF9411L, is used before the MC13142 to improve sensitivity. Detailed noise analysis supports this conclusion.

Front-end IC. The front-end IC circuit is shown in **Figure 6**. The matching network is optimized for noise figure, gain, and input VSWR. Small-signal scattering parameters and noise parameters are found in the IC data sheet. An RF filter is used before the LNA and mixer to provide image rejection. A variety of filters—SAW, ceramic, and dielectric—are offered by manufacturers like Toko, Motorola, and Murata. Both Toko (Part # 4DFA-926A-11 at 926.5 MHz and Part # 4DFA-904A-10 at 904.5 MHz) and Motorola (Part # KFF6140A at 906.5 MHz and Part # KFF6141A at 926.5 MHz[9]) make ceramic filters for 902 to 928-MHz Part 15 applications. The above filters have 3 dB bandwidths of 2 MHz.

IF output matching. The IF output is converted to 50 ohms via a 16:1 impedance transformer. The transformer provides DC through its center tap on the high side; 800 ohms is used across the high side to set the impedance for the 16:1 transformation to 50 ohms. An optional IF preamplifier follows the mixer IF output. This IF preamp provides additional gain with low noise figure and is used to lower the secondary

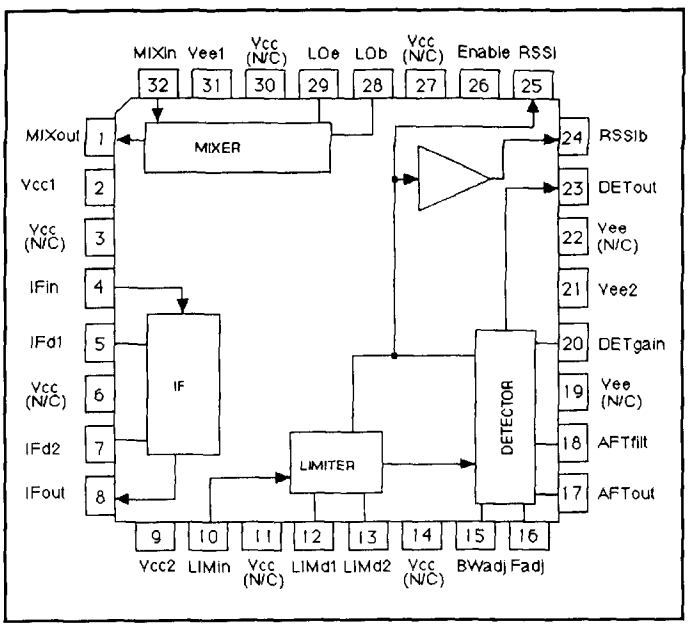

Figure 4. MC13150FTB block diagram and pin connections.

noise figure contribution of the back-end portion of the receiver system. A receiver noise analysis that shows the results with and without the preamp is presented later (**Table 1**).

The first of the IFs is tuned to 83.16 MHz because some manufacturers, such as Toko (Part # SWS.83GBWA) and Murata (Part # SAFC83.161MA40X), offer surface-mounted SAW filters with high attenuation at fc ± 910 kHz. This first IF filter is designed to provide at least 60 dB of second image rejection in a typi-

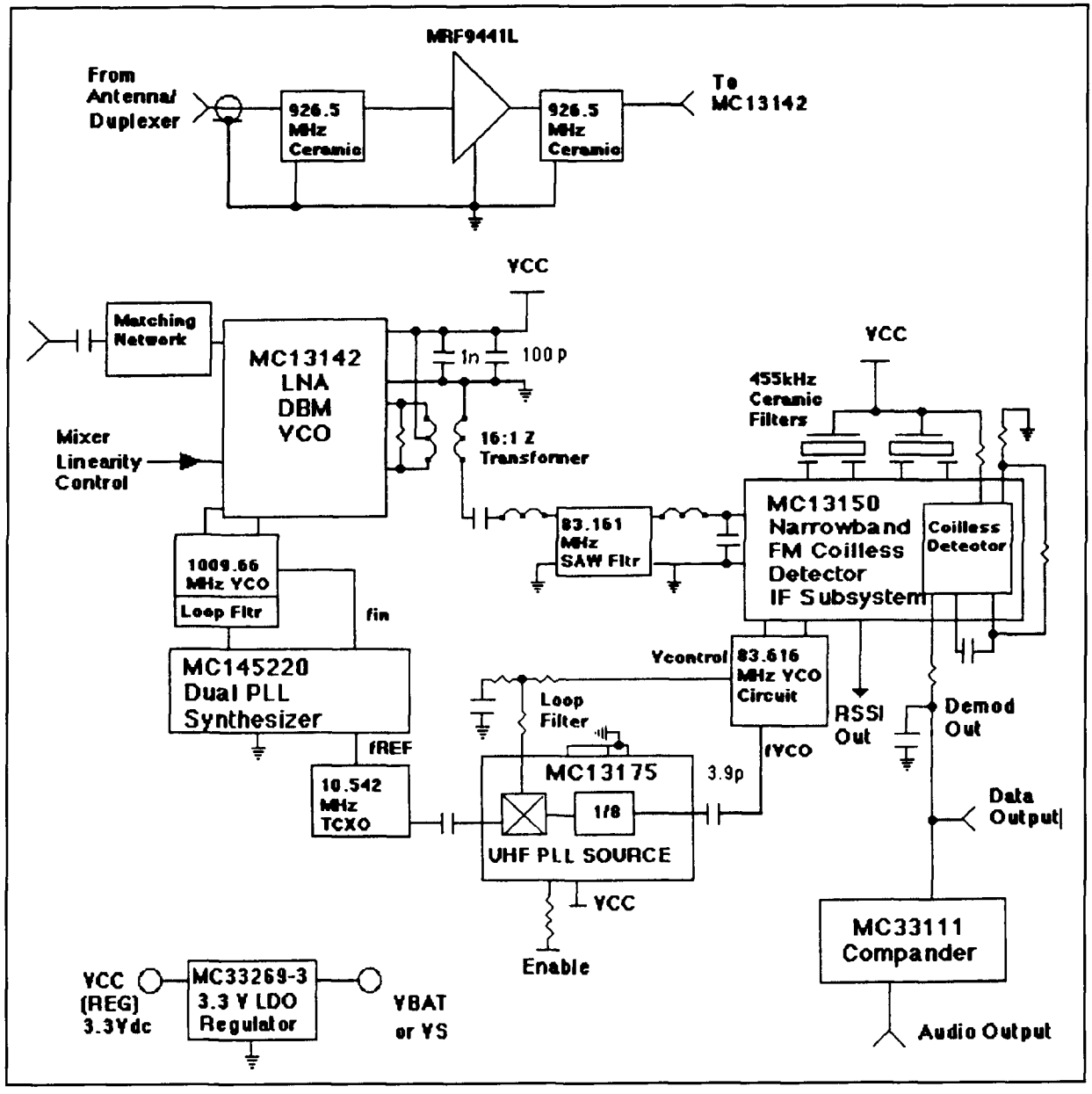

Figure 5. 926.5-MHz receiver system block diagram.

cal narrowband FM receiver with a 455 or 450-kHz limiting IF.

First local oscillator. The first local oscillator is PLL controlled with a MC145220 dual PLL synthesizer. The MC13142 has an onboard transistor with the emitter base and collector pinned out. **Figure 7** shows the VCO circuit, which uses a common collector configuration. The following equation is used to calculate the center frequency of the varactor-controlled oscillator at a nominal 2-volt control voltage:

$$f_{osc} = 0.159 \{L[(C1C2/(C1+C2))+(CvCB/(Cv+CB)) +Cp]\}^{-1/2}$$

where Cp is the parasitic capacitance of the IC and pc board layout; Cp is typically 4 pF.

The sensitivity may be adjusted by changing CB; if CB>>Cv, then Cv dominates and the VCO sensitivity is maximized; thus:

$$CvCB/(Cv+CB) \sim Cv$$

If CB~Cv, then the effect of Cv is minimized and the VCO sensitivity is minimized.

The parasitic capacitance, Cp, is minimized by keeping the interconnects short and maintaining small component mounting pads. Components should be chosen that are high Q with minimum parasitics. The Q of the inductor is important to maintain phase noise performance and power developed in the VCO. Also, the varactor should have sufficient Q at the

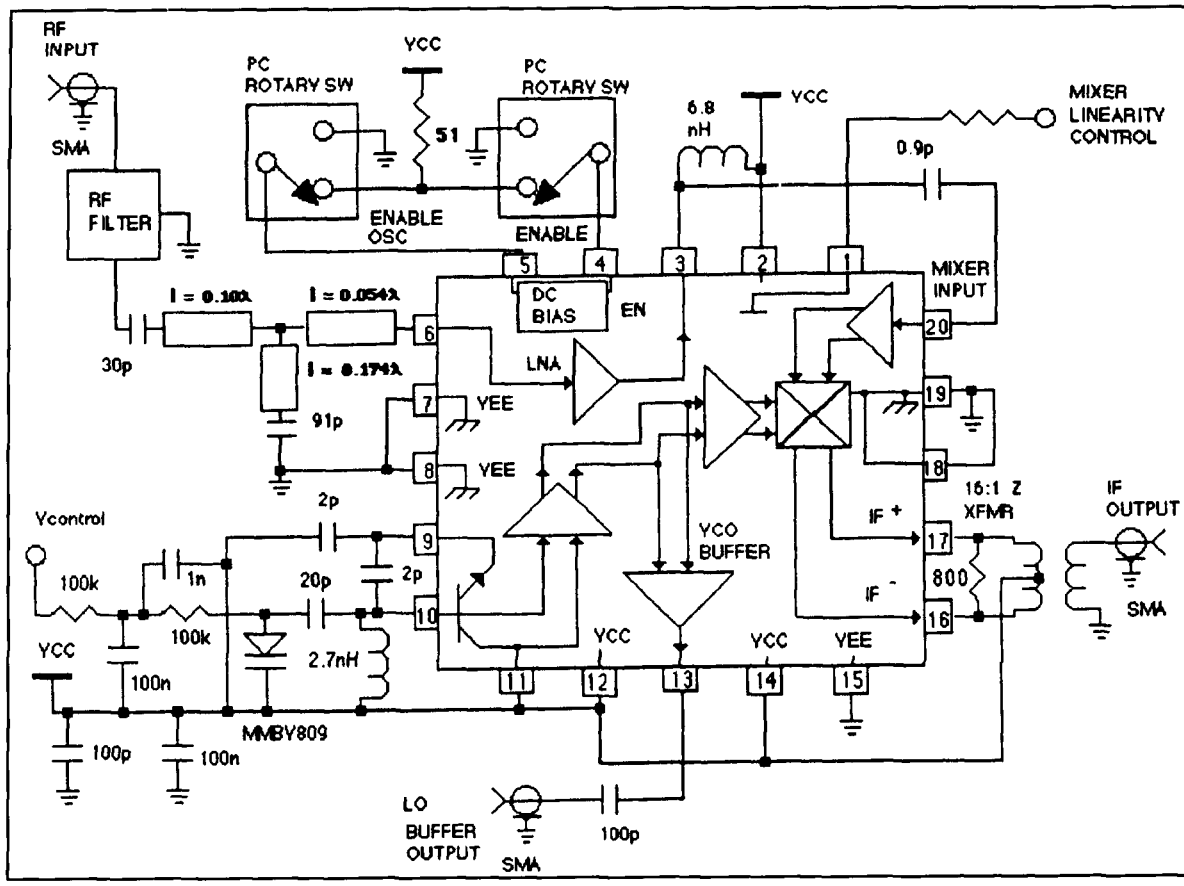

Figure 6. MC13142FTB front-end receiver circuit.

VCO frequency. The MMBV809 offers high Q (150) with 6 pF at 2 volts. Thus, the nominal center frequency of the VCO with 2-volt varactor-controlled voltage is calculated to be 1003 MHz; the required LO center frequency is 1009.661 MHz.

Back-end receiver IC. The back-end function of the receiver makes use of the coil-less detec-

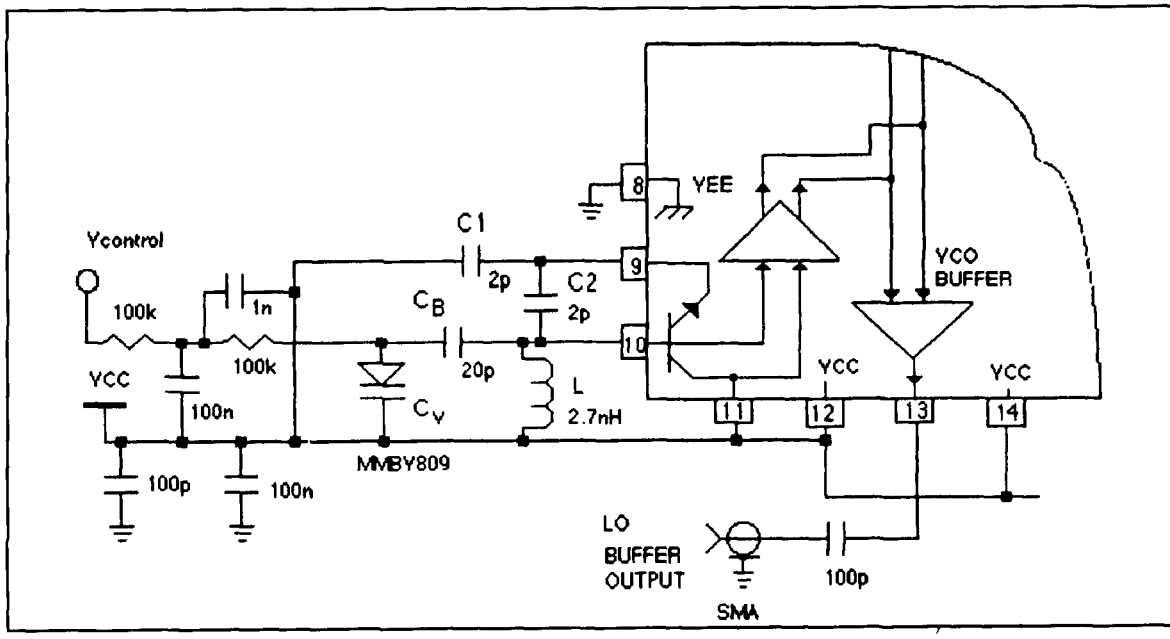

Figure 7. First local oscillator "VCO" circuit.

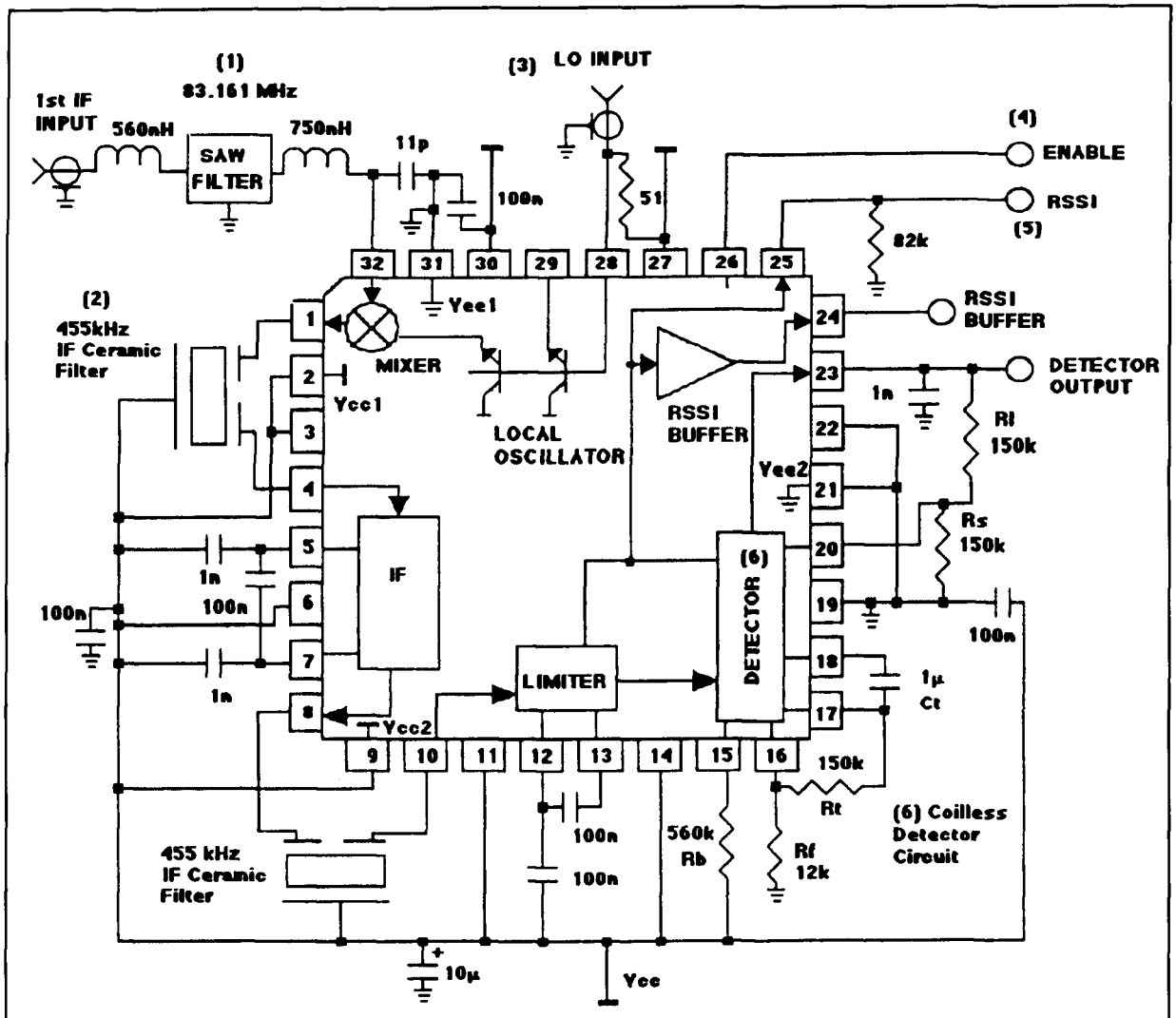

NOTES:
(1) SURFACE MOUNT SAW FILTERS AT 83.16 MHZ IF CENTER FREQUENCY REQUIRED A SERIES INDUCTOR ON THE INPUT AND OUTPUT TO MATCH TO 50 Ω. TOKO AND MURATA ARE EXCELLENT SOURCES FOR THESE FILTERS.
(2) 455kHz CERAMIC FILTERS (SOURCE MURATA CFU455 SERIES WHICH ARE SELECTED FOR VARIOUS BANDWIDTHS).
(3) FOR EXTERNAL LO SOURCE, A 51 OHM PULL-UP RESISTOR IS USED TO BIAS THE BASE OF THE ON-BOARD TRANSISTOR AS SHOWN IN FIGURE 9.
DESIGNER MAY PROVIDE LOCAL OSCILLATOR WITH 3RD, 5TH, OR 7TH OVERTONE CRYSTAL OSCILLATOR CIRCUIT (SEE IC DATA SHEET FOR DETAILS).
(4) ENABLE IC BY SWITCHING THE PIN TO VEE.
(5) THE RESISTOR IS CHOSEN TO SET THE RANGE OF RSSI VOLTAGE OUTPUT SWING.
(6) DETAILS REGARDING THE EXTERNAL COMPONENTS TO SETUP THE COILLESS DETECTOR ARE PROVIDED IN THE APPLICATION SECTION OF THE IC DATA SHEET.

Figure 8. Back-end receiver circuit.

tor in the MC13150 (see **Figure 8**). The coilless detector external circuit design (pins 15 to 22) is explained in detail in the IC data sheet. When the external components are properly chosen, no detector tuning is required in production manufacturing.

Second local oscillator. The second local oscillator is set at 83.616 MHz. It may be crystal controlled using a fifth overtone crystal, as shown in the MC13150 data sheet, or PLL controlled, in which case the master PLL reference oscillator is used. The latter method eliminates an expensive overtone crystal and the required tuning to ensure lockup. Because the master PLL reference oscillator is a narrowband FM system that uses a very stable TCXO with 1 to 2 ppm frequency tolerance and 1 ppm/year aging, reference tuning isn't necessary.

The MC13175 may be used to implement the second LO by using its fixed divide by 8

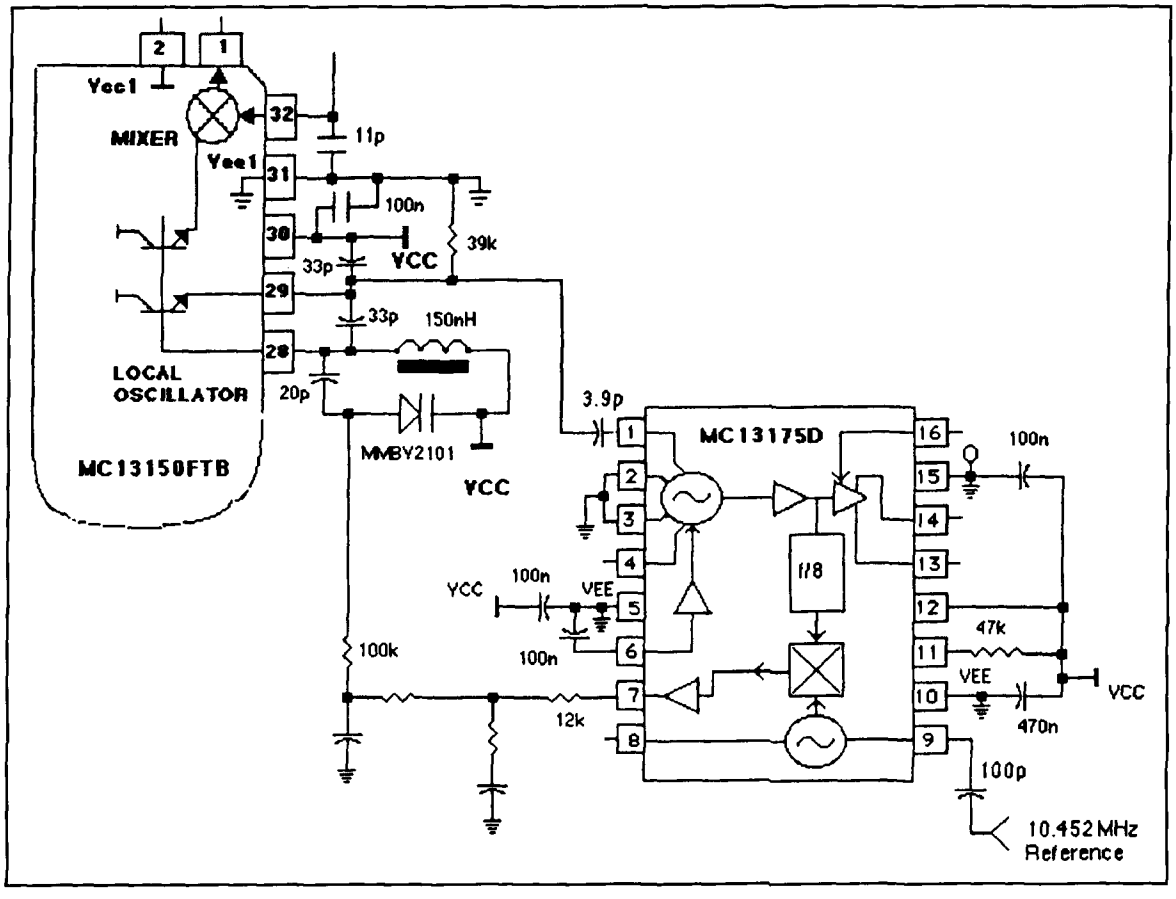

Figure 9. 83.616-MHz VCO (2nd LO).

prescalar and phase detector. The 10.452-MHz reference is AC coupled at pin 9. The phase detector output at pin 7 is used to drive a passive loop filter that drives an external varactor-controlled LC tank circuit at pins 28 and 29—the internal common collector transistor oscillator. The VCO circuit for the 83.616 oscillator is shown in **Figure 9**. Implementing the 83.616-MHz oscillator in this way offers appreciable savings in material and engineering cost while providing better system frequency, stability, and performance.

System noise analysis

The system noise analysis compares several possible configurations using a public domain software application published by Hewlett Packard called AppCAD. A summary of the system noise figure, overall gain, input 3rd order intercept point (IIP3), IMD, and SINAD is presented in **Tables 1** and **2**.

Front-end analysis

Noise analysis of the front and back-end IC circuits is done separately based on the performance characterization of the ICs. **Figure 10** shows the model used for the MC13142. A low-noise amplifier (LNA), MRF9411 (**Figure 11**), is used to improve the front-end noise performance. Design of the matching network is detailed in a paper by Nagaraj Dixit in March 1994.[10] Noise performance with or without this discrete device is shown in **Table 1** (see circuit examples 1 and 2). Although using the discrete transistor requires a few more external components to match and interface with the MC13142, it is preferable for the following reasons:

1. Provides better overall system noise figure and SINAD performance due to added gain and lower noise figure.
2. Improves reverse isolation of the LO at the antenna port. While the TQFP package is excellent and is appreciably better than the SOIC package, it only provides 45 dB maximum isolation between any two pins.

The additional LNA circuit preceding the MC13142FTB improves the reverse isolation by the contribution of the discrete transistor and the RF bandpass filters. The RF LNA provides improvement in noise performance, while it reduces the IIP3. The RF ceramic or SAW preselector filter contributes to 1.5 to 3.8 dB inser-

Table 2. Noise Analysis of System Receiver (Consisting of Front and Back-End Combinations)

Input Power = -30 dBm

Circuit Reference Number	Circuit Configuration Description	Cascaded Gain (dB)	Cascaded NF (dB)	Input IP3 (dBm)	Minimum Detectable Signal (dBm)	Output IP3 IM3 O/P Level (dBm)
1 + 3	MC13142 w/o Preamp MC13150 w/o Preamp	117.5	12.07	-12.5	-117.1	105 52.56
1 + 4	MC13142 w/o Preamp MC13150 w Preamp	135.5	6.43	-26.1	-122.7	109.4 97.7
2 + 3	MC13142 w Preamp MC13150 w/o Preamp	128	6.42	-22.7	-122.8	105.3 83.4
2 + 4	MC1342 w Preamp MC13150 w Preamp	145.5	5.08	-36.1	-124.1	*109.4 127.7

**Note that intermod products exceed the output intercept point in this example.*

tion loss. This adds directly to the system noise figure, but the filter is necessary to provide first image frequency rejection.

Back-end noise analysis

Figure 12 shows the noise model of the MC13150 at 83.16 MHz using the first IF SAW filter specified in the application. Performance is shown with and without a preamp as in the MC13142 analysis. **Figure 13** shows the circuit with a preamp. Examination of the data in **Table 1** (circuits 3 and 4) clearly shows the performance tradeoff with and without a preamp. The noise figure improves from 21.8 dB without the preamp to 6.3 dB with the preamp.

Cascaded receiver system noise analysis

The front and back-end circuits in **Table 1** are cascaded together in four possible combina-

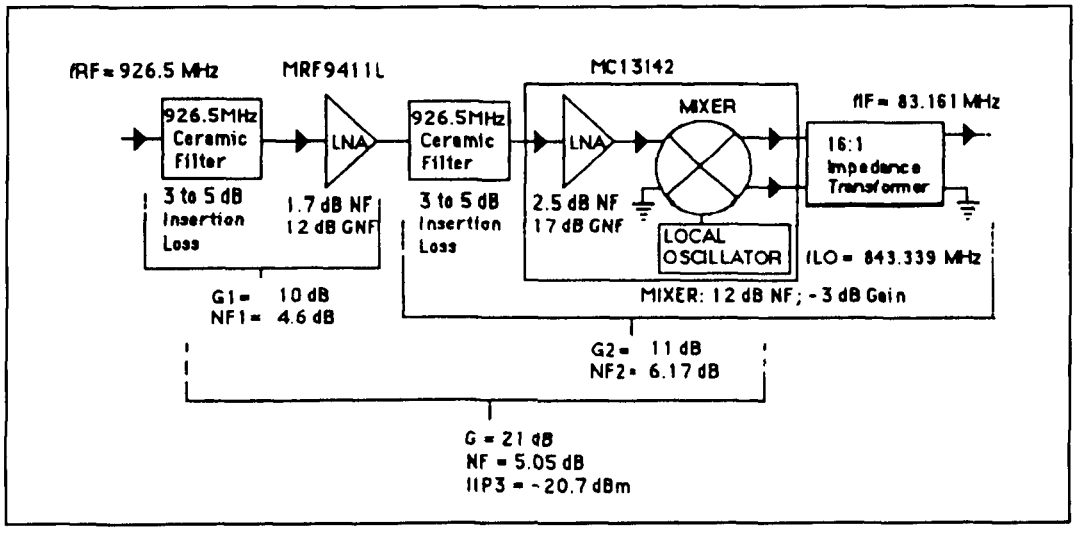

Figure 10. Noise analysis diagram of MC13142 with/without MRF9411L preamp.

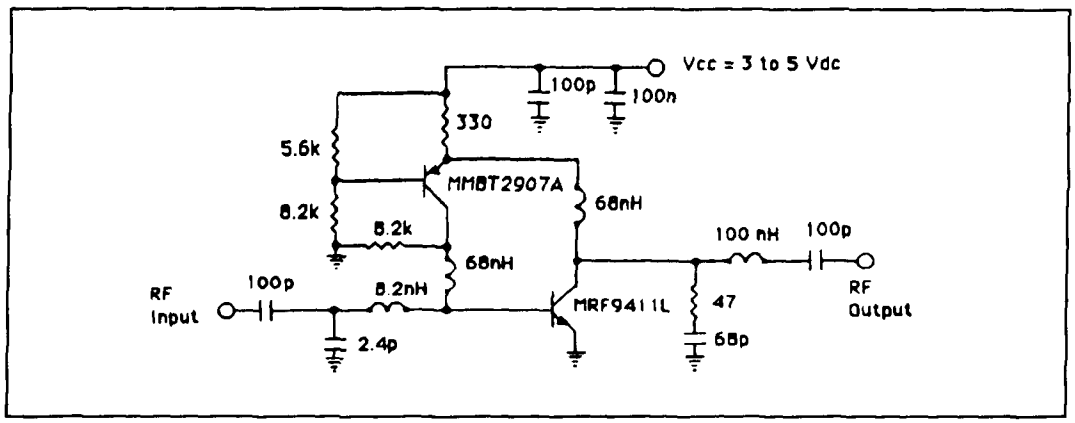

Figure 11. MRF9411L RF LNA.

tions. **Table 2** shows the analysis of overall gain and noise figure, receiver sensitivity, intermodulation, and intercept point performance. The receiver system consisting of the MC13142 with an external preamp and the MC13150 with no external preamp is chosen over the others because it offers the best overall performance. The cascaded noise figure and sensitivity are optimized with maintaining reasonable third order intercept point and intermod performance. The worst performances for IIP3 and intermod occur when preamps are used with both the front and back-end ICs. At -30 dBm input power level, the output intermod exceeds the output IP3.

Performance Criteria

The receiver outlined in **Figure 5** has the following performance:

- System noise figure is typically 6.5 to 7 dB
- 12-dB SINAD performance -116 dBm to -118 dBm
- Input third order intercept point of -23 dBm
- Second image rejection >70 dB
- RSSI dynamic range of typically 100 dB

Other design considerations

Component selection. Component selection is a critical issue in RF circuit design. Components used in these radio and wireless systems must be well characterized and consistent from lot to lot. The Q and tolerance of the components used in fixed tuned circuits should be tightly specified. Of the several manufacturers of RF SAW and dielectric bandpass filters for cellular and cordless phone applications, the specifications for maximum insertion loss are somewhat relaxed and varied. If the RF preselector filter has wide and uncertain specification limits, this will adversely affect receiver system performance because the preselector filter insertion loss adds directly to system noise figure. These filters are optimized for 50-ohm load and source terminations; it's important

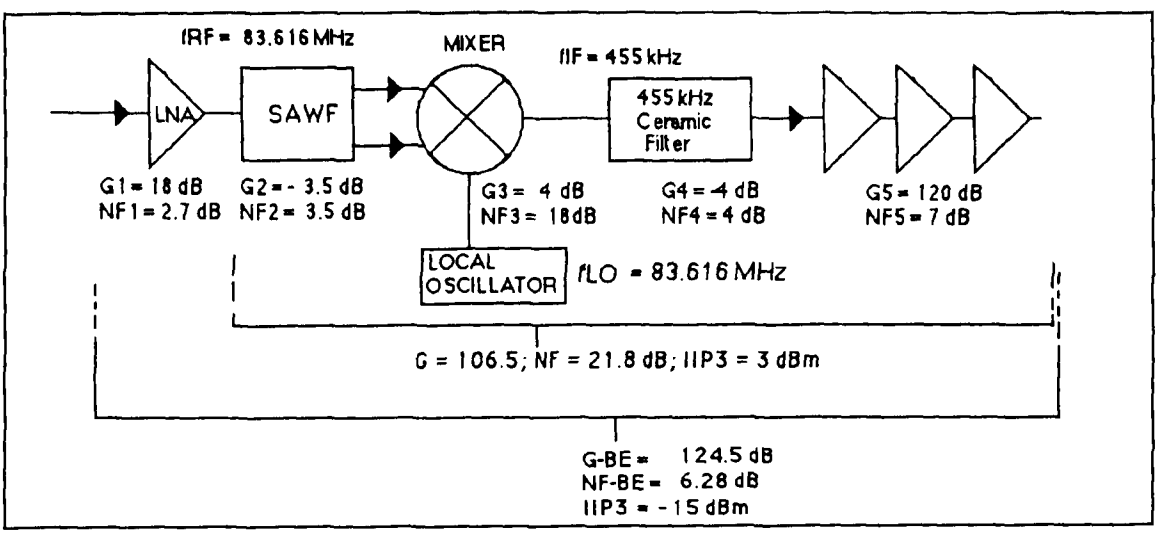

Figure 12. Noise analysis diagram of MC13150 back-end with/without IF preamp.

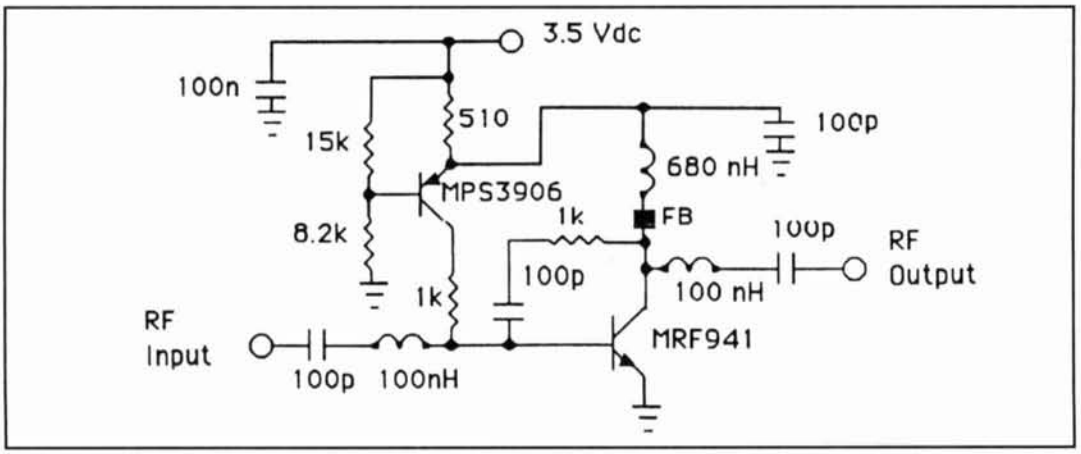

Figure 13. MRF9411L IF preamp.

that the interface matching is implemented correctly and that it can be repeated in a production manufacturing environment.

PC board layout. In RF circuit design, controlled impedance lines are used to reduce lump component count and to cut down on manufacturing cost. Microstrip techniques are successfully used in 900-MHz RF circuit design. The ICs specified in this receiver are all surface mount components. Use of these ICs and other surface mount passive components provides a very compact layout. The demonstration receiver pc board is an example of good RF layout and grounding practices. Chapter 8 of the *Analog IC Data Book* discusses the criteria for good RF layout.

FCC regulation and approval. The receiver system discussed here isn't considered a final product, nor is it approved by the FCC. It is the manufacturer's responsibility to obtain the acceptance and the licenses required by the Code of Federal Regulation (CFR Title 47) to manufacture and market a radio frequency product. The main purpose here is to help the radio designer in his quest with design techniques, application solutions, and recommendation of suitable semiconductor and passive components that achieve the performance criteria of the wireless communication system. ■

REFERENCES
1. Code of Federal Regulations, Title 47, U.S. Government Printing Office, Washington 1994, Part 15 and 95.
2. MC13142/D, Motorola Semiconductor Technical Data, Motorola, Inc., Tempe, Arizona, 1995.
3. MC13150/D, Motorola Semiconductor Technical Data, Motorola, Inc., Tempe, Arizona, 1995.
4. MC131175/D, Motorola Semiconductor Technical Data, Motorola, Inc., Tempe, Arizona, 1992.
5. MC33111/D, Motorola Semiconductor Technical Data, Motorola, Inc., Tempe, Arizona, 1993.
6. MC332269/D, Motorola Semiconductor Technical Data, Motorola, Inc., Tempe, Arizona, 1994.
7. MC145220/D, Motorola Semiconductor Technical Data, Motorola, Inc., Tempe, Arizona 1994.
8. MRF9411/D, Motorola Semiconductor Technical Data, Motorola, Inc., Tempe, Arizona, 1994.
9. KFF6141A Ceramic Bandpass filters Data, Motorola Components Division, Motorola, Inc., Albuquerque, New Mexico, 1994.
10. V. Nagarai Dixit, "Design and Performance of a Low Voltage, Low Noise 900-MHz Amplifier," *RF Design*, March 1994, Argus Business, Skokie, Illinois, pages 48 to 53.

PRODUCT INFORMATION

RFM® Publishes New Data Book

RF Monolithics has published a new, comprehensive data book detailing its 200-plus standard products. The 432-page data book, available at no cost, covers the company's four rapidly growing product lines: low-power components, Virtual Wire® radio systems, frequency control modules, and filters. To help designers determine which product is best suited to their applications, the book contains four master indexes by product type, part number, frequency, and lid symbolization. Also included are overviews of each product line, selection guides, and short-form catalogs. In addition, application notes and article reprints are provided to support each of the product lines. The free data book can be obtained by contacting a local RFM sales representative, listed on RFM's Web site at <http://www.rfm.com>, or by contacting the company directly at 4441 Sigma Road, Dallas, Texas 75244; Phone: (972) 448-3700, (800) 704-6079; Fax: (972) 387-8148.

Richard A. Formato, Ph.D., *K1POO*
P.O. Box 747
Boylston, Massachusetts 01505-0747

LOADING PROFILES FOR WIDEBAND ANTENNAS

Maintain high radiation efficiency with increased bandwidth

Adding impedance loading (resistance and reactance) to an antenna is one of the most effective ways to increase bandwidth. This approach has received progressively more attention since the early 1980s, and today it's state of the art for wideband systems. The choice of a suitable "loading profile" can maintain high radiation efficiency while providing a remarkable increase in bandwidth.

Certain types of communication systems benefit substantially from wideband antennas—typical examples are spread spectrum, frequency-agile, and ALE (automatic link establishment) systems. In each case, it is desirable to maximize antenna bandwidth while maintaining acceptable power gain and radiation pattern. One way to meet this objective is to intentionally add impedance loading to the antenna. As an example of how effective this technique can be, the dipole design described below provides continuous coverage from 6 to 150 MHz with no tuner or matching network.

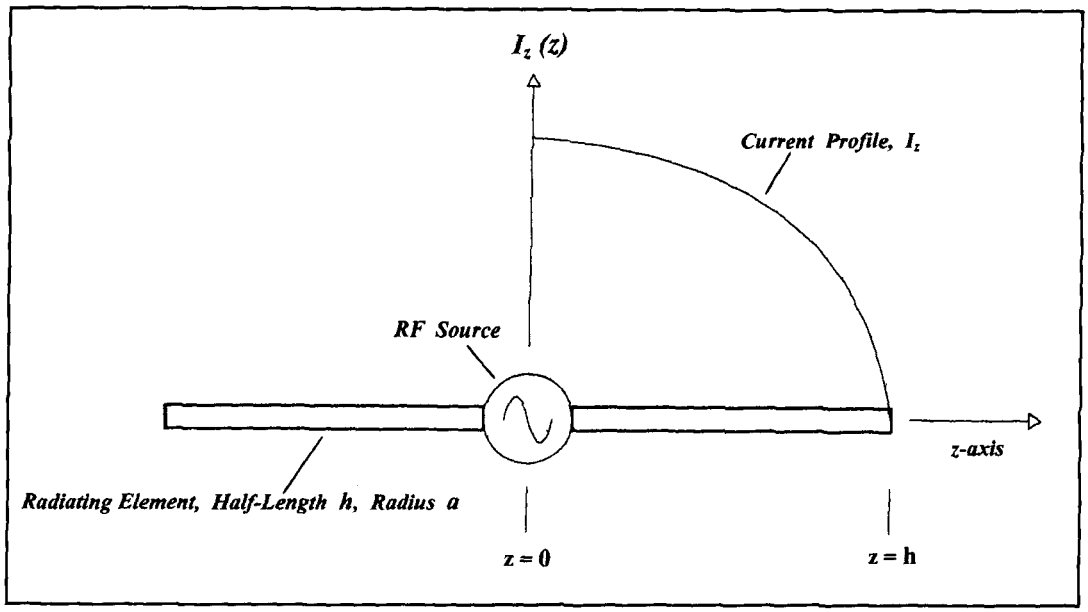

Figure 1. Center-fed dipole.

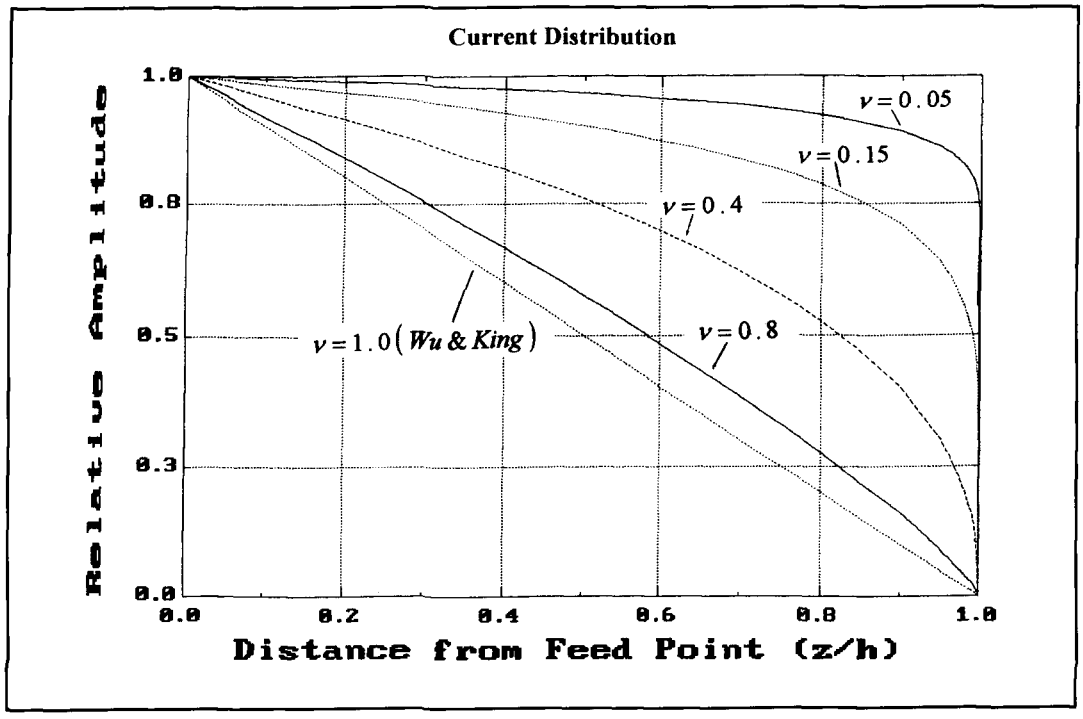

Figure 2. Typical current amplitude distributions parametric in profile exponent *v*.

When designing a loaded antenna, the question is how to select an "optimum" loading profile, because selecting the wrong one can produce dismal results. Indiscriminately adding resistance to an antenna obviously deteriorates performance, and the reduction can be quite severe. This article describes an improved technique for computing the required loading profile for simple wire antenna elements and analyzes several design parameters important in selecting good profiles. Design guidelines are then developed for maximizing antenna bandwidth. Some results are rather surprising, but they can lead to substantial performance improvements over unloaded antennas.

Background

The notion of adding resistance to an antenna to improve frequency response has been around for a long time. In 1953, Willoughby[1] described resistively loaded wires in a variety of configurations, including Vees and Rhombics, used as wideband transmit and receive antennas. The wires were loaded either with discrete resistors or with a gradually tapered resistance profile so the end nearest the RF source had the lowest resistivity and the end farthest from the source had the highest.

Resistance can transform a resonant, standing-wave antenna element into a nonresonant, traveling-wave element, increasing the loaded antenna's bandwidth. The distinction between resonant (standing-wave) and nonresonant (traveling-wave) antenna elements can be illustrated by considering the center-fed dipole (CFD) in **Figure 1**. In the unloaded antenna, resonance results from the superposition of outward-traveling waves produced by the RF source and reflected waves generated at the impedance discontinuity at the CFD's free ends.

These two oppositely propagating waves combine to produce a standing wave that determines the CFD's resonant frequency. However, if the outward-traveling wave were not reflected, no standing wave would exist and the CFD would not exhibit resonance. One way to minimize reflections is to add resistance near the ends of the element to absorb incident energy that has not been radiated away from the antenna, reducing the reflected wave amplitude. This general principle underlies all resistive loading schemes. Of course, there are many ways in which resistance can be added to an antenna, and different approaches can produce dramatically different results.

The simplest loading scheme is to insert a resistor in the antenna, as Altshuler[2] did in the early 1960s. Altshuler theoretically analyzed and built a CFD whose input impedance was for practical purposes flat over a 2:1 frequency range as a result of adding resistance. Each arm of the dipole was loaded with one 240-watt resistor placed a quarter-wavelength from the end, which resulted in an essentially traveling-wave current distribution. Because resistance

reduces the radiated power through Joule heating (i^2R loss), the antenna's bandwidth was increased at the expense of radiation efficiency, which was reduced by about 50 percent. This is the inevitable tradeoff in designing impedance-loaded wire antennas. Bandwidth is best in heavily loaded antennas, but the resulting penalty in radiation efficiency may be too high to provide acceptable power gain.

Altshuler's work was a precursor to Wu and King's[3] landmark paper on continuously loaded antennas. Their theoretical study forms the basis of all recent efforts to improve antenna bandwidth by adding resistance. Unlike the discrete resistor approach, the Wu and King loading profile varies continuously along the antenna element and can be implemented with a conductive surface layer of different materials (aluminum and carbon, for example) of varying thickness. Profiles based on the Wu-King (WK) theory provide good bandwidth but, unfortunately, relatively poor radiation efficiency because the antenna is heavily loaded.

The performance of continuously loaded antennas has been impressive. Using the full WK profile, for example, Kanda[4] built a small loaded-CFD receive-only field probe with essentially flat response from HF to beyond 1 GHz. It was resistively and capacitively loaded by depositing a segmented, conductive thin-film of varying thickness on a glass rod substrate. Narrow rings were burned away using a laser to separate conductive segments and provide the reactive component of the loading profile. This sensor was so heavily loaded, however, that its radiation efficiency was far too low for it to be useful as a transmit antenna (transfer function typically below -22 dB).

Of perhaps greater interest is the continuously loaded HF monopole designed, built, and tested by Rama Rao and Debroux.[5,6] Their 35-foot high antenna provided SWR $\leq$ 2 from 5 to 30 MHz and radiation efficiency in the 15 to 36 percent range. Because the full WK profile generally results in poor radiation efficiency, Rama Rao and Debroux used a fractional loading profile equal to 0.3 times the Wu-King profile ("30 percent profile"), along with a fixed, lumped-element matching network. In addition to fractional loading profiles, other profiles have been proposed that combine resistance and inductance to improve bandwidth and efficiency,[7] but these aren't discussed in detail here.

This article describes a modification to the WK profile that increases the average antenna current, resulting in higher radiation efficiency, while maintaining the traveling-wave current mode necessary for increased bandwidth. Because the fields radiated by an antenna are proportional to its *Idl* product (current moment), increasing the average current increases the radiated fields, which in turn improves efficiency. The current distribution produced by the WK loading profile decays lin-

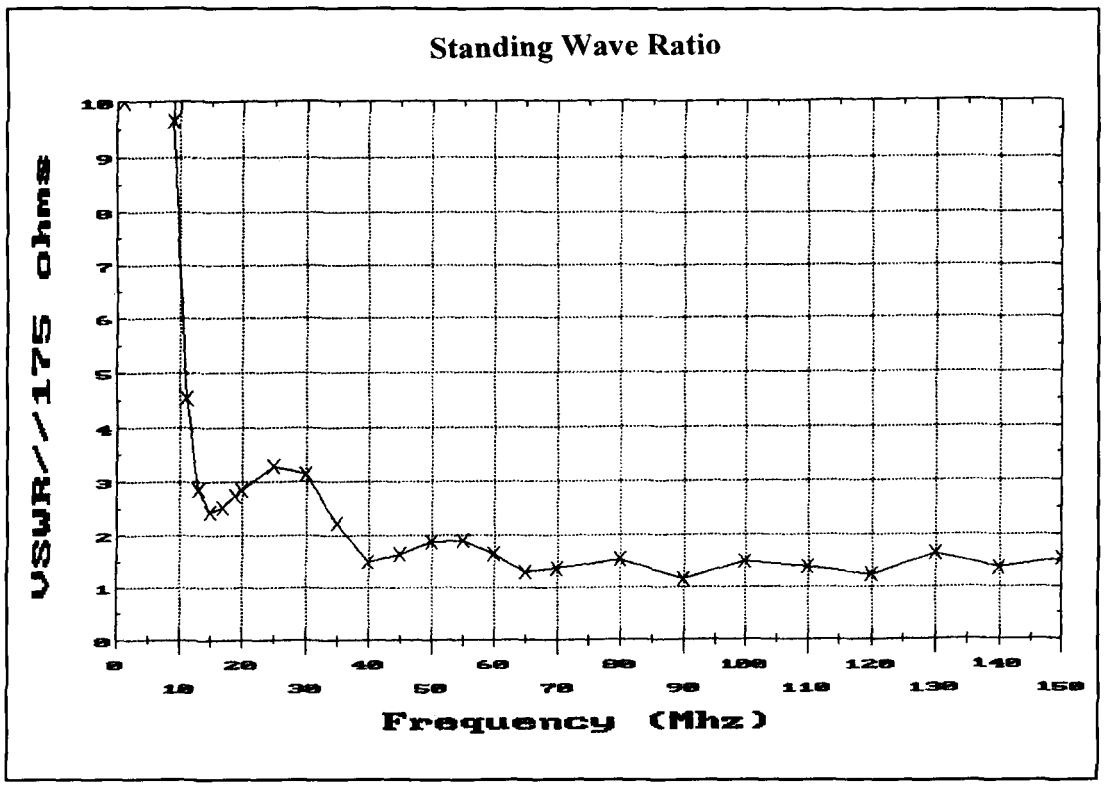

Figure 3. Computed input SWR for 175-ohm feed system impedance.

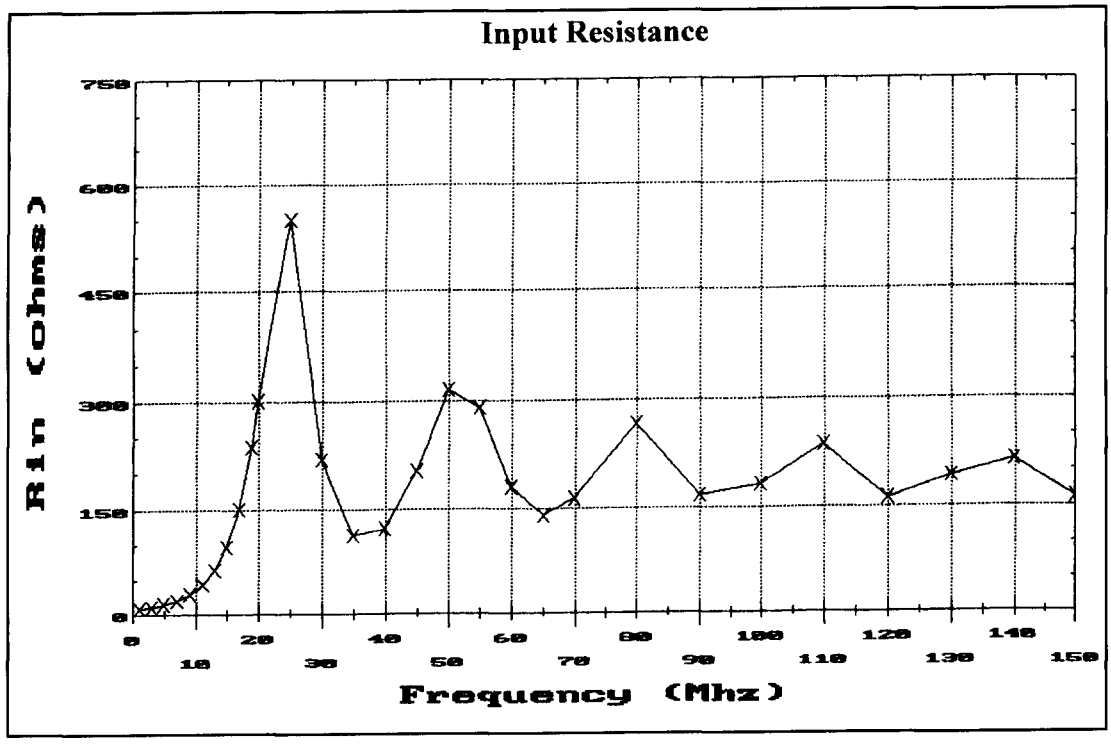

Figure 4. Monopole input resistance.

early along the antenna. The improved profile produces a traveling-wave current mode with a power law amplitude decay, of which the WK profile is a special case.

Wu-King Theory

Figure 1 shows a CFD antenna consisting of two radiating elements of length h and radius a. The amplitude of the current profile is plotted schematically along one element's length. Maximum current occurs at the RF source at the feedpoint, and the current magnitude decreases along each arm until reaching zero at the end.

In the WK model, the CFD is assumed to have an internal impedance profile along the wire element given by $Z^i(z) = R^i(z)$, where Z^i is the (complex) internal impedance per unit length (ohms/meter) consisting of lineal resistance and reactance R^i, and where $j = \sqrt{-1}$. Wu-King develops the differential equation satisfied by the current I_z, and then determines *by inspection* that a traveling-wave current mode exists for one particular impedance profile Z^i.

The WK current distribution is:

$$I_z(z) \approx \underbrace{\left(1 - \frac{|z|}{h}\right)}_{\textit{Linear Amplitude Decay}} \underbrace{\exp(-jk_o\,|z|)}_{\textit{Traveling Wave Factor}}. \qquad (1)$$

which consists of the product of a linearly decreasing ("straight line") amplitude and a traveling-wave propagation factor in the complex exponential term. The wave number is $k_o = 2\pi/\lambda_o$. The propagation factor represents a current wave progressing outward along each dipole arm. There is no reflected wave propagating toward the source to form a standing wave pattern, and consequently no resonance effect.

This current distribution exists only when the CFD element has a specific "1/z" internal impedance profile. The required profile is given by:

$$Z^i(z) = \frac{60(\psi/h)}{1 - \frac{|z|}{h}}, \qquad (2)$$

where $\psi = \psi_R + j\psi_I$ is the complex expansion parameter discussed in Altshuler[2] with real and imaginary parts subscripted R and I, respectively. ψ is the ratio of the antenna element's vector potential to current and is approximately constant along its length. The 1/z profile **Equation 2** is the basis for the resistive loading used in **References 4, 5,** and **6**.

The expansion parameter is defined as:[3]

$$\psi = 2\left[\sinh^{-1}\left(\frac{h}{a}\right) - C(2k_o a, 2k_o h) - jS(2k_o a, 2k_o h)\right] + \frac{j}{k_o h}\left[1 - \exp(-j2k_o h)\right] \qquad (3)$$

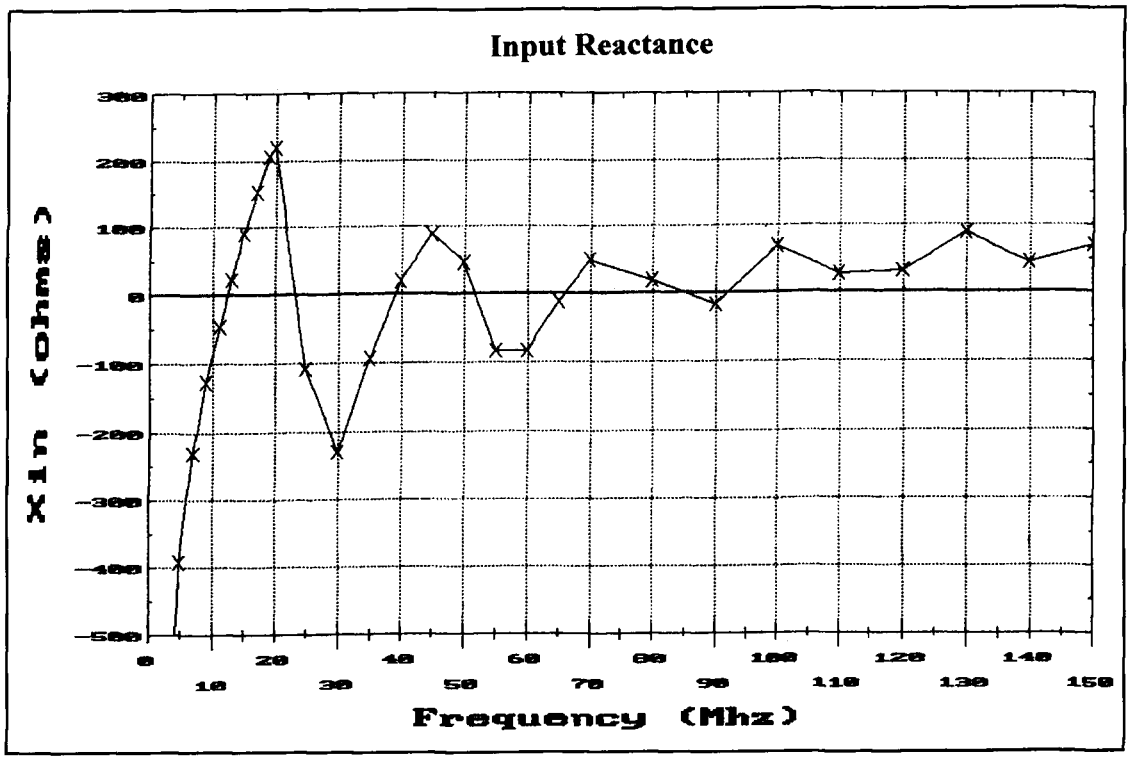

Figure 5. Monopole input reactance.

C and S are the *generalized* sine and cosine integrals[3,8] given by:

$$C(b,x) = \int_0^x \frac{1-\cos W}{W}\,du \qquad \textbf{(4a)}$$

$$S(b,x) = \int_0^x \frac{\sin W}{W}\,du \qquad \textbf{(4b)}$$

where $W = (u^2 + b^2)^{1/2}$.

Because ψ is frequency dependent, it is usually evaluated at the antenna's fundamental half-wave resonance; that is, $\lambda_0 = 4h$ (see **Reference 3** for details). However, this choice is not necessarily the best. The design frequency f_o(Hz) and the corresponding wavelength λ_0 (meters) are related by $f_o\lambda_o = c$, where $c \cong 2.998 \times 10^8$ meters per second is the free-space velocity of light. Note that the design frequency f_o for evaluating ψ is not the RF source frequency.

Improved loading profile

The 1/z profile is a special case of a more general profile that results in higher radiation efficiency. The first step in deriving the generalized profile is to assume a power law traveling-wave current distribution. The next step is to substitute this assumed current distribution into the current equation developed by Wu and King, which then yields the condition that must be satisfied by the element's internal impedance in order to generate traveling-wave-only modes. This approach is fundamentally different from the WK approach, because the loading profile for a particular traveling-wave current mode is now an unknown determined by solving the appropriate equations.

The generalized CFD current distribution is assumed to be of the form:

$$I_z(z) = C\,(h-|z|)^{v}\,\exp(-jk_o|z|), \qquad (5)$$

Power Law Amplitude Decay — *Traveling Wave Factor*

where C is a complex constant determined by the current at the feedpoint. The current amplitude decays with a power law variation with exponent v, instead of a linear decay. When $v = 1$ the Wu and King case is recovered, but when $v \neq 1$ the more general case is obtained. **Figure 2** shows typical current amplitude distributions parametric in the *profile exponent v*. It is apparent that values of v less than 1 can lead to significantly higher average antenna currents. Radiating elements with these current distributions are more efficient than those using the 1/z loading profile that corresponds to $v = 1$.

The internal impedance profile that produces traveling-wave-only currents of the form in

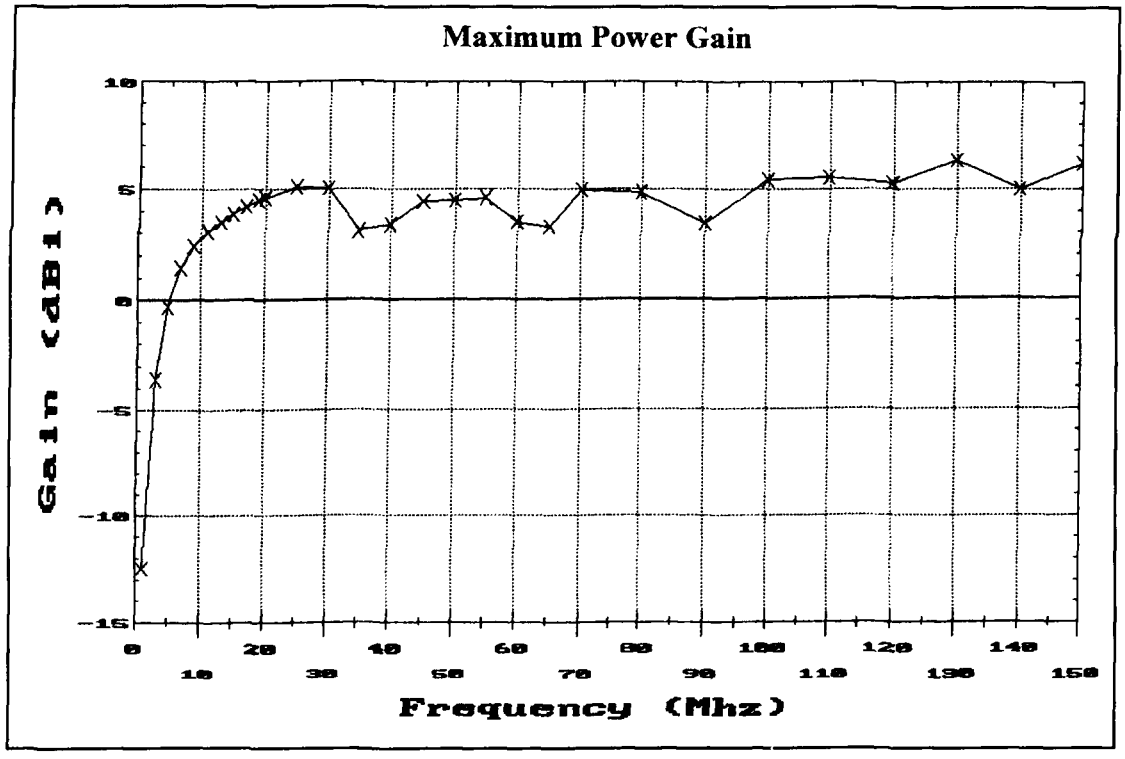

Figure 6. Loaded monopole's maximum power gain.

Equation 5 is determined as follows. The derivatives $\frac{dI_z}{dz}$ and $\frac{d^2 I_z}{dz^2}$ are computed and substituted into the equation satisfied by $I_z(z)$, which is Wu and King's **Equation 11**. This generates the equation that must be satisfied by the auxiliary function $f(z)$ introduced in WK **Equation 9**. Its solution is:

$$f(z) = 2\nu (h-|z|)^{\nu-2} \left\{ 1 - j \frac{\nu - 1}{2 k_o (h-|z|)} \right\} \quad (6)$$

The impedance profile is determined by $f(z)$. **Equation 6** generalizes Wu and King's **Equation 12** and recovers their results exactly when $\nu = 1$.

The loading profile resistance and reactance per unit length are computed from $f(z)$ and are given explicitly by:

$$R^i(z) = 60\nu (h-|z|)^{\nu-2} \left\{ \psi_R - \frac{(1-\nu)\psi_I}{2 k_o (h-|z|)} \right\} \quad \textbf{(7a)}$$

$$X^i(z) = 60\nu (h-|z|)^{\nu-2} \left\{ \psi_I - \frac{(1-\nu)\psi_R}{2 k_o (h-|z|)} \right\} \quad \textbf{(7b)}$$

where $k_o = \frac{2\pi}{\lambda_o}$ is the wavenumber.

The corresponding lineal inductance (henry/meter) or capacitance (farad/meter) are given by $L^i = X^i/\omega_o$ and $C^i = 1/(\omega_o X^i)$, respectively, for $X^i > 0$ and $X^i < 0$. The circular frequency is $\omega_o = 2\pi f_o$ where f_o is the design frequency (Hz) at which ψ is computed and $f_o = c/\lambda_o$.

The improved loading profile in **Equation 7** contains both resistance and reactance. But adding reactance to a wire antenna, especially capacitive reactance, can complicate construction. As a consequence, many practical designs employ only resistive loading, because excellent results are often achieved even without the profile's reactive component (see **References 5** and **6**, for example). In the antenna designs discussed below, only resistive loading is considered.

Discrete loading

Building a continuously loaded antenna can be a formidable task—especially if some exotic technique is required (for example, vapor deposition of a conductive thin-film layer), or if reactive loading is included. An effective alternative to the continuous-loading profile in **Equation 7** is to construct an approximate profile using only discrete resistors at intervals along the antenna.

The discretely loaded antenna consists of highly conducting (for practical purposes, per-

fectly conducting) cylindrical wire segments connected together by resistors. Single resistors can be used; large diameter radiators are preferred for multiple resistors. Discrete loading can provide exceptional bandwidth and efficiency, better even than a continuous profile, and it does so without the problems associated with continuous profiles or reactive loading. Because of these advantages, only discrete loading profiles are considered here.

A discrete profile may be computed by first dividing the CFD into an odd number of equal length segments, N. The center segment, which contains the RF source, is not loaded. All other segments are loaded with a lumped resistance placed at the segment center. The value of the resistor is computed as the product of the segment length (in meters) and the value of the continuous loading profile evaluated at the segment center (R^i in ohms/meter from **Equation 7A**). Loading profiles for monopole antennas are computed in the same way, but the number of segments isn't restricted. This approach provides a piecewise linear (step) approximation to the continuous loading profile. There is, of course, an infinite number of discrete approximations, and nonuniform profiles might result in even better antenna performance. However, only the uniform step approximation is considered here.

In the next section, I describe a discretely loaded monopole design that provides continuous coverage from about 12 MHz to beyond 150 MHz with no antenna tuner or matching network. In subsequent sections, we'll investigate the effects of key loaded antenna design parameters by examining the computer-modeled performance of a typical HF-VHF CFD using discrete resistance-only loading.

Loaded HF-VHF monopole

To illustrate the effect of loading an antenna, a profile was computed for a monopole element fed at its base against an infinite, perfectly conducting ground plane. The radiating element height is 5.83 meters and its radius is 2.54 centimeters. The design frequency, f_o, is 12.86 MHz (approximately the fundamental resonance), and the power law exponent v is 0.05. At the design frequency, $\psi = 8.961\text{-}j2.431$.

A resistance-only profile was computed at 14 discrete, equally spaced loading points along the antenna using **Equation 7A**. The profile is tabulated in **Table 1**. It increases very gradually from 0.419 ohms near the base of the monopole to about 787 ohms near the top. Reactive loading from **Equation 7B**, in this case inductive, was not included.

The monopole antenna's performance was computed-modeled for RF source frequencies from 1 to 150 MHz (upper limit of the model). The computed input SWR for a feed system

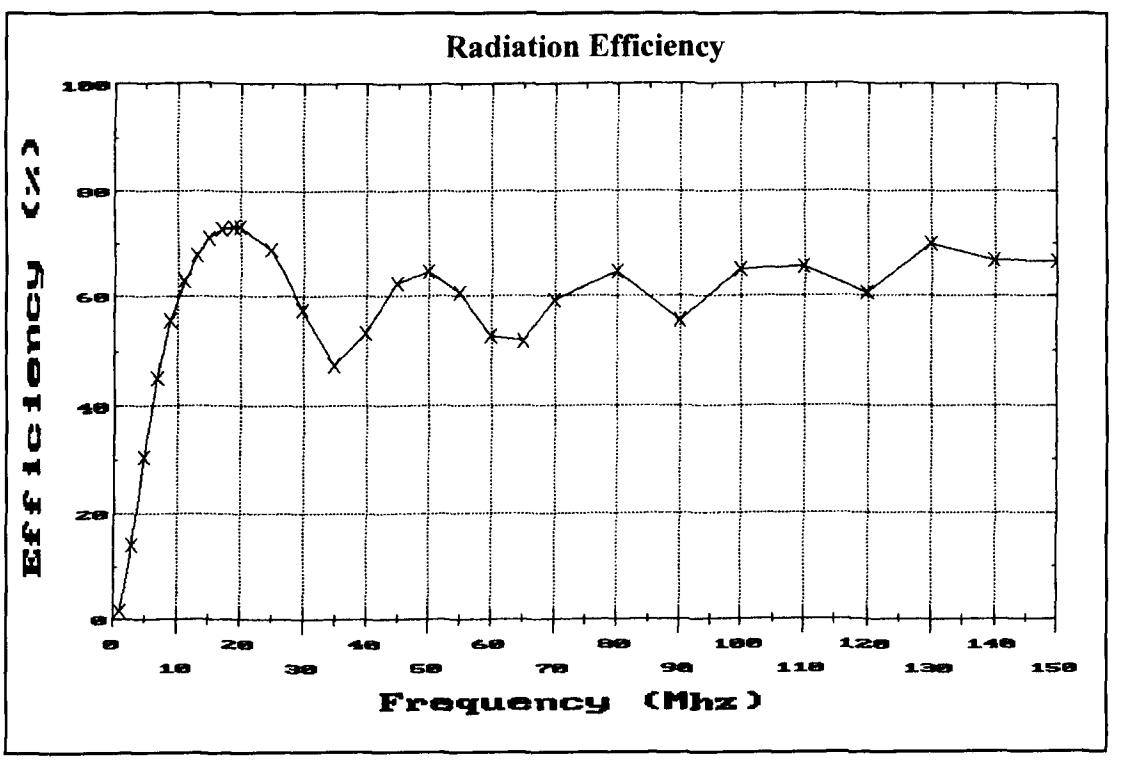

Figure 7. Monopole's radiation efficiency.

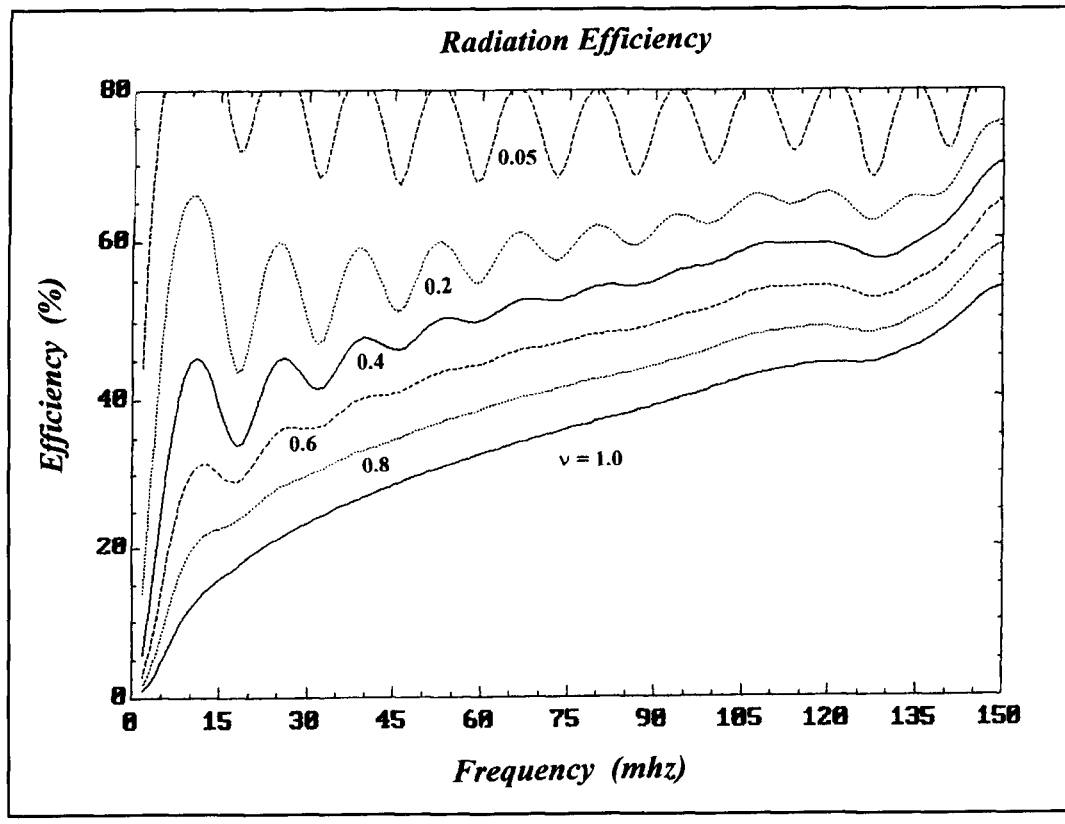

Figure 8. Radiation efficiency where $\nu = 1$.

Height (meters)	Resistance (ohms)	Height (meters)	Resistance (ohms)
0.208	0.419	3.123	1.889
0.625	0.489	3.539	2.689
1.041	0.581	3.956	4.129
1.458	0.699	4.373	7.131
1.874	0.859	4.789	15.102
2.290	1.080	5.205	49.473
2.707	1.401	5.622	786.910

Table 1. Monopole loading profile.

impedance of 175 ohms appears in **Figure 3** (calculated points are marked by X). Because SWR was computed for a 175-ohm characteristic impedance, feeding this antenna with the usual 50-ohm coaxial line requires a 3.5:1 unun or another suitable broadband transformer.

The monopole's performance is excellent at all frequencies above 36 MHz. The SWR is below 2 from 36 to 150 MHz. It's somewhat worse from approximately 12 to 36 MHz, reaching a maximum of 3.3 at 25 MHz. Below 11 MHz, SWR increases rapidly due to increasing capacitive reactance and decreasing radiation resistance. This behavior is characteristic of electrically short antennas and is evident in the monopole's feedpoint resistance and reactance plots in **Figures 4** and **5**, respectively. The data in these curves were used to compute the SWR plot in **Figure 3**.

The impedance bandwidth is remarkably good, especially considering that there is no matching network and only discrete resistive loading is used. No attempt was made to further improve the loading profile by, for example, modifying computed resistance values (typically a fractional or a nonuniform profile) or by adding reactance. Such adjustments can frequently yield even better performance, but they aren't considered further.

The following comparison illustrates just how dramatic the effect of loading an antenna can be. For an unloaded monopole, the bandwidth for SWR ≤ 2.5 (50-ohm feed) is typically 15 to 25 percent of its $\lambda/4$ frequency, depending on the length-to-diameter ratio. A monopole $\lambda/4$ high at 12.86 MHz, like the one considered here, would exhibit a bandwidth no greater than 3.2 MHz. In marked contrast, the same antenna with loading has a bandwidth of more than 115 MHz, a very substantial improvement indeed!

Of course, SWR bandwidth by itself doesn't guarantee a good antenna. For example, consider a dummy load: its response is flat, typically well into the UHF range, but its radiation efficiency is practically zero. The dummy load

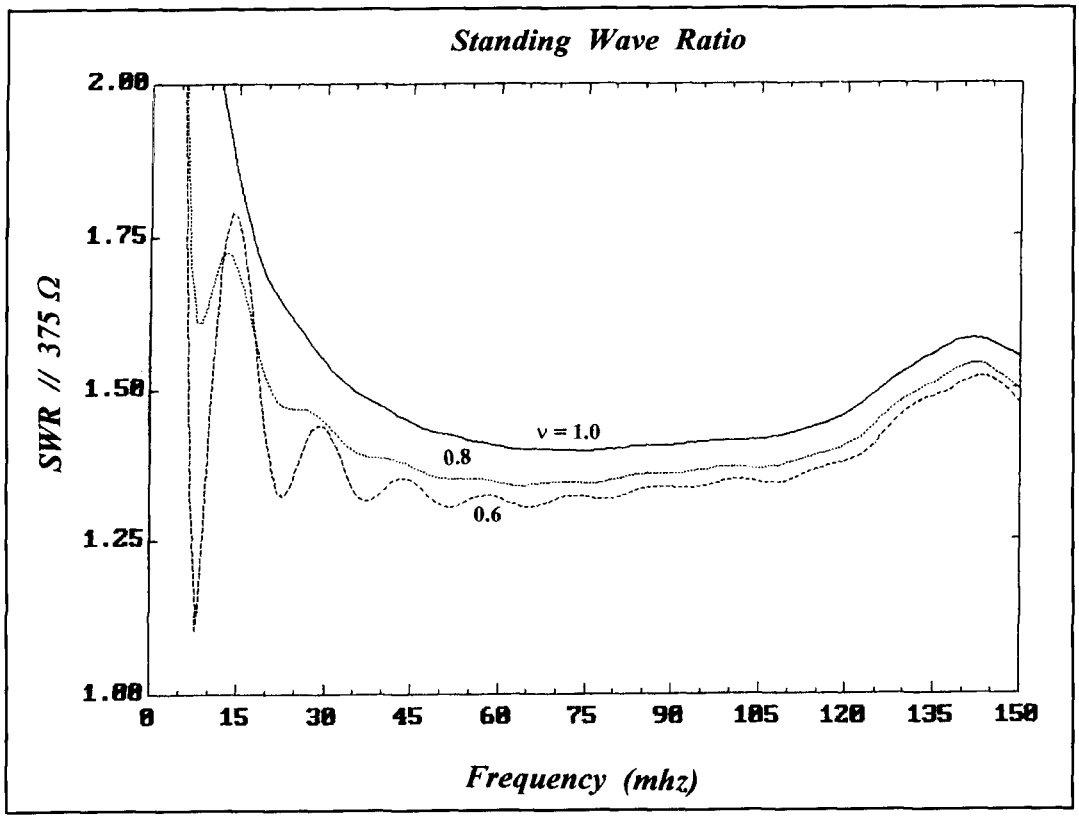

Figure 9. (A) Standing wave ratio (SWR) for ν = 1.0.

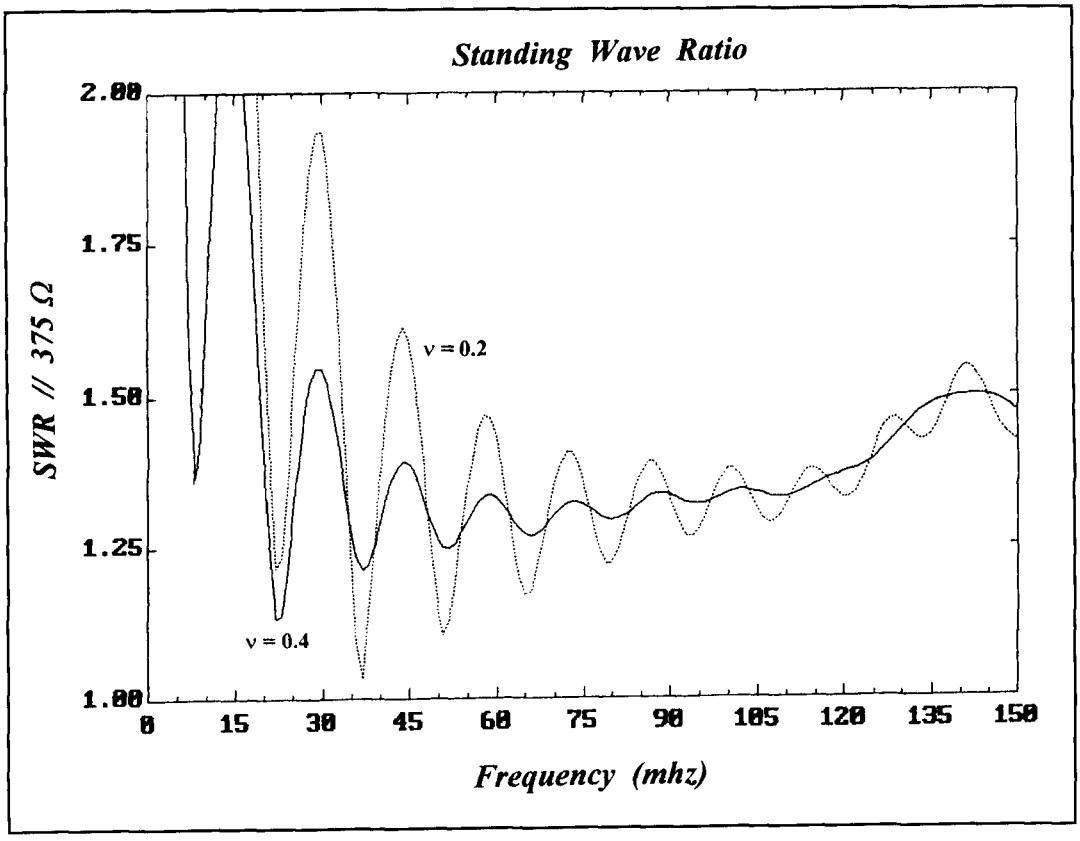

Figure 9. (B) SWR for ν = 0.2 and 0.4.

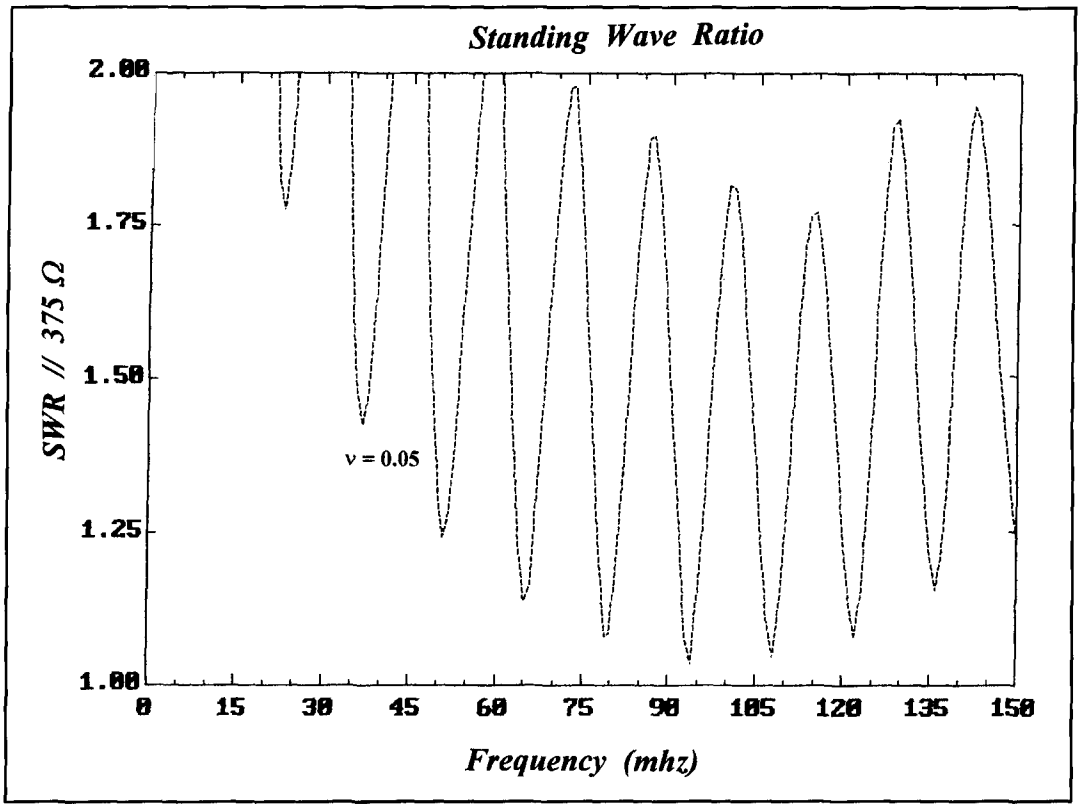

Figure 9. (C) SWR for 0.05.

Distance (meters)	Resistance (ohms)	Distance (meters)	Resistance (ohms)
0.00	0.00	6.07	12.30
0.76	3.86	6.83	15.99
1.52	4.36	7.59	21.89
2.28	4.98	8.34	32.31
3.03	5.76	9.10	53.90
3.79	6.75	9.86	113.47
4.55	8.05	10.62	438.06
5.31	9.82		

Table 2. Prototype CFD loading profile.

is obviously not suitable as an antenna, even though it has excellent SWR bandwidth. Two other key measures of antenna performance, maximum gain and radiation efficiency, must also be considered.

The loaded monopole's power gain (product of directive gain and efficiency) is plotted in **Figure 6** in dBi (decibels relative to an isotropic radiator). The gain at 10 MHz is nearly 3 dBi, and from 10 to 150 MHz it's mostly in the 4- to 6-dBi range. For comparison, the maximum power gain of a half-wave CFD in free space is 2.15 dBi. The monopole with the improved resistance profile exhibits power gains comparable to those of similar antennas with no loading at all. These maximum gain values are surprisingly good for an antenna providing as much bandwidth as the loaded monopole.

Of course, the fundamental issue in choosing an effective impedance-loading profile is the tradeoff between bandwidth and radiation efficiency. The merit of a particular profile is determined primarily by these two performance measures. An examination of the monopole's SWR curve (**Figure 3**) showed it to be more or less flat from 36 to 150 MHz, with somewhat higher, but still acceptable, SWR from 12 to 36 MHz. The second measure of merit, radiation efficiency, is plotted in **Figure 7**. The efficiency is generally above 60 percent over the entire range from 10 to 150 MHz, with only minor dips below 60 percent and in some regions where it is near or above 70 percent. Even the minimum efficiency value of 45 percent or so near 35 MHz is quite acceptable. The improved resistive loading profile has resulted in an antenna with exceptionally good SWR bandwidth, relatively high power gain, and very acceptable radiation efficiency.

Profile design parameters

There are several parameters that influence how well a particular loading profile performs, and there is not one "best" profile. Important

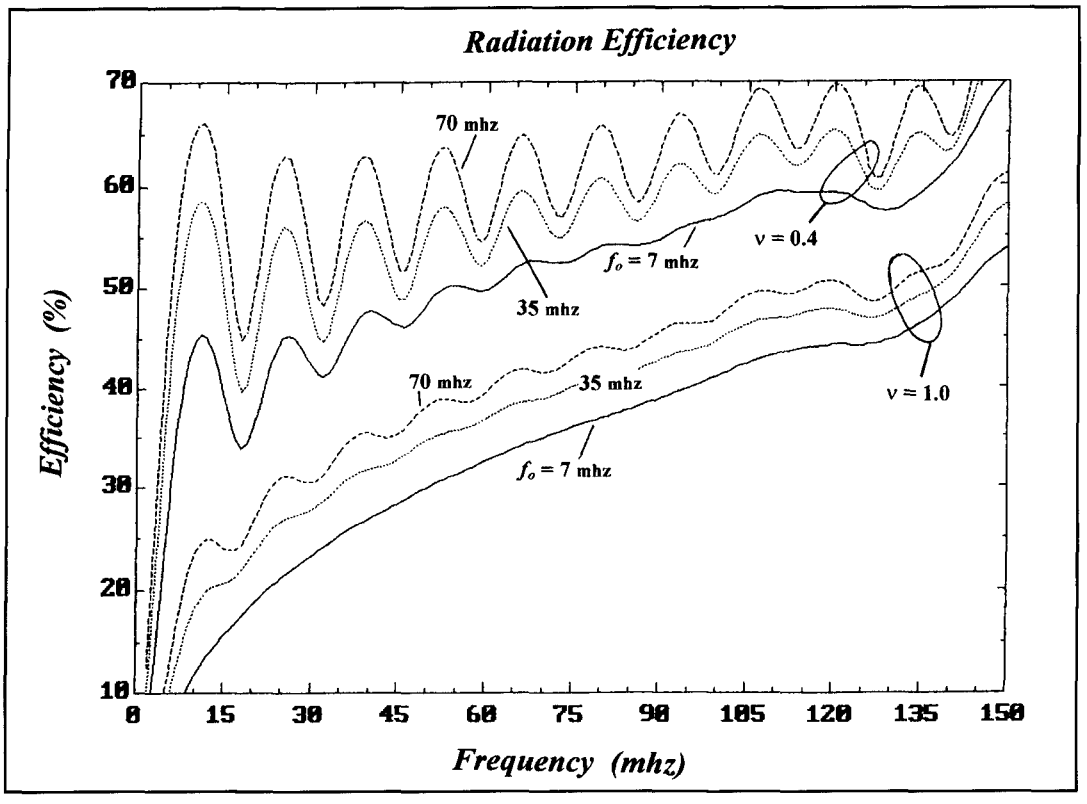

Figure 10. Radiation efficiency plot for a 22-meter-long, 10-centimeter-diameter CFD.

design parameters include: (1) value of the profile exponent, (2) design frequency, (3) wire length-to-diameter ratio, and (4) number of antenna segments (number of discrete resistors). Certain parameters are more important than others (in the sense of having a relatively greater impact on performance), and for some parameters the results are unexpected.

These four design parameters are discussed below for typical HF/VHF CFD designs. Radiation efficiency and SWR are examined for RF source frequencies between 2 and 150 MHz. Other important measures of antenna performance (power gain and pattern, for example) aren't considered in detail because they are usually acceptable in an impedance-loaded antenna with a good loading profile. For example, the maximum gain figures for the monopole antenna described above are typical of well-designed impedance-loaded radiators.

The prototype CFD considered below has the following design parameters: L = 22 meters, D = 10 centimeters, f_o = 7 MHz, v = 0.4, N = 29, ψ = 8.822-j2.464. In the following sections, individual parameters will be varied to study their influence on antenna performance. There is no reactive or feedpoint loading, and the full (100 percent) profile is used.

The prototype CFD's discrete resistance-only profile, computed as described above using **Equation 7A**, appears in **Table 2**. Distance is measured from the origin, and the loading is symmetrical in each arm of the CFD. The loading resistance increases slowly from 3.86 ohms on either side of the RF source (±0.76 meter from the center) to just over 438 ohms in the last segment (located ±10.62 meters from the source). This very gradual increase in resistance is typical of more efficient loading profiles.

Profile exponent

Probably the most important design parameter in determining radiation efficiency is the value of the profile exponent, v, which determines how quickly the current amplitude decays along the dipole. Slower decay (lower v) results in a higher average antenna current, which increases the radiated fields and, consequently, the efficiency. The efficiency improvement can be quite dramatic. The tradeoff is that decreasing v increases the peak standing-wave ratio (SWR) and causes it to fluctuate more with frequency.

The influence that v has on radiation efficiency and SWR is illustrated in **Figures 8** and **9**. These plots show computer-modeled data for the 10-centimeter diameter, 22-meter long CFD with N = 29 and a 100-percent, resistance-only loading profile computed at a

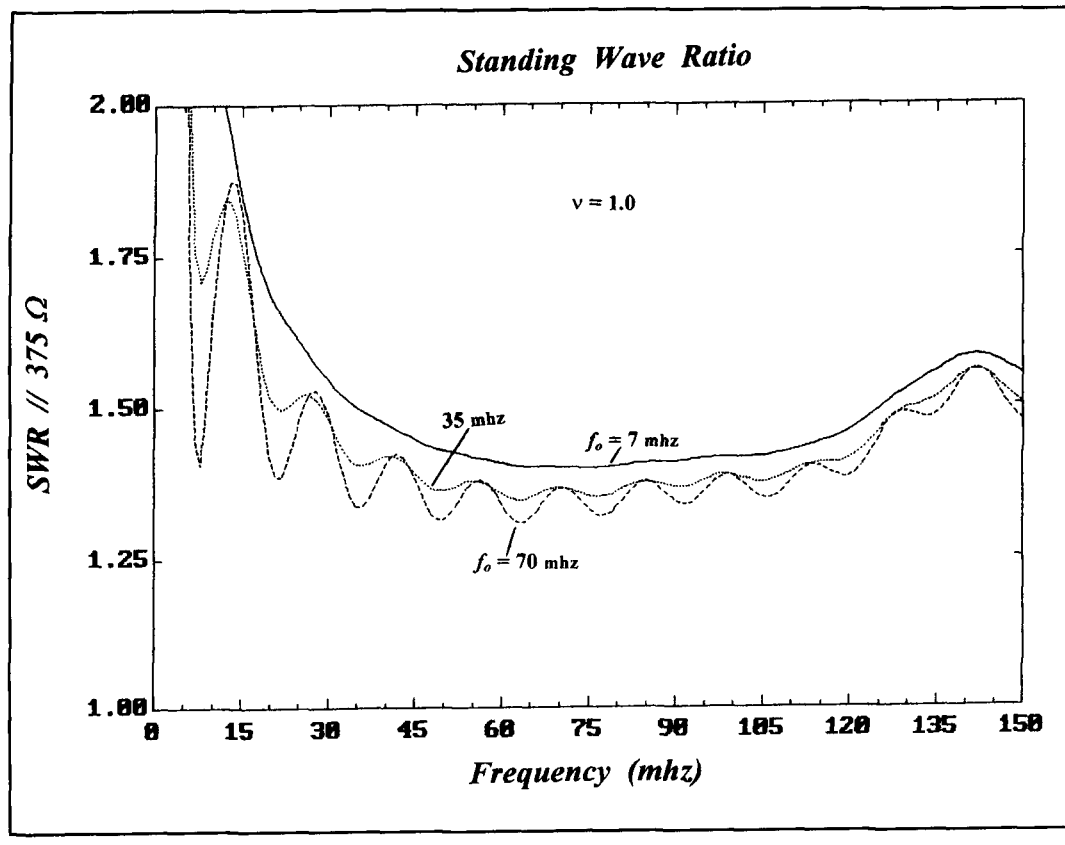

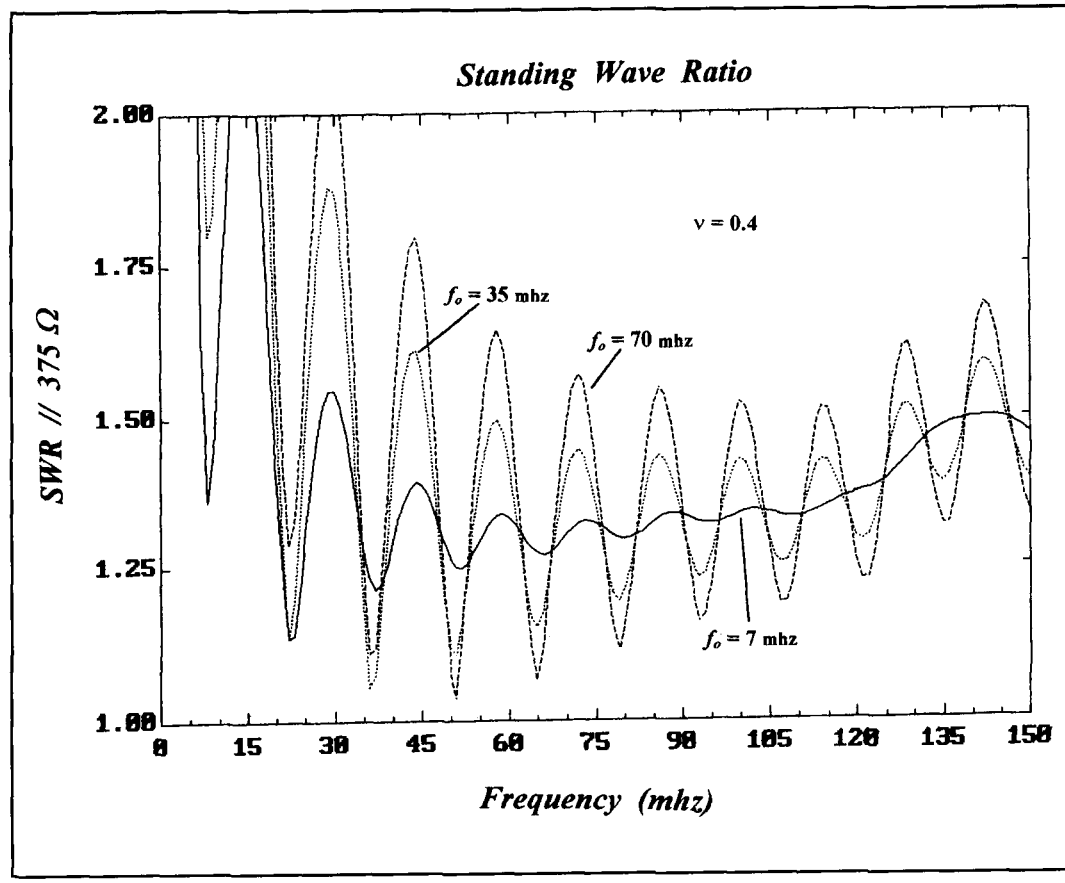

Figure 11. (A) Selecting f_0 = 70 MHz when ν = 1.0 results in generally the lowest SWR. (B) When ν = 0.4, f_0 results in an SWR ≤ 2 across most of the band.

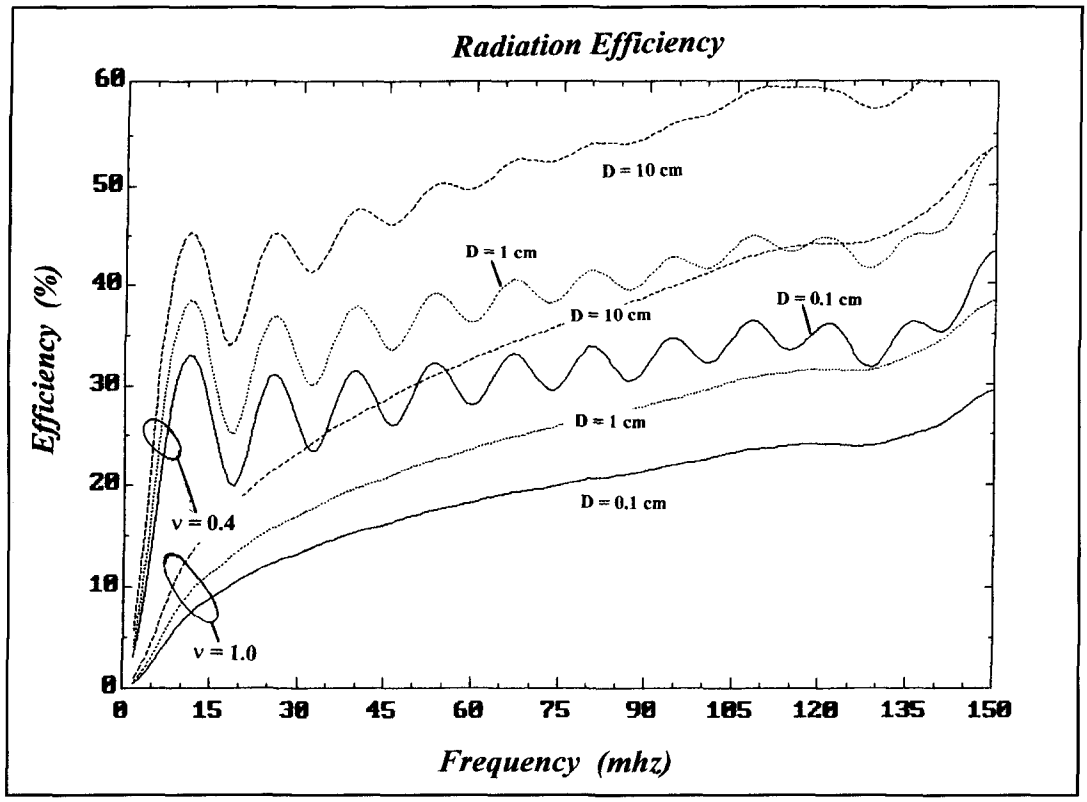

Figure 12. Larger diameter antennas have better radiation efficiency at all frequencies for both values of *v*.

design frequency f_o = 7 MHz. Efficiency and SWR are plotted as a function of the RF source frequency from 2 to 150 MHz. Calculations were made every 1 MHz.

The profile exponent v has a very significant effect on radiation efficiency, with lower values resulting in higher efficiencies. The curve in **Figure 8** for v = 1, which corresponds to the 100-percent WK loading profile, shows that the efficiency increases from about 1 percent at 2 MHz to about 54 percent at 150 MHz. The variation with frequency is smooth and monotonic. But as v decreases, the efficiency increases progressively more rapidly, especially at lower frequencies. When v = 0.2, the efficiency increases from about 14 percent at 2 MHz to more than 65 percent at 10 MHz—a 51-percent increase in a span of only 8 MHz. Beyond 10 MHz, the efficiency fluctuates more or less periodically, with a gradually increasing trend until it reaches a maximum above 75 percent at 150 MHz. For v = 0.05, the efficiency exhibits a pronounced quasi-periodic fluctuation. But its minimum value is more than 68 percent and the maximum is well above 80 percent.

Figure 9 plots SWR parametric in v for an RF source characteristic impedance of 375 ohms. If a different feed system impedance is used, an appropriate balun or other broadband transformer is required. For v = 1.0, the SWR varies smoothly from a maximum of greater than 2:1 at 12 MHz to a minimum of about 1.45 near 67 MHz. It then increases gradually above 67 MHz with a slight dip near 150 MHz. The curves for v = 0.8 and 0.6 show the same general trend. But, significantly, the SWR is generally lower with decreasing v, even though it fluctuates more at lower frequencies.

Figure 9B plots the SWR for v = 0.4 and 0.2. The SWR is generally lower for v = 0.4 than it is for v = 0.6, but the variability with frequency is much greater and the peak values are higher at some frequencies. For v = 0.4, the SWR exceeds 2:1 between about 12 and 16 MHz, but it is below 2 for v = 0.6. As v decreases to 0.2 and then to 0.05, **Figure 9C**, the SWR fluctuation becomes more pronounced and the peak values are higher. The minimum SWR values, however, are generally lower, and, on average, the SWR is still well below 2:1.

The best choice for v is evidently the lowest value that provides acceptable SWR at frequencies of interest. Choosing v in this way ensures the highest possible radiation efficiency, and the improvement is usually substantial.

Design frequency

The design frequency, f_o, is another important parameter in determining a good loading profile. Although it appears to be accepted

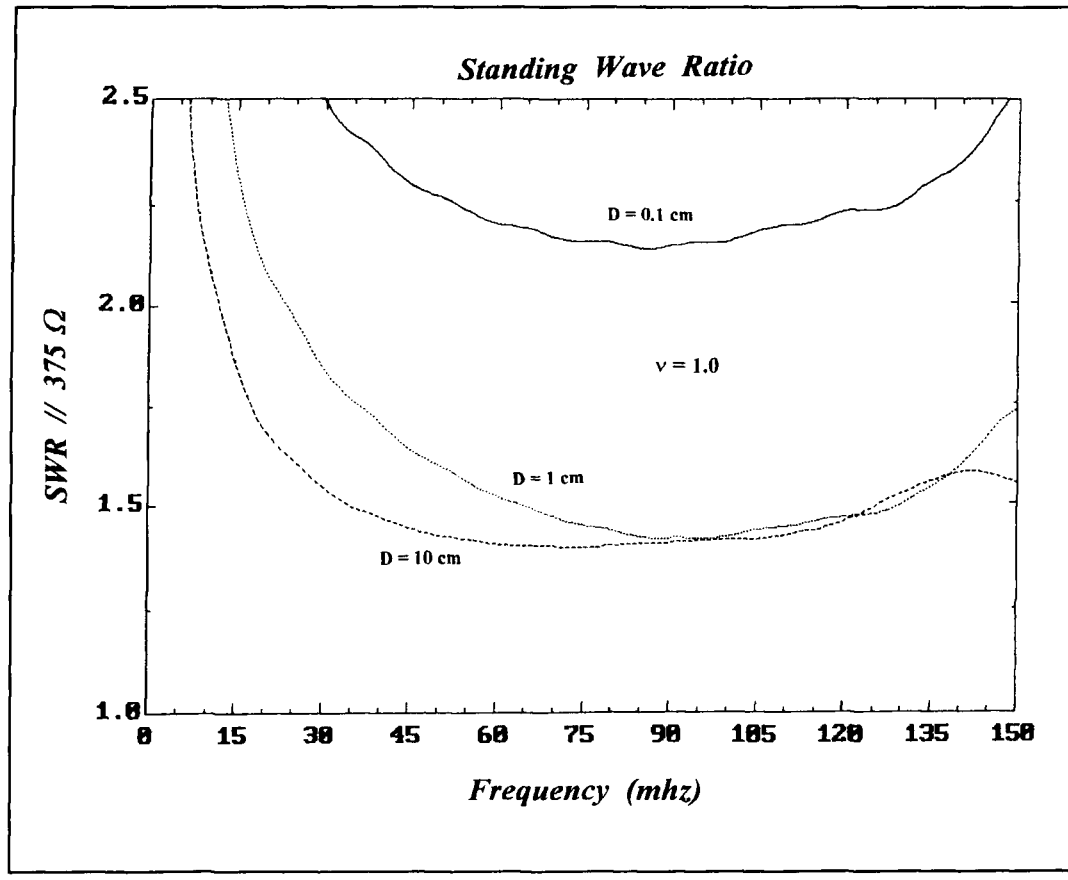

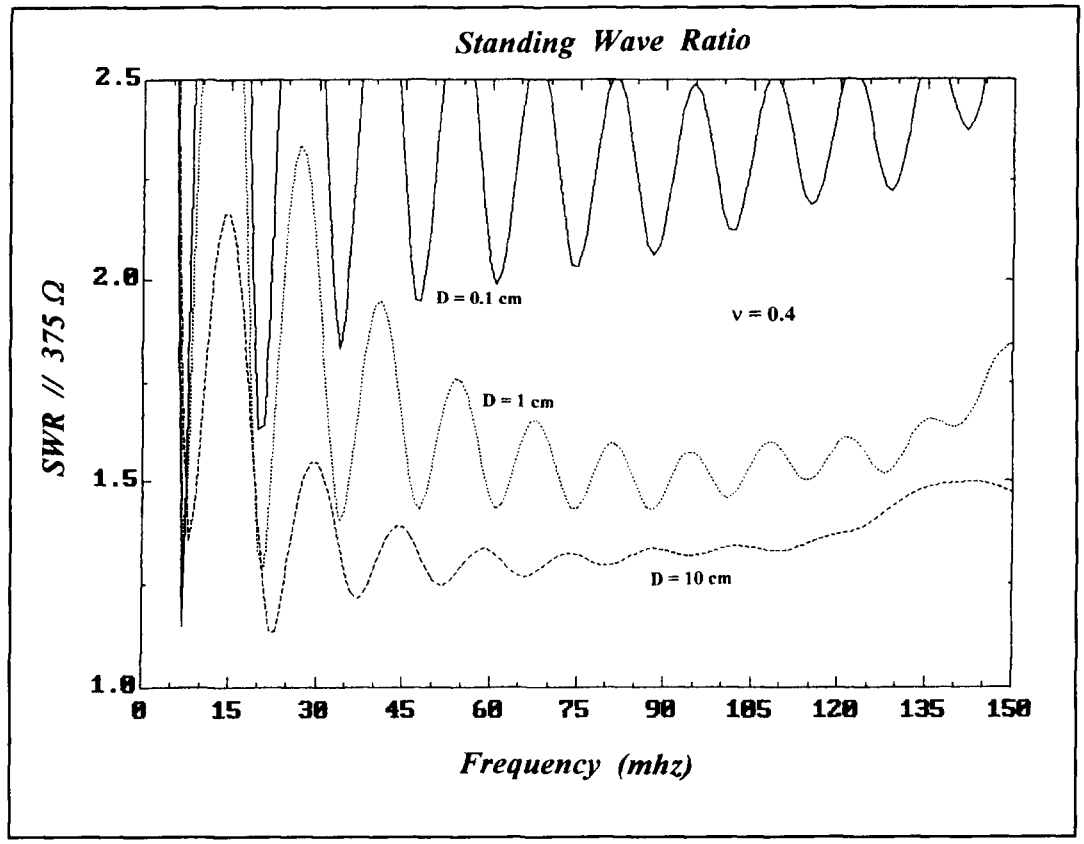

Figure 13. (A) SWR curves for $\nu = 1.0$. (B) SWR curves for $\nu = 0.4$.

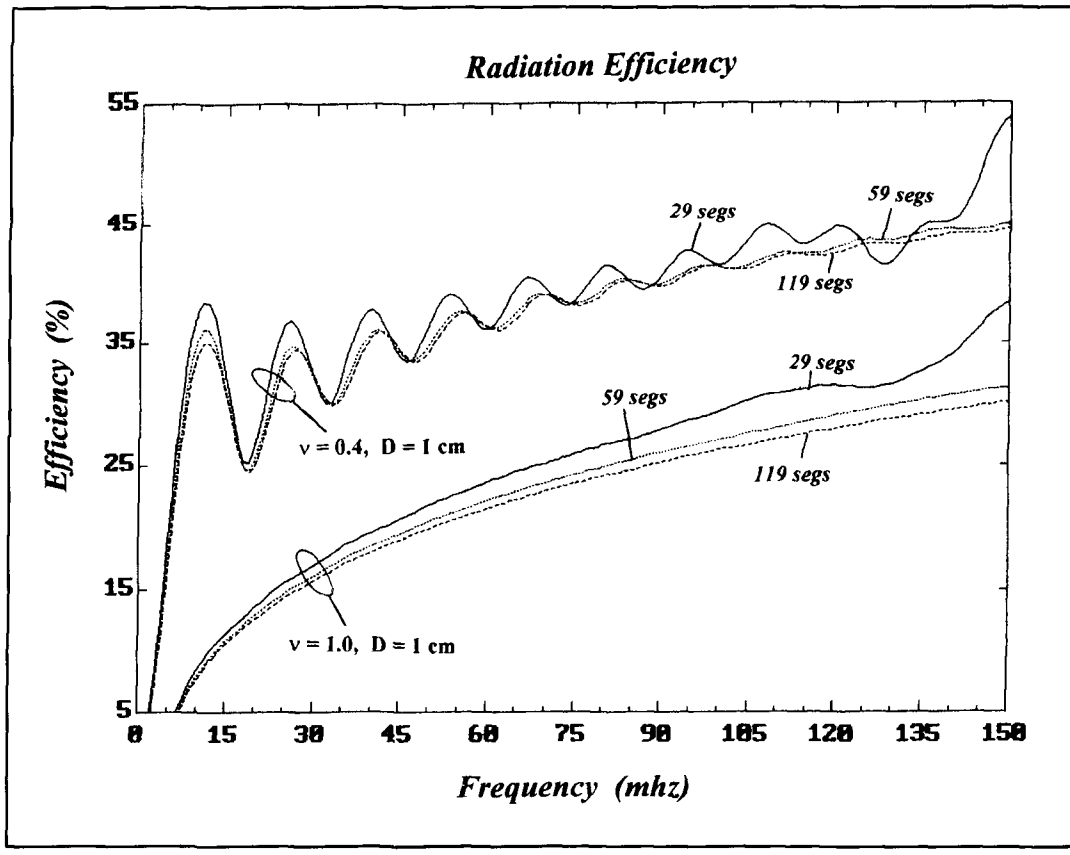

Figure 14. Efficiency curves show the least segmented area provides the best performance.

practice to choose f_o close to the CFD half-wave resonance frequency (see **Reference 3**, for example), this choice isn't necessarily the best. Because the expansion parameter, which plays a major role in determining the loading profile, is frequency dependent, the actual choice of design frequency must be based on how much a given loading profile improves bandwidth while still providing good radiation efficiency. There's no other sensible scheme for determining f_o, because there's no theoretical basis for choosing one value over another. Therefore the best approach is empirical, which is the approach adopted here.

Radiation efficiency and SWR plots for three design frequencies and two values of the profile exponent v are shown in **Figures 10** and **11** for a 22-meter-long, 10-centimeter-diameter CFD with N=29 and a 100-percent, resistance-only loading profile. Values of 7 MHz (approximately the half-wave frequency), 35 MHz, and 70 MHz were used for f_o, with v = 1.0 and 0.4 at each frequency. Except for the fundamental resonance, f_o was chosen arbitrarily. Other choices would yield different results, but the observations made here are still generally applicable.

As expected, the lowest efficiencies in **Figure 10** result from the most heavily loaded profile (v = 1.0). The efficiency increases with frequency and shows slightly more variability at the higher design frequencies. The less heavily loaded profile (v = 0.4) is much better, especially between 2 and 10 MHz. The higher values of f_o increase the fluctuation in the efficiency, but the variability isn't great.

The most important feature of the efficiency data is that higher design frequencies result in substantial improvements. f_o has a major impact on radiation efficiency, and its influence is greater for profiles with lower values of v. Because the efficiency increases with decreasing v, the influence that f_o has becomes even more important. Thus, even though the 22-meter CFD has a fundamental resonance near 7 MHz, choosing a design frequency that is *10 times greater* provides better performance. For example, as the curve for v = 0.4 shows, the radiation efficiency at 10 MHz is about 45 percent when f_o = 7 MHz, but it increases to 67 percent when f_o is increased to 70 MHz. The higher design frequency produced a much better antenna.

The advantage of a higher design frequency is also evident in the SWR plots of **Figure 11**. It's quite significant that selecting f_o = 70 MHz when v = 1.0 (**Figure 11A**) results in generally the lowest SWR across the entire 2- to 150-

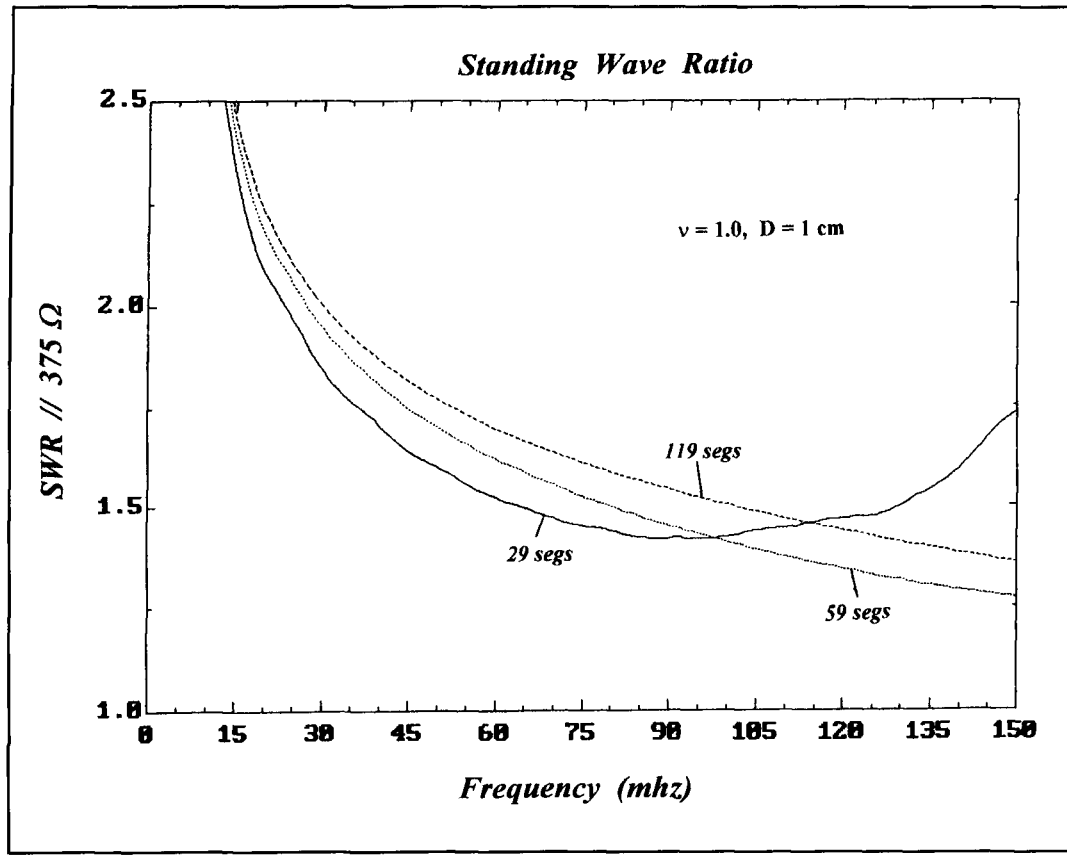

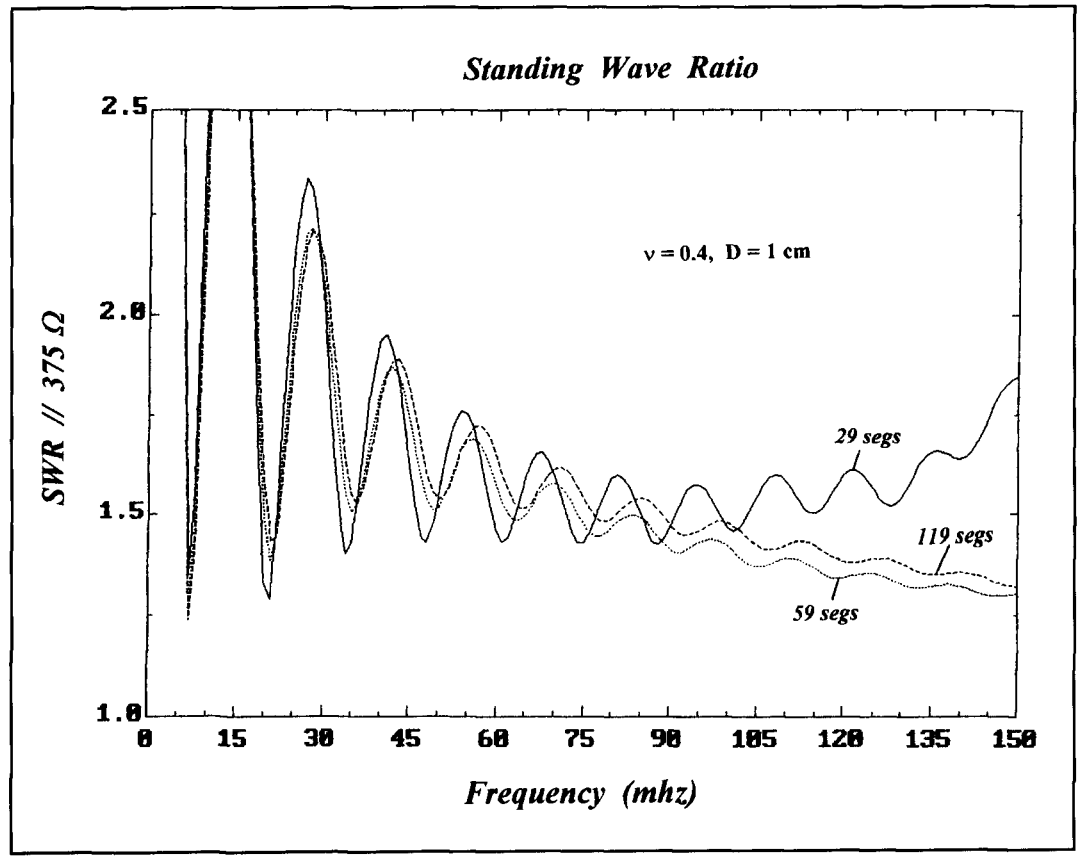

Figure 15. Lowest segmentation probably provides the best overall performance. (A) v = 1.0, D = 1 centimeter. (B) v = 0.4, D = 1 centimeter.

MHz band. When $v = 0.4$ (**Figure 11B**), choosing $f_o = 70$ MHz results in SWR ≤ 2 across most of the band. The variability is greater and the SWR is not consistently lower with increasing f_o, as it is when $v = 1.0$. But these effects are minor and better overall performance usually results from higher values of f_o.

Radiating element length-to-diameter ratio

Performance data for various L/D ratios appear in **Figures 12** and **13**. Radiation efficiency and SWR were computed for radiating element diameters of 0.1, 1, and 10 centimeters with profile exponents of $v = 1.0$ and 0.4. The corresponding L/D ratios are 22,000, 2200, and 220, which represent antennas ranging from "extremely thin" to "thin." The CFD is 22 meters long with 29 segments and a 100-percent resistance-only loading profile computed at a design frequency of $f_o = 7$ MHz.

Increasing the element diameter is a standard broadbanding technique for wire radiators. It is, therefore, not surprising that a larger diameter impedance-loaded CFD exhibits better overall performance than its thin counterpart. In **Figure 12**, for example, larger diameter antennas have better radiation efficiency at all frequencies for both values of v. The improvement in efficiency becomes progressively greater at higher frequencies and approaches a factor of 2 at the high end of the band. For the profiles with $v = 0.4$, increasing the element diameter also reduces fluctuations in the efficiency curve. The curve for D = 10 centimeter, for example, is much flatter than the curve for D = 0.1 centimeter. This effect isn't evident in the heavily loaded profiles when $v = 1.0$.

SWR curves for $v = 1.0$ appear in **Figure 13A**. The largest diameter element provides the best performance, especially at lower frequencies. Its SWR is below 2.5 at all frequencies above 6.5 MHz and is below 2 above approximately 12 MHz. The SWR decreases quickly up to about 30 MHz and flattens out below 1.5 for most of the rest of the band. By contrast, SWR for the very thin element (D = 0.1 centimeter) is high, being above 2 throughout the band and above 2.5 below 30 MHz. The very thin radiator thus fails to provide acceptable SWR even though it is very heavily loaded.

Similar SWR behavior appears in the curves for $v = 0.4$ in **Figure 13B**. The fattest element provides the best performance. Its SWR is below 1.5 over most of the band and below 2.15 at all frequencies above 6 MHz. Decreasing the diameter to 0.1 centimeter increases the SWR, but not as much as it did for the more heavily loaded profile with $v =$ 1.0. When $v = 0.4$, however, the SWR variability becomes much more pronounced for smaller element diameters.

Building an antenna with a low L/D ratio—that is, making it "fatter"—may be difficult if too large a diameter conductor is required. Fortunately, a continuous cylindrical surface often can be approximated by a sufficient number of parallel wires (usually ≤ 8) uniformly spaced around the cylinder's circumference. This dipole structure, sometimes called a "cage dipole" because of its resemblance to a bird cage, offers a convenient and effective alternative to large diameter cylinders for low L/D ratio designs, which are clearly superior.

Segmentation

Radiation efficiency and SWR data for different segmentation (values of N) appear in **Figures 14** and **15**. The results are somewhat surprising. A 22-meter-long, 1-centimeter-diameter CFD was modeled with N = 29, 59, and 119 segments. A 100-percent, resistance-only loading profile with $v = 1.0$ and 0.4 was computed at a design frequency of $f_o = 7$ MHz.

The efficiency curves in **Figure 14** show that the least segmented antenna (N = 29) provides the best overall performance. As the segmentation increases, radiation efficiency generally decreases, although the change isn't great from N = 59 to 119. This result is unexpected, as increasing segmentation presumably provides a better approximation to the continuous loading profile. However, the data show quite convincingly that the net effect of adding more discrete resistance is to increase the i^2R losses more than the radiated power, resulting in lowered efficiency. This effect occurs for both values of the profile exponent v. As is typically the case, the efficiency fluctuates more with frequency as v decreases, and the variability is greatest at the low end of the band. One beneficial effect of increasing N is to reduce the fluctuation somewhat, but the change is not pronounced, and it occurs only when $v = 0.4$.

The SWR data in **Figure 15** aren't as clear cut as the efficiency data in **Figure 14**, but the general conclusion is still that the lowest segmentation probably provides the best overall performance. For $v = 1.0$, the SWR is lowest for N = 29 at frequencies below approximately 90 MHz (roughly 12 times the fundamental resonance). In the same frequency range, it is not significantly different from the N = 59 or 119 values, even when $v = 0.4$. Above 90 MHz, the antenna with N = 59 performs best for both values of v, but the 119-segment design is very close. Nevertheless, in that same frequency range, "eyeball average" SWRs for N = 29 are,

say, 1.6 for $v = 1.0$ and 1.65 for $v = 0.4$, which are very good indeed. Thus, the least segmented antenna provides very robust SWR performance at all frequencies across the entire band.

Conclusion

This article has examined impedance-loaded wideband antenna elements and described an improved loading profile. Adding resistance and reactance to an antenna can dramatically improve bandwidth, but doing so reduces radiation efficiency. The tradeoff between greater bandwidth and reduced efficiency is not arbitrary. Some loading profiles are far better than others for designing wideband antennas.

Previous theoretical profiles, especially when modified as fractional profiles, provide a sound basis for loaded element design that yields good results. The improved loading profile described here generalizes the previous theoretical work to a power law traveling-wave current mode, which increases the average antenna current, improving radiation efficiency. Computer-modeled SWR and efficiency data show that the improved profile does indeed provide better performance than previously used profiles. The new method for calculating element loading promises to yield better antennas in terms of bandwidth and efficiency and will, hopefully, be put to good use to accomplish this goal.

This article has also investigated key design parameters for wire radiators loaded with uniform-step, discrete, resistance-only profiles. Observing the following guidelines should result in wideband antenna designs with very good performance:

(a) Perhaps the most important design parameter is the profile exponent v. Lower values of v result in higher radiation efficiencies and the improvement is very significant. The optimum value for v is the smallest value that provides acceptable SWR at frequencies of interest.

(b) Because the design frequency f_o is usually chosen near the fundamental CFD resonance, it is somewhat surprising that higher frequencies generally result in substantially better radiation efficiency. This effect is especially evident in loading profiles with smaller values of v. Higher values of f_o also usually give better overall SWR performance. The optimum value for f_o is, therefore, the highest value that provides acceptable SWR at frequencies of interest.

(c) The lower the L/D ratio, the better. Large diameter radiating elements provide much more bandwidth than thin ones in any wire antenna, even antennas without impedance loading. A large diameter radiator makes it easier for impedance loading to maximize bandwidth even further. If necessary, large diameter conductors can be approximated by a sufficient number of parallel wires (usually at least eight).

(d) Reducing segmentation (the number of discrete resistors used to approximate a continuous loading profile) results in somewhat better radiation efficiency. SWR isn't particularly sensitive to segmentation at "low" frequencies, and it is slightly better with increased segmentation at "high" frequencies. For a thin antenna, low frequencies are less than about 12 times the fundamental resonance, and high frequencies are greater, but this boundary is not well defined. The segmentation design guideline is, therefore, to use the smallest number of discrete resistors that meets the SWR objectives. ■

REFERENCES

1. E.O. Willoughby, "An Improved Wideband Aerial," Patent Specification No. 162,009, Commonwealth of Australia, August 13, 1953.
2. E.E. Altshuler, "The Traveling-Wave Linear Antenna," *IRE Transactions on Antennas and Propagation*, July 1961, p. 324.
3. T.T. Wu and R.W.P. King, "The Cylindrical Antenna with Nonreflecting Resistive Loading," *IEEE Transactions on Antennas and Propagation*, May 1965, pp. 369–373 (see also Corrections, p. 998, *IEEE Trans. Ant. Prop.*, November 1965).
4. M. Kanda, "Time Domain Sensors for Radiated Impulsive Measurements," *IEEE Transactions on Antennas and Propagation*, May 1983, p. 438.
5. B. Rama Rao and P.S. Debroux, "Wideband HF Monopole Antennas with Tapered Resistivity Loading," IEEE Military Communications Conference, Monterey, California, September 30–October 3, 1990 (MILCOM '90).
6. B. Rama Rao, "Optimized Tapered Resistivity Profiles for Wideband HF Monopole Antenna," 1991 IEEE Ant. & Prop. Soc. Symposium, London, Ontario, Canada.
7. L. Little, O. Ramabi, and R. Mittra, "Combined Tapered Resistive and Inductive Loading to Increase the Bandwidth of Small Antennas," *Proceedings of the IEEE Ant. & Prop. Soc. Symposium*, July 1992, p. 2089.
8. M. Abramowitz and I. Stegun, *Handbook of Mathematical Functions With Formulas, Graphs, and Mathematical Tables*, U.S. Department of Commerce, National Bureau of Standards Applied Mathematics Series 55 (AMS 55), Ninth Printing, November 1970, p. 231.

PRODUCT INFORMATION

New Toshiba MCUs for Handheld Battery-powered Applications

Toshiba America Electronic Components, Inc. (TAEC) has added six new members to its TLCS-870 microcontroller (MCU) line. These devices can operate at voltage levels as low as 1.8 volts and are ideal for handheld battery-powered applications.

The MCUs are equipped with a six-channel, 8-bit S/D converter that operates down to 1.8 volts. They also have 412 basic instructions allowing for a reduced program size. Ten interrupt sources let the MCU respond faster to real-time system requirements.

To learn more contact TAEC, 9775 Toledo Way, Irvine, California 92718; Phone: (800) 879-4963.

Because we were unable to obtain reproduction permission from the author, the following article does not appear in the *ARRL Communications Quarterly Collection*...

Transmission Line Transformers

By Donald A. McClure, KB2Z

12 West Azalea Lane
Mt Laurel, NH 08054

Summary: A detailed discussion of family of transmission line transformers that offers optimum flexibility in impedance transformations (compared to Guanella devices).

Summer 1997 issue, pages 45-58.

Please contact the author for additional information.

PRODUCT INFORMATION

High Grade VCXOs Made to Order and Expedited by Jan Crystals

High stability VXCOs are now being made to order by Jan Crystals, in frequencies from 1 MHz to 40 MHz. Expedited service is available for orders of any size.

Jan offers voltage controlled crystal oscillators made to customer specifications, in either 14 pin DIP or 8 pin DIP packages with rugged resistance welds. High stability, ±3ppm @ 5V ±10%, and wide pullability, maximum 300 ppm ±150, make the Jan oscillators suitable for a wide range of applications. All feature tight linearity and output symmetry, 50% ±10%, with control voltage of +2.5 ±2V and an output load of 10 TTL +15pF. Other standards include a VoH level of +2.4V minimum, VoL level +0.4V maximum, and rise and fall time of 6 ns maximum.

Jan VCXOs are stable over wide temperature ranges, operating from -35°C to +80°C and storing from -125°C to +155°C.

For more information, contact Jan Crystals; Phone: (800)-JAN-XTAL (526-9825); Fax: (941) 936-3750.

R.P. Haviland, *W4MB*
1035 Green Acres Circle North
Daytona Beach, Florida 32119

THE INFLUENCE OF GROUND ON HORIZONTAL ANTENNAS

And on Ground Effect Calculation

When an antenna is operated close to ground, the close-in electric field is modified because the ground dielectric constant is different from that of free space, or of air. Only in rare cases is there a direct change in the magnetic field of the antenna, as most soils are nonmagnetic. However, a loss is almost always introduced because most soils are partly conductive.

Because these factors cause the near fields of even simple antennas above ground to become markedly nonsymmetric, the magnitude of the effects is especially difficult to analyze. Several very approximate methods have been developed. One is to assume that the effect on the antenna can be neglected, that the antenna characteristics are the same as in free space. This gives a value of 73+j42.5 for an infinitely thin half-wave dipole. For very great heights, this "no calculation method" is nearly true, but the effects of the ground start to be noticeable for heights of 3 to 5 wavelengths.

Another method assumes that the ground can be replaced by a sheet of metal, a perfect reflector. Such analysis is easy. Simple geometry is maintained and the ground can be replaced by a mirror-image antenna, the two spaced twice the height above ground. This leads to the thin dipole drive resistance curve of **Figure 1**, developed from data in Kraus.[1] However, the curve below 0.2 wavelength is highly suspect because the zero ground resistance would lead to nearly infinite current in a resonant antenna just above ground. (There is an equivalent curve for drive reactance, but this variation is universally ignored in texts.)

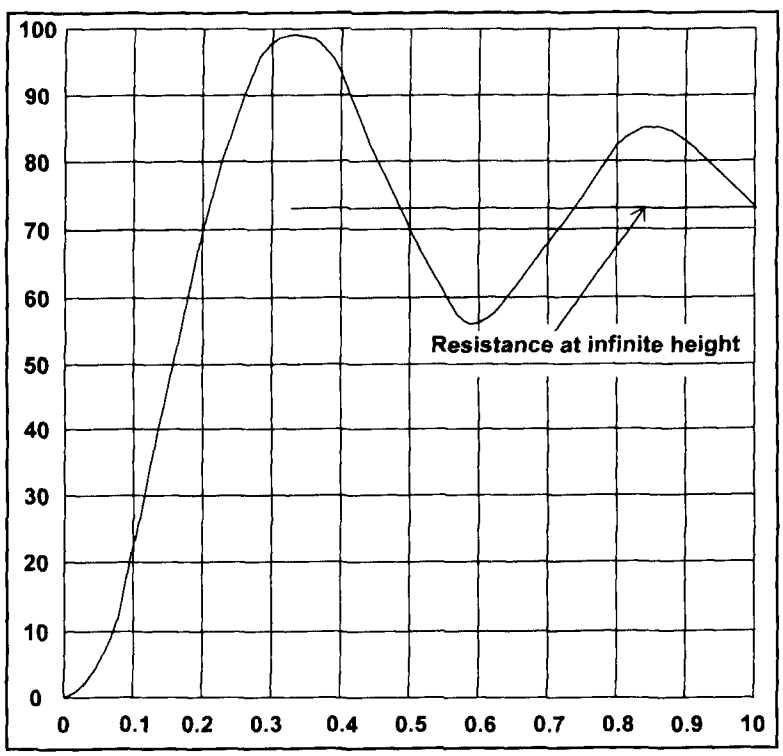

Figure 1. Drive resistance of an infinitely thin dipole antenna above perfect ground. The free-space value is shown. After Reference 1.

Remember that these two methods were the

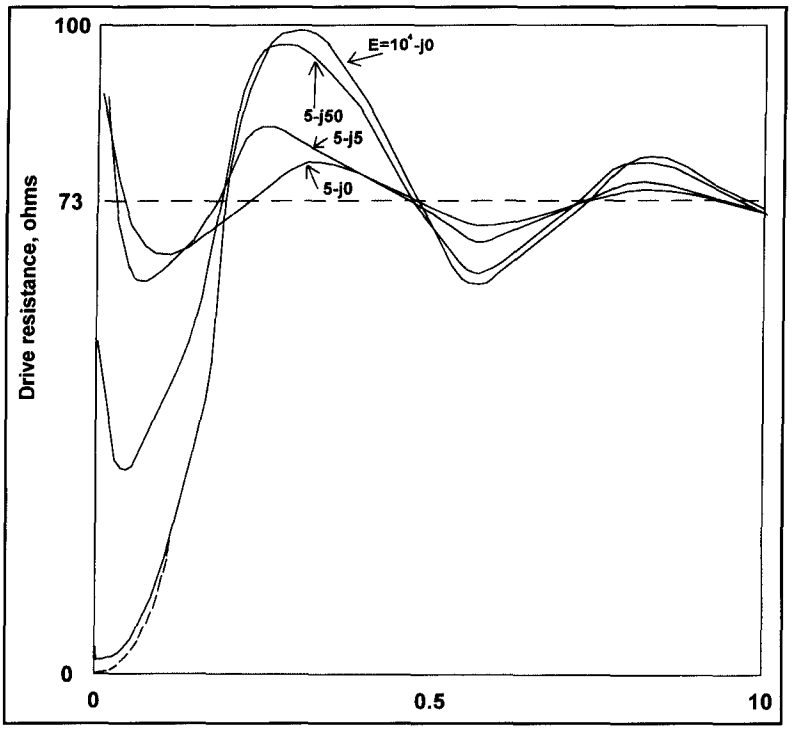

Figure 2. Drive resistance of an infinitely thin dipole above earth as calculated by the "exact image" theory. The curve parameters are the complex ground dielectric constant, A+jB. The perfect ground case is shown dotted. After Reference 4.

only ones available for practical use until recently—as in the popular antenna analysis program, MININEC, and its derivatives. For MININEC, one must be suspicious of the drive characteristics for low height antennas. Note

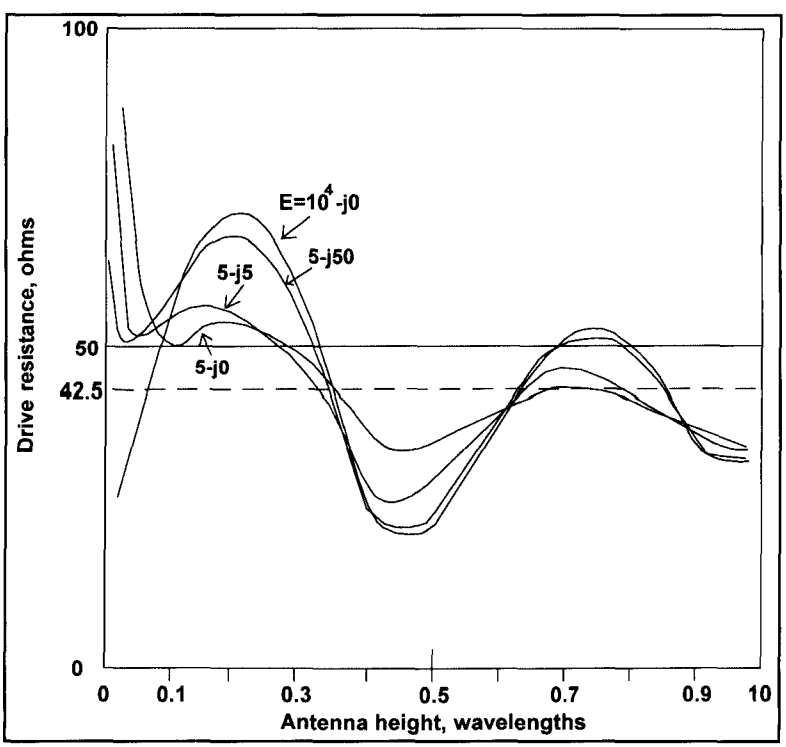

Figure 3. As Figure 2, but showing drive reactance. After Reference 4.

that there may be secondary effects, the most noticeable being overly optimistic values of lobe nulls.

More accurate methods

There are several more accurate analysis methods. The first is based on the concept that the reflection from the ground is not the unity value implied by the perfect ground analysis, but some smaller value instead. This is expressed as a complex number to account for both loss and dielectric constant. While appreciably better than the ideal ground method, this "reflection coefficient analysis" analogy isn't perfect. In the case of segmented antennas, it exaggerates the influence of a segment on its mirror image and approximates that of other segments. Read **References 2** and **3** for additional data on this method.

Another technique is based on solution of what are known as the Sommerfield equations, a mathematically exact method nearly 100 years old. The problem with this method is that the relations become so complex that approximate solutions must be used. The Sommerfield method is known to be more accurate than the reflection method, with both better than the free-space or ideal ground method. Unfortunately, the calculation approximations mean that results at low heights must also be viewed with suspicion.

I haven't undertaken a full study of the limitations of these methods, nor have I found one in the literature. I have not found a comprehensive comparison of measured antenna impedances versus height where the ground characteristics have been determined accurately. Without a full theory or a set of careful measurements, it isn't possible to be certain of the range of usefulness of the above approximations.

The "exact image" method

There is, in the literature, another approach to ground effects calculation.[4] This is based on the image antenna concept, but modifies the current on the image antenna to account for the presence of ground, so it's called "the exact image" method. The equations are also complex and must be solved by approximations, but the form indicates that results accuracy is not too sensitive to height. Also, several special cases can be compared with exact theory, and indicate that the relations are "well-behaved."

The results given in the reference show what's happening with a half-wave dipole close to earth. **Figure 2** is the drive resistance for several values of ground parameters. Here the form A+jB indicates the complex dielectric constant, also expressed as Er-jS/(2*Pi*F*Eo),

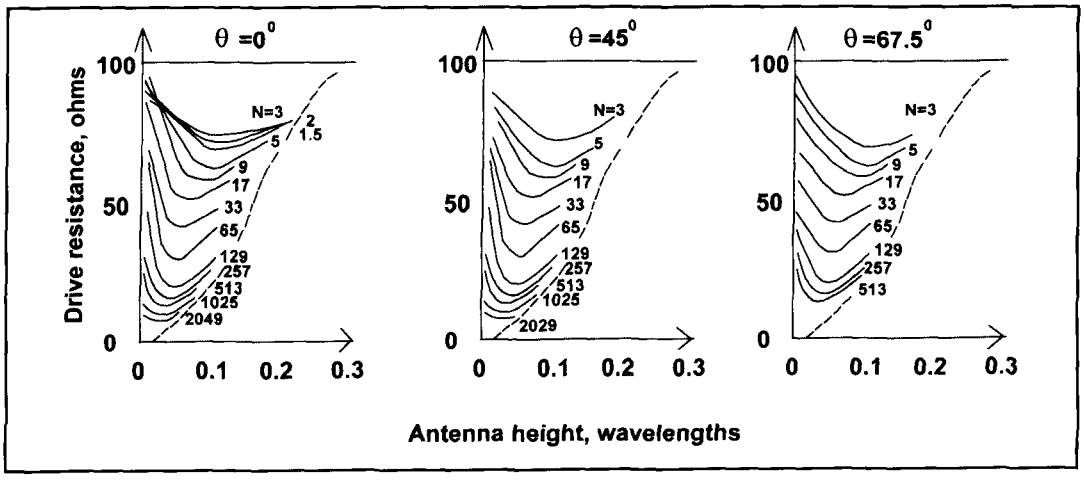

Figure 4. Drive resistance variation with antenna diameter and height. Omega is the thickness parameter, 2*Logn(2*Pi*b/a), where b is the length of the antenna and a is its radius. After Reference 4.

where Er is the relative permittivity of the earth, S is its conductivity, F is the frequency, and Eo is the permittivity of free space.

The curve labeled 5-j5 represents a poor soil. For such soils, the drive resistance oscillates about the free space value of 73 ohms. A larger value of the j-term means higher soil conductivity. With higher conductivity soils, the drive resistance tends toward the ideal earth values (shown dotted). Note that certain heights can provide the same drive resistance for different soils, a fact which complicates use of antenna input impedance for measurement of soil conditions.

Figure 3 shows the drive reactance. The same oscillation about the free-space reactance occurs, around 42.5 ohms (dipoles must be shorter than a half wave to show resonance). At low heights, the amount of shortening needed for resonance increases for most soil conditions. Comparing curves shows that very high conductivity with antennas close to the ground essentially leads to a short-circuited antenna of zero drive impedance.

Figure 4 shows, in detail, the behavior of the drive resistance as the ground conditions move toward ideal earth. The ground parameter is expressed in the form E=(1+2^n)*e^-jTheta, with n and theta plotted. The drive resistance is sensitive to the magnitude of the complex dielectric constant, E, but insensitive to its phase angle.

For low conductivity soils low in water content, very low antennas behave as if they were partly surrounded by fairly good insulation. This reduces the wave velocity, thereby effectively increasing the antenna length, without much change in drive resistance. Where high conductivity is due to large moisture content, the drive resistance moves toward the ideal earth condition: due to the high dielectric constant of water there is also a change in effective length, which

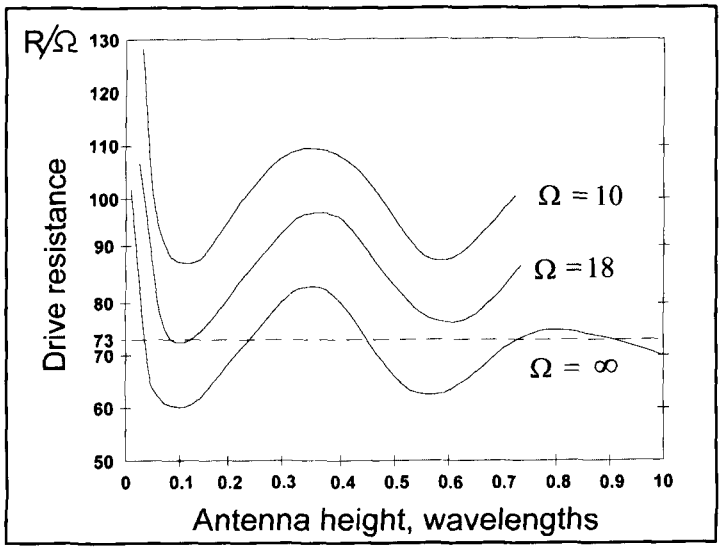

Figure 5. Drive resistance of an infinitely thin antenna for various values of the complex ground dielectric constant in the complex form, see text. The perfect ground case is shown dotted. After Reference 4.

shows as an increase in the reactance.

These curves are for infinitely thin dipoles. One of the features of this analysis method is that the drive impedance Zd is of the form Zd=Zf+Zg, where Zf is the free space impedance and Zg is the contribution of the ground (actually, that of the exact image of the antenna). This leads to the drive resistance curves of **Figure 5**. The parameter here is the thickness factor, 10 representing a dipole of tubing, 18 one of fairly heavy wire, and infinity representing an extremely thin wire—perhaps an "invisible" antenna. These curves are for the 5-j5 soil type.

Measuring up

Table 1 is a compilation of the calculated drive impedance of a half-wave dipole at vari-

Table 1. Comparison of Ground Analysis Methods

	METHOD OF ANALYSIS				
HEIGHT	EXACT IMAGE	SOMMER-FIELD	REFL. COEFF. R+JX	PERFECT EARTH	IDEAL R only
1.0	82+j36	74+j41	74+J41	75+j36	74
0.9	79+j39	80+j41	80+j41	89+j40	83
0.8	81+j45	83+j47	82+j48	86+j54	82
0.7	70+j50	76+j52	76+j52	71+j58	68
0.6	61+j50	69+J48	69+j47	61+j44	57
0.5	67+j37	70+J38	72+j38	72+j27	69
0.4	83+j38	83+j36	83+j36	95+j31	92
0.3	86+J45	90+j48	91+j48	102+j61	97
0.2	78+j58	81+j61	81+j64	72+j85	70
0.1	45+j55	68+j60	59+j64	23+j67	24
1/20	33+j57	76+j62	55+j72	6+j38	5
1/100	50+j83	121+j128	110+j1274	.2+j8	~1
Conditions		f=5 MHz 15 segments cond.=1.39E-3	e=5-j5 K=5	a=.0001	

Comparison of antenna drive impedances of a 30-meter-long antenna at 5 MHz, as calculated by various methods. The Sommerfield, reflection coefficient, and perfect earth values are calculated by NEC for a wire diameter of 0.0001 meter (omega=29), with a ground dielectric constant of 5 and a conductivity of 1.39E-3. The exact image values are for the same ground parameters, but for an infinitely thin antenna. The ideal resistance is also for an infinitely thin antenna.

ous heights as determined by the methods available. These are for poor soil, (5+j5), for a dielectric constant of 5, and a conductivity of 1.39E-3 at 5 MHz. The Sommerfield, reflection coefficient, and ideal earth values are calculated by NEC with 15 segments and a diameter of 0.0001 meter. Other values are read from the curves of the figures. Values are given from left to right in order of best to worst approximation.

Comparison of these values leads to the following information:

- The free space value is nearly correct for heights above about 3 wavelengths.
- The ideal earth approximation is usable above about 1 wavelength height, poor below this, and very poor below about 0.2 wavelengths.
- The reflection coefficient method as used by NEC is usable above about 0.2 wavelengths, but is poor below this height.
- The Sommerfield method as used by NEC is usable down to about 0.1 wavelengths, but is poor below this height.
- All methods indicate that the effect of ground on dipole drive characteristics can be completely neglected in the practical sense for heights greater than one wavelength, and usually for heights above 0.2 wavelengths.

The NEC calculation methods can be applied to any antenna. While this is possible in principle with the exact image method, the calculations become complex. A combination of the moment and the exact image method could be developed to apply to any antenna. This hasn't seemed to be justified, especially in view of the likelihood of unknown ground parameter values in a real situation and the variability of parameters with time as soil moisture changes.

In other words, the practical accuracy of all calculation methods is likely to be determined more by the problems of determination of ground conditions than by limitations in the calculation method. Because of this, when investigating the performance of very low antennas, it is suggested that calculations be repeated with differing ground parameters to determine sensitivity to this factor. If a high sensitivity is found, plan on measurement of drive characteristics of the real-world antenna.

Most of the antenna drive problems introduced by the earth when using low antennas can be eliminated with the implementation of a good antenna tuner. However, the pattern will be that of a low antenna, and there may be reduced signal level if the ground is lossy. A change in ground moisture is likely to cause a change in drive characteristics. ■

REFERENCES

1. John D. Kraus, *Antennas*, 2nd edition, McGraw-Hill, 1988.
2. *ARRL Antenna Handbook*, current edition, the American Radio Relay League, Newington, Connecticut, 1995.
3. George H. Hagn, "HF Ground Measurements at the LLNL Field Site," *ACES Journal*, V3N2, Fall 1988.
4. Ismo Lindell et al., "Exact Image Method for Impedance Computation of Antennas Above the Ground," *IEEE Trans. Ant. Prop.*, AP-33, September 1985.

Joseph J. Carr, *K4IPV*
P.O. Box 1099
Falls Church, Virginia 22041
e-mail: <carrjj@aol.com>

HOW JUNK SCIENCE GOES WRONG (SOMETIMES)

Some further ruminations on a tantalizing topic

Junk science, and revisionist history, is sometimes offered up by people who make serious errors in interpreting data. They're not dishonest, just wrong. And it isn't always so easy to spot one's own mistakes. Let's take a look at some common forms of error:

1. The underlying order mistake
2. The familiarity ("But I Know Someone Who...") mistake
3. The regression mistake
4. The false consensus mistake
5. The one-sided evidence mistake
6. The misframed question mistake
7. The necessary-versus-sufficient mistake
8. The secondhand sources mistake
9. The imprecise criteria mistake
10. The overcritical response mistake
11. The incomplete evidence mistake
12. The Post Hoc Ergo Propter Hoc mistake

These mistakes can cause misinterpretation of data. Some mistakes are particularly bad when dealing with survey, sociological, psychological, and other forms of supposedly "soft" data that are hard to quantify. However, hard numerical data can also suffer from the same abuses of misinterpretation. Let's take a closer look.

The underlying order mistake

Humans are uncomfortable with disorder because order implies predictability, while disorder implies unpredictability. Chaos, fear, and the inability to cope are the rewards of disorder. This tendency may be especially common in the West because of our scientific tradition. Our science is based explicitly on the assumption that there is a fundamental underlying order at the root of every phenomenon, no matter how disorderly it appears on the surface.

The expectation of order causes us to impose order where there is none. Some people see an "image" in the swirls of cumulus clouds. Others see a "man in the moon" or a strange "face" on the surface of Mars. When we look at data without imposing a rigorous scientific discipline, we may see many "Martian faces" emerging from a collection of purely random data.

Part of the problem is that we often don't know what randomness truly looks like. Many

"The tendency to impute structure and coherence to purely random patterns is wired deep into our cognitive machinery, and it is unlikely to ever be completely eliminated."

— Thomas Gilovich
How We Know What Isn't So
MacMillan/Free Press (1991)

people erroneously believe that randomness implies there are no short-term orderly sequences in data. In coin flipping, for example, when we see several "heads" come up in a row, we may assume that the coin is somehow biased. Gilovitch[1] calls this the "clustering illusion." When we look at data and see a pattern, we often don't look further; thereby erroneously believing that the pattern indicates a real phenomenon is emerging from the experiment. This effect is particularly strong if the short-term pattern confirms a favored preconceived theory about the final results.

The familiarity ("But I know someone who...") mistake

Individual data points are rarely important when deciding how to evaluate an entire body of data. This is especially true when the system is in what quality experts call "statistical control," and all variation is due to non-attributable common causes. But our psychology persists in making us try to see significance in single data points. A local TV news anchor recently questioned the FBI report that violent crime is down 3 percent this year compared with last year on the grounds that her husband had been mugged a few weeks before.

The regression mistake

If a process is truly random, then occasional individual events fall far from the mean. Data points close to or beyond the $\pm 3\ \sigma$ points may have a low probability of occurring, but it is not zero. Furthermore, when such an event occurs, there is a high probability that the next data point will be much closer to the mean. This is the well-known "regression to the mean" phenomenon. When we see unusually good results, we tend to expect the next result to be equally good or better.

If a process is truly random, then prediction is impossible for individual (as opposed to mass) events. In addition, the next event is likely to be much closer to the system mean rather than to the unusually good result. In the random system, it is virtually useless to compare isolated individual data points to each other because their difference is due to random occurrence.[2]

The false consensus mistake

Most of us believe at some deep level that we are well within the mainstream. We believe that our preconceived opinions, biases, and perceptions are representative of the mass of people rather than some smaller, more limited set. When looking at data, we may see trends where there are none, especially if some short trend in otherwise random data supports our view of things (see mistake no. 1). By either giving too much attention to confirming data (i.e., "sharpening"), or unconsciously suppressing discomfirming data (i.e., "leveling"), we may arrive at an incorrect conclusion. Such a conclusion may seem right, very right indeed, simply because: a) it matches our preconception of what it ought to be, and b) it seems to agree with an ambiguous alleged "consensus" of others.

The one-sided evidence mistake

This type of mistake emerges from situations where only one class of evidence is abundantly available. I've seen grown men—professional engineers—seriously claim that more elevators in our office building go up than go down! The reason for the misperception is that they were going down, and while they waited several "up" elevators went past their floor. Because they got on the first "down" elevator to arrive, they could only count one. Because elevators are cyclic, the only logical way their observation could be true is for elevators to be assembled in the basement and then either disassembled or stored on the roof. Or perhaps they return to the basement by another route that is hidden from view. By now, the building should be showing a distinct list to starboard from all those elevators on the roof! Data collection schemes in which only one of two (or more) possible outcomes can easily be captured are inherently flawed.

The misframed question mistake

The way that a survey question or experiment hypothesis is framed can have a profound effect on outcomes. If we ask "what evidence supports this view...", then we tend to pre-bias ourselves to look for confirming evidence rather

than all of the evidence. We may overlook valid disconfirming evidence because we either did not look for it, or failed to recognize it when it surfaced. We also see this effect when asking about similarities or differences between two classes of event, or when comparing evidence against some pre-existing model.

Misframing questions is easy enough when trying to conduct an honest study, but it seems to be a way of life in the case of advocacy research. If the point of a research study is to "prove" a pre-selected outcome, then the questions asked will be overwhelmingly biased towards the ideological prejudice of the questions' framers.

The necessary-versus-sufficient mistake

Just because an item of evidence *supports* a hypothesis doesn't mean that it *proves* it. Even if the evidence is totally necessary for the proof, it may not be *sufficient* for the proof. More elements of evidence may be needed to prove the case.

This form of error often comes from expecting too much information from too little data. It's especially likely to occur when, early in an experiment or study, a rather high number of confirming data points are noted. If there's a fair number of these confirming data points, then we may take a logical leap of faith and assert that those data prove that the hypothesis is true. Psychologists tell us that confirming data are cognitively easier for us to deal with, so we may tend to see confirmation where there is none.[1]

The secondhand sources mistake

This mistake is the result of accepting hearsay evidence from secondary or tertiary sources, rather than going to the primary sources for confirmation. Whether it's eyewitness accounts, expert opinion, or physical data collected according to good scientific principles, the fact that the information is reported secondhand through a third party makes the evidence subject to large errors. The game of "Telephone " (where a sentence is passed in whispers from ear-to-ear and then repeated out loud at the end of a chain of several recipients) clearly demonstrates how reporting of evidence can get badly garbled.

There's also a tendency for secondhand sources to interpret, embellish, selectively filter, or otherwise alter evidence they pass on. Quite apart from intentional alterations, made with deceit in mind, it's quite normal for honest, but fallible, humans to make such mistakes when transmitting evidence to others.

We often see cases where the results of a research paper or technical report are said to be better than they were in the original. In some cases, a relatively minor experimental result is amplified by each retelling, until eventually the result that's widely reported bears little resemblance to the original. Research is sometimes reported with great enthusiasm, often critically, and only later is it discovered that the reporter had never actually read the original research paper. There's a word for that: Bull#&*$.

Be particularly wary of reports cited not from the original source but from a derivative work that, in turn, cites the original. Such twice removed data is even more likely to be distorted, even when there's no intent to deceive.

There are a number of reasons why the secondhand source mistake occurs (absent deception, of course). One reason is the normal human need to tell a good story. The secondhand source may feel compelled to advocate a cause, or entertain the recipient, or to simply tell a well-received tale. Sometimes, because of space or time constraints, or because the one that offers the information assumes that mundane qualifying details are too boring or unimportant, critical facts about a study are omitted.

There's also the phenomena of "leveling" and "sharpening." If some portion of the results are de-emphasized in the retelling, then a kind of leveling effect occurs that tends to distort the actual result. Similarly, if a portion of the results are given unwarranted special emphasis, then that information tends to bias the conclusion towards that end of spectrum. Be cautious of wording such as "...as much as..." or "...as few as..." because they may indicate that there's some leveling or sharpening toward one end of a confidence interval.

The key to avoiding the secondhand source mistake is to rely on primary data as much as possible—even if it means taking the trouble to look up the original source. The primary source rule usually permits one to better evaluate the reliability of the evidence, to make further inquiries of the source, or to see the entire set of data within the context in which it was collected.

The imprecise criteria mistake

This mistake is caused by failing to precisely define what constitutes good data and what does not. The classes into which any given event falls may be vague or ambiguous enough that different observers, or the same observer at different times or under different conditions, will classify the same event differently. It becomes all too easy to subconsciously filter what is accepted and what is rejected when the criteria aren't

crisply defined. There's a natural tendency to accept a wide band of data as "confirming" a pet theory, while severely narrowing the band of data seen as disconfirming the theory.

The overcritical response mistake

If two or more tentative theories are in competition, advocates of one theory may submit the alternative theory to intense scrutiny, while at the same time barely scrutinizing the favored theory. Nearly all studies are flawed, and that can create problems. Although good experiment design can reduce the problem considerably, Nature is rarely so crisp and well-defined as our mental models imply.

There always seem to be unknown or poorly understood interactions and complexities that make the outcome uncertain. That's one of the reasons why C.I. Lewis'[3] view of knowledge, cited by W. Edwards Deming in his "Profound Knowledge" teachings,[4] is essentially probabilistic rather than definite. Because of this natural vagueness, intense scrutiny of any experiment can usually turn up flaws.

While it's proper to criticize any study in this manner (which is what the scientific process does), it is also proper to subject all competing theories to the same level of scrutiny. Unfortunately, our tendency is to closely scrutinize the opposition and not even look twice at our own positions.

Incomplete evidence mistake

If only part of the available evidence is considered, then it's likely that a poor decision will be made. This problem showed up in startling video news footage in January 1986 when the space shuttle Challenger exploded little more than a minute into the flight, killing all seven astronauts on board. The investigating commission blamed the fatal event on O-ring seals on the solid-fuel rocket boosters. The material of the O-rings tends to become brittle as temperature drops below a certain point.

Unfortunately, they graphed only the O-ring failure data, and it looked random. This error had the effect of making the team think that the overnight freeze wouldn't be a problem. But when the O-ring data for all of the flights is graphed, it demonstrates that all of the flights on which no failures occurred were at temperatures above 63 degrees. There emerges a distinct nonrandomness when all data are examined.

A variant on this fallacy is the decision taken on the basis of assumptions of alleged facts that aren't in evidence. An executive had lunch with a client in an expensive downtown restaurant. When she was ready to leave, she was surprised to see the headwaiter was holding her coat ready without seeing the claim check. "How did you know it was my coat?" asked the executive. "I don't know that it is your coat, Madame, I only know that it is the one you were wearing when you arrived." It is necessary to examine the facts, assumptions, and premises on which a decision is based in order to see whether or not they are true.

The Post Hoc Ergo Propter Hoc ("After This, Therefore Because of This") mistake

Another of our apparently deep psychological flaws in evaluating data is the need to see causality when data are merely correlated. We naturally tend to believe that if event B always follows event A, then somehow A caused B. When we make a scatter diagram of data, and see points seemingly clustered about a rising or falling imaginary line, then we know that some correlation exists, but we cannot properly say that the X-axis data causes the Y-axis data.

Causality, unfortunately, isn't the only reason for correlation. One reason for correlation might be an unaccounted for third factor. The classic example, often used in college logic classes, is the interesting observation that there's a positive correlation between the number of marriages and the number of armed robberies in Los Angeles over the period 1920 to 1980. Depending on which data we use as the X- and Y-axis of our graph, we might fairly conclude that either marriages cause armed robberies, or armed robberies cause marriages. The overlooked third factor, namely the huge (and nearly continuous) growth of Los Angeles' population between 1920 and 1980, may independently account for the increase in both marriages and armed robberies.

The Tukey-Mosteller[5] criteria provide a means for checking causality. Three conditions must be satisfied before one may reasonably propose causality: a) consistency, b) responsiveness, and c) mechanism. The consistency requirement means that the two correlated factors are routinely found together. If a test is run multiple times, and nearly the same correlation is always found, then we may assume that the consistency requirement is met.

Responsiveness means that a change in the independent variable results in a change in the dependent variable. The mechanism requirement is met if an adequate and testable theory is available to explain the relationship in causal terms. Deming[6] insisted on having a theory to explain results as a requirement for Profound

Knowledge. Otherwise, all we have is data and not information.

Conclusion

Very few people disagree that good decisions are based on good data. Just as important, however, is to not ruin the usefulness of good data by faulty interpretation. Being aware of these "dirty dozen" will help keep faulty interpretation from being a problem.

Acknowledgment

Thanks are due to Robert P. Reid, Director of the Organizational Effectiveness Institute, for sharing his knowledge and wisdom with me over the past several years. ■

REFERENCES

1. Thomas Gilovitch, *How We Know What Isn't So: The Fallibility of Human Reason in Everyday Life*, Macmillan/Free Press, New York, 1991.
2. Brian Joiner, *Fourth Generation Management: The New Business Consciousness*, McGraw-Hill, New York, 1994.
3. C.I. Lewis, *Mind and the World Order*, Charles Scribner & Sons, New York, 1929. Reprint edition: Dover Publications.
4. W.W. Scherkenbach, "Profound Knowledge," The W. Edwards Deming Memorial Lecture to American Society for Quality Control (ASQC), Northern Virginia Section (0511), June 16, Ritz-Carlton Hotel, Arlington, Virginia.
5. John Tukey and Frederick Mosteller, *Data Analysis and Regression*, Addison-Wesley, Reading, Massachusetts, 1977.
6. W. Edwards Deming, *The New Economics*, Massachusetts Institute of Technology, Center for Advanced Engineering Study, Cambridge, Massachusetts, 1993.

BIBLIOGRAPHY

1. Joseph J. Carr, *The Art of Science*, HighText Publications, Inc., San Diego, 1993.
2. Joseph J. Carr, *CrashCourse(r) in Statistics*, HighText Publications, Inc., San Diego, 1994. A book/CD-ROM multi-media product.
3. W. Edwards Deming, *Out of the Crisis*, Massachusetts Institute of Technology, Center for Advanced Engineering Study, Cambridge, Massachusetts, 1982, 1986.
4. David Futrell, "Ten Reasons Why Surveys Fail," *Quality Progress*, April 1994, pages 65-69.

PRODUCT INFORMATION

Svetlana 3CX300A1 Power Triode

Svetlana Electron Devices, Inc. announces the availability of its new 3CX300A1 metal-ceramic power triode. The device is usable for audio amplifiers, in Class A, AB, or B, or as a power-supply pass device.

Manufactured at the Svetlana facility in Russia, the 3XC300A1 features high transconductance (20,000 micro-Siemens typ.); low plate resistance (450 ohms typ.); plate ratings of 1800 volts maximum DC supply voltage, 300 watts maximum dissipation with forced-air cooling; increased peak emission from new cathode materials; stable operation from extended processing and aging; exceptional linearity, well suited for push-pull amplifiers (a single pair can produce 800 watts in Class B).

The unit's ceramic-metal construction, with cathode and grid rigidly mounted on coaxial cones, reduces microphonic effects and resists mechanical and thermal shocks. The external anode is machined from solid copper, for ruggedness and tolerance of high temperatures.

The 3CX300A1s undergo comprehensive testing before and after aging; are suitable for retrofitting of audio amplifiers (they can substitute for 212E, 805, 211, etc. with equipment mods.); and fit Svetlana SK2A sockets, standard loktal sockets, or special sockets intended for the 4CX250B tetrode.

For additional information, contact Svetlana Electron Devices, Headquarters, 8200 South Memorial Parkway, Huntsville, AL 35802, or call (205) 882-1344; Fax: (205) 880-8077.

Free Catalog from Mouser

Mouser Electronics' latest electronic component catalog contains 340 pages featuring new products from 3M, Amp, NEC, SGS Thomson, Rectron Teccor, E-Switch, BI Technologies, and others. A guide for buyers and engineers, the catalog offers complete specification drawings and guaranteed prices. For your free copy call (800) 992-9943; e-mail <catalog@mouser.com>; or visit Mouser's Web site at <http://www.mouser.com>.

Popular 30-Year-Old HP Application Note on Web Site

Hewlett-Packard has given one of its most popular and long-lived application notes an updated, multimedia format on the company's Web site. The 30-year-old technical note illustrates S-Parameter techniques for designing electrical networks used in oscillators and amplifiers. The note can be found on HP Web site at: <http://www.hp.com/go/tminteractive>.

Phil Salas, *AD5X*
1517 Creekside Drive
Richardson, Texas 75081
e-mail: <psalas@aud.alcatel.com>

MEASURE YOUR COAX CABLE LOSS

Turn in your calculator for an Excel spreadsheet

How good is your coax feedline? It can certainly degrade with time, especially when it's out in the weather. Is it time to consider replacing it? Maybe now is the time to measure the loss and see.

To determine loss, you can use a power meter to measure the power at your transmitter output, and again at the end of the coax cable at the antenna. However, it's also very easy to measure the loss with just an SWR analyzer, or with your transmitter and an SWR meter—along with a few simple calculations. I recommend an SWR analyzer as the best way to make the necessary measurements, because the method described here requires that your transmitter be able put out some power into a high SWR without damage.

Transmission line loss

In order to understand the methodology used in this article, let's review the transmission line loss equations.

The reflection coefficient at the input of a lossy cable is given as:

$$\rho = \rho_1 e^{-2\alpha} \quad (1)$$

where:

ρ_1 = reflection coefficient at the antenna
α = cable loss in nepers = cable loss in dB/20log e = cable loss in dB/8.6859

You can see that $\rho = \rho_1$ for a lossless cable (i.e, $\alpha = 0$).

If you short or open (disconnect) your feedline at the antenna, the reflection coefficient at the antenna is unity (1); i.e., an infinite SWR. Therefore, for a feedline open or shorted at the antenna, the input reflection coefficient equation simplifies to:

$$\rho = e^{-2\alpha} \quad (2)$$

Now, we can rearrange this equation to solve for the cable loss:

α (nepers) = -0.5 ln ρ, or

Cable loss in dB = α (nepers) X 8.6859 = -4.343 ln ρ

Because ρ = (SWR-1)/(SWR+1), we have our final equation:

Cable loss in dB = -4.343 ln [(SWR-1)/(SWR+1)] (3)

Measuring SWR

Unfortunately, some SWR meters and SWR analyzers only have meter scales calibrated to a maximum SWR of 3:1. If your SWR meter also has a calibrated linear scale (say, from 1 to 10), you can accurately calculate SWR in excess of this amount using the following equation:

SWR = (Forward Reading + Reflected Reading)/(Forward Reading - Reflected Reading) (4)

If you're using an SWR meter or SWR analyzer that has no linear scale and is only calibrated in SWR to 3:1 maximum, there is a way to obtain a fairly good approximation of higher SWRs. Mentally divide the range above 3:1

Table 1

Feedline Loss Calculations — Phil Salas-AD5X (1/18/97)

Input Parameters	**Input Data**	
Feedline Length (ft.)	70	
Open/Short Circuit or Out-of-Band SWR	5	
Frequency (MHz) of SWR measurement	28	
Desired Frequency of interest of cable loss	18.1	
Expected Loss @ SWR freq. (from Table)	0.812	
Expected Loss @ desired freq. (from Table)	0.652	
	Results	
Actual Cable loss (dB) @ SWR Freq.	**1.761**	
Excess Cable Loss (dB) @ SWR Freq.	**0.949**	
Actual Cable Loss (dB) @ Desired Freq.	**1.416**	
Excess Cable Loss (dB) @ Desired Freq.	**0.764**	

Cable Loss Table

Feedline	**SWR Frequency Expected Loss(dB)**	**Desired Frequency Expected Loss (dB)**
RG-58	1.758	1.414
RG-8X	1.353	1.087
RG-213	0.812	0.652
LMR-240	0.879	0.707
LMR-400	0.473	0.381
9913	0.135	0.109

Table 1. Calculation of feedline loss from SWR measurement as compared to expected line loss calculated from coax cable specifications.

SWR into thirds, and assume the top of the first third is 5:1 and the top of the second third is 10:1. The top end of the scale is infinite SWR. Always measure SWR at the highest frequency possible. Cable loss is greater at higher frequencies, resulting in a lower measured SWR which gives you higher accuracy.

Finally, in many cases, you can even accurately measure your cable loss without disconnecting your feedline! Just measure the SWR at a frequency well removed from the antenna resonant frequency. Normally, the off-frequency antenna SWR is very high, so measure your 20-meter beam at 10 MHz, or your 40-meter vertical on 20 meters. You can then go back into the spreadsheet and see what the loss is at your frequency of interest. If you make the SWR measurements outside of the ham bands, you'll obviously need an SWR analyzer because you can't legally key up your transmitter outside these bands.

Cable loss at other frequencies

Once you know the loss at one frequency, you can calculate the loss at any other frequency using the following equation:

$$L_{df} = L_{kf}(df/kf)^{1/2} \quad (5)$$

where

L_{df} = Loss at desired frequency

L_{kf} = Known loss at a specific frequency

df = desired frequency

kf = frequency at which the loss is known

This equation is pretty accurate over a broad frequency range.

Example

To simplify these calculations, you can write a BASIC program to do the number crunching for you. Better yet, I've found an Excel spreadsheet is very flexible and can pull these equations together nicely. My spreadsheet (**Table 1**) was done in Excel 5.0. It calculates the feedline loss from the SWR measurement and compares it to the expected line loss, which is calculated from the coax cable specifications for RG-58, RG-8X, RG-213, LMR-240, LMR-400, and 9913 cables.

Enter the information in the "Expected Loss (db) @ SWR Freq." column. The spreadsheet will give you the excess loss (as calculated from the SWR) over the expected value. From this, you can decide the status of your feedline—be it good or bad. You can then go back

Table 2

Feedline Loss Calculations	Phil Salas-AD5X (1/18/97)	
Input Parameters	**Input Data**	
Feedline Length (ft.)	70 <- B4	
Open/Short Circuit or Out-of-Band SWR	5 <- B5	
Frequency (MHz) of SWR measurement	28 <-B6	
Desired Frequency of interest of cable loss	18.1 <- B7	
Expected Loss @ SWR freq. (from Table)	0.812 <-B8	
Expected Loss @ desired freq. (from Table)	0.652 <-B9	
	Results	
Actual Cable Loss (dB) @ SWR Freq.	-4.343*LN(($B$5-1)/($B$5+1))	
Excess Cable Loss (dB) @ SWR Freq.	$B$12-$B$8	
Actual Cable Loss (dB) @ Desired Freq.	$B$12*($B$7/$B$6)^0.5	
Excess Cable Loss (dB) @ Desired Freq.	$B$14-$B$9	
Cable Loss Table	**SWR Frequency**	**Desired Frequency**
Feedline	**Expected Loss (dB)**	**Expected Loss (dB)**
RG-58	0.026*($B$6/30)^0.5*$B$4	0.026*($B$7/30)^0.5*$B$4
RG-8X	0.020*($B$6/30)^0.5*$B$4	0.020*($B$7/30)^0.5*$B$4
RG-213	0.012*($B$6/30)^0.5*$B$4	0.012*($B$7/30)^0.5*$B$4
LMR-240	0.013*($B$6/30)^0.5*$B$4	0.013*($B$7/30)^0.5*$B$4
LMR-400	0.007*($B$6/30)^0.5*$B$4	0.007*($B$7/30)^0.5*$B$4
9913	0.002*($B$6/30)^0.5*$B$4	0.002*($B$7/30)^0.5*$B$4

Table 2. Feedline loss calculations including reference equations.

into the spreadsheet and see what the actual feedline loss is at any other frequency.

For example, I have 70 feet of RG-213 coax cable running from my shack to my vertical antenna in the back yard. I disconnected the feedline at the antenna and measured the SWR in the shack. It was 5:1 at 28 MHz (for a lossless feedline, the SWR would be infinite). From the spreadsheet, I determined my actual feedline loss is 1.76 dB. New RG-213 has a loss of about 1.3 dB/100 feet at 28 MHz. A 70-foot length should have a loss of 0.8 dB. Although it's about one dB worse than this, my feedline may actually be in fairly good shape because I'm also including a bypassed antenna tuner, a low-pass filter, three coax switches, two line isolators, and some short interconnecting pieces of RG-8X along with the feedline.

Okay, so I measured the SWR at a high frequency for accuracy, but what's the actual loss on 17 meters (18.1 MHz)? That's easy to find. Just go back into the spreadsheet, enter the desired frequency (18.1 MHz), and input the expected coax loss from the table. As you can see, the loss is 1.4 dB, which is 0.76 dB worse than was expected.

The second spreadsheet table (**Table 2**) shows the equations used in the spreadsheet cells, so you may key them in. Notice that I started with the published cable loss per foot at 30 MHz for all my reference calculations for the coax cables considered. If you operate primarily above 30 MHz, you'll get slightly better accuracy if you base your cable loss reference equations on published loss figures closer to your actual operating frequencies.

Conclusion

The use of spreadsheets is a great way to take the drudgery out of making repetitive calculations. I have found Excel very easy to use for many applications that once required me to write BASIC programs. Give this cable loss spreadsheet a try and you'll see what I mean. ■

L.B. Cebik, *W4RNL*
1434 High Mesa Drive
Knoxville, Tennessee 37938-4443
e-mail: <cebik@utkvx.utk.edu

MODELING AND UNDERSTANDING SMALL BEAMS: PART 7

Shrunken Quads

Quad beams remain one of the most controversial antennas around, simply because we inevitably want to compare them to linear Yagis of similar element numbers. Entire books have been written on the quad, the two most notable of which are the Orr and Cowan classics and the more recent detailed study by Haviland.[1] The foundation of the quad is the full-wavelength loop, which builders have constructed in squares, rectangles, diamonds, and even circles.[2] Whatever the shape of this structure, it is mechanically ungainly, requiring a nonconductive support structure (or at least one in which the conductive portions are broken into nonresonant or nondetuning lengths) for a wire loop. Putting two or more such elements together has been a challenge for commercial and home builders alike. If high winds mangle Yagis and quads equally, ice has shown a distinct preference for the destruction of quads.

Reducing the dimensions of the quad loop has been an enterprise almost as old as the quad itself. If the quad loop can be shrunk considerably, then the mechanical problems diminish almost as the square of the percentage of shrinkage. The ingenuity of home builders in trying schemes for shortening the quad has produced diverse techniques. In his own "corner-inductor" version of the shortened quad, KA2OIG/TI2 noted that "in the literature on reduced quads there are examples of top-hat or capacitive loading, linear loading, stub loading, trap and coil loading, a folded-mini, and finally coil loading."[3] Almost all of these systems add

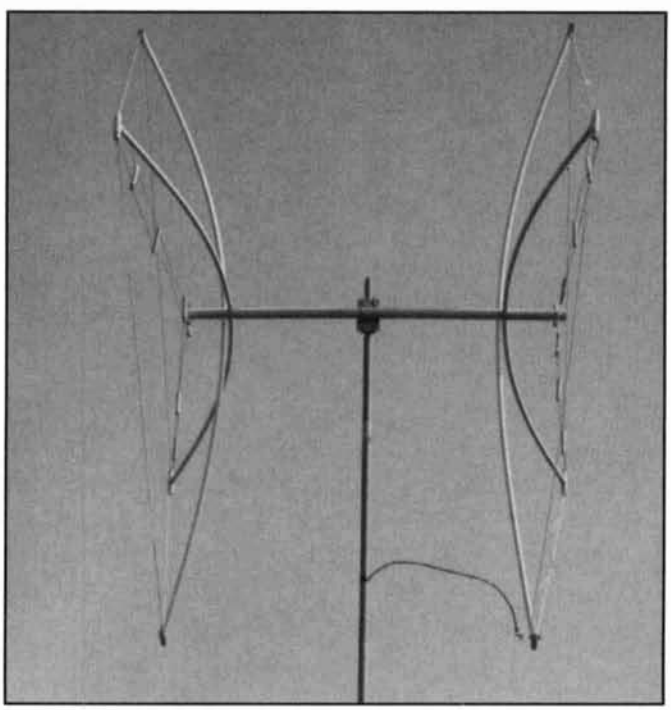

Photo A. The shrunken quad antenna.

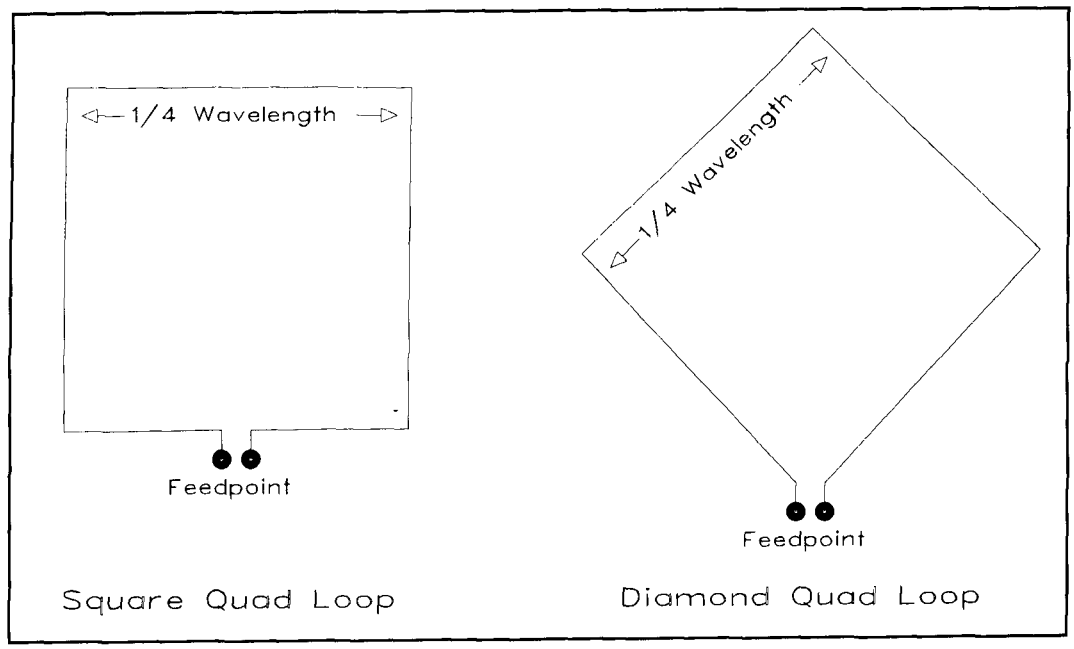

Figure 1. Simplified outlines of full square and diamond quad loops.

one or another physical complexity to quad construction as repayment for the reduction in overall antenna loop size.

More recently, N4PC has experimented with a diamond-shaped "squished quad" using linear loading at the voltage nodes, which are located halfway up the vertical sides in a square design and at the horizontal apexes of the diamond design. The object was to leave as much as possible of the high-current portion of the antenna unaffected by loading, thereby maximizing gain. The added wire at the voltage nodes could be a continuation of the overall wire loop, thereby simplifying mechanical construction.[4] Except for the copper wire losses, the mid-sole or voltage-node loading scheme

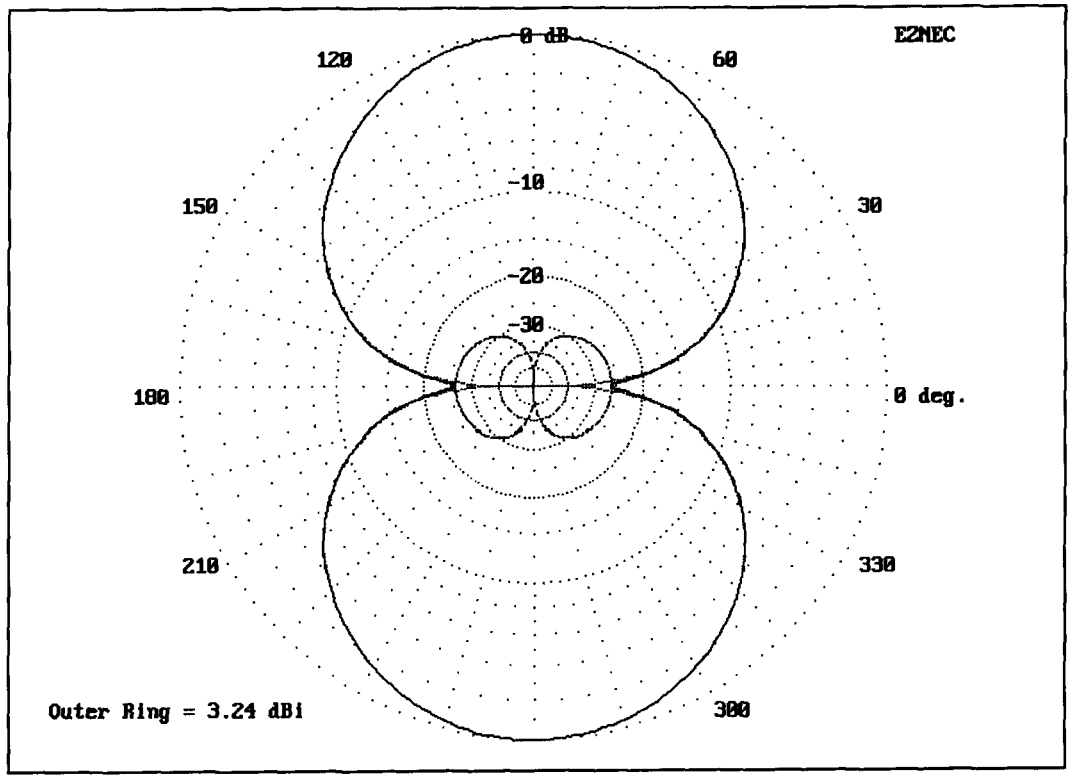

Figure 2. Free-space azimuth pattern of a full-size quad loop.

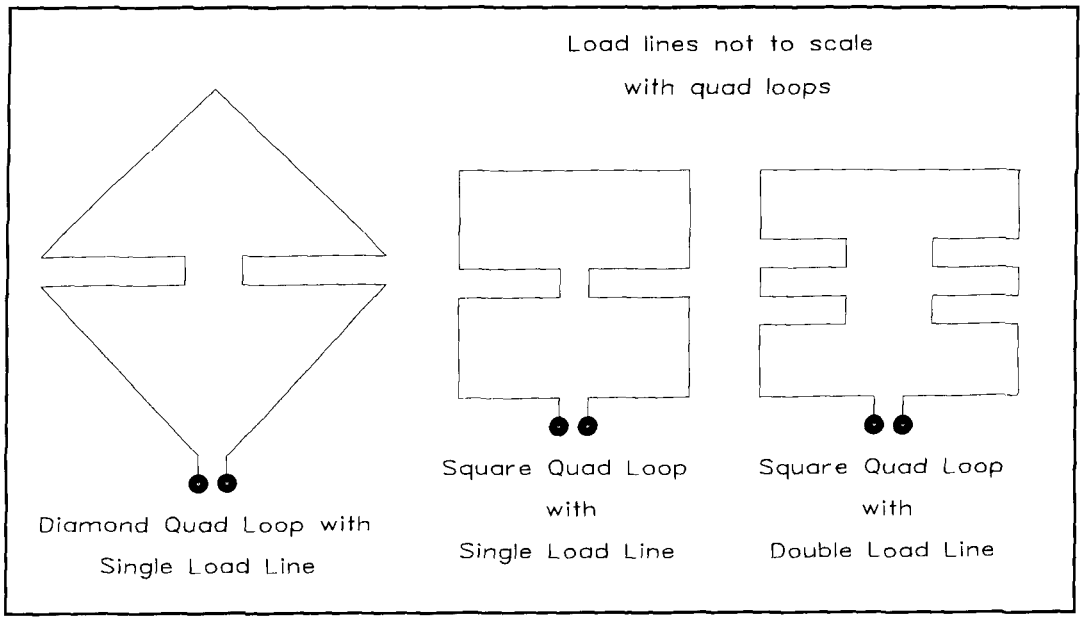

Figure 3. General outline of three test models used to establish shrunken quad loop performance potentials.

avoids losses associated with the use of coils and capacitors as loading elements. In addition, voltage-node loading is usable with both diamond and square quad loops.

N4PC's success with the "squad" left some question as to what sort of performance we might be able to expect from such an antenna in advance of building one. If, as he noted, 85 percent of the antenna current occurs in the centermost 65 percent of the antenna wire, what

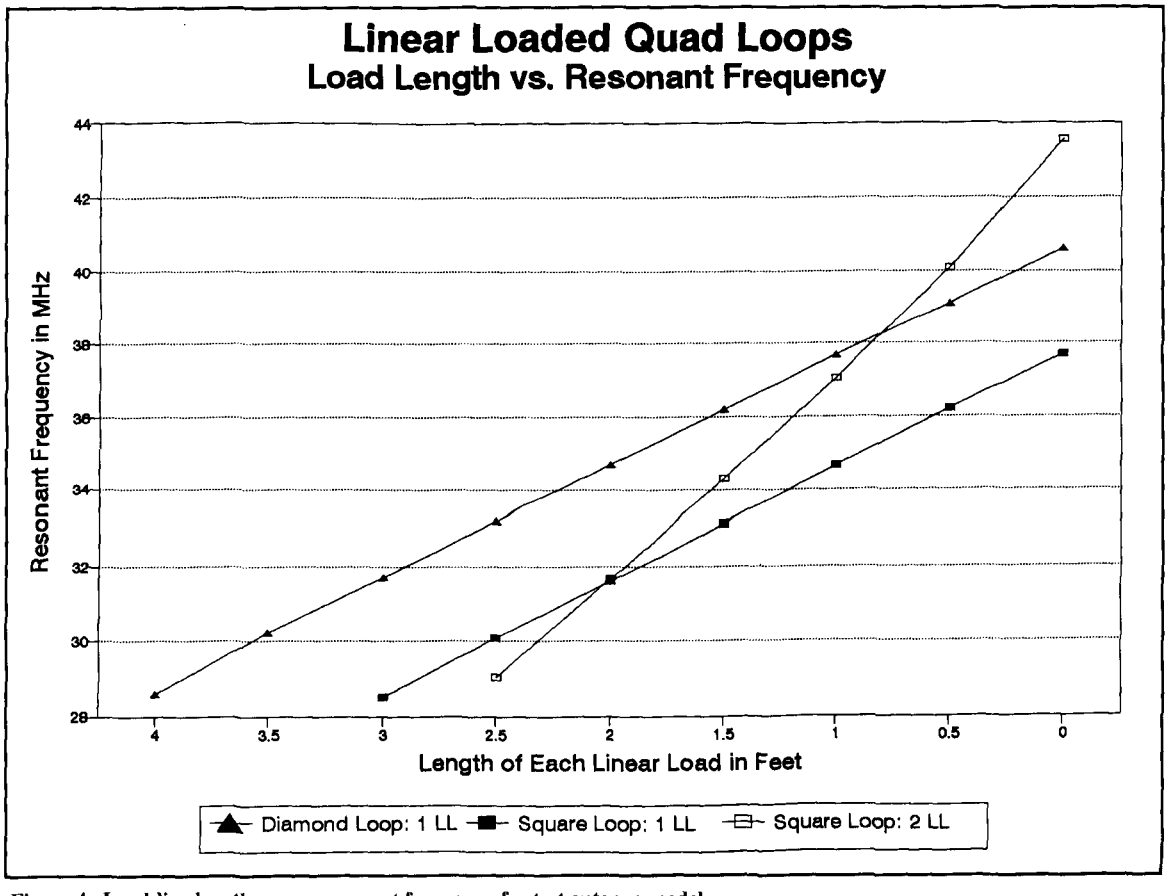

Figure 4. Load-line length versus resonant frequency for test antenna models.

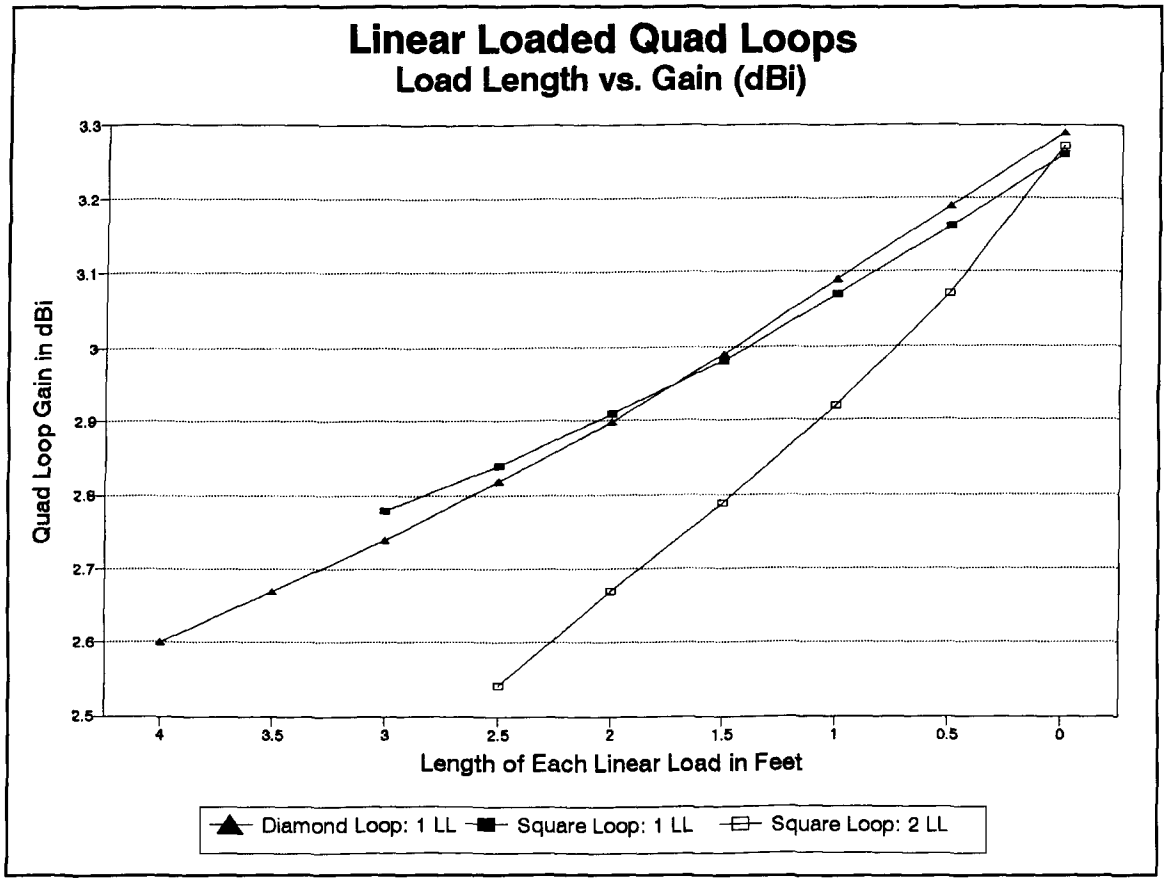

Figure 5. Load-line length versus free-space gain for test antenna models.

would this mean in terms of overall antenna performance? The availability of NEC-2, which can handle complex geometries with some ease (as long as the wire diameter doesn't change) suggested that modeling both the squad and the loops that compose its elements might be an instructive exercise. The result was my own version of a shrunken diamond-form, two-element quad for 10 meters with dimensions less than 7 feet per side.

Full-size and shrunken quad loops

Despite the plethora of articles on quads, data on the proper dimensions for a simple quad loop are hard to come by. The traditional formula, L (in feet) = 1005/f (in MHz) is simply wrong for bare copper wire. Additionally, the diameter of the wire will have an influence on the total length of the quad loop. Thus, any formula given must be specified for the wire size as well. On 10 meters (28.5-MHz design center), the proper length (in feet) for a resonant quad loop of #14 bare copper wire is approximately 1045/f (in MHz). At 28.5 MHz, this yields a circumference of about 36.5 feet or about 9.13 feet per side. These dimensions apply to both the square and diamond configurations shown in **Figure 1**.

Whether square or diamond, the loop provides a free space gain of about 3.25 dBi (about 1.1 dB greater than a free space dipole of similar materials). The pattern shown in **Figure 2** displays both the horizontal and vertical components of the total far field pattern: the vertical component is insignificantly larger for the square loop. The feedpoint impedance is between 125 and 130 ohms resistive for both configurations.[5] Free space gain and feedpoint impedance figures can be used with confidence for the comparisons that follow, because none of the models exhibited any surprising changes in characteristics when modeled over real ground. If a shrunken model exhibits a reduced gain relative to a full-size model of 1 dB in free space, an equivalent reduction will be found in models over real ground.

Three types of shrunken quad loops, shown in **Figure 3**, were modeled for performance comparisons. All use #14 copper wire, the diamond loop (referred to as "Diamond loop: 1LL" on graphs) has a circumference (in feet) of 725/f (in MHz), about 25.5 feet or about 6.36 feet per side. The diamond is thus about

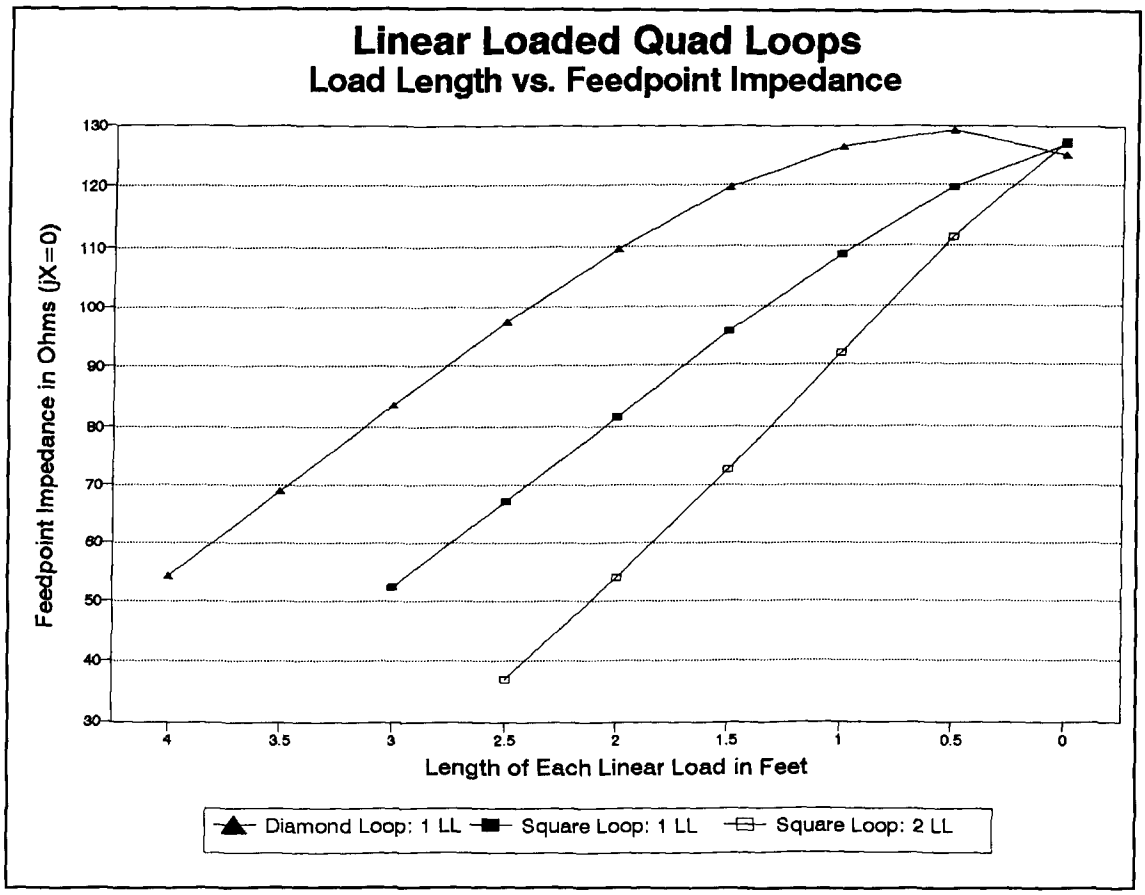

Figure 6. Load-line length versus feedpoint impedance gain for test antenna models.

70 percent full size. One advantage of the diamond is that it allows the most room for the voltage-node linear load, shown as the side insets on the diagram. The model uses a short horizontal feed wire to reflect usual diamond quad loop construction. Using a perfect diamond with a split feed yielded linear load lengths only 3/4-inch longer than those indicated by the single feed model at 28.5 MHz, with no change in feedpoint impedance.

A comparable square requires a larger circumference to permit resonance at the design center frequency of 28.5 MHz, since the maximum inset linear load is shorter. The model used here (designated "Square Loop: 1LL on graphs) is based on the formula 789/f (in MHz), which is about 27.7 feet overall and 6.92 feet per side. The resulting quad loop is about 76 percent full size. Its advantage mechanically is that the X-members or spreaders supporting the wire can be 10 feet long, a convenient hardware store supply dimension.

N4PC used a double inset linear load on his squad. Therefore, a third version seemed appropriate for modeling: a square with a double inset (designated "Square Loop: 2LL" on graphs). The double inset permits a reduction of the circumference to about 689/f (in MHz) or 66 percent of full size. The 24-foot circumference is distributed at 6 feet per side.

Initially, all voltage-node loads were identically constructed (except for length). Composed of #14 copper wire, they are 3 inches (0.25 feet) wide and extend inward from the side wires horizontally toward the center of the element assembly, as shown in **Figure 3**.

For each type of loop, the resonant frequency is close to a linear function of the load length, as **Figure 4** illustrates. Each loop size was chosen to resonate at 28.5 MHz with the load length at or near its practical maximum length to achieve the smallest loop size possible. The diamond loop allowed 4-foot load lines on each side of center, while the single-load square allows 3-foot load lines. The double-load square is arbitrarily chosen to be 3 feet on a side by fiat, which yielded a load-length on each side of 2.595 feet for resonance at 28.5 MHz. With an even 2.5 feet of load length per side, the resonant frequency rises to 29.05 MHz as the starting point of the graph.

The single-load diamond and square loops show nearly parallel linear rises in frequency at almost twice the rate of either single-load loop. Thus, the double-load line is much more frequency-sensitive to adjustments.

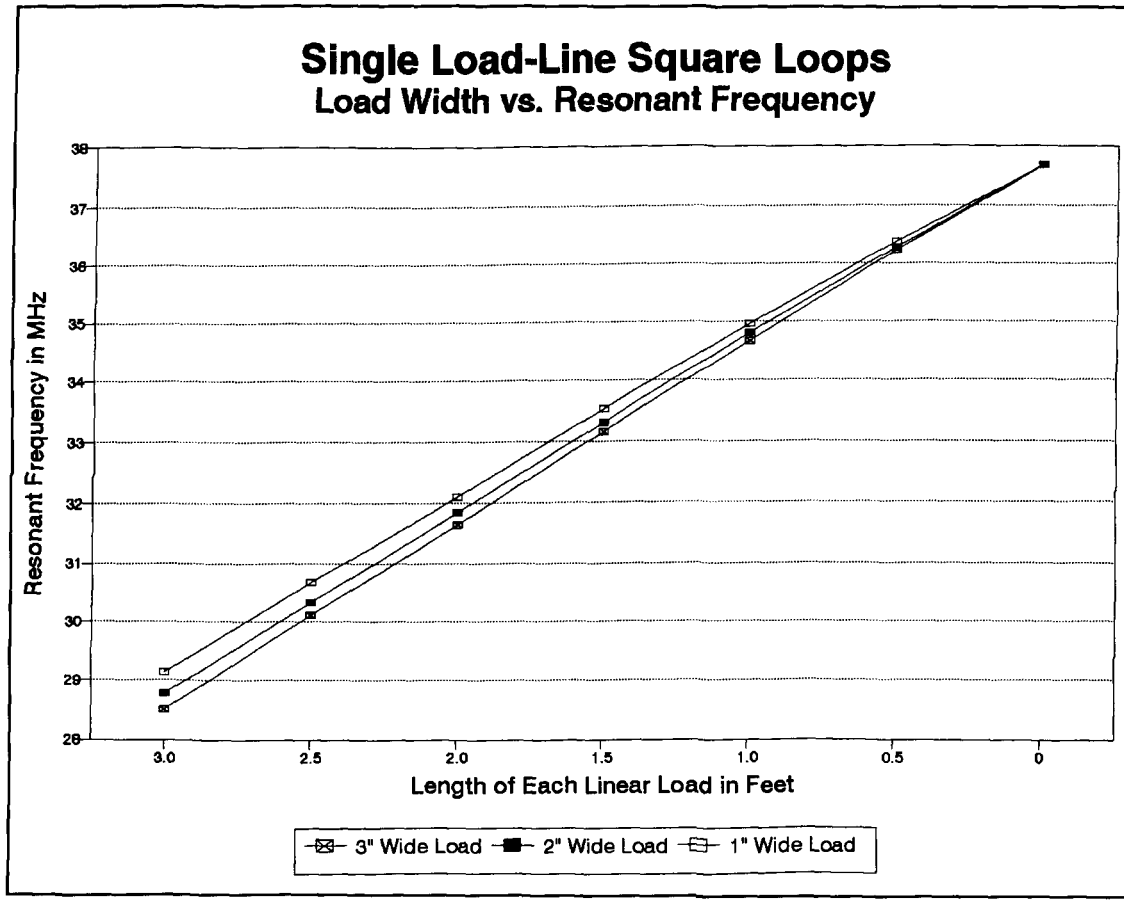

Figure 7. Single load-line width versus resonant frequency for test square-loop models.

As one might expect, the longer the load line at resonance of the loop, the lower the gain of the loop. Because the load lines are of the same material as the element, the only losses are those of the copper wire in the line, which are too small to account for the reduction of gain in all loaded quad loops. The gain of a quad loop is in part dependent upon its physical size.

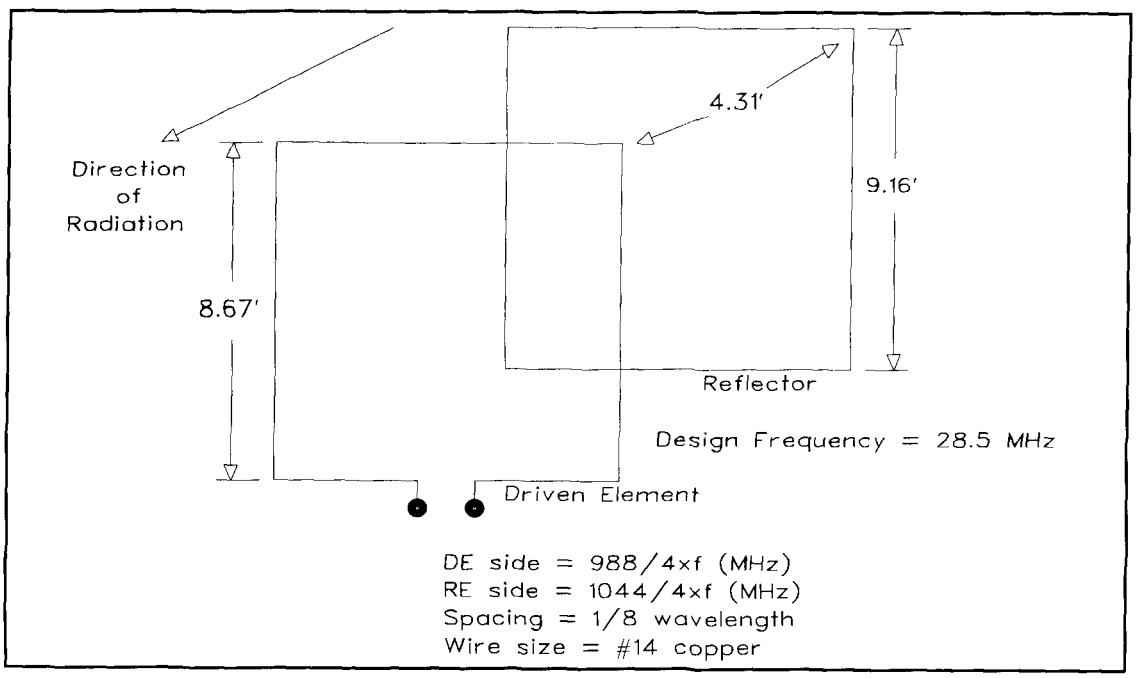

Figure 8. Outline of a full-size, two-element quad beam model.

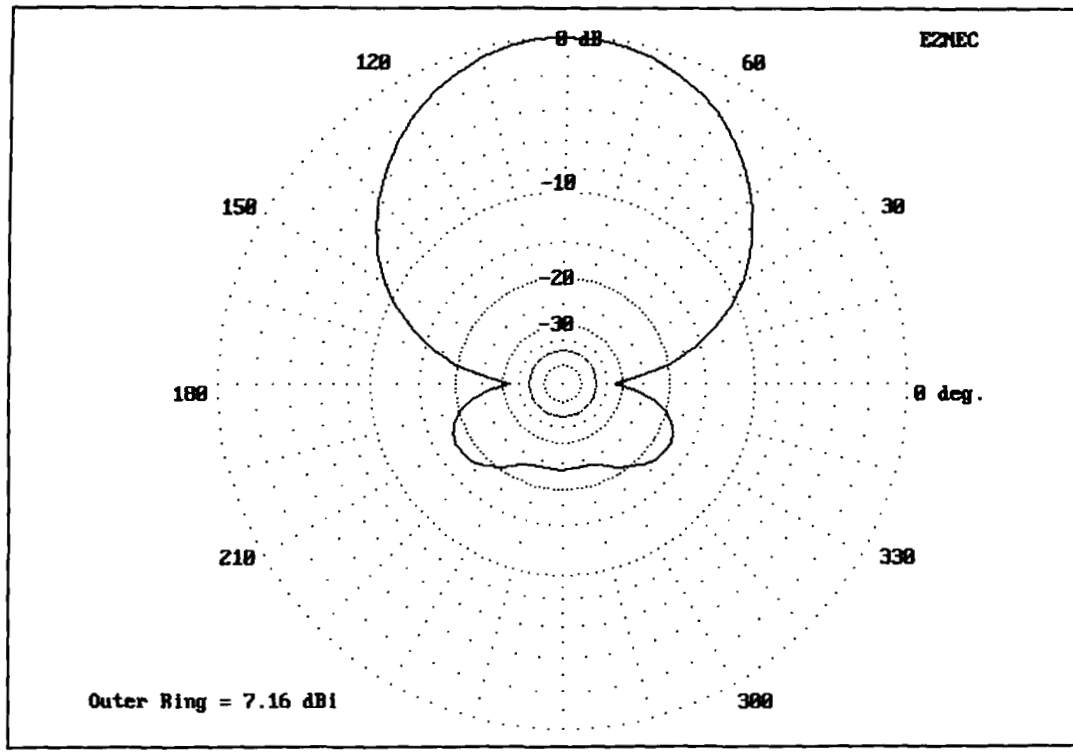

Figure 9. Free space azimuth pattern of a full-size, two-element quad beam model.

Hence, any shrinkage of the loop relative to a full-size loop at resonance will reduce its gain. In turn, reduction of loop gain will limit the gain obtainable from a multi-element quad beam using these shrunken loops.

Figure 5 shows the gain of loops using voltage-node loading, with each length of linear load corresponding to a resonant frequency for the assembly (**Figure 4**). Comparisons are possible only where corresponding loops have the

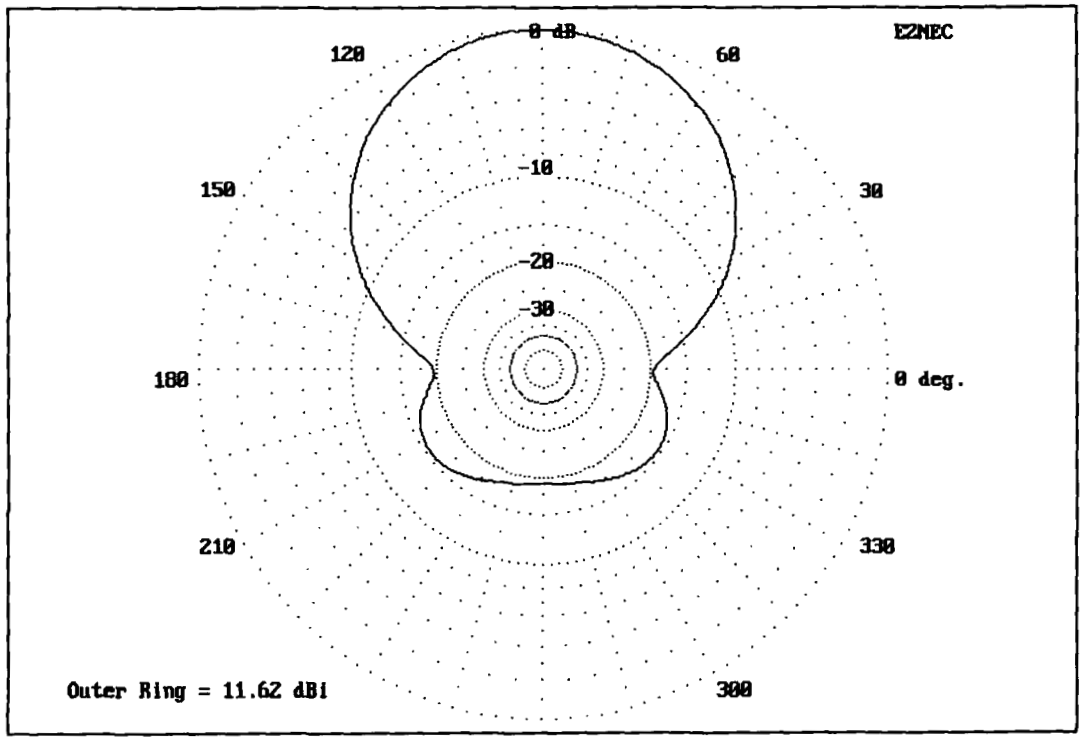

Figure 10. Full-size, two-element quad beam model azimuth pattern at the angle of maximum radiation for a height of 20 feet over medium earth.

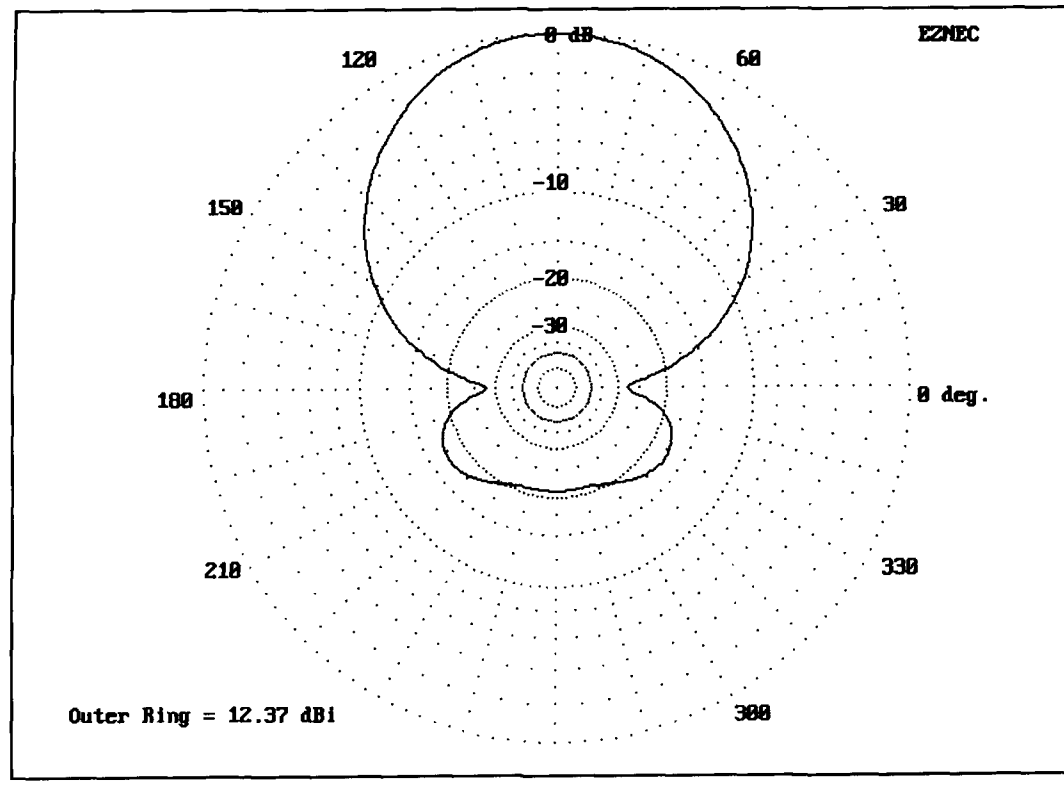

Figure 11. Full-size, two-element quad beam model azimuth pattern at the angle of maximum radiation for a height of 25 feet over medium earth.

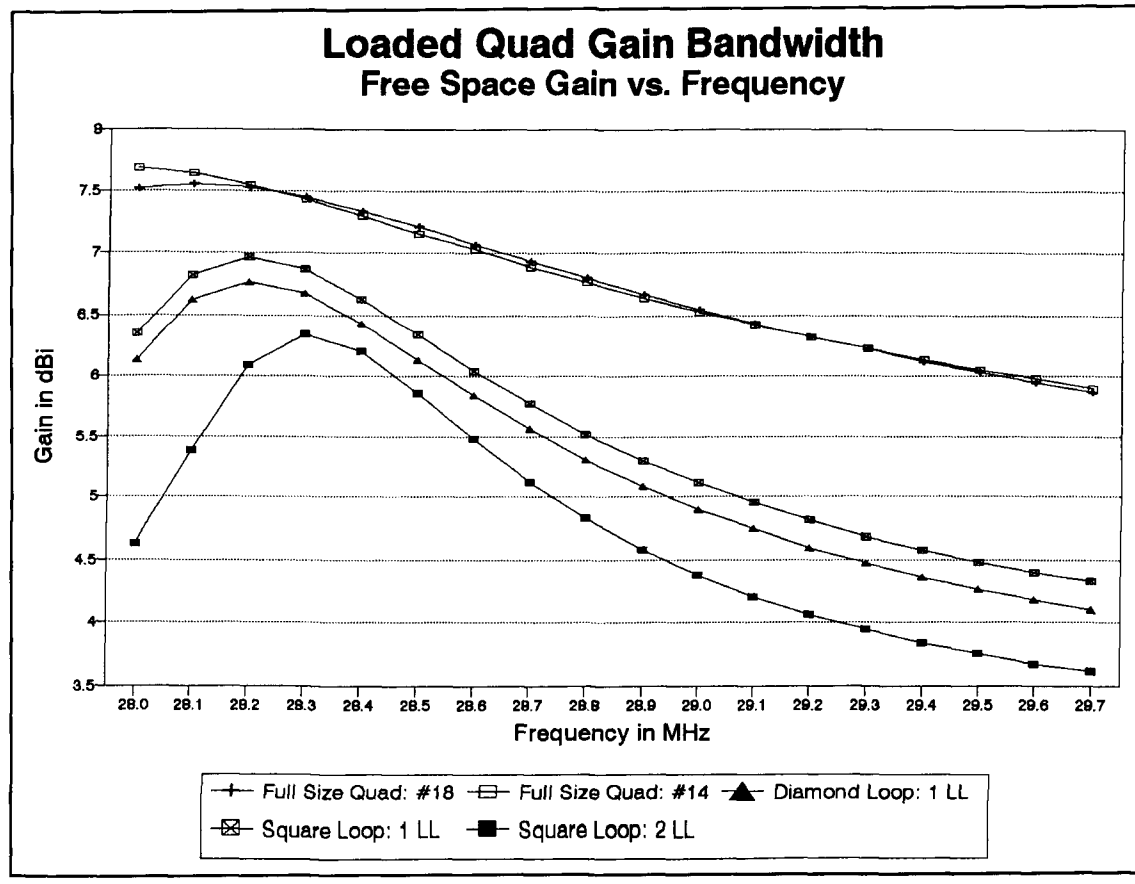

Figure 12. Comparative free space gains of full-size and shrunken quad beam models across 10 meters.

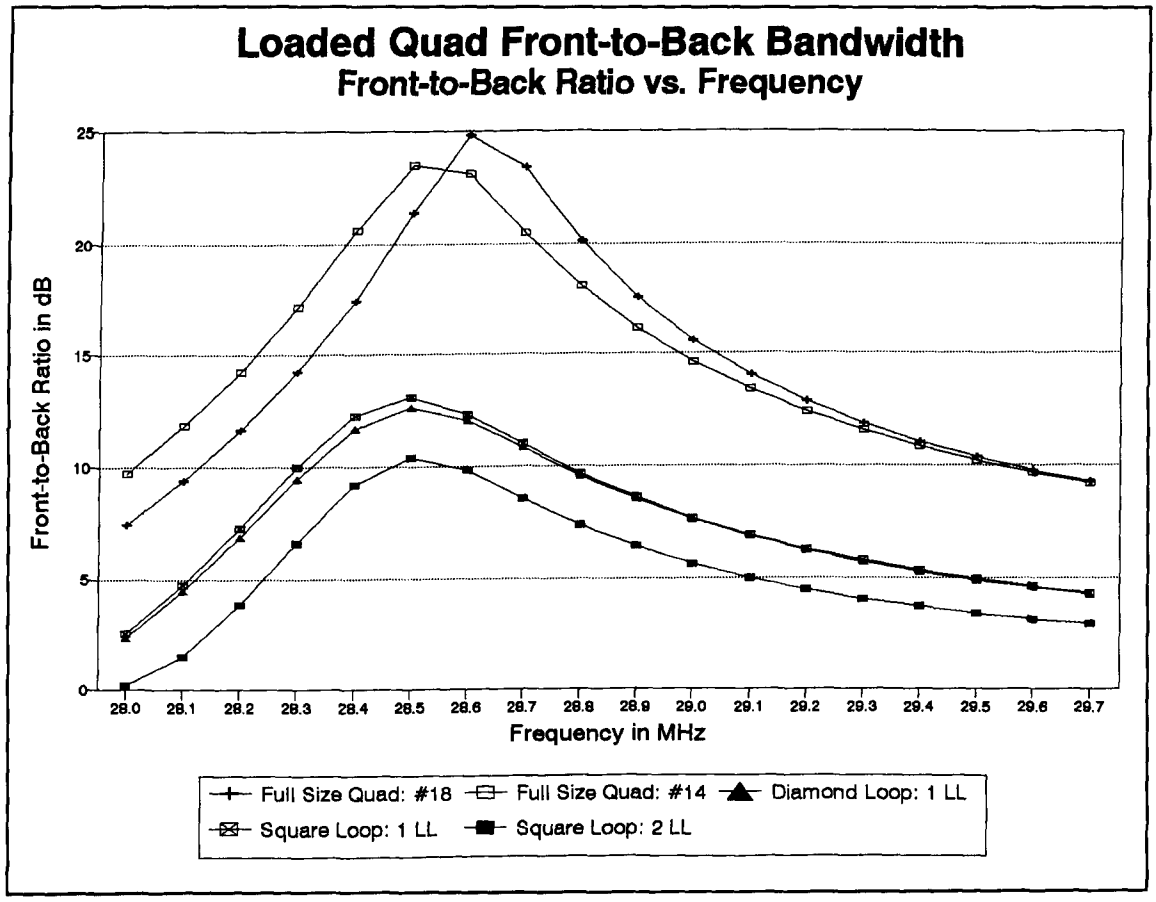

Figure 13. Comparative free space front-to-back ratios of full-size and shrunken quad beam models across 10 meters.

same length of load line. For all practical purposes, the gains of the single-load elements, diamond and square, are the same (under 0.05 dB difference). However, the gain of the double-load-line square is significantly less than that of either single-load configuration, reaching more than 0.25 dB difference at a 2.5-foot load length. At that load length, the single-load elements have lost about half the advantage of a full-size quad over a dipole; the double-load element is only slightly better than a dipole.

Both of the single-load loops show a resonant feedpoint impedance just about 50 ohms, as shown in **Figure 6**. The square element progresses in near linear fashion toward the impedance value of an unloaded resonant quad as the load line is shortened. However, the diamond loop reaches a peak value with load lines of 0.5 feet each. Like the single-load square, the double-load line square displays a near-linear rise in impedance value. Near the design center frequency, its feedpoint impedance is in the 35-ohm region.

Of the three configurations, the double-load-line element shows the least promise, despite its great compactness. Its low feedpoint impedance and noticeably reduced gain relative to the other shrunken loops suggest inferior beam performance. Add to these factors the frequency-sensitivity of the assembly to adjustments, and the configuration loses more appeal. A 6-foot wide and high 10-meter quad would not likely be worth the effort to build; however, a 7-foot wide and high quad beam may be well worth the effort, especially at about 58 percent of the volume required by a full size beam.[6]

Before attempting a two-element antenna, we should note that changing the spacing of the wires in the linear loads also changes the characteristics of a single-element quad loop slightly. Although gain and feedpoint impedance do not change enough to alter design considerations, the resonant frequency for a given length of load on each side of the loop will create design concerns. **Figure 7** shows part of the curve of load length and resonant frequency for these different load widths. Narrowing the spacing between load lines for a give load length raises the resonant frequency of the loop. The amount of resonant frequency increase is proportional to the percentage of decrease. The decrease from 2 to 1 inch yields a larger increase in resonant frequency than the decrease from 3 to 2 inches of load width.

Looking at the assembly from a different perspective, the narrower the line width, the longer

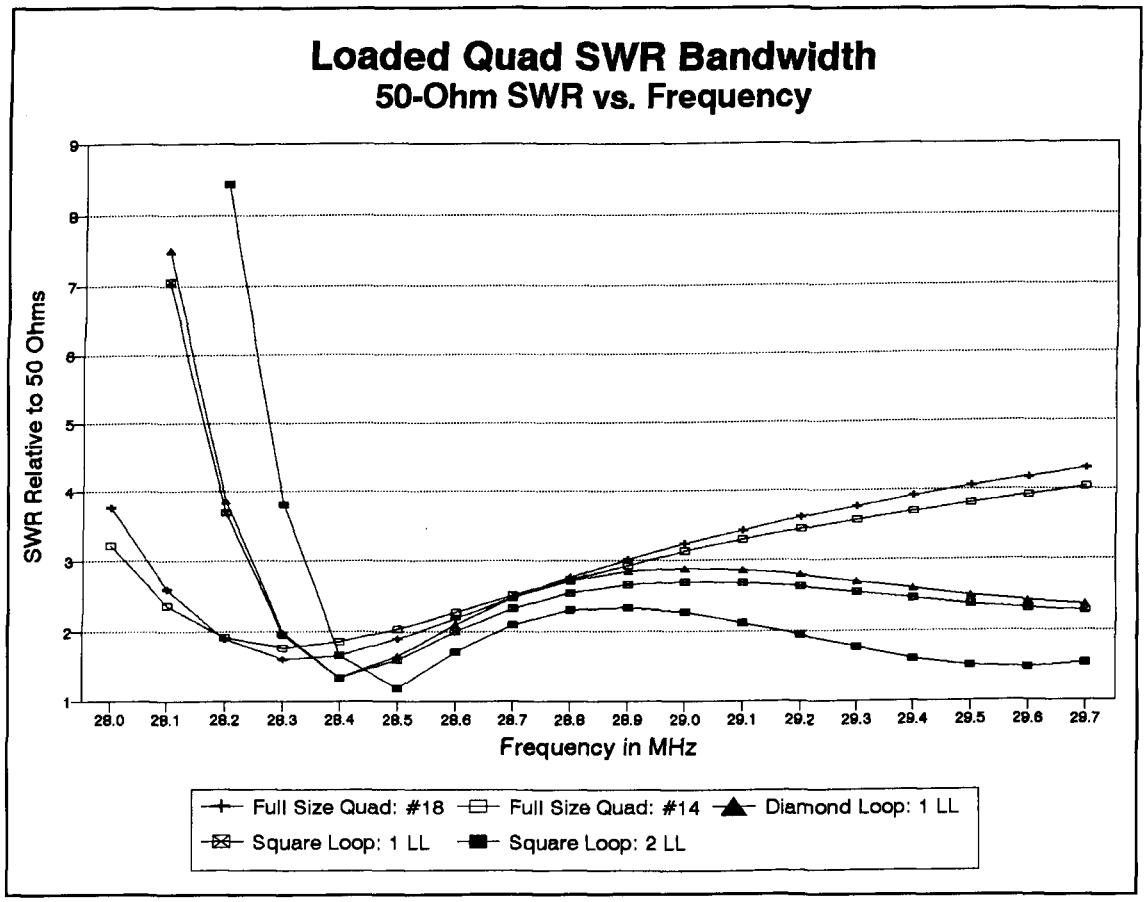

Figure 14. Comparative free space 50-ohm SWR bandwidths of full-size and shrunken quad beam models across 10 meters.

the load line needs to be for desired resonant frequency. Resonating a 1-inch wide load line at 28.5 MHz would have required a line longer than the 3.46 feet from side wire to the center of the quad element. At the far right end of the scale, of course, all three curves on the graph converge as the load line reaches 0 length.

Wider spacing between the load lines reduces the necessary line length for a given resonant frequency. However, increasing the spacing beyond 3 inches (say, to 6, 9, or 12 inches) produces only marginal shortening. Lines spaced 1 foot apart are only half a foot shorter for the single-line square and the diamond than lines spaced 3 inches apart for resonance at 28.5 MHz. Since maintaining the larger spacing would add weight to the small 10-meter structure, the 3-inch line spacing represents a good compromise between mechanical and electrical efficiency. Wider spacing might be used in a pinch if a given load-line length doesn't quite reach down to the desired resonant frequency: increasing the spacing an inch or two is equal to adding a few inches to the line length at its narrower spacing.

Because a quad loop, loaded or unloaded, has gain over a dipole, it qualifies as an array of sorts. However, it is barely an array (two bent dipoles touching ends). If one goes to the trouble to construct a full wavelength loop, one might as well construct two and have a classic two-element quad beam.

Full-size and shrunken quad beams

A full-size two-element quad beam consists of two quad loops cut to optimal dimensions spaced for the closest conjunction of gain and front-to-back ratio. Many formula sets are available, for example in Orr and Cowan, the *ARRL Antenna Book*, and Haviland. **Figure 8** outlines the parasitic quad beam and provides formulas for a close-spaced version (1/8th wavelength). Using #14 wire at a design center frequency of 28.5 MHz, the beam shows a free space gain of over 7 dBi with a front-to-back ratio over 23 dB. With a feedpoint impedance of about 100 ohms, the antenna falls in the middle of the 75 to 125-ohm feedpoint impedance range common with quad designs.

The sample quad beam is neither the best performer nor the broadest-banded of possible quads, as its spacing is somewhat close by quad standards. However, it demonstrates the perfor-

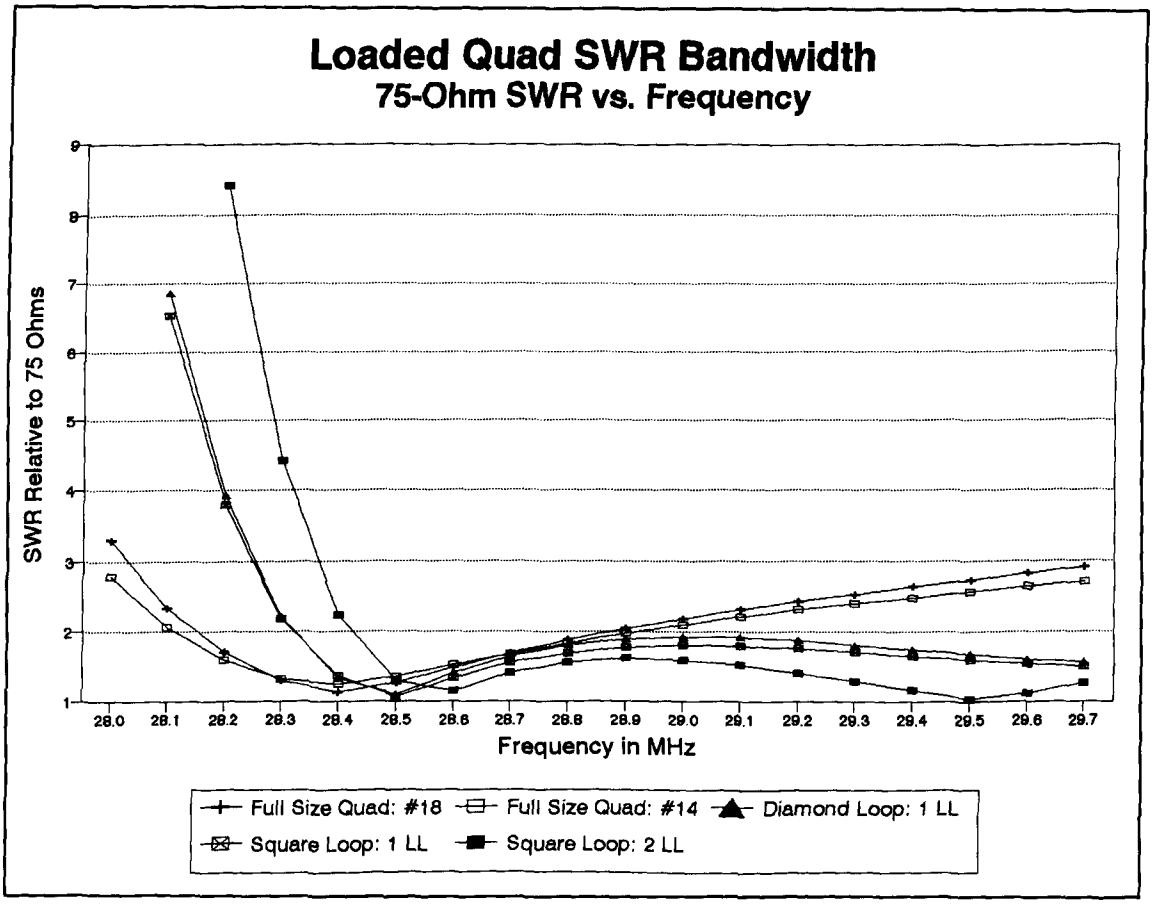

Figure 15. Comparative free space 75-ohm SWR bandwidths of full-size and shrunken quad beam models across 10 meters.

Table 1. Construction Values for Three Models of Side-Loaded Shrunken Quads

Type	Formula	Total L	L/side	DE load L	RE load L	L-Support
Diamond	725/f (MHz)	25.44'	6.36'	3.64'	4.07'	9.0'
Square: 1LL	789/f (MHz)	27.68'	6.92'	2.62'	2.98'	9.8'
Square: 2LL	684/f (MHz)	24.00'	6.00'	2.42'	2.58'	8.5'

Notes:

1. DE and RE load lengths refer to the length of each of two identical load lines at the center of each vertical wire on the square and at the horizontal apexes of the diamond model. See **Figure 3** for reference.

2. L= length of wire or wire assembly, including the total circumference of each loop, the length per side, the length of each load assembly consisting of two wires and a junction, and the length of the support element reaching across the antenna from apex to apex.

3. All three models use \$14 copper wire.

Table 1. Construction values for three 1/8 λ spaced shrunken quad beams, using side-loading for both the driven element and the reflector.

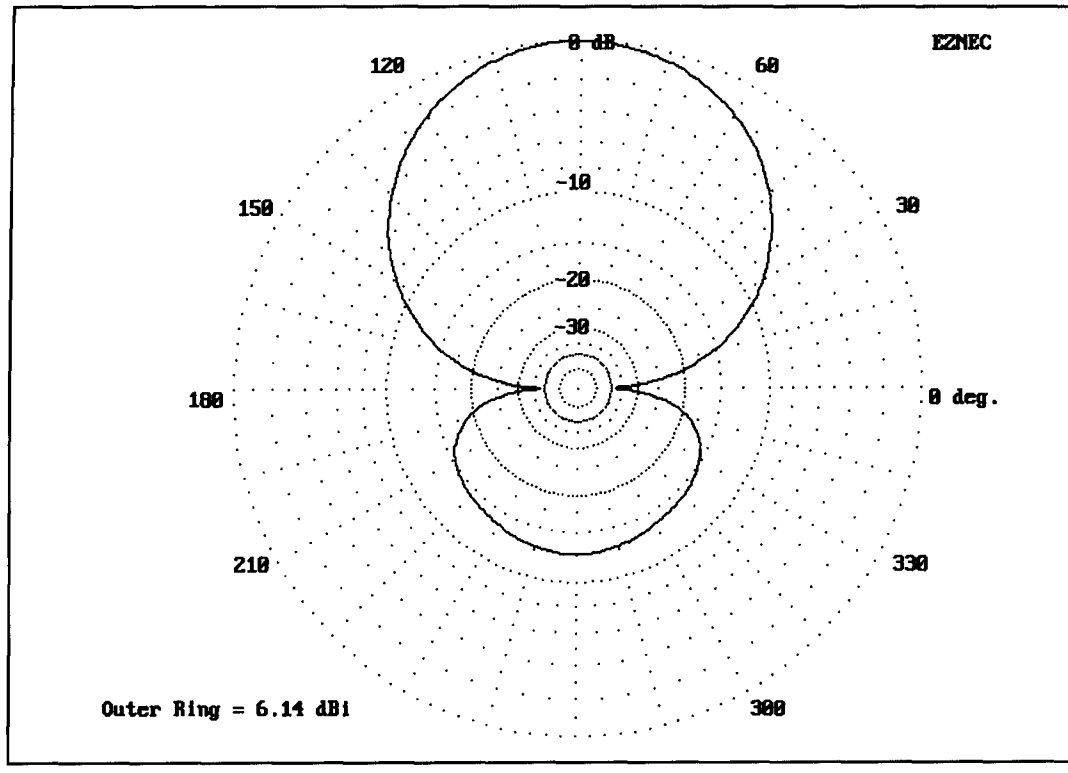

Figure 16. Free space azimuth pattern of the shrunken diamond-shaped, two-element quad beam model.

mance characteristics that lead many to choose quads over two-element or three-element trap Yagis: it has higher gain and a very respectable front-to-back radio (in fact, a good front-to-rear ratio, if we look at everything to the rear of the main lobe). **Figure 9** shows the antenna's free space azimuth pattern.

Full-size quads tend to perform well at mod-

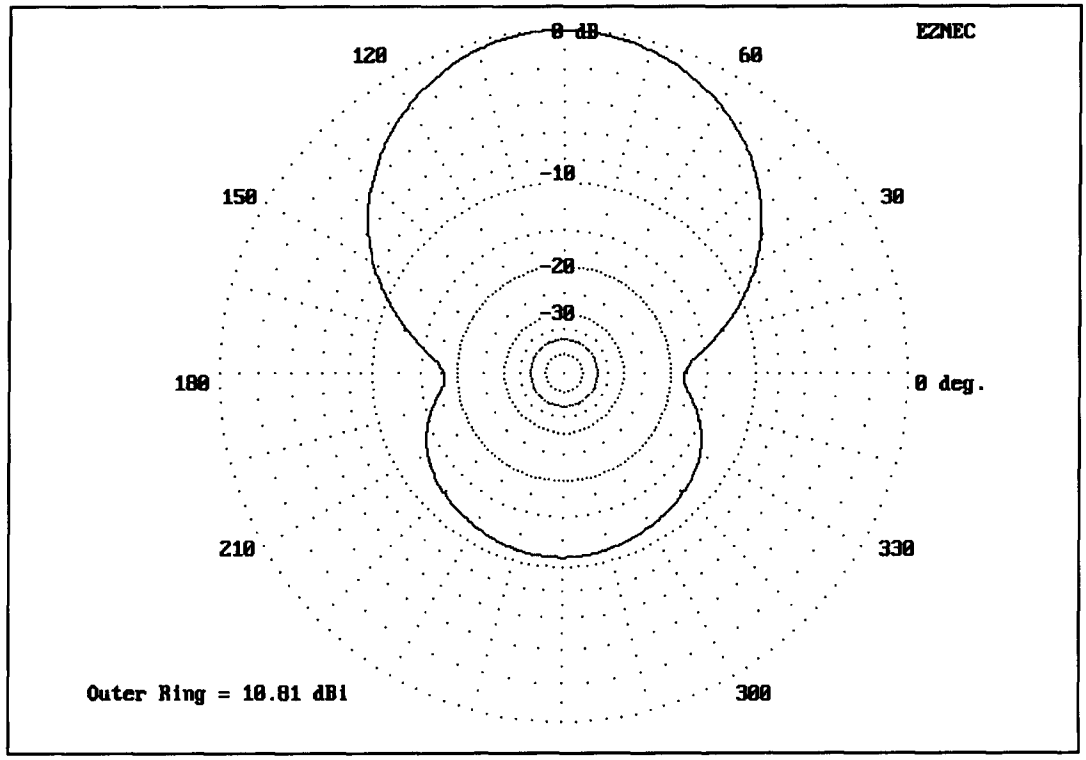

Figure 17. Shrunken diamond-shaped, two-element quad beam model azimuth pattern at the angle of maximum radiation for a height of 20 feet over medium earth.

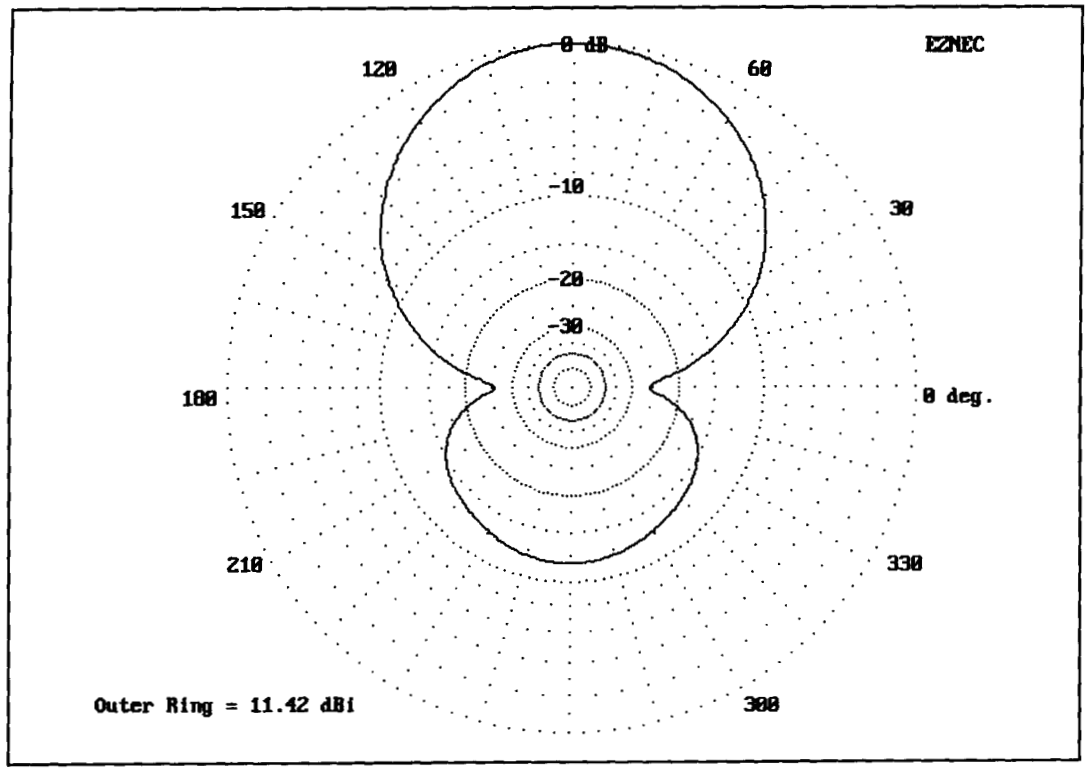

Figure 18. Shrunken diamond-shaped, two-element quad beam model azimuth pattern at the angle of maximum radiation for a height of 35 feet over medium earth.

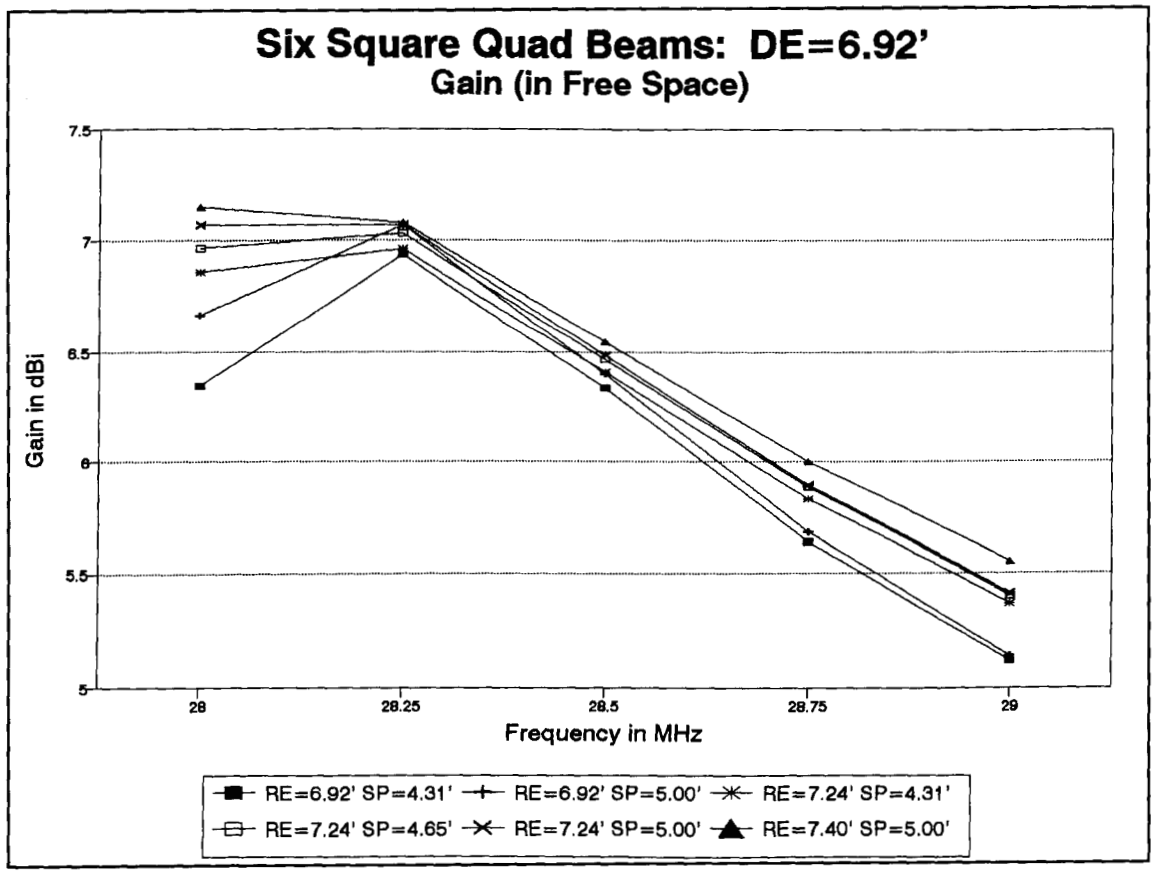

Figure 19. Comparative free-space gains of shrunken, two-element quad beams with increased spacing and/or enlarged reflectors.

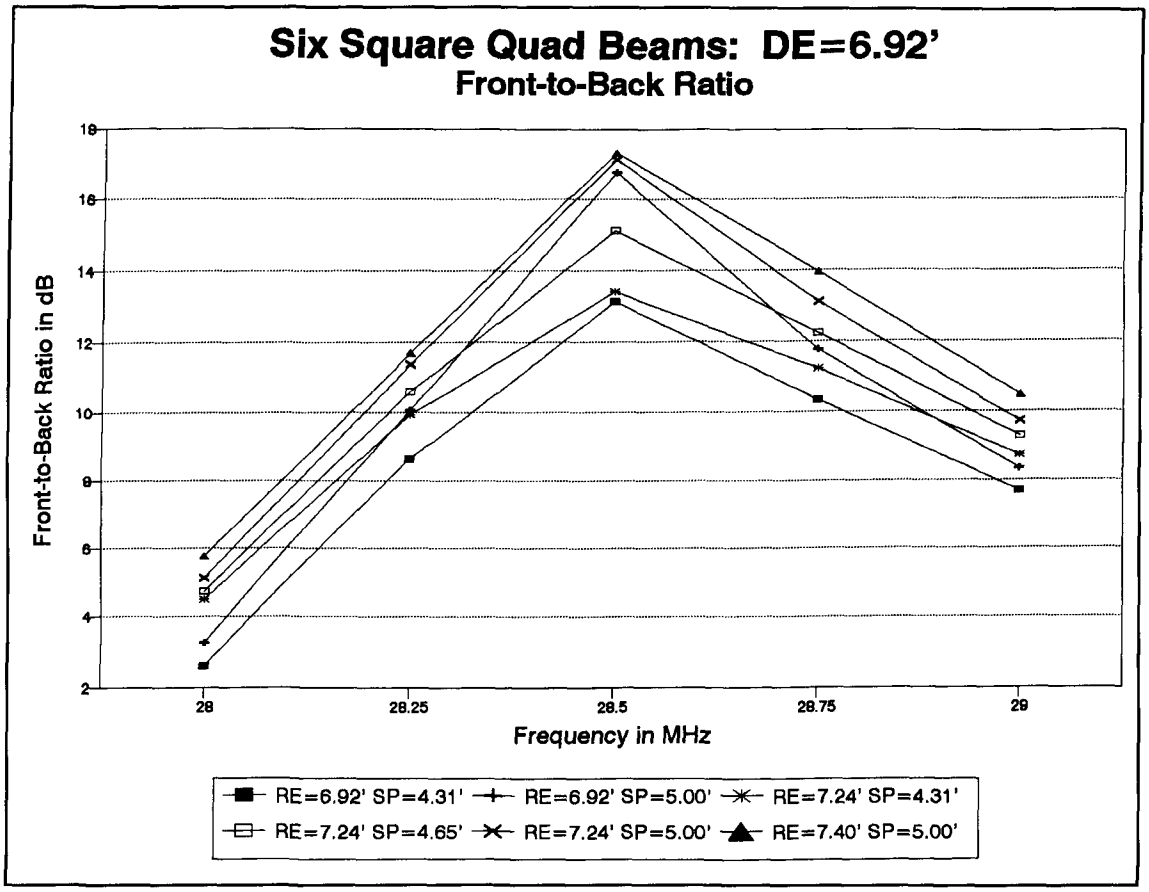

Figure 20. Comparative free-space front-to-back ratios of shrunken, two-element quad beams with increased spacing and/or enlarged reflectors.

est heights. **Figures 10** and **11** illustrate the beam azimuth pattern at the angle of maximum radiation for the antenna at heights of approximately 5/8 wavelength and about a full wavelength above medium ground. Although the pattern of ground reflections tends to degrade the rearward performance at the lower height, at a wavelength, the antenna recovers close to free-space front-to-back ratio. The broad beamwidth provides good forward coverage for general operation.

These notes on full-size quads are not a recommendation of the antenna. Instead, they provide a set of standards against which to compare shrunken quads with side (voltage-node) loading. Whereas the full-size quad requires either that the reflector be physically larger than the driven element or that an inductive stub be added to electrically lengthen the reflector, any model of a side-loaded shrunken quad can be adjusted solely by lengthening or shortening the linear load elements. In fact, for most models, the driven element will require a shorter load and the reflector a longer than a resonant single quad element.

Table 1 provides initial dimensions for test model shrunken quads for each of the three types of loops investigated. Spacing is a constant 4.31 feet (1/8 wavelength at 28.5 MHz). Each driven element was resonated and each reflector adjusted for maximum front-to-back ratio at approximately 28.5 MHz. Although reflector adjustment affects primarily the antenna feedpoint resistance and driven element adjustment affects primarily the feedpoint reactance, the two adjustments are sufficiently interactive to require a few iterations before optimal values are obtained.

All three types of loaded quad loops can be molded into a reasonable parasitic beam. Assessing how well how we might expect them to perform requires that we look at some of the parameters that can be modeled and compare those values with numbers for a full-size quad. Using the entire 10-meter band as a baseline, we can better appreciate what some of those numbers may mean.

Figure 12 provides a snapshot of the gain performance of the shrunken beams in comparison with two full-size quads, one using #18 wire, the other using #14 wire. Because quad gain doesn't peak at the same point as the front-to-back ratio, the two full-size quads show a decreasing gain across the band. The #14 full-

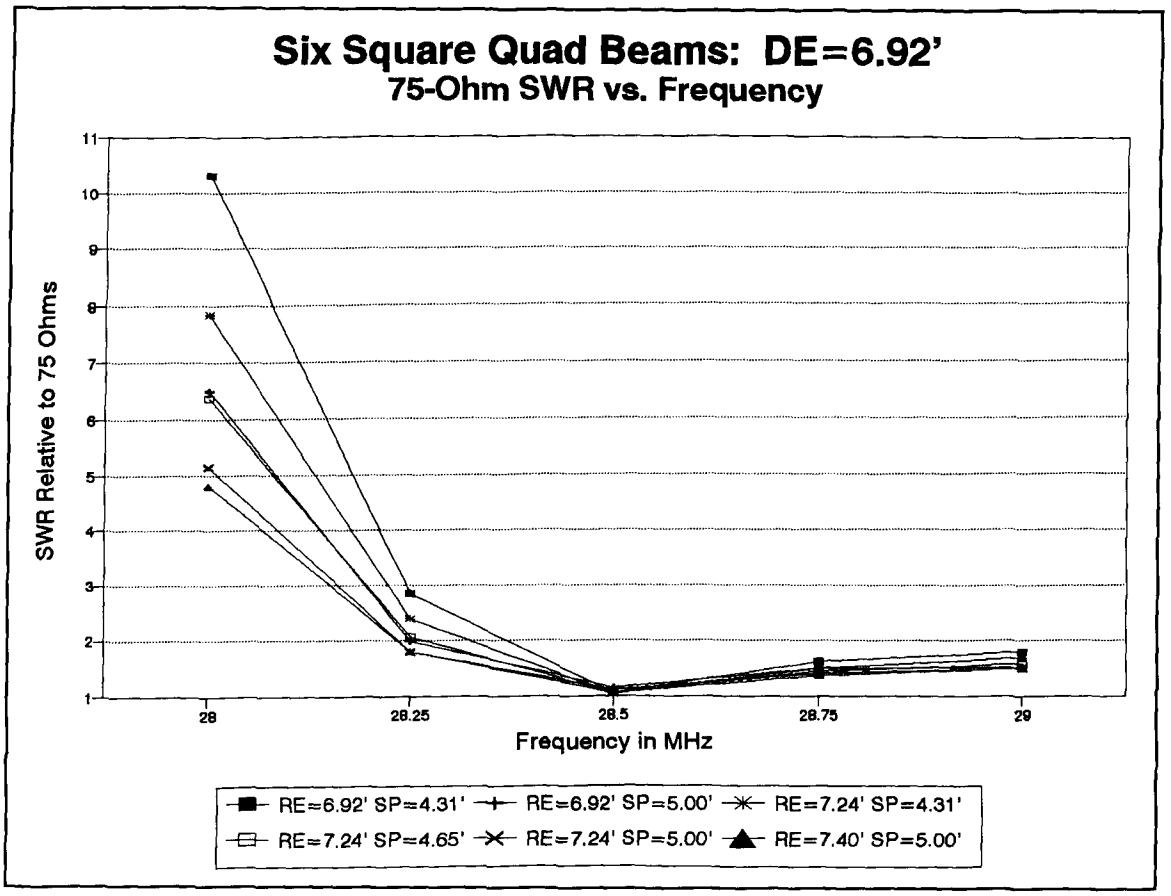

Figure 21. Comparative free-space 75-ohm SWR bandwidths of shrunken, two-element quad beams with increased spacing and/or enlarged reflectors.

size quad peaks outside the lower end of the band. However, both beams maintain above 6.5 dBi gain for the first MHz of the band, peaking above 7.15 dBi. For comparison, the broadband two-element Yagi used as a standard in other parts of this series has a maximum gain of about 6.1 dBi.

The two single-load-per-element quads show a considerable peak in gain above 6.7 dBi, but only over a smaller segment of the band. Like any shortened antenna, the gain cannot approach that of a full-size model; like any loaded antenna, the bandwidth for most characteristics will be smaller than that of a full-size model. The square double-load-line model provides the lowest gain and the narrowest gain bandwidth of all three. At the upper end of the band, its gain drops to that of a full-size single and quad loop.

Similar comments apply to the front-to-back ratios of the quad beams, as displayed in **Figure 13**. The two full-size beams have front-to-back ratios that peak above 25 dB (but at frequencies between the check points that form the graph). The ratio falls off fairly rapidly below design center frequency and more slowly above that frequency.

There is little to distinguish the front-to-back performance of the single-load-line shrunken quads. The front-to-back ratio peaks at about 13 dB, falling off rapidly at the lower end of the band and more slowly at the higher end. The standard broadband Yagi, by contrast, holds its front-to-back ratio at about 10 dB or better across the first MHz of 10 meters. The double-load-line model not only has a lower peak front-to-back (less than 10.5 dB), but its band-edge values fall well below 5 dB as well. Except for a 200-kHz window, its ability to reject QRM is marginal or worse.

The SWR curves relative to 50 and to 75 ohms, respectively, shown in **Figures 14** and **15**, provide a lesson in some of the illusions of a low SWR. For the full-size quads, a quarter-wave 75-ohm matching section or a 2:1 transformer would provide a good match between the antenna and a 50-ohm coaxial cable. At the high end of the band, the SWR performance appears worse than that of the shrunken quad, which exhibits a good match to 75-ohm cable from the design center frequency to the upper edge of the band.

However, one cannot take these numbers in isolation. The steep portion of the shrunken

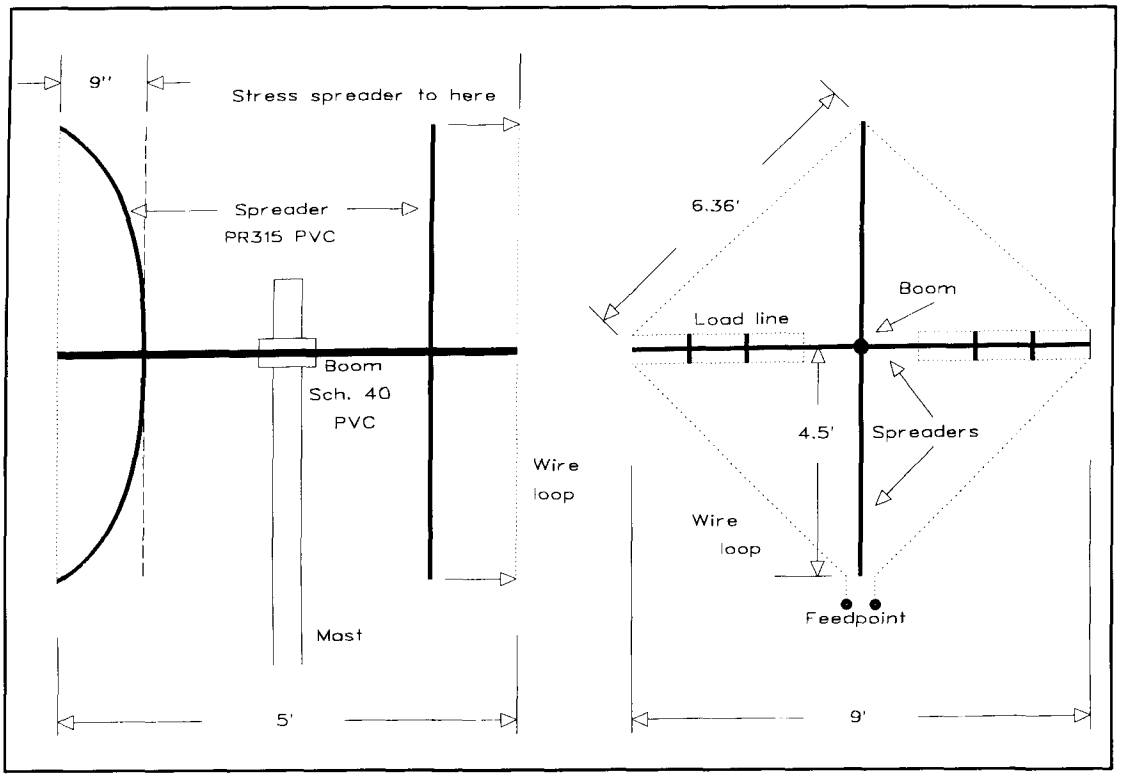

Figure 22. Overall structural features of a PVC-support 10-meter shrunken quad.

quad SWR curves at the lower end of the band overlaps that antenna's gain peak: the curves input impedance is most variable where the antennas perform best. In contrast, the curve is flattest in the region where the antennas barely show beam characteristics. The SWR bandwidth curves of the shrunken quads are essentially exaggerated versions of the curves for full-size quads, but those exaggerations have more pronounced negative affects upon antenna performance across 10 meters.

In essence, all three shrunken quads are narrow-band performers when gain, front-to-back ratio, and SWR (or feedpoint impedance) are taken together. Optimal performance covers about 200 kHz of 10 meters, with reasonable performance for about an additional 100 kHz each way.

The single-line models, whether diamond or square, clearly outperform the double-line model. Moreover, in optimizing models of the double load-line model for maximum performance, adjustments as small as 0.001 foot made a somewhat significant difference. In adjusting the single-line models, change minimums of 0.01 foot made a somewhat significant difference. In adjusting the single-line models, change minimums of 0.01 foot sufficed to optimize the model. (An inch is 0.0833 foot.)

Between the diamond and the square there is little to choose in terms of performance. **Figure 16** shows the azimuth pattern of the diamond in free space; the pattern of the square is too similar to need reproduction. In evaluating either or both of these small beams, investigate the patterns over real ground at the planned height. The azimuth pattern of the diamond (taken at the angle of maximum radiation in **Figure 17**) at 5/8 wavelength height shows a considerable rear lobe that is unlikely to provide much rejection. (The equivalent rear pattern of the standard broadband Yagi is smaller.) At a full wavelength up (**Figure 18**), matters improve, especially with respect to side rejection, but not to the level of a full-size quad.

Because these initial models used close spacing and identical loops, with their electrical sizes adjusted by changing the length of the loading lines, they do not achieve all of the gain and front-to-back ratio possible from a shrunken quad beam. Just how much more you can obtain from side-loaded elements depends to a great extent on how much you are willing to unshrink the loops and spread them apart.

Unshrinking the shrunken quad for better performance

In an attempt to improve the anticipated performance of a shrunken quad, I explored several models that alternately increased the spacing between elements and gradually enlarged the

physical size of the reflector. The basic dimensional properties of these models are listed in **Table 2.** Model 1 is the same square quad with a single load line per element used above. Model 2 increases the spacing to 5 feet (about 0.14 wavelength) close to the optimum value recommended by Orr and Cowan for a full-size two-element quad. Model 3 returns to the 1/8-wavelength spacing, but enlarges the reflector about 4.5 percent. Using the new reflector size, Model 4 increases spacing to 4.65 feet and Model 5 further increases spacing to the 5-foot mark. With this new spacing, Model 6 further increases the reflector size to 7 percent over the original. All models were optimized for maximum front-to-back ratio at a design center frequency of 28.5 MHz.

Figures 19, **20**, and **21** graph the results of these modeling experiments. Because performance falls below usable values above 29 MHz, the graphs are limited to data for the first MHz of 10 meters.

In general, gain increases with spacing, as **Figure 19** demonstrates. All three models with 5-foot spacing show the highest gain peak (at 28.25 MHz). However, the smaller the reflector, the more quickly the gain decreases as the frequency departs from the gain center. In fact, Model 6, with the largest reflector in the sequence, actually shows a slight increase in gain toward 28 MHz. Merely enlarging the reflector will not increase peak gain, as a comparison of Models 3 and 1 at 28.25 MHz will establish. However, enlarging the reflector will increase the gain-bandwidth. Model 3's gain falls off more slowly than that of Model 1.

The front-to-back ratio of the antenna, shown in **Figure 20**, also increases most dramatically with increased spacing between the two loaded elements. Model 2, with equal size elements but 5-foot spacing, rivals the largest reflector for peak front-to-back ratio. The models with the largest reflector dimensions show the slowest decrease in front-to-back ratio as the frequency departs from the design center. However, none of the models is a stellar performer at the low end of 10 meters.

The SWR bandwidth relative to 75 ohms is shown in **Figure 21.** All of the models show a fairly flat line and a good 75-ohm match above the design center frequency. Below design center, greater spacing flattens the SWR curve more dramatically than does a larger reflector. Notice that Model 2's (equal size squares at 5 feet) SWR curve largely overlaps the curve of Model 4 (an intermediate size reflector at an

Table 2. Some Variations on the Single Load-Line Quad

Model		Length of Driven Element per side in feet		Length of Reflector per side in feet		Spacing in feet
1[1]		6.92		6.92		4.31
	LL		2.62		2.98 [2]	
2		6.92		6.92		5.00
	LL		2.72		3.01	
3		6.92		7.24		4.31
	LL		2.64		2.69	
4		6.92		7.24		4.65
	LL		2.68		2.71	
5		6.92		7.24		5.00
	LL		2.72		2.73	
6		6.92		7.40		5.00
	LL		2.72		2.56	

Notes:

1. Model 1 is the same as the single-load line model used in the comparison with other loaded configurations above. Models 2 through 6 vary the size of the reflector or the spacing or both.

2. LL = length of load-line assembly on each side of the element. All load lines are #14 copper wire (same as the antenna element) with a spacing of 3 inches between lines.

Table 2. Some variations on the single load-line square to improve performance.

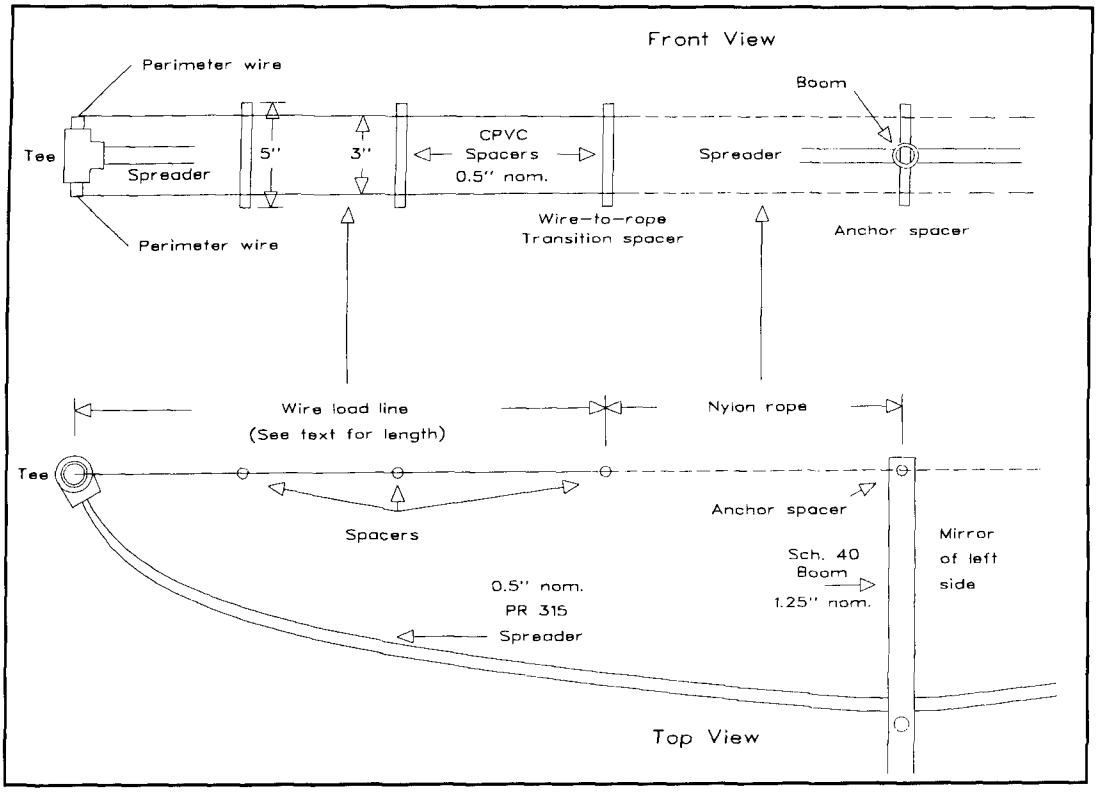

Figure 23. Load-line assembly details for the PVC-supported 10-meter shrunken quad.

intermediate size reflector at an intermediate spacing). However, the combination of the two factors, as in Models 5 and 6, produces an antenna that is a direct match for 75-ohm coax from 28.25 to 29 MHz.

Summing up the three sets of characteristics: wide spacing and a physically larger reflector produce the maximum gain, highest front-to-back ratio, and the flattest SWR curve. However, the antenna remains superior to a standard two-element Yagi only over about 500 kHz, with usable directional characteristics for about another 250 kHz. For effective use at the low end of 10 meters, the design center should be set another 250 kHz lower to bring the front-to-back ratio up to the productive levels and to bring the feedpoint impedance to levels easily matched in a 75-ohm system. However, the practical upper limit of the antenna as something better than a single full-size quad loop would then be about 28.75 MHz.

If the narrower bandwidth for full performance is acceptable and there is a need for compactness, then a shrunken quad can be a good choice. If hardware store supplies are the source of the antenna parts (except for the #14 wire, a RadioShack staple), then perhaps the model having equal-size loops and 5-foot spacing may be the best choice. Larger reflectors would require supports longer than the standard 10-foot lengths of thin-wall PVC. The diamond tends to shed ice and water better than the square. However, the square requires less horizontal space.

A test model of a shrunken quad

The test antenna was a diamond single-load-line quad with equal size loops spaced 5 feet apart. This configuration permitted an all-PVC support system on a 5-foot boom of 1.25 inch nominal Schedule 40 PVC. The spreaders are 9.1-foot lengths of PR 315 0.5 inch nominal PVC. Each piece fits through a 0.875-inch hole through the boom, and there are adjacent holes for spreaders at each end. Number 10 stainless steel (SS) hardware fixes each spreader in place. As shown in **Figure 22**, spreaders are mounted about 9 to 10 inches from the ends of the boom. To carry the wire, glue a half-inch Tee to the end of each spread.

The total circumference of the diamond loop is approximately 25.4 feet. With expendable twine, create a loop through the Tees, stressing the spreaders outward towards the end of the boom. The twine loop should be about the right circumference, as the spreaders bend in a plane with the end of the boom. Stressing the spreaders prevents them from waving front to back in the wind and strengthens the overall structure.

I drilled the end of the boom for an additional

short piece of half-inch diameter CPVC about 5 inches long. (Tan CPVC is closer than white PVC to its listed diameter: 0.5-inch nominal diameter CPVC has an outside diameter just enough larger than a 5/8-inch hole cutter to require a small amount of filing for a fit.) Drilled at a 3-inch spacing, this piece anchors the load lines. A pair of short sections of 1/8-inch nylon rope will attach to the final spacer of the lines at each side of center.

Models of the test antenna in free space, as well as 20 and 35 feet over real medium ground, suggest driven element load line lengths of 3.6 to 3.8 feet each for the driven element and 4.0 to 4.1 feet for the reflector. I chose to install driven element lines (without a shorted end) of 4 feet and reflector lines of 4.25 feet to allow for variables of building. Although there is a slight mismatch with the model, since the Tees round the quad corners, the most significant variable concerns the stressing of the spreaders. I found that I tended to overstress the assembly, and, in the process, lost a half inch or so of wire length per side. The longer load lines permit on-site adjustments before final soldering.

I used a single piece of wire for the top two sides and the top wire of each load line. Install at least two spacers (4-inch pieces of half-inch CPVC, drilled at a 3-inch spacing) on each load wire and tie off the load wire to a third spacer. Tie this last spacer to the one on the boom with the end of the nylon rope. **Figure 23** shows some of the details of the load-line arrangement. A single wire for the reflector lower half and load-line bottom wire replicated the top half, including load-line spacing and termination. Separate wires for the remaining sides and their associated bottom wire for loads of the driven element completed the basic assembly. Add thin position-locking wires, soldered to the main wire at each major corner, including the top spreader. A coax connector on an L-shaped piece of plastic completes assembly.

The resulting structure, with outward-curved spreaders at each end of the boom has its own aesthetic appeal. More significantly, it is sufficiently rigid to hold its shape in a gale, but flexible enough to withstand the breezes, transferring spot stress throughout the structure.

Initial testing can be done with the beam pointed skyward. Temporary shorting bars permit easy adjustment. I used short lengths of #12 copper wire terminated with ring connectors. Around the load-line wires, I crimped half-inch L-brackets, passing a #6 bolt through the two holes and the ring connector on one end of the #12 wire.

If it's not off the mark by more than a half MHz, you can initially adjust the driven element for lowest SWR as a marker of resonance. Adjusting the reflector will either be a matter of guess work or of in-place adjustment. A low-level signal source at a distance of at least 10 wavelengths (about 350 feet on 10 meters) will help you find and adjust the minimum signal off the rear of the beam. On my test model, my initial guesswork settings, based on the computer models and upon my estimates of how much I shortened the beam during construction, allowed the reflector adjustment to be made in one trial, with no further work needed on the driven element. (I am not always, or even usually, this lucky, even with computer guidance.)

I added about 2.5 inches to each load line initially to compensate for loop compression during building (about half an inch short on each of the diamond's four sides). With a 50-ohm coax line connected directly to this feedpoint, the final settings placed a minimum SWR window of 1.6:1 from about 28.3 to 28.7 MHz, with under 2:1 SWR from 28.1 to over 29 MHz. At a 25-foot height, these frequencies climbed about 0.2 MHz.

Reflector adjustment was also close to the compensated mark, requiring about a half-inch of load-line lengthening to place the maximum null at 28.5 MHz. Rechecks of the driven-element SWR proved that further adjustment was unnecessary. The reflector null was fairly sharp, with noticeable drops, as low as 50 kHz off maximum. However, within the limits of simple S-meter rezadings of uncalibrated test signals, the curve tracked the models predictions quite well. Once set, the difference between maximum null and the rearward signal at the band edges of 10 meters was about 2 S-units.

Although the shrunken quad can be operated as-is over a fair portion of 10 meters, its impedance is a better match for 75-ohm cable than for the 50-ohm test cable. A quarter-wave section of 75-ohm cable might well improve the SWR bandwidth, although a 1.5:1 broadband transformer of transmission-line transformer might produce a more accurate match. The basic narrow bandwidth of the antenna's gain and front-to-back ratio will not be affected by these measures.

Summary

Because the shrunken quad can be built from wire and PVC, it is among the cheapest of the beams so far tested, even requiring the least hardware. N4PC's sturdier all-Schedule 40 construction for 17 meters is a model for lower band use.[7] In fact, on the WARC bands, the narrow bandwidth of the shrunken quad's peak performance figures is no hindrance; in deed, the antenna may have its best home on those bands. It is also at home wherever one requires

a small footprint, but can tolerate some offsetting vertical dimensions.

Alternatives to the use of linear load lines are unlikely to improve performance in any noticeable way. R.G.D. Stone, G3YDW, reported the same narrowness of performance and SWR bandwidth on his capacitively loaded miniquad for 20 meters.[8] Indeed, voltage-node loading, whether by load-lines or linear capacitive "hats," is likely to yield the fewest loss sources of the many schemes used to shrink quads.

Capacitive hats, of course, are not limited to quads or verticals. I wonder what they might do for a shortened Yagi. ■

REFERENCES

1. William Orr, W6SAI, and Stuart Cowan, W2LX, *Cubical Quad Antennas, 3rd Edition*, (Radio Amateur Callbook, Lakewood, New Jersey, 1993); and Bob Haviland, W4MB, *The Quad Antenna*, (CQ Communications, Hicksville, New York, 1993). The number of articles on quads is legion, and this piece makes legion + 1.

2. Howard Hawkins, WB8IGU, "12-Meter Quad," *The ARRL Antenna Compendium, Volume 2* (ARRL, Newington, Connecticut, 1989), page 90. See this article for a circular quad.

3. Kris Merschrod, KA2OIG/TI2, "Coil Shortened Quads—A Half-Size Example on 40 Meters," *The ARRL Antenna Compendium, Volume 2* (ARRL, Newington, Connecticut, 1989), page 90. See this article for references in the literature to each of these loading schemes.

4. Paul Carr, N4PC, "The N4PC SQUAD (Squished Quad)" in Lew McCoy, W1ICP, *Lew McCoy on Antennas* (CQ Communications, Hicksville, New York, 1994), pages 83–85. See this article for references to earlier work on the mid-side loaded quad.

5. All patterns and figures in this study are derived from NEC-2 in the EZNEC 1.0 package available from W7EL. It should be noted that tapered models in MININEC tend to show resonance with a length formula between 1044 and 1045 divided by the frequency in MHz, all other factors held constant. Because NEC-2 doesn't "cut" corners, it is used as a basis for discussion here.

The preference applies only where the wire diameter is constant throughout the model. NEC-2 has difficulty with changes in wire diameter, especially in models with some degree of geometric complexity. The diameter change difficulty can be minimized by adding separate wires for the last portion of each corner. Using this technique for quads with tubing for the horizontal members and wire for the sides brings the gain figures into close coincidence with MININIC models, although the feedpoint impedance in the two modeling systems continues to diverge significantly.

The diamond models used here generally have a short horizontal three-segment wire at the lower apex as the feedpoint. Compared to a pure diamond, fed at the apex under a combined split feed modeling system, the diamond models with the flattened bottoms tend to need a slightly smaller circumference (about 0.5 percent), which would make no significant difference in actual construction.

6. With each dimension approximately 75 percent of full size, the area is less than 58 percent of a full-size quad loop. However, element spacing would remain unchanged from a full-size model, yielding 58 percent as the volume gain as well.

7. Carr, N4PC, "The N4PC SQUAD (Squished Quad)" in Lew McCoy, W1ICP, Lew McCoy on Antennas, pages 83–85.

8. R.G.D. Stone, "Practical Design for a Top-hat Loaded 14 MHz Miniquad," *Radio Communications*, October 1976, as quoted in Moxon, *HF Antennas for All Locations, 2nd Edition*, (RSGB, Herts, U.K., 1993), pages 207–208.

Appendix: Capacity Loading versus End-Stub Loading a Shrunken Quad

Long after I completed my foray into shrunken quads, my highly perceptive YL, N4TZP, noticed my brief remarks on capacity-loaded quads. These versions of shortened quads use a single wire from the side points instead of the parallel lines that I used, following Paul Carr's lead. She asked me a simple question: "Is there any advantage to one system of loading over the other?"

The answer comes in two parts: 1. There is no electrical advantage to one system over the other. 2. There may be a mechanical advantage to one over the other, depending upon your quad construction technique.

Figure 24 shows the physical layout of a two-element diamond quad beam using a capacity "side" hat (the electrical equivalent of a vertical's top hat) to permit tuning the elements to resonance or other points. The diamond's dimensions are the same as the model built and tested from **Figures 22** and **23**. Capacity hat dimensions are shown on one side for the driven element and on the other for the reflector. Element spacing remains the same at 5 feet. I derived the dimensions by a simple modeling technique. From the final model of the quad I built, I erased one of the elements in each of two separate models and determined the resonant frequency of each element. Then I eliminated the parallel stubs and joined the side peaks. Finally, I creased a capacity hat with a wire inset plus two wires paralleling the main element, adjusting their lengths until the loop was resonant on the same frequency as its stub-predecessor. I then rejoined the two separate elements in one model.

You can adapt this technique to the actual construction of antennas. Build one element at a time and tune it to a resonant frequency given by a model that you have previously broken down into separate elements. Combining the elements should assure that you're close to optimal performance without concern for interpreting element interactions during tuneup.

The technique of replacing the stub by a capacity hat is justified on the basis that the two points originally separated by the parallel stub have the same current and can, therefore, be connected. However, a capacity hat in one dimension (ignoring wire thickness) requires a greater length than a two-dimensional flat disk-type hat. The dimensions shown are applicable to #14 copper wire and to the separation wire length (0.5 feet in this model). As with the parallel wire stub, careful pruning is necessary.

Figure 25 shows the free-space pattern that resulted from this exercise. Forward gain (nearly 6.2 dBi) and front-to-back ratio (about 18 dB) are too close to the corresponding numbers

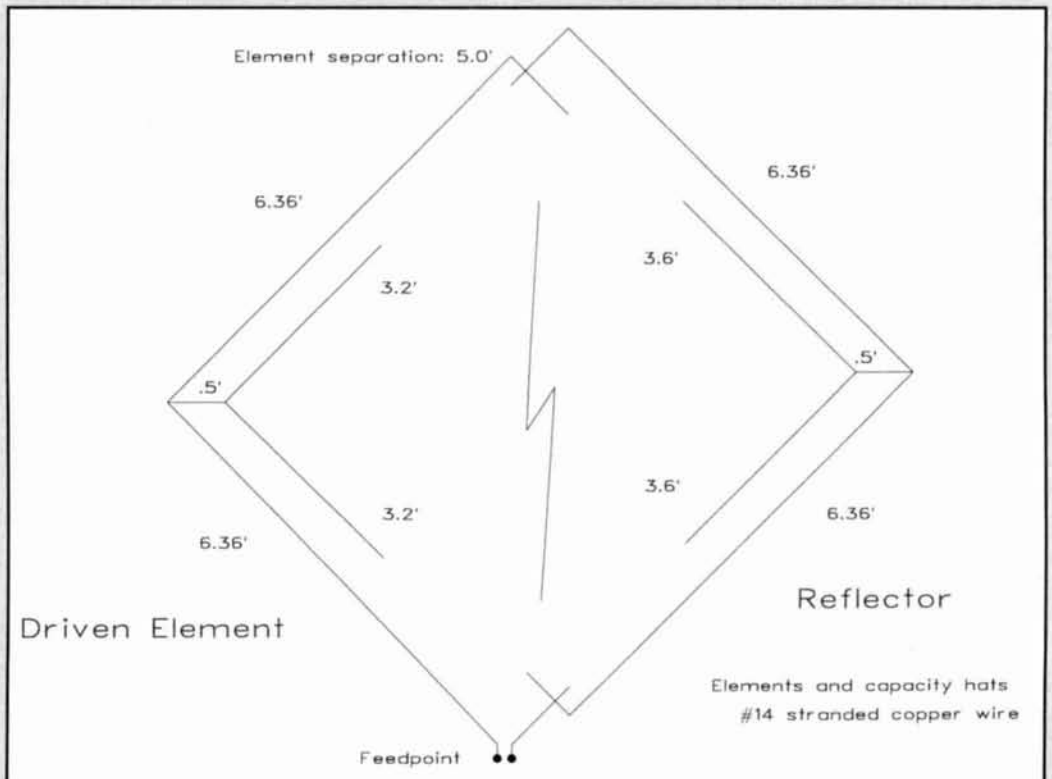

Figure 24. General outlines of a capacity-loaded shrunken quad, with driven element dimensions to the left and reflector dimensions to the right. The missing parts of the diagram are mirror images of the parts shown.

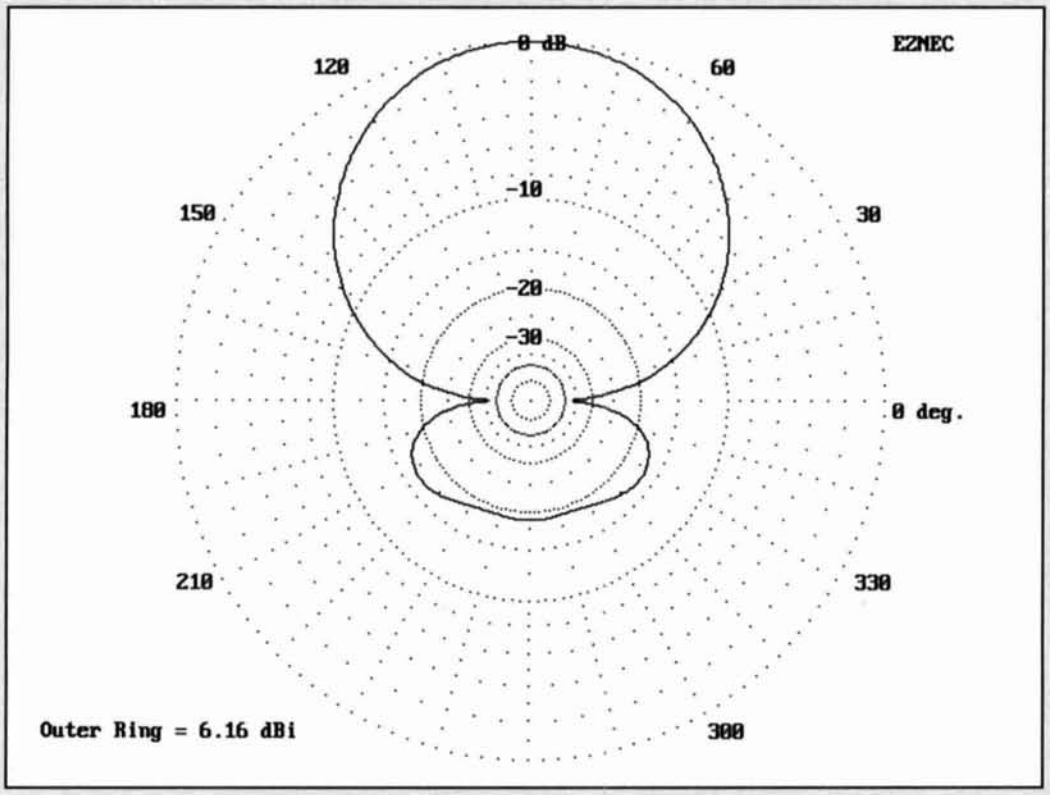

Figure 25. Free space azimuth pattern for a two-element capacity-hat-loaded shrunken quad of the dimensions shown in Figure 24.

for the stub-quad to make any difference in performance. SWR, gain, and front-to-back figures over 10 meters correlate well with those for the stub quad.

The shortening technique you use likely will depend on your construction method. The stubs in the shrunken quad I built are preferable with the stressed support arms, because each stub rides free, with no nearby metallic masses to detune it. Scaling up the antenna for lower bands, however, may call for the capacity hat technique. If you use flat-face Xs to support the quad wires, and if there is any metal in them, then the capacity hat technique may be better suited to your needs. It would reduce coupling to the support framework.

End loading of antenna elements is a technique that deserves further study. Although capacity hats are somewhat out of vogue in amateur antenna-making, except for vertical mobile antennas, they do offer somewhat higher efficiencies than other forms of loading. They load where the current is least, rather than adding coil losses at high current points or otherwise distorting the radiation pattern near the feedpoint. Although near-circular hats are somewhat ungainly, they may still have a place in at least monoband horizontal antennas.

An Invitation To Authors

Communications Quarterly welcomes manuscript submissions from its readers. If you have an article outline or finished manuscript that you'd like to have considered for publication, we'd like the chance to review it.

Those of you who are thinking of writing, but aren't sure how to put a piece together, or what programs we accept, can write for a free copy of our author's guidelines (SASE appreciated).

Interested?

Send your manuscripts or requests for author's guidelines to: Editorial Offices, *Communications Quarterly*, P.O. Box 465, Barrington, New Hampshire 03825.

We're waiting to hear from you.

PRODUCT INFORMATION

High Energy Surge Protectors for RS-232/422/485 Comm Lines

A new line of heavy duty surge protectors from B&B Electronics is designed to help protect data and communication lines against lightning strikes, power surges, and other types of voltage disturbances. Up to five lines are protected.

The new models offer three stages of protection: a gas discharge tube, a series resistor, and a transient voltage suppresser. The heavy metal case of the B&B Electronics High Energy Surge Protectors offers two terminal posts and two metal mounting brackets to provide a good solid ground connection, which is important for the units' proper operation.

The units have been tested to meet IEC 1000-4-5 and IEEE C62.41 specifications; they also meet CE regulations.

Standard connectors are five-position blocks. An RS-232 model with M/F DB-25 connectors is also available. Size is 4 1/2" x 3 1/4" x 1 3/4" (LWH) and weight is 7 ounces.

The new High Energy Surge Protectors from B&B Electronics range from $74.95 to $124.95. For a free catalog, contact B&B Electronics Manufacturing Co., 707 Dayton Rd., Ottawa, IL 61350; Phone: (815) 433-5100: Fax: (815) 434-7094; e-mail: <catrqst@bb-elec.com>; WWW: <http://www.bb-elec.com>.

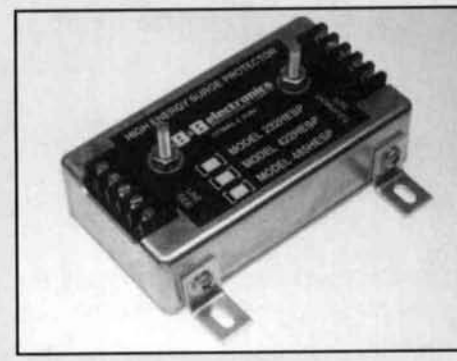

L.B. Cebik, *W4RNL*
1434 High Mesa Drive
Knoxville, Tennessee 37938
e-mail: <cebik@utk.edu>

QUARTERLY COMPUTING

HFx 1.1: The CCIR alternative in HF propagation analysis and prediction

Although most current HF propagation software for Windows uses a version of IONCAP as its foundation, HFx by Pacific-Sierra Research Corporation uses the vertical incidence critical frequency foF2 model recommended by the International Radio Consultative Committee (CCIR) in 1966–67. The mathematical model is based on long-term empirical observations. The propagation model is based on ray geometry and uses another CCIR-recommended algorithm.

From these calculations, HFx produces three types of outputs: a global model (with rectangular or spherical mapping) of MUF, FOT, and HPF world wide; a temporal or clock-hour graph of MUF, FOT, and HPF for a given path; and a display of skip or "hop modes" in either graphical or tabular form. The familiar Maximum Usable Frequency (MUF) concept is joined by the Optimum Traffic Frequency (FOT) and the Highest Possible Frequency (HPF) to provide the user with varying levels of confidence in various paths at various frequencies of interest.

HFx is surprisingly simple to use and requires rather minimal user inputs. Among the basic inputs are a date and time (or an option to use the host computer figures), an option to use short or long great circle paths, transmitter power and antenna (as some aspects of the calculations depend upon this figure), minimum take-off angle for the antenna used, and an option to enable *E*-layer bending for greater computational accuracy. Additionally, one enters the station location as a latitude and longitude (or as a callsign prefix to preset a default figure) and, for two of the outputs, a receiver location somewhere else in the world. If the user is graphically oriented, he can enter locations using the left and right mouse buttons to click locations from the interactive world map (**Figure 1**) to transfer them to the data entry box. The user also has the option of linking all three program outputs to these figures or of entering separate figures for each.

The only required input data that's not a matter of time, place, or options are the solar activity number and the K-index. Solar activity may be entered as either the sunspot number or the daily 10.7-centimeter solar flux figure. The former, along with the current three-hour geomagnetic K-index, are broadcast hourly by WWV and available on the World Wide Web from NOAA and other sources.

Once entered, the user selects the desired output and lets the program do its work. The world map MUF function graphically displays FOT, MUF, or HPF as a series of easily readable blocks atop either a rectangular or spherical world map. One can alter the center of the displayed half sphere to any convenient latitude and longitude and click between rectangular and spherical displays.

The MUF map may be most useful for exercises in learning what happens with varying sunspot and K-index conditions. Taking in the world at a glance quickly familiarizes one with the concept of Maximum Usable Frequency (MUF) and its operating consequences.

Detailed DXpedition, contest, and even general operation planning requires access to the 24-hour graphs of the MUF/FOT/HPF for specific paths, normally from the anticipated operating point to various areas of the world. A

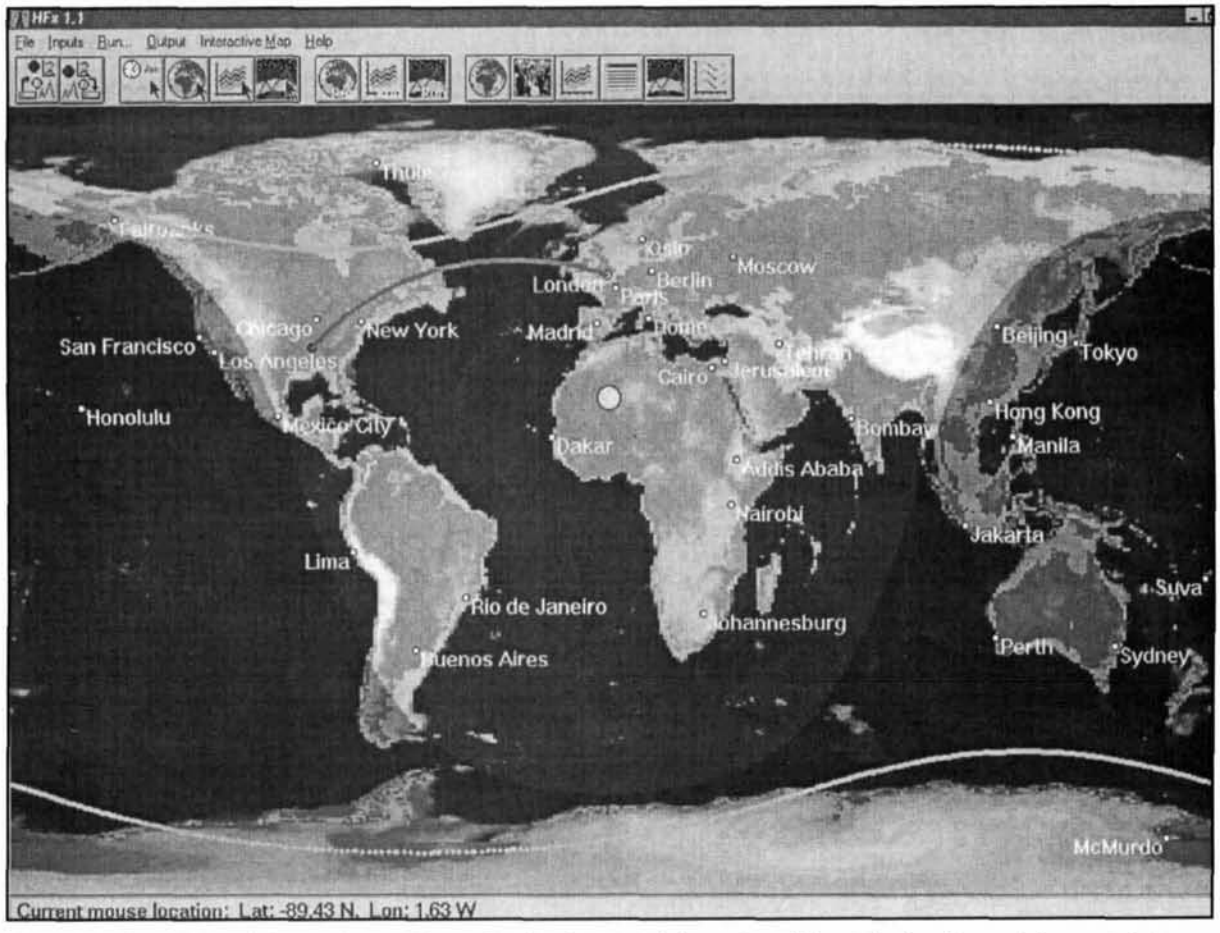

Figure 1. A view of the main interactive world map, showing the transmitting and receiving station locations and the great circle path between them, the sun location, the auroral areas, and the daylight terminator. This gray-scale reproduction of the screen cannot do justice to the quality of the color graphics of HFx.

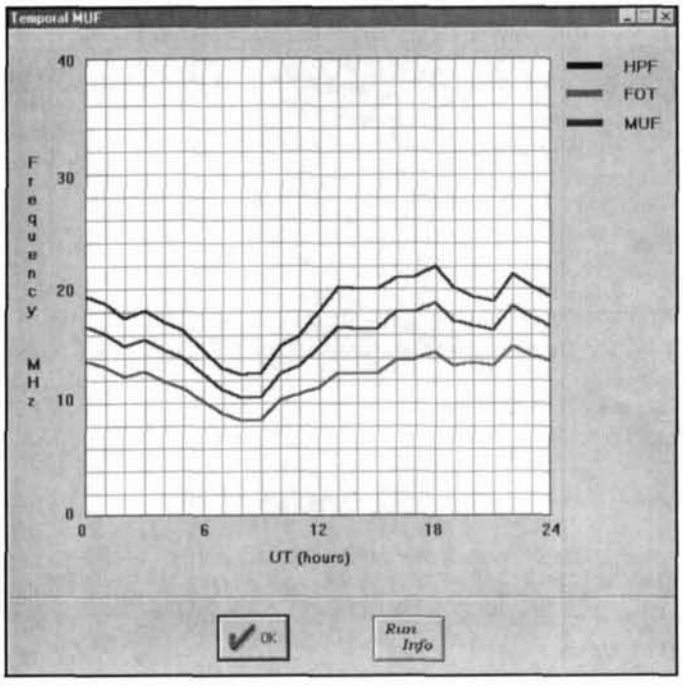

Figure 2. A typical hourly chart of MUF, FOT, and HPF from a planning exercise. The color-coded lines for this Tennessee—England exercise tend to favor 20 meters in the UTC afternoon.

sample is shown in **Figure 2**. One can develop a planning exercise for each ham band for representative areas of the world and also find the best times of day for contacts with each. A compilation of this data soon sorts itself into a detailed plan of attack for maximizing QSOs and minimizing search time.

For detailed path investigations, HFx offers both graphical and tabular skywave "hop" geometries. The data is available for up to 10 HF frequencies and tabular output includes calculations of the e-field at the reception site. A simple 14-MHz hop path from Tennessee to London appears in **Figure 3**. Although one might think of this mode as a graphical extra without much utility in amateur communications, serious operators and students of propagation can gain significant insight into propagation path physics from this mode of analysis. The tabular data on anticipated signal strength, signal-to-noise ratio, and path availability is especially useful.

In the end, HFx will provide the user with much more information if he brings to the software a well-developed planning or study exercise to make the available output data meaning-

ful and useful. Software sessions, in turn, will likely help one in developing the exercises even further. Gradually, a program like HFx becomes a natural tool. Then come the refined questions. How do actual experiences correlate with predictions? How useful is the three-hour K-index in planning actual operations?

New users may wish to review the extensive HFx manual in partial reverse order. After installing the software, study the glossary of basic propagation terms (Chapter 7), then read carefully the explanation of ionospheric propagation (Chapter 6). Finally, work through the tutorial in Chapter 5 (referring often to the interface information in Chapter 4) to quickly master the art of putting data into and getting data out of the program. Finally, spend some time before and after each session in developing new or expanded uses of the program.

Although HFx has much to offer serious students of HF propagation, one can hope for future print functions for graphics and save-to-file functions for tabular data to help glean the most information from each session. HFx is available from Pacific-Sierra Research Corporation, 2901 28th Street, Santa Monica, California 90405-2938, at a cost of $129. ■

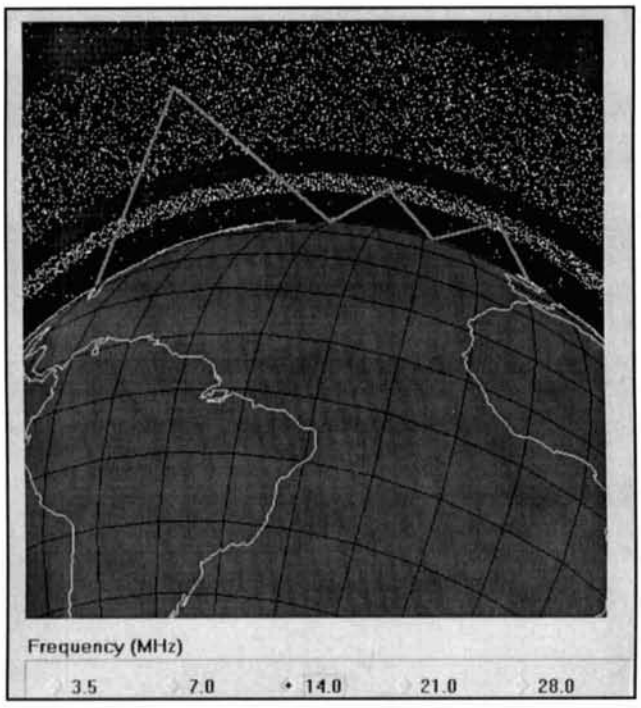

Figure 3. The 20-meter skip or hop analysis for the same Tennessee—England path in the same exercise. Again, gray-scale reproduction reduces the vividness of the actual color screen display.

PRODUCT INFORMATION

Slewing Operational Amplifier Sets Speed Benchmark

Analog Devices has introduced the industry's fastest slewing monolithic operational amplifier. The current-feedback AD8009 features a 5500 V/μs slew rate—more than twice that of its nearest competitor with 10% faster rise and fall times at 725 ps for a 4-V step.

Small signal (-3dB) bandwidth is 1 GHz at unity gain and 700 MHz with a gain of +2. Spurious free dynamic range is 74 dBc at 5 MHz, 53 dBc at 70 MHz, and 44 dBc at 150 MHz. For multitone signals, such as RF/IF signals, the 3rd-order intercept is specified at 26 dBm at 70 MHz and 18 dBm at 150 MHz. Settling time to within 0.1% of full scale signals is 10 ns.

The AD8009's high-speed performance is available with no penalty to output power drive. From 6 V supplies it drives 175 mA (150 mA minimum) of output current through a 10-Ω load, and it can drive four back terminated video loads with a guaranteed maximum 0.03% differential gin and 0.03° differential phase error. Maximum quiescent current is 16 mA and maximum input offset is guaranteed to be less than 5 mV (typically 2 mV).

The AD8009 costs $2.99 in 1,000s, is available in standard 8-pin SOIC packaging, and will operate over the industrial temperature range -40 to +85°C. An evaluation board (model number AD8009-EB) is available for custom device characterization.

For more information, contact Analog Devices, Inc., Ray Stata Technology Center, 804 Woburn Street, Wilmington, MA 01887; Phone: (617) 937-1428; Fax: (617) 821-4273.

Rick Littlefield , *K1BQT*
109A McDaniel Shore Drive
Barrington, New Hampshire 03825
e-mail: <k1bqt@aol.com>

QUARTERLY DEVICES

The Den-On SC7000Z Vacuum Desolderer

Few designers or low-volume repair technicians can afford the luxury of a full-blown SMD rework station. Instead, most of us improvise with what we've got, while keeping an eye open for new low-cost tools to make the job easier. For example, to solder, I use a combination iron and vacuum-sucker soldering station liberated from a flea market at a fraction of its as-new price.

This works OK, but what I really want is an all-in-one gizmo that can wire-solder, air-reflow, extricate SMD parts, and free tight leads from stubborn plate-throughs. I'd also like to get rid of the compressor, air tank, hoses, tangled cords, and shoe-box sized vacuum unit presently cluttering up my lab.

Photo A. The Den-On SC7000Z Vacuum Desolder.

Although this "R & D dream machine" probably doesn't exist, the Den-On SC7000Z desoldering tool comes amazingly close!

Description

The Den-On SC7000Z is a handheld desoldering device with a built-in suction pump and filter. It performs the same basic function as a much-larger bench-mounted vacuum system. However, there are several differences and added features that make the SC-7000Z more versatile. For one thing, the unit is fully self-contained in a high-impact plastic case about the size of a standard soldering gun. The case is carbon-impregnated and the tip grounded, making the SC-7000Z ESD-safe for C-MOS devices. The unit's vacuum pump, flow valve, and filter are located in the body, and the pump's drive motor is inside the handle. This may sound like a hefty handful of hardware, but the entire package barely weighs a pound. Operation is totally silent, except for pump noise when the trigger switch is depressed.

Compared to a bench-top vacuum unit powered by compressed air, the SC-7000Z not only saves space, but also a considerable amount of money. To illustrate how much money, the current list price for my bench-top station is over $1,100, plus another $250 for a small compressed-air setup with all the required hoses and attachments. The SC-7000Z, on the other hand, sells for $395 (current sale price with stand). If this were simply a powered vacuum-sucker alone, you'd already be $1,000 ahead of the game. But, its more!

Unlike my fixed-temperature bench-top station, the Den-On unit is temperature-adjustable from 350 to 500 degrees Celsius (662 to 932 degrees Fahrenheit). This means you can set

the tip temperature to accommodate a wide variety of components and pc boards. Heat is generated by a barrel-mounted, 100-watt ceramic element. This unified design minimizes conduction distance to the tip, and temperature is held constant by a sensor-feedback control circuit. A thermostat LED indicator remains lit during warmup and blinks when the unit is at temperature. Warmup from a cold start takes about two minutes.

Perhaps the most significant feature of the SC-7000Z is its ability to reverse air flow and function as a positive-pressure hot-blow system. This adds the capability to air-desolder LSI chips and other SMD parts. It also allows you to use reflow pastes for installing parts with pin spacings too close to wire-solder with an iron. To change modes from powered suction to hot-blow soldering, you'll need to change tips, substitute a bypass cartridge for the unit's suction filter, flick the air-direction lever, and turn up the heat. This procedure is simpler than it sounds and takes less than a minute to complete.

In comparing the SC-7000Z to a bench unit, I should note that most vacuum stations are designed to run all day—every day—in a high-volume production environment where compressed air is readily available. Most of them also provide a high-quality temperature-controlled soldering iron as part of the package (something the SC-7000Z does not). The SC-7000Z, on the other hand, is designed for intermittent use in a low-volume shop, field-service, or lab environment. Here, small size and versatility are especially valued features. It's simply a matter of choosing the right tool for the job; for many of us, a production-line vacuum station is overkill.

Using the SC-7000Z

Manufacturer's specifications and claims are always interesting to read, but using a product for real-world tasks is more telling. When I set the product literature aside and applied power to the SC-7000Z, I wondered how a small handheld unit could seriously compete with an industrial-grade vacuum sucker. About two minutes later, the thermostat LED started to blink and it was time to find out.

To provide a true acid test, I pulled a rejected radio transceiver board from my junk box. Unlike most digital boards, this particular RF layout harbored a host of nasty-to-remove through-hole parts stuffed into large heat-absorbing ground-plane areas—a nightmare for most removal systems. For openers, I took aim on a 10-mm shielded RF transformer and pulled the trigger. The SC-7000Z's vacuum pump kicked in with a muffled "brrupp." As soon as I desoldered the last pin, the 10-mm shield can literally fell out of the board! I tried several more parts, and each one came out with equal ease. Through a combination of solid thermal capacity, stiff temperature control, and strong suction, the SC-7000Z lived up to its claims. It's a real performer!

The "gun" technique for removing parts is simple—just make sure the tip is well-tinned and the plate-through is completely heated before you pull the trigger. Thorough heating ensures complete evacuation of the hole and pad area. One note of caution: the manual advises against suctioning up clipped wire leads. This can result in an unscheduled stop for a tip cleaning.

The spec sheet states that the SC-7000Z can clear plate-throughs on multilayer boards up to eight layers deep, and even 12 layers deep when supplemental heat is applied to the bottom of the board. I believe it—the unit's internal pump develops over 650 mmHg of vacuum in a mere 1/10 of a second! In fact, this is the only low or moderately priced system I've seen that has enough suction and thermal recovery to reliably clear plate-throughs implanted in large land areas.

Encouraged by the unit's performance on through-mount boards, I switched over to hot-blow mode. As long as you have a safe way to handle and cool the extracted tip, you can switch modes while the unit is still hot. To use the hot-blow mode effectively, however, you'll need to purchase the accessory SMD Tool Kit ($42). This package includes a special elongated tip that delivers superior air heating, a baffled bypass cartridge to replace the fiber-filled suction filter, and a SMD removal tool with a collection of stainless-steel wires and blades for lifting various SMD packages.

After setting up for hot-blow operation, I *located a scrap board containing an SMD IC* with 0.05-inch pin spacing. To ensure sufficient air temperature, I set the thermostat for 450° C (more tip heat is required for hot-blow procedures than for suction removal). To remove the IC, I installed a thin stainless-steel wire in the SMD removal tool and slipped it behind the IC pins on one side. After preheating the pad area for a couple seconds, I began to pop each lead off its pad with the SMD tool, moving down the length of the chip while continuing to apply heat. This procedure worked exactly as advertised, and the chip came out cleanly without damage to the board.

Next, I extracted a few 1206 resistors, heating each one with a jet of hot air and plucking it off the board with tweezers. The SMD tool may also be used for removing discrete parts such as capacitors, resistors, and inductors. Simply sub-

stitute a small blade in place of the wire. Finally, to push the envelope, I reinstalled the same IC I had removed, using solder paste and a construction aid to hold the chip in place. This was a slightly more challenging task, but, once again, the gun's air temperature was more than adequate to heat the pads quickly and reflow the paste.

Maintenance

As with any vacuum desoldering system, the SC-7000Z requires periodic maintenance. However, thanks to some forethought on the part of the manufacturer, I found this quick and easy to perform.

The pathway from tip to filter cartridge is short, straight, and very hot, so there's little opportunity for solder to ball up and become trapped in the either the tip or suction line. To clear solid debris, the instructions suggest reversing the air flow briefly prior to shutdown. A more thorough tip cleaning is accomplished with a cleaning pin (a set of these comes with the unit). For dissolving residual flux, the literature suggests occasionally removing the tip and soaking it overnight in acetone.

To protect the unit—and to protect yourself from the hot tip—I strongly recommend ordering the SC-7000Z with the ST-800 stand. This heat-resistant holder not only allows safe storage when the unit is turned on, but also provides a cleaning sponge for keeping the tip bright and clean. Also, to prolong life, the instructions recommend tinning the tip occasionally with fresh solder and remembering to turn the unit's thermostat down to minimum heat during prolonged periods of inactivity.

The other important maintenance item on the SC-7000Z is the unit's filter. All vacuum systems require an in-line air filter to prevent solder debris from being sucked into the pump. The disposable Den-On filter cartridge is made from shatter-proof high-temperature plastic, and it ejects easily from the top of the unit with the pull of a release lever. Routine cleaning is easy, and cartridge handling is far less touchy than with the high-temperature glass-tube filters used in many bench-top stations. A catch-plate (or baffle) in the Den-On cartridge prevents rapid fouling of the filter's fibrous material and prolongs the filter's useful life. When the fibrous material finally becomes contaminated, replacement cartridges are available for about $3.00 each.

The Bottom Line

Overall, I found the SC-7000Z to be a first-class performer. For one thing, it did everything the promotional literature claimed it would. More importantly, however, it fulfilled several valuable functions I routinely need when prototyping new designs for both through-lead and SMD style packaging. If you're looking for a low-cost way to add vacuum-powered suction and hot-blow capability to your bench, this unit is a hard act to beat!

The Den-On SC-7000Z is presently available from Howard Electronic Instruments, Inc. for a sale price of $395. This price includes the ST-800 stand, a standard-profile 1 mm-ID suction tip, a spare filter, and a tip-cleaning tool ($375 without stand). Other standard and slim-profile tips are also available as accessories in 0.8 mm, 1.0, and 1.5 mm ID sizes, along with disposable replacement filter cartridges.

In addition to purchasing the basic unit and stand, I strongly suggest ordering the 51-78-00 SMD Tool Kit ($42). This accessory is essential if you wish to use the hot-blow feature of the unit for SMD work. Other accessories, such as the 71-11-00 SMD suction-removal assembly for LSIs ($65), are also available to perform specialized operations normally found only in high-end bench-top SMD rework units.

You may contact Howard Electronic Instruments, Inc. for literature and more information at 1-800-394-1984 and 1-316-744-1993 via voice, or at 1-316-774-1994 via Fax. The e-mail address is <sales@heinc.com>, and the Web site is at <http://www.heinc.com>. The regular mailing address is Howard Electronic Instruments, Inc., 6222 North Oliver, Kechi, KS, 67067. All units purchased carry a 30-day fully refundable money-back guarantee, and a one-year warranty. Qualified buyers may be eligible for a free 15-day trial. The unit may be returned at no charge if you decide not to buy. The company also carries a line of Den-On premium-grade temperature-controlled soldering irons to compliment the SC-7000Z. ■

Edited by Peter Bertini, K1ZJH
Senior Technical Editor

A Note on the Radiation Resistance of Loop Antennas with Short Circumferences

Loop antenna fans, take note.

Peter Bertram, DJ2ZS

Small loop antennas with radius b and circumference C are increasingly popular, as is evidenced by the number of publications dedicated to such antennas. The number of most interest is the radiation resistance, which is always calculated by the expression:

$$R_s \cong 320\pi^6 \left(\frac{b}{\lambda}\right)^4 \bullet \Omega \qquad (1)$$

which equals:

$$R_s \cong 20\pi^2 \bullet C_\lambda{}^4 \bullet \Omega \qquad (2)$$

where C_λ is short for C/λ.

The above-mentioned equation is an approximation, valid only for very small loops with a constant current distribution whose derivation can be found in almost any antenna textbook. It isn't a good approximation for $C_\lambda \leq 0.1$, which

Table 1. Values of R_S.

C_λ	R_F mΩ	R_M mΩ
0.052	1.5	1.5
0.105	23.8	27.0
0.157	121	163
0.210	381	664
0.262	931	2330
0.315	1930	8106

Table 2. Results of R.W.P.

C_λ	Re_K Ω	Im_K Ω	Re_M Ω	Im_M Ω
0.05	0.0013	80	0.0013	81
0.10	0.0222	166	0.0222	167
0.15	0.1317	263	0.1312	265
0.20	0.5212	380	0.5238	384
0.25	1.7153	534	1.7780	544
0.30	5.4935	760	5.867	784

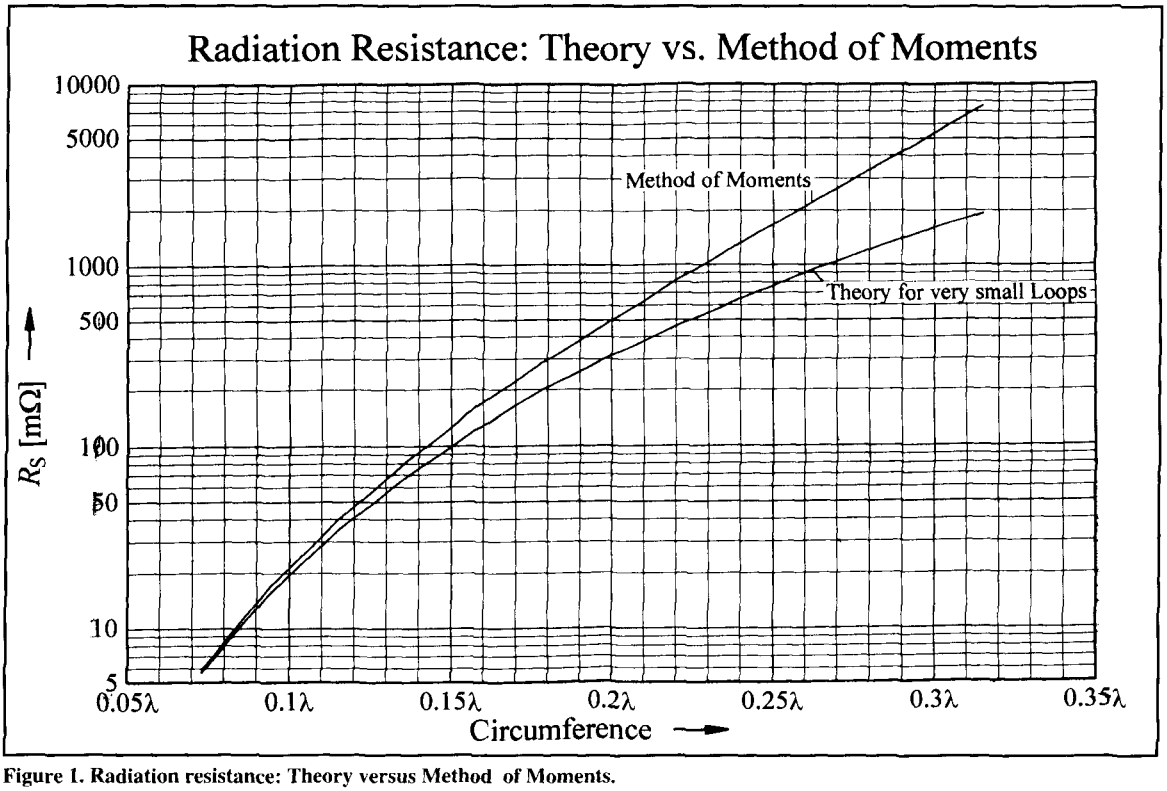

Figure 1. Radiation resistance: Theory versus Method of Moments.

is easily shown by a simulation using the method of moments (MOM). **Table 1** lists some values of R_S where R_F stands for radiation resistance predicted by the formula and R_M for the radiation resistance gained by the method of moments. And, there's good news: R_S is greater as is usually supposed!

Figure 1 is a graph that should enable you to read off the values of interest. For those who prefer a pocket calculator, **Equation 3** shows three approximations for three ranges of C_λ. Note the different exponents!

$$R_S \approx \left\{ \begin{array}{ll} 200 \cdot U_\lambda^4 & \Leftrightarrow 0.000 \le U_\lambda \le 0.110 \\ 1240 \cdot U_\lambda^{4,8} & \Leftrightarrow 0.105 \le U_\lambda \le 0.250 \\ 7820 \cdot U_\lambda^6 & \Leftrightarrow 0.200 \le U_\lambda \le 0.320 \end{array} \right\} \text{Ohm} \quad (3)$$

For those who are still skeptical, I include the results of R.W.P. King (**Table 2**) after a rigorous mathematical treatment of loop antennas of arbitrary size. The subscripts K and M stand for King and MOM, respectively. The level of agreement speaks for itself.

So, if you find your loop antenna works better than expected, you'll know why!

New Relays for Old

Choosing the right relay for the right job.

S.F. Brown, G4LU

The relay has been around in its many forms since the earliest days of line telegraphy. The fact that these devices still figure in the major suppliers' catalogs shows they still have many applications.

Relay selection

When you select a relay for a particular project, it's probably because the contact arrangement is correct; however, the operating voltage may not be suitable for the application. You can look around for another relay with a coil of similar dimensions and the required operating voltage rating, or you can make hit-and-miss attempts at rewinding the original coil. If you adopt the latter course, the relay may only operate weakly, or the modified coil may overheat. Usually ad hoc methods don't produce a satisfactory solution, nor is the time you spend rewinding the coil used efficiently.

To avoid excess experimentation, the following formulas were devised some 40 years ago, and have proved successful on many occasions since. The method depends on making a reasonably accurate estimate of the ampere-turns required to operate the relay in its unaltered form. This is done using knowledge of the original operating voltage, by measuring the physical dimensions of the coil, and calculating the number of turns and the gauge of wire employed from those properties. (In some cases the wire is revealed near the coil terminals and a direct measurement can be made.) Having determined these factors, it's a relatively easy matter to find the gauge of wire and number of turns for the desired operating voltage.

The math

The mathematics aren't difficult for those who are versed in the art/science of calculations. For those who are not so blessed, the important conclusions appear in the boxes.

Consider the relay core shown in **Figure 1**. If "W" cms is the distance between the cheeks of the coil former and "t" cms is the overall diameter of the wire used, it follows that the turns per layer will be W/t.

Similarly, if "d" is the diameter of the iron core plus, say 0.1 cms for insulation, and "D" is the outside diameter of the coil less 0.1 cms for the protective insulation, then the height of the winding will be (D-d)/2 and the number of layers will be (D-d)/2t. (The diameter of the core should be measured at the fixing end because the other end is often enlarged to retain the outer cheek of the coil former.)

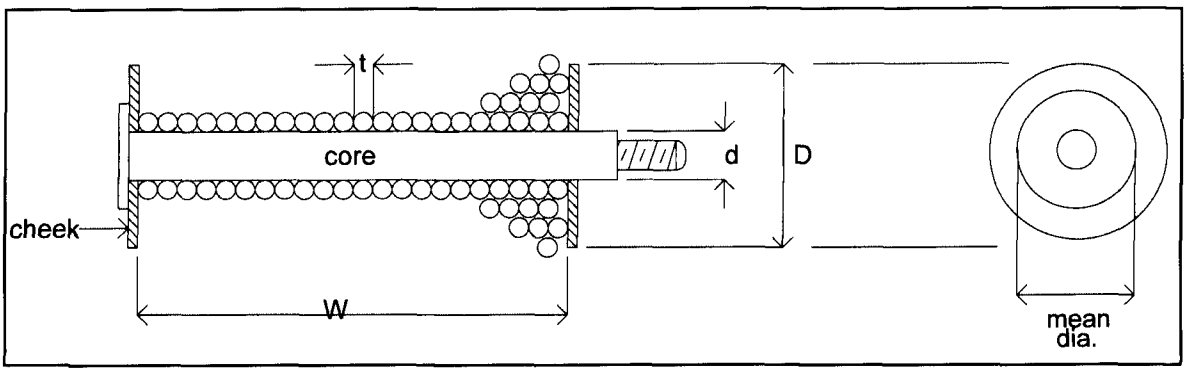

Figure 1. Relay core.

It follows, then, that the total turns, T, will be the product of these two terms,

$$T = \frac{W\,(D - d)}{2t^2} \qquad (1)$$

This is a general expression that applies to any coil of the shape shown.

If we can strip the coil of its wire, we can measure its thickness and it will then be a simple matter of substitution in **Equation 1** to find the number of turns employed. (For accurate work, you'll need a micrometer or wire gauge, but it will be sufficient to close-wind an inch length of turns on a pencil and calculate the thickness.) Some relay coils carry a label that provides this information, and if we're lucky, the wire gauge along with the coil resistance. (See the example at the end of the article.)

Usually, this isn't the case; but once we've obtained this information and know the resistance of the winding, the ampere-turns may be determined. This is a constant for a given relay because the magnetic flux, and hence the pull on the armature, are in direct proportion. This value isn't much use in itself, because what we really want to know is how to achieve the same value when the coil is rewound for the desired operating voltage. This we must set about doing, but first we must develop some equations for the resistance of the coil.

A digression

Let's digress to another set of formulas concerning coil resistance. This information is usually printed on the outside of the coil, but, if not, it can be determined by measurement. Also, we know the resistance is a function of the length and cross-sectional area of wire, as related by the following well-known formula:

$$R = \mu \bullet \frac{\text{length of wire}}{\text{cross-sectional area of wire}}$$

where μ is the resistivity of the wire material, which for copper is 1.724 μ x ohms/cm^3.

It's obvious that some turns, where they are next to the core, will have a small circumference, while those on the outside of the winding will be correspondingly larger. As a result, we must introduce the concept of "mean length of turn," or MLT. The MLT will clearly be pi times the mean diameter of coil, i.e.,

$$MLT = \pi \bullet \frac{(D + d)}{2}$$

If the mean length of the turns is multiplied by the number of turns, we shall obtain the length of wire used in the coil. Thus if "L" is the length of wire in the coil, then using **Equation 1**:

$$L = \frac{W\,(D - d)}{2t^2} \bullet \frac{\pi\,(D + d)}{2}$$

$$L = \frac{\pi\,W\,(D^2 - d^2)}{4t^2} \qquad (2)$$

Now the cross-sectional area of the wire is

$$\left(\frac{\pi t^2}{4}\right)$$

By substituting this expression in the resistance formula, together with the length given by **Equation 2**, we have:

$$R = \mu \bullet \frac{\pi W(D^2 - d^2)}{4t^2} \bullet \frac{4}{\pi t^2}$$

$$R = \mu\,\frac{W\,(D^2 - d^2)}{t^4} \qquad (3)$$

The only unknown quantity in this formula is "t", the thickness of the wire. By transposing the quantities, we can easily derive a formula for it, thus:

$$t^4 = \frac{\mu W(D^2 - d^2)}{R}$$

$$\text{or } t = 4\sqrt{\left[\mu W(D^2 - d^2)/R\right]} \qquad (4)$$

The fourth root will have to be evaluated using log tables, a slide rule or pocket calculator, or even by dredging up a double helping of the longhand method of square rooting once taught in schools.

This formula enables us to find the thickness of the wire without wrecking the original winding. But, by whatever means we use to deduce the size of the wire, the value can be put back into **Equation 1** to calculate the turns on the original winding.

We now must find an expression for the ampere-turns, AT, in terms of the voltage and coil dimensions. Because we have a formula for the resistance of the coil given in **Equation 3** above, we can find an expression for the current in the coil. Thus, if the applied voltage is "E", the current "I" will be:

$$I = \frac{E}{R} = E \bullet \frac{t^4}{\mu W(D^2 - d^2)}$$

and the ampere-turns will be given by multi-

plying this by the expression for the turns derived in **Equation 1**:

$$AT = E \bullet \frac{t^4}{\mu W(D^2 - d^2)} \bullet \frac{W(D - d)}{2t^2}$$

$$= E \bullet \frac{t^2}{2\mu (D + d)}$$

We can now set up conditions for the new and old coils. The dimensions of the coils will be the same in both cases. The only things that will be different are the voltages and the wire diameters. If the new operating voltage is "E_n", and the wire thickness for the new winding is "t_n", then because the ampere-turns are the same in each case, it follows that:

$$AT = E \bullet \frac{t^2}{2\mu (D + d)} = E_n \bullet \frac{t^2}{2\mu (D + d)}$$

Because the denominators on both sides are the same, by transposing we can achieve the simple formula:

$$t_n = t \bullet \sqrt{ [E / E_n] } \qquad (5)$$

Thus, if the relay originally operated on 24 volts and is needed to work with 12 volts, the new winding will require wire 1.4 times (i.e. $\sqrt{2}$) the thickness of the old.

If we return to **Equation 1** and do a little transposing there, we find that:

$$2Tt^2 = W (D - d)$$

and $$2T_n t_n^2 = W (D - d)$$

hence $$T_n = \frac{Tt^2}{t_n^2}$$

And using **Equation 5** above:

$$T_n = \frac{E_n}{E} \qquad (6)$$

Thus, in the example above, the new relay would have twice the turns of the old one.

Using the resistance formula, it can also be shown that the power dissipation in the two coils will be the same, so the new one will run as cool as the old.

Example

As an example of the degree of accuracy obtainable from these formulas, I used a 50-volt relay of U.S. Navy provenance found in the junkbox. The relay coil had a resistance of 800 ohms and it also specified on its label the turns on the coil and the wire gauge employed. Thus, using its dimensions, the turns and wire thickness could be calculated and checked against the label specification.

Using the previous nomenclature, it measured as follows:

D = (1.8 - 0.1)cms taking the insulation into account

d = (0.65 + 0.1) cms taking the insulation into account

W = 3.5 cms

μ = 1.724 μohms/cm^3

$$\therefore\ t4 = \frac{1.724 \text{ x } 3.5 (1.72 - 0.75^2)}{1{,}000{,}000 \text{ x } 800}$$

$$= 0.0000000176$$

and $\therefore$ t = 0.0115 cms.

The label on the relay said it was wound with 37 AWG (t = 0.011 cms), which shows that the error is about 5 percent.

The turns on the relay will be given by substituting this value for "t" in **Equation 1**:

$$\text{thus turns} = \frac{3.5 \text{ x } (1.7 - 0.75)}{2 \text{ x } 0.0115^2}$$

$$= 12571 \text{ turns}$$

The label said there were 11800 turns, making the error about 6.5 percent. The magnitudes of the errors are quite acceptable, as most relays will usually pull in with an applied voltage much reduced on the specified rating.

The errors in all probability arise because of the assumptions on the thickness of insulation around the core, the protective covering around the coil, and also because no account has been taken of the wire insulation. In addition, it has been assumed that the layers are wound exactly on top of each other, which isn't necessarily the case. Some turns will fall in the "valleys" between the turns beneath them.

If the relay in our example were to be used on a 12-volt supply, the thickness of the wire would need to be increased to $\sqrt{[50/12]}$x0.0115, which is 0.0235 cms (22/23 AWG) or, because I am on this side of the "Pond," approximately 34 British Standard Wire Gauge. The new turns will be 12571 x [12/50] = 3017 turns.

Many relays on the surplus market are designed for use in 24 or 50-volts DC circuits, but in amateur practice a 12-volt supply is more common. Using the preceding formulas, there should be no difficulty in rewinding relays for any DC supply voltage.

The 2-Meter PVC-EDZ Antenna

The Plumber's Delight, 1990s Style.

Rick Littlefield, K1BQT

To an old-timer, a "plumber's-delight" antenna might conjure up recollections of copper pipe, blue flames, and the acrid tang of hot flux. However, PVC and Genova Cement™ are the new materials of choice for plumbers and antenna builders alike. These inexpensive supplies provide the backbone for this high-performance, side-mount 2-meter antenna. Build it carefully and, for the price of lunch at McDonald's™, you'll have a skyhook that performs with the best.

Technical description

The PVC-EDZ is a 1-1/4 wavelength extended double zepp consisting of back-to-back 5/8-wavelength radiators fed in the center. When mounted vertically, it yields 3-dB gain over a 1/2-wavelength dipole by flattening out the pattern and forcing more radiation toward the horizon. When side mounted, you'll realize yet another 1 to 2 dB gain due to reflector action from its support mast. Of course, this extra gain comes at a price: side-mount verticals exhibit a shadow, or a shallow null, off the back side. However, if you can tolerate a few dB attenuation in one quadrant, the PVC-EDZ will perform exceptionally well in all other directions.

Each 5/8-wavelength radiator is 1/8 wavelength short of resonance at 3/4 wavelength and exhibits capacitive reactance (**Figure 1**). Normally, antenna manufacturers use a small base-mounted series inductor to tune this reactance out. However, the PVC-EDZ takes a different approach, using a short coaxial delay line cut from a scrap of 50-ohm cable to perform the same task. This method avoids the need for cut-and-try inductor tuning.

With reactance tuned out, each 5/8-wavelength radiator approximates a 50-ohm resistive load. Connecting the two radiators in series yields a 100-ohm balanced load. This, in turn, requires a 2:1 impedance transformer and balun for interface with 50-ohm unbalanced line. Both conditions are satisfied by installing a 3/4-wavelength line transformer made with 75-ohm cable and wound into a current choke around the antenna's PVC horizontal support arm.

Construction

I bought my coax off-the-reel at RadioShack, but you can use other sources. To make the delay lines, cut two 12-inch pieces of solid-dielectric RG-58 and prepare them as shown in **Figure 2**. Be careful not to nick the center conductor—it breaks easily. Next, cut a 46-1/2 inch length of RG-59 foam cable. Install a PL-259 on one end and prepare 1/2-inch pigtails at the other end. The antenna's 23-inch center section is cut from 1/2-inch ID PVC water pipe. The horizontal support is a 36-inch length of 1-1/2 inch thin-wall pressure pipe. Drill both of these pieces, along with the two PVC end caps, as shown in **Figure 3**. Finally, make a 6-inch aluminum insert from 1-1/2 inch

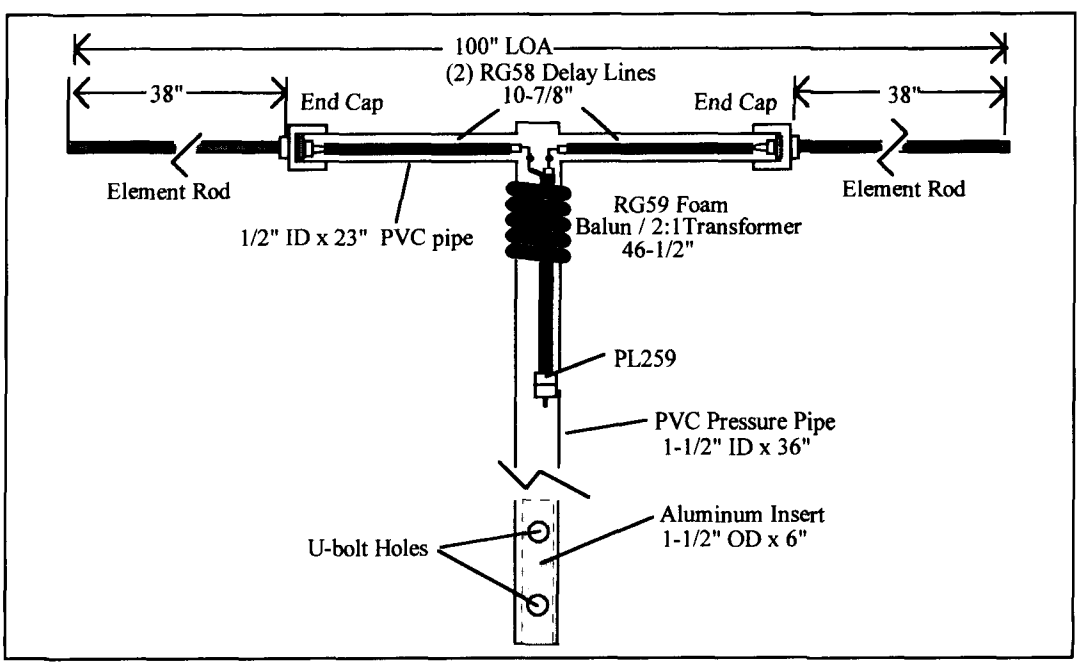

Figure 1. Two-meter PVC-EDZ antenna.

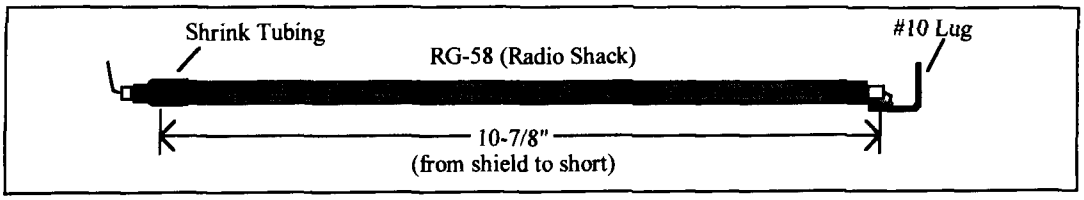

Figure 2. Delay line construction detail.

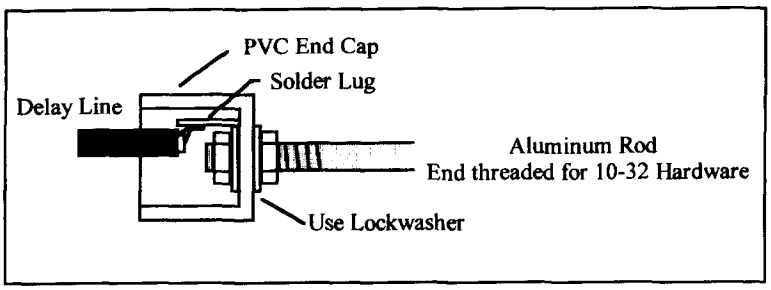

Figure 3. Element mounting detail.

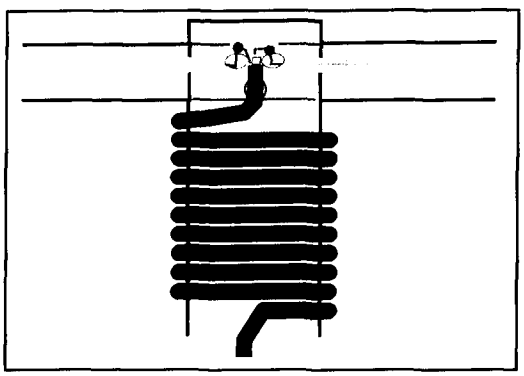

Figure 4. Feedline connection and choke detail.

OD stock and drill it for a standard TV-mount U-bolt. This will prevent the PVC pipe from crushing when it's clamped onto the mast. The two aluminum-element segments are made from 3/16 x 48-inch rod stock threaded for #10-24 on one end (collapsible whips may be substituted for portable use).

After installation, each aluminum rod is cut to 38 inches from element tip to the top of the PVC end cap. Prep delay lines as shown, installing a #10 lug on one end and protective shrink tubing on the other. Assemble an element rod and delay line onto each PVC end cap, tightening hardware securely. Carefully drill a small drain hole in the cap that will go on the lower leg of the antenna.

To begin final assembly, slip the antenna's center section into the horizontal support boom and secure it in place with Genova Cement™. Allow the assembly to dry and cure thoroughly before continuing. Next, insert each delay-line (as shown), making sure the prepared end is accessible through the center-point access hole. If all is okay, glue each end cap in piace and allow to dry. To connect the feedline, carefully pull each delay line center conductor through its respective center holes using hemostats (**Figure 4**), being sure to bend each conductor over so it can't pop back inside (this is tricky). Next, insert the pigtail end of the RG-59 line through the cable hole in the boom and solder each lead to a delay line. Secure the cable in place with PVC electrical tape, then wind the RG-59 around the mast to form a coaxial choke. Secure in place with μV-resistant electrical tape and install mast-mounting hardware at the opposite end. Finally, install a plastic cover of some sort on the end of the support boom to protect the feedpoint from the weather.

Mounting and testing

When mounting the antenna, provide a minimum of 20 inches of separation above and below each element tip. Connect a 50-ohm feedline onto the 75-ohm line transformer using a barrel connector, then waterproof the splice with rubber tape or Coax Seal™. Remember to orient the antenna so its shadow falls in a non-critical direction. This could be a quadrant where no important activity takes place, or an area where stations are all local and no gain advantage is necessary for coverage. My PVC-EDZ exhibited 1.1:1 VSWR at resonance and covered the band with a VSWR of 1.5:1 or less. If resonance falls outside the band, or if minimum VSWR exceeds 1.2:1, check for dimensional errors. Also, check continuity between the feedline and elements.

Conclusion

The PVC-EDZ is based on a proven antenna design and it performs well. I built it as a weekend project to cure an RFI problem at my computer desk—a condition that rendered my C-108 useless with its rubber-duck antenna. With the PVC-EDZ mounted at 35 feet outside the office, all computer interference disappeared, and I can now access most repeaters in southern New Hampshire with the Standard's 250-mW signal. Another plus is that out-of-band reception of public service and air-band traffic is outstanding.

If you're looking for an inexpensive antenna with a little extra boost in performance, why not take $5 and head for the local hardware store. The plumbing department may yield the best deal in town. ■

CQ Books & more...

NEW!

33 Simple Weekend Projects

by Dave Ingram, K4TWJ

A wide ranging collection of do-it-yourself electronics projects from the most basic to the fairly sophisticated, and even touching on the frivolous. You'll find an interesting and very do-able array of useful devices: station accessories for VHF FMing, working OSCAR satellites, joining the fun on HF, trying CW, building simple antennas, even a complete working HF station you can build for $100.

Add a measure of practical tips and techniques on how to build electronic projects yourself, and you've got an information-packed book that will keep the newcomer or the most experienced homebrewer busy for many a pleasant weekend.

Order No. 33PROJ..... $15.95

1997 Amateur Radio Almanac

by Doug Grant, K1DG

This volume is filled with over 600 pages of ham radio facts, figures and information. CQ's almanac is a resource you'll refer to over and over again. If it's ham radio, it's in The Source!

Order No. BALM97 ... $19.95

McCoy on Antennas

by Lew McCoy, W1ICP

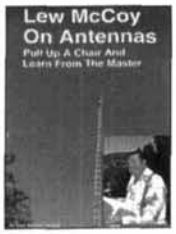

This is truly a unique antenna book that's a must read for every amateur. Unlike many technical publications, Lew presents his invaluable antenna information in a casual, non-intimidating way for anyone!

Order No. MCCOY $15.95

Keys, Keys, Keys

by Dave Ingram, K4TWJ

You'll enjoy nostalgia with this visual celebration of amateur radio's favorite accessory. This book is full of pictures and historical insight. If you've ever wondered about the old days of Morse, this book's for you.

Order No. KEYS $9.95

W6SAI HF Antenna Handbook

by Bill Orr, W6SAI

Nearly 200 pages filled with dozens of in expensive, practical antenna projects that work! This invaluable resource will guide you through the construction of wire, loop, yagi and vertical antennas.

Order No. HFANT..... $19.95

The NEW Shortwave Propagation Handbook

by W3ASK, N4XX & K6GKU

The most comprehensive source of information on HF propagation is available from CQ! Read about propagation principles, sunspots, ionospheric predictions, with photography, charts and tables galore—it's all in this unique reference volume!

Order No. SWP..... $19.95

The Quad Antenna

by Bob Haviland, W4MB

Second Printing

You'll enjoy this authoritative book on the design, construction, characteristics and applications of quad antennas.

Order No. QUAD..... $15.95

The Vertical Antenna Handbook

by *Paul Lee, N6PL*

Learn basic theory and practice of the vertical antenna. Discover easy-to-build construction projects for anyone!

Order No. VAH..... $9.95

Where Do We Go Next?

by Martti Laine, OH2BH

Ever dream about what it's like to go on a DXpedition? Have you ever imagined thousands of stations calling only you? Whether it's from the wind-mills of Penguin Island or the volcanoes of Revillagigedo each chapter conveys a unique story that you won't be able to put down.

Order No. WGN..... $9.95

The VHF "How-To" Book

by Joe Lynch, N6CL

This book is the perfect operating guide for the new and experienced VHF enthusiast.

Order No. BVHF..... $15.95

The Packet Radio Operator's Manual

by Buck Rogers, K4ABT

CQ has published an excellent introduction and guide to packet operation. It's the perfect single source, whether you're an advanced user or just starting out.

Order No. PROM. $15.95

Building and Using Baluns and Ununs

by Jerry Sevick, W2FMI

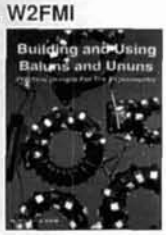

This volume is the source for the latest information and designs on transmission line transformer theory. Discover new applications for dipoles, yagis, log periodics, beverages, antenna tuners, and countless other examples.

Order No. BALUN . . . $19.95

SPECIAL!

Ham Radio Horizons: The Book

by Peter O'Dell, WB2D

Written by Peter O'Dell, WB2D, this is a book about ham radio that every beginner can enjoy! If you want to get in on the fun and excitement of Amateur Radio, Ham Radio Horizons is the perfect way to get started. HRH is full of tips from expert hams in: DXing, Contesting, Serving the Public, Ham Radio in Space, Experimenting, Digital Communications — you name it! This exciting book is an excellent gift to a prospective ham or for use in your club's licensing classes and library.

Order No. BHOR..... ~~$12.95~~ $8.95

CQ Videos, Calendars & more...

Videos

These videos are filled with easy to understand advice and tips that can't be found anywhere else.

Only $19.95 each!

Ham Radio Horizons: The Video.....Order No. VHOR
Getting Started in VHF.....Order No. VVHF
Getting Started in Ham Radio.....Order No. VHR
Getting Started in DXing.....Order No. VDX
Getting Started In Packet Radio.....Order No. VPAC
Getting Started in Amateur Satellites.....Order No. VSAT
Getting Started in Contesting.....Order No. VCON

Hats

A Must for Every Ham

This hat says that you're a part of the world's greatest hobby! Poplin cap with adjustable strap has 5 panels with fused buckram backing, 1/4" thick braid and a visor with eight solid rows of stitching.

Order No. : 97G (Green), 97B (Black)

.....$12.00

1997/98 Calendars

Fifteen month calendars - January '97 through March '98

Backpacks

Go Ahead! Load it up!

Load it up with all your ham "stuff." This useful and rugged backpack will be your greatest asset when carrying around your ham accessories. Embroidered design, 2 front pockets.

Order No.: 96N (Navy), 96G (Green), 96B (Black)

Glass Steins

Heavyweight!

This oversized glass stein holds a whopping 19 oz. With CQ's logo etched into the heavyweight glass, this collectible will look great forever!

Order No. 91 .....$9.95

Phone: 800-853-9797 | **FAX: 516-681-2926** | **MAIL**

YES! Rush me my book(s), calendar(s), video(s) right away!

Qty	Item #	Description	Price	Total Price
		Please add $4 shipping & handling. FREE shipping & handling for orders $50 and over.		
		NY State Residents add applicable sales tax.	Total	

Name _____

Callsign _____ Phone/Fax No. _____

Street Address _____

City _____ State _____ Zip _____

CQ Communications, Inc.
76 North Broadway, Hicksville, NY 11801, Phone: 516-681-2922/Fax: 516-681-2926

or call toll-free 800-853-9797

ADVERTISER'S INDEX

Reach this dynamic audience with your advertising message, contact Don Allen, W9CW at 217-344-8653, FAX 217-344-8656, or e-mail: QtrlyAds@aol.com

QuickCheck

The Xplorer Test Receiver. The professional choice when speed, performance, and reliability are an issue !

For Commercial and Mobile Radio testing, the **Optoelectronics Xplorer** stands alone. Let the Xplorer perform all your quick radio checks, instantly determining the radio's frequency, **CTCSS, DCS, DTMF**, deviation or signal strength. The Xplorer automatically locks on to any nearfield signal from **30MHz - 2GHz** in less than a second.

There is **no setup necessary**-Whether you're in the field or in the shop, the Xplorer is the portable, compact and **economical solution** for any two-way communications business.

Patent No. 5,471,408

FEATURES

- Nearfield receiver, sweeps 30MHz-2GHz in <1 second (Cellular bands are blocked on all U.S. versions)
- Decodes CTCSS, DCS, and DTMF. Manually record tones into memory
- Lockout up to 1000 frequencies
- Store 500 frequencies in memory with time & date stamp, as well as number of hits per frequency
- NMEA-0183 GPS interface for recording Latitude & Longitude coordinates (GPS Required)
- VFO mode for tuning to specific frequencies
- PC interface for downloading data from memory
- FM demodulation / Built-in speaker
- Auto or manual frequency hold
- Maximum nearfield reception / Up to 1/4 mile away

$899

Summer Special Includes: Spectrum CD & CC30 Case

Xplorer includes: TA100S antenna, NiCads, Charger, PC Download cable and software

SPECIFICATIONS	
Freq. Range	30MHz - 2GHz
Modulation	FM Deviation
Freq. Response	50 - 3000Hz
Auto Sweep Time	<1 second
Input 50 Ohm	-59dBm @100MHz
	-25dBm @1GHz
Display	2 line LCD
Power	Internal NiCad

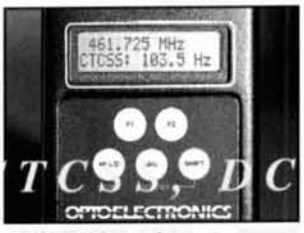

CTCSS Decode

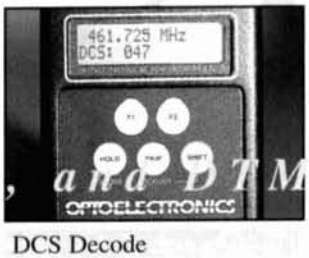

DCS Decode

DTMF Decode

FACTORY DIRECT ORDER LINE: 800•327•5912

OPTOELECTRONICS®

Check out our Web Site
www.optoelectronics.com

MADE IN U.S.A.

5821 NE 14th Avenue • Ft. Lauderdale, FL • 33334
Telephone: 954•771•2050 Fax: 954•771•2052 EMail: sales@optoelectronics.com
Prices and specifications are subject to change without notice or obligation.
Payment terms are Visa, MasterCard or C.O.D. (Cash or MoneyOrder)

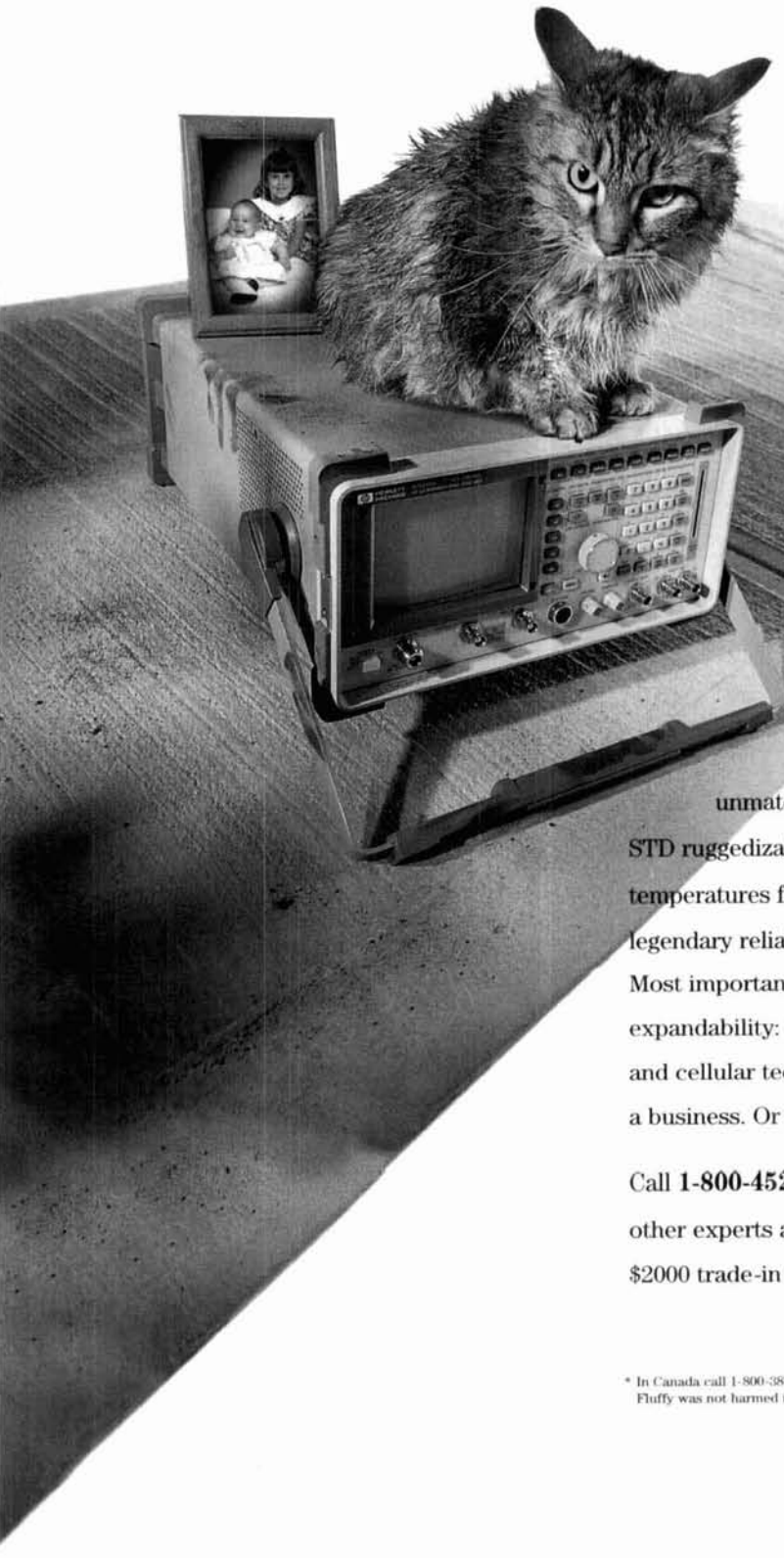

October 2, 1996.

Bob Jensen had
a fire at his mobile
radio repair shop.

He had only a
few seconds to
save things.

Thanks for the vote of
confidence, Bob.

No offense, Fluffy, but the HP 8920A is irreplaceable, too. Because the HP 8920A service monitor provides the edge you need to survive in today's tough business environment. It offers unmatched accuracy (frequency to within .1 ppm). MIL-STD ruggedization means it can withstand shock forces up to 30 g's, temperatures from 0 to 50 °C, and humidity from 0 to 95%. With the legendary reliability of HP (20,000 hrs mean time between failures). Most importantly, the 8920A service monitor offers superior expandability: it can test everything from two-way radios to pagers and cellular technologies. Which is important when you're building a business. Or rebuilding one, as the case may be.

Call **1-800-452-4844,* Ext. 5308**. Talk to Charlie or one of our other experts about the HP 8920A and find out how you can get a $2000 trade-in value for your old service monitor.

* In Canada call 1-800-387-3154, program number TMU310.
Fluffy was not harmed in the making of this ad. She's as rambunctious as ever, and enjoying Bob's new location.

HEWLETT® PACKARD